Aerogel based delivery of furanones for the inhibition of quorum sensing and biofilm formation in the wound pathogen *Pseudomonas aeruginosa*

A thesis presented for the degree of

Doctor of Philosophy

Chris Ryan Proctor B.N. B.Sc. M.Res.

School of Biomedical Sciences & School of Pharmacy and Pharmaceutical Sciences

December 2020

I confirm that the word count of this thesis is less than 100,000

Contents

Chapter 1 – General Introduction

Chapter 2 – Formulation and characterisation of PVA borate hydrogels as furanone delivery systems

Chapter 3 - Formulation and characterisation of a novel PVA aerogel for the delivery of furanones to wound biofilms

Chapter 4 - Furanones as antibiofilm molecules against *Pseudomonas aeruginosa*

Chapter 5 - Development of a novel in-vitro chronic wound biofilm model

Chapter 6 – General Discussion

Chapter 7 - Proposal for future work: In-situ degrading polymer aerogels as drug delivery systems for use in both acute and chronic wounds.

Appendix 1

Acknowledgements

I would like to acknowledge my supervisors, Dr Nigel Ternan and Professor Paul McCarron, for their continuous support and guidance and freedom to make this project a success. I have been grateful for all the advice you have given me both in the lab and in my many other ventures over the last three years. You both made competing this PhD immeasurably easier.

I would also like to thank all of my friends and staff from both the School of Biomedical Sciences and the School of Pharmacy and Pharmaceutical Sciences for any and all advice they have given. You have all made the last three years a lot of fun.

Finally, and most importantly, I would like to thank my family. Without their continuous support and understanding I would not have been able to push through and keep going, even when everything was going wrong.

Summary

A chronic wound is any wound that does not progress through the normal stages of healing. These wounds can take months or even years to resolve and, in many cases, will never fully heal. Chronic wounds are highly prevalent, with up to 3% of people over 60 and as many as 5% of people over 80 suffering from a chronic wound. Patients with chronic wounds often suffer from chronic pain, limited mobility, social isolation, and poorer mental health. Not only are these wounds highly traumatic for patients, but they are also a significant burden for the NHS, with their treatment costing approximately £5.3 billion per annum.

There are several reasons why a wound might fail to heal. The most common cause, however, is bacterial infection, and one of the most common causative organisms is *Pseudomonas aeruginosa*. When present in a wound, *P. aeruginosa* grows primarily in the form of a biofilm, a collection of bacterial cells encased in a self-produced polymer matrix. This matrix makes the bacteria highly resistant to antibiotic treatment, making wound infections very difficult, and often impossible, to eradicate.

The formation of bacterial biofilms is governed by a process known as quorum sensing, in which bacteria produce and detect small signalling molecules known as autoinducers. This form of communication allows the cells to coordinate complex, population-wide, behaviours such as virulence factor expression, and biofilm formation.

Several methods of disrupting quorum sensing, for example, via enzymatic degradation of the signalling molecules, have been proposed. One method competitive inhibition wherein a compound which competitively binds to the bacterial quorum sensing signalling receptors, effectively blocks the cell's ability to take part in quorum

sensing. Many synthetic and natural compounds have been shown to be capable of such competitive inhibition but perhaps the most well studied of these are furanones.

Furanones are one such family of naturally occurring chemicals which are structurally similar to the signalling molecules used by *P. aeruginosa*. This allows furanones to competitively bind to the quorum sensing signal receptor, thus, minimising biofilm formation by *P. aeruginosa* populations.

This thesis aimed to develop a novel method of delivering furanones to chronically infected wounds. This work demonstrated that, due to their inherent instability, a minimally crosslinked polymer aerogel was the most appropriate system for the controlled delivery of these compounds. Further, this thesis has demonstrated that, whether they are applied early in the biofilm formation process or to mature biofilms, two furanones, 4-hydroxy-2,5-dimethyl-3(2H) furanone (HDMF) and sotolon, are capable of significantly reducing biofilm biomass *in vitro*. The final experimental chapter of this thesis aimed to develop a novel, clinically representative, *in vitro* model of chronic wound biofilm that could be used to assess furanone loaded aerogels as potential antibiofilm wound therapeutics. The developed model was validated by showing efficacy of clinically relevant wound dressings and, subsequently, was used to demonstrate that sotolon-loaded aerogels showed great potential for reducing biofilm in chronic wounds.

This thesis concludes that, though complex to include in pharmaceutical formulations, naturally occurring furanones have excellent potential to be used as antibiofilm wound therapeutics. Furthermore, when incorporated into a minimally crosslinked poly (vinyl alcohol) aerogel material, these compounds retain their activity and can be delivered to clinically representative biofilms where they reduce biofilm biomass.

List of Abbreviations

ACP – 3-oxo-acyl carrier protein

AHL – Acyl-homoserine lactone

AI – Autoinducer

AMPS - 2-acrylamido-2-methylpropane sulfonic acid

AMR – Antimicrobial resistance

BBF – Bicyclic brominated furanone

BHL – N-butanoyl homoserine lactone

BSA – Bovine serum albumin

COC – Critical overlap concentration

CT – Computerised tomography

e-DNA – Extracellular DNA

EPSRC - Engineering and Physical Sciences Research Council

HDMF/DMHF – 4-hydroxy-2,5-dimethyl 3(2H) furanone

HPMC – Hydroxypropyl methylcellulose

IUK – Innovate UK

IVIS - *In Vivo* Imaging System

LB - Lysogeny broth

LVR – linear viscoelastic region

MCP1 - monocyte chemoattractant protein 1

MHB – Mueller-Hinton broth

MIC – Minimum inhibitory concentration

MRC – Medical Research Council

MTHF – 2-methyltetrahydrofuran-3-one

NCBI – National Centre for Biotechnology Information

OdDHL – Oxo-dodecanoyl homoserine lactone

PAA – Poly (acrylic acid)

PBS – Phosphate buffered saline

PEG – Poly (ethylene glycol)

PHMB - polyhexamethylene biguanide

PI – Propidium iodide

PML – Porcine myocyte lysate

PQS – Pseudomonas quinolone signal

PsaDM – *Pseudomonas aeruginosa* diffusible materials

PVA – Poly (vinyl alcohol)

QS – Quorum sensing

QSI – Quorum sensing inhibitor

SBF – Simulated body fluid

SWBA - semi-synthetic wound bed agar

TMOS – Tetramethyl orthosilicate

TNF α – Tissue necrosis factor alpha

TSB – Tryptone soy broth

TTC – 2,3,5 – triphenyl tetrazolium chloride

UKRI – United Kingdom Research and Innovation

‘I hereby declare that with effect from the date on which the dissertation is deposited in the Library of the University of Ulster I permit the Librarian of the University to allow the dissertation to be copied in whole or in part without reference to me on the understanding that such authority applies to the provision of single copies made for study purposes or for inclusion within the stock of another library. This restriction does not apply to the copying or publication of the title and abstract of the dissertation. “IT IS A CONDITION OF USE OF THIS DISSERTATION THAT ANYONE WHO CONSULTS IT MUST RECOGNISE THAT THE COPYRIGHT RESTS WITH THE AUTHOR AND THAT NO QUOTATION FROM THE DISSERTATION AND NO INFORMATION DERIVED FROM IT MAY BE PUBLISHED UNLESS THE SOURCE IS PROPERLY ACKNOWLEDGE

Chapter 1

General Introduction

Pseudomonas aeruginosa is a gram-negative bacterium which can be found in a diverse range of environments including soil and water. It is also commonly found in healthcare settings such as hospitals, clinics and nursing homes. This ubiquitous pathogen is capable of causing a range of infections in humans. These infections range in severity from mild skin infections to potentially fatal bacteraemia (Rybtke *et al.*, 2015). *P. aeruginosa* is an opportunistic pathogen and, as such, often affects chronically unwell patients, such as those with long-term respiratory conditions (e.g. cystic fibrosis or chronic obstructive pulmonary disease), those with open wounds such as burns and open fractures, and those who are immunocompromised (e.g. neutropenic patients) (Streeter and Katouli, 2016). One of the main reasons for the success of *P. aeruginosa* as a clinical pathogen is the numerous virulence factors it has at its disposal. These include mechanisms for evading host immune processes like phagocytosis and opsonisation, as well as the ability to produce enzymes such as elastase and collagenase which degrade and damage host tissues. However, while these mechanisms allow *P. aeruginosa* to colonise and attack a host effectively, they must be tightly controlled and regulated. As such, many of these virulence factors are controlled through a phenomenon known as quorum sensing.

1.1 Quorum sensing in *Pseudomonas aeruginosa*

Quorum sensing (QS) is a cell density dependent method of cell-cell communication which is seen in both gram-negative and gram-positive bacterial species as well as some species of fungi. Organisms which utilise QS do so to control processes including biofilm formation, cell motility and virulence associated gene expression (Fuqua, Winans and Greenberg, 1994). Bacterial QS is a complex process which varies

widely between species. In general, QS is dependent on the production and detection of small signalling molecules. In brief, bacteria constitutively express low molecular weight signalling molecules called autoinducers. In gram-negative organisms, the primary autoinducers are a group of molecules known as the N-acyl homoserine lactones (AHLs). These AHLs either diffuse or are actively effluxed from the cell and accumulate in the extra-cellular environment. Once a critical environmental AHL concentration is reached the signalling molecules will diffuse across the membrane of another, adjacent, bacterial cell and interact with their cognate receptor protein. This interaction causes a conformational change in the receptor structure allowing it to act as a transcriptional promoter, thus, inducing the expression of a group of target genes. These target genes encode a wide range of products including molecules such as endotoxins and enzymes and polymers (Lee and Zhang, 2014). While QS often upregulates the expression of virulence genes it can also down regulate the expression of some genes. Genes which are downregulated in response to QS include surface antigens such as OprH so that a cell may avoid detection by a host's immune system (Arevalo-Ferro *et al.*, 2003).

1.2 The quorum sensing systems of *Pseudomonas aeruginosa*

P. aeruginosa is perhaps the most well characterised QS bacterial species and, indeed, it is often used as a model organism in which gram-negative QS can be studied. The process of QS in *P. aeruginosa* is highly complex with several QS systems working in tandem, positively or negatively regulating the others. *P. aeruginosa* has 3 known QS systems; the Las system, the Rhl system and the PQS system. A fourth system, known as the IQS system, has been proposed but, to date, remains poorly understood

(Lee *et al.*, 2013). Each of these systems has a cognate autoinducer which controls it. Each of these four systems and their autoinducers are discussed here.

1.2.1 Acyl-homoserine lactones

AHLs are the primary QS signalling molecules used by gram-negative bacteria (Papenfort and Bassler, 2016). These AHLs have a common base structure that consists of a lactone ring and an acyl side chain (Figure 1.1).

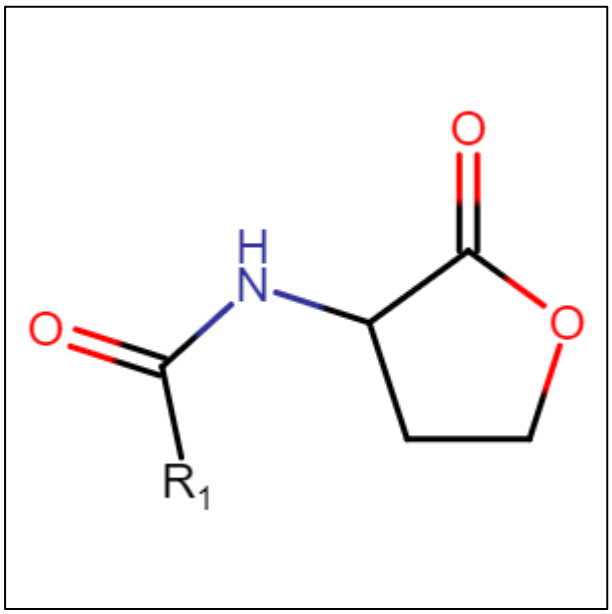

Figure 1.1 – General structure of AHL molecules.

The lactone ring remains constant across all AHL molecules while the acyl chain can vary in both length and presence of side groups.

It is variations in the length of this side chain and the various side groups that makes the AHLs produced by different organisms so distinct. For example, if an AHL has a twelve-carbon chain at R1 it would be oxo dodecanoyl homoserine lactone, the AHL used in the Las QS system of *P. aeruginosa*. However, if the R1 group is a cinnamoyl

moiety then AHL will be cinnamoyl homoserine lactone, an AHL used by *Bradyrhizobium spp*. (Ahlgren *et al.*, 2011).

1.2.2 The Las quorum sensing system

The Las system was the first QS system to be characterised within *P. aeruginosa* and remains the most well-studied system to date. The Las QS system is responsible for the production of many virulence factors including the LasA, LasB, and Apr protease enzymes (Gambello and Iglewski, 1991; Toder, Gambello and Iglewski, 1991; Gambello, Kaye and Iglewski, 1993). While the Las QS system is only one of four QS systems used by *P. aeruginosa* it is typically thought of as being at the top of the QS hierarchy, mainly because the activation of the Las system causes a subsequent activation of both the Rhl system and the PQS system.

The Las system makes use of the AHL N-(3-oxododecanoyl)-L-homoserine lactone (OdDHL) (Figure 1.2).

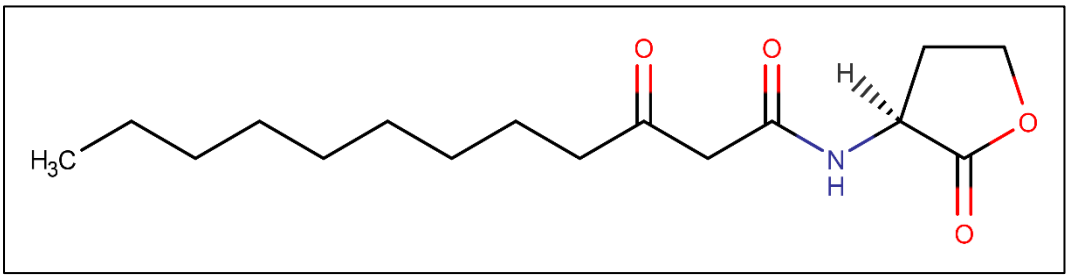

Figure 1.2 – Chemical structure of autoinducer N-(3oxododecanoyl)-L-homoserine lactone (OdDHL).

This autoinducer, like all AHLs consists of a lactone ring with a 12-carbon acyl chain.

Prior to its isolation and characterisation, it was known that that OdDHL (then known as Pseudomonas autoinducer or PAI) had a high structural homology to the autoinducer responsible for the regulation of luminescence in the bacterium *Vibrio fischeri* and, indeed, it was believed that *P. aeruginosa* may in fact also be using VAI as an autoinducer (Jones *et al.*, 1993). However, in 1994, Pearson *et al.* showed that PAI was structurally distinct from its *V. fischeri* counterpart. While VAI was known to be N-(3-oxohexanoyl) homoserine lactone, PAI was found to be the structurally similar N-(3-oxododecanoyl) homoserine lactone.

In the Las QS system, OdDHL is constitutively expressed at low levels by the bacteria and is actively transported out of the cell via the MexAB-OprM efflux system (Pearson, Van Delden and Iglewski, 1999). This active efflux causes OdDHL to accumulate in the extracellular environment and when a critical threshold has been reached, OdDHL enters the cell and associates with its cognate receptor which is known as LasR. Upon complexing with OdDHL the LasR undergoes a conformational change. It has been suggested that the binding of OdDHL causes a LasR to dimerise, resulting in a conformational change in the LasR protein (Kiratisin, Tucker and Passador, 2002; Schuster, Urbanowski and Greenberg, 2004). This dimeristion and conformational change means that LasR can adopt a biologically active form (Sappington *et al.*, 2011). This active LasR-OdDHL complex then binds to the target genes and activates their transcription. The Las system controls the transcription of numerous genes including the virulence factors LasA protease and LasB elastase. In addition to increasing transcription of several virulence factors the LasR/OdDHL complex also positively regulates the transcription of the AHL synthase gene, *LasI*.

The upregulation of this AHL synthase gene causes a greater production of OdDHL (Seed, Passador and Iglewski, 1995). This results in the first positive feedback QS loop (Figure 1.3).

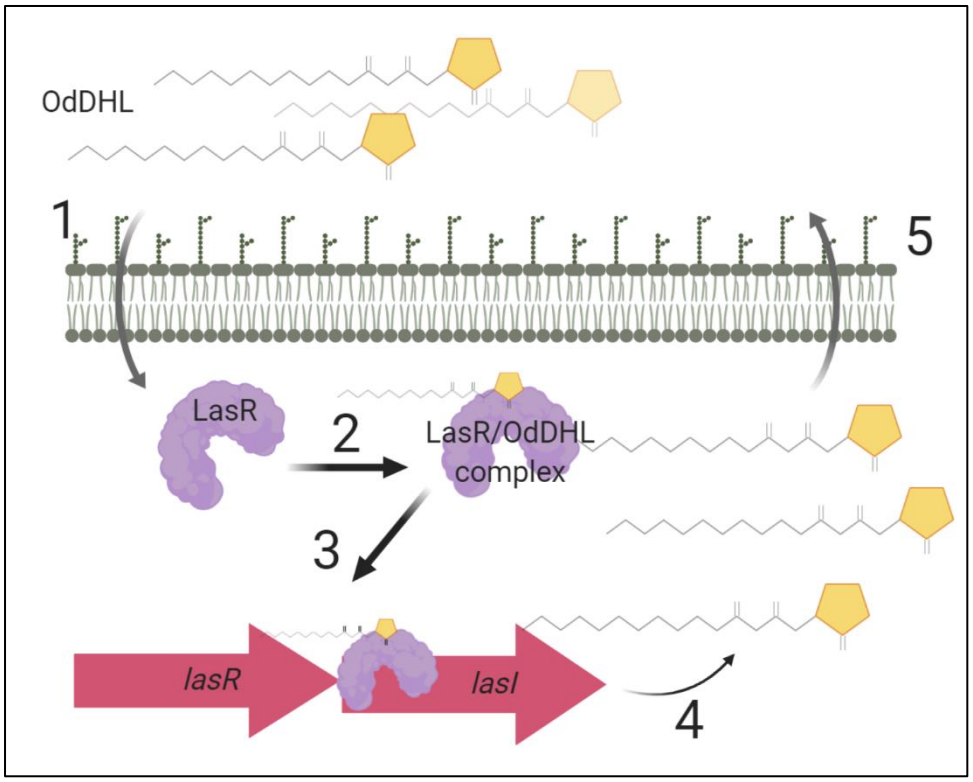

Figure 1.3 – The Las quorum sensing system of *P. aeruginosa*.

(1) OdDHL accumulates in the extracellular environment and when a critical threshold concentration is reached it diffuses into the bacterial cell. (2) OdDHL complexes with the receptor protein LasR causing a conformational change resulting in the active LasR/OdDHL comples. (3) The active LasR OdDHL complex bind to a set of target genes initiating their transcription. (4) One of the induced genes is lasI which encodes for the production of an AHL synthase which results in increased production of OdDHL. (5) The produced OdDHL is actively effluxed from the cell and begins to accumulate in the extracellular environment.

As well as the production of virulence factors and additional OdDHL, activation of the Las system leads to the transcription of both *rhlR* (which encodes for the RhlR, the

receptor protein of the Rhl QS system) and *PqsR* (which encodes for the PqsR receptor protein for the PQS QS system). As stated previously, due to the activation of these other QS systems, the Las QS system is considered the most important QS system used by *P. aeruginosa*.

1.2.3 The Rhl quorum sensing system

The Rhl QS system is the second QS system of *P. aeruginosa* and main constituents are the Acyl-homoserine lactone synthase, RhlI and the receptor RhlR. The product of RhlI synthase is an AHL known as N-butyryl homoserine lactone (BHL). BHL is the autoinducer responsible for the activation of the Rhl quorum sensing system (Winson *et al,* 1995) and has a similar mode of action to OdDHL. Binding of BHL to the RhlR protein causes RhlR to become active. This activation is again suggested occur via dimerization of the receptor protein (Ventre *et al.*, 2003). The RhlR dimer then binds to the promoter region of its associated regulon initiating transcription. This QS system governs the transcription of a distinct set of virulence associated genes such as those involved in rhamnolipid, pyocyanin, and hydrogen cyanide production (Pearson, Pesci and Iglewski, 1997; Pessi and Haas, 2000)

BHL also shares structural homology with both VAI and OdDHL differing only in the length of its acyl chain (Figure 1.4).

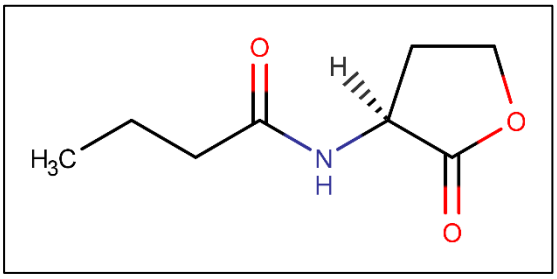

Figure 1.4- Chemical structure of N-butyryl-homoserine lactone.

This AHL has the characteristic structure of an AHL, consisting of a lactone ring and a 4 carbon acyl chain.

As is the case with the Las quorum sensing system, the Rhl QS system is not wholly independent. While BHL is constitutively expressed at low levels and subject to a positive feedback loop when RhlR is active, the presence of the LasR-OdDHL complex activates the expression of both the *rhlR* and *rhlI* genes (Papenfort and Bassler, 2016) (Figure 1.5).

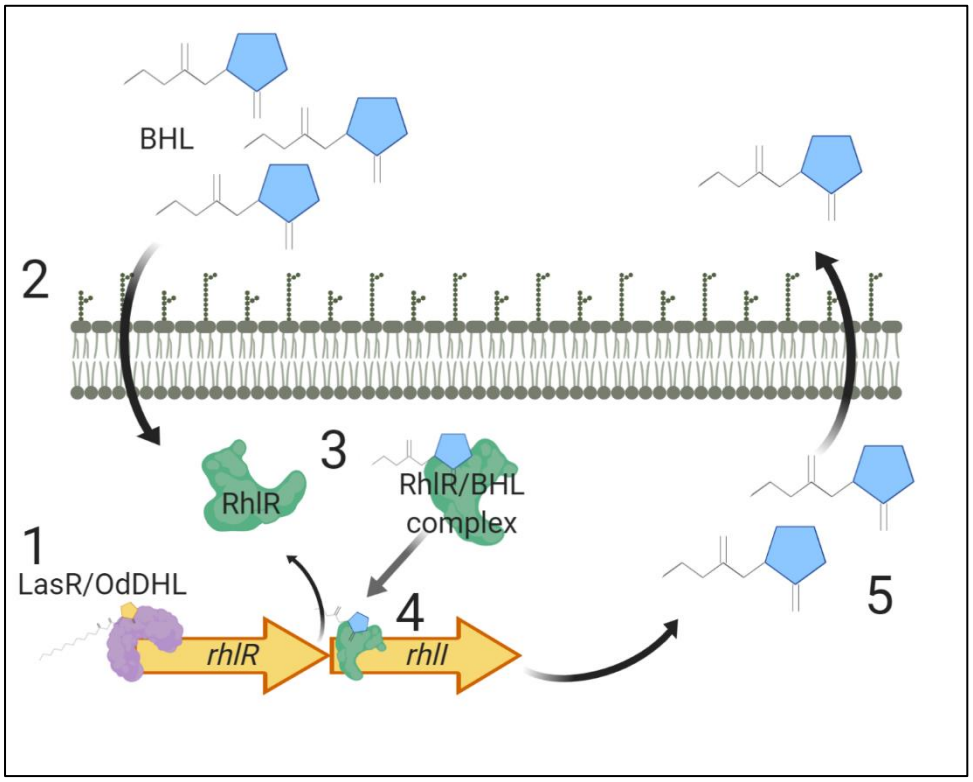

Figure 1.5 – The Rhl quorum sensing system of *P. aeruginosa*.

(1) LasR/OdDHL complex initiates the transcription of the rhlR gene encoding for the RhlR receptor protein. (2) BHL in the extracellular environment enters the cell. (3) BHL complexes with the receptor protein RhlR and causes a conformation change. (4) The RhlR/BHL complex initiates the transcription of target genes including the AHL synthase encoding gene rhlI. (5) BHL is produced and it exits the cell and begins to accumulate in the extracellular environment.

The RhlR-BHL complex has been shown to be capable of inhibiting the expression of the *pqsR* gene and the *pqsABCDE* operon. The inhibition of these genes results in a decrease in the autoinducer of the PQS system (Wade *et al.*, 2005). Interestingly, the PqsR receptor protein, when in complex with PQS, can induce the expression of both RhlR and RhlI. This may suggest that this RhlR-BHL dependant negative regulation

of the PQS QS system allows for fine control of the genes under both the Rhl and PQS systems as well as maintaining an optimal balance between autoinducers.

1.2.4 The PQS quorum sensing system

The PQS quorum sensing system is the third system used by *P. aeruginosa*. The autoinducer of this system is 2-heptyl-3-hydroxy-4-quinolone, also known as the Pseudomonas quinolone signal or PQS. Although PQS is an autoinducer, it is not part of the homoserine lactone family and does not share any structural homology with OdDHL or BHL (Figure 1.6).

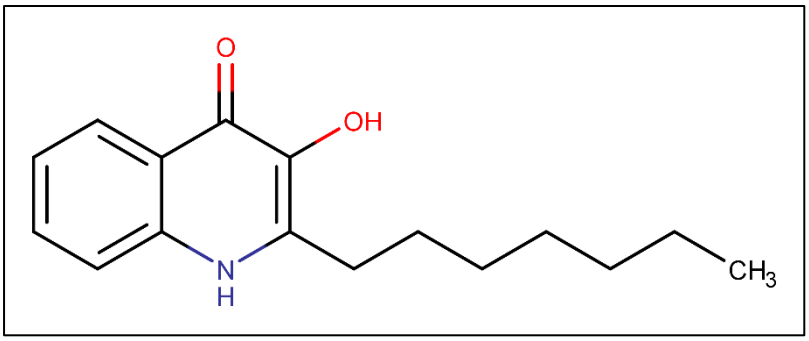

Figure 1.6 – Chemical structure of 2-heptyl-3-hydroxy-4-quinolone also known as the Pseudomonas quinolone signal (PQS).

This autoinducer is not part of the AHL family of signalling molecule and, thus, does not share a structural homology with OdDHL or BHL

PQS is a product of a biosynthetic pathway initiated by an anthranilate-coenzyme A ligase, the transcriptional product of *pqsA.* This biosynthetic pathway is completed by the enzyme PqsH, which converts a PQS precursor into the active PQS molecule. As noted above, the PQS system is influenced by other quorum sensing systems. The transcription of the *pqsH* gene is positively controlled by LasR and the production of

the transcriptional activator PqsR is controlled by the LasR/OdDhl complex. Not only this, but the production of the transcriptional activator PqsR is negatively regulated by RhlR-BHL (Wade *et al.*, 2005) (Figure 1.7).

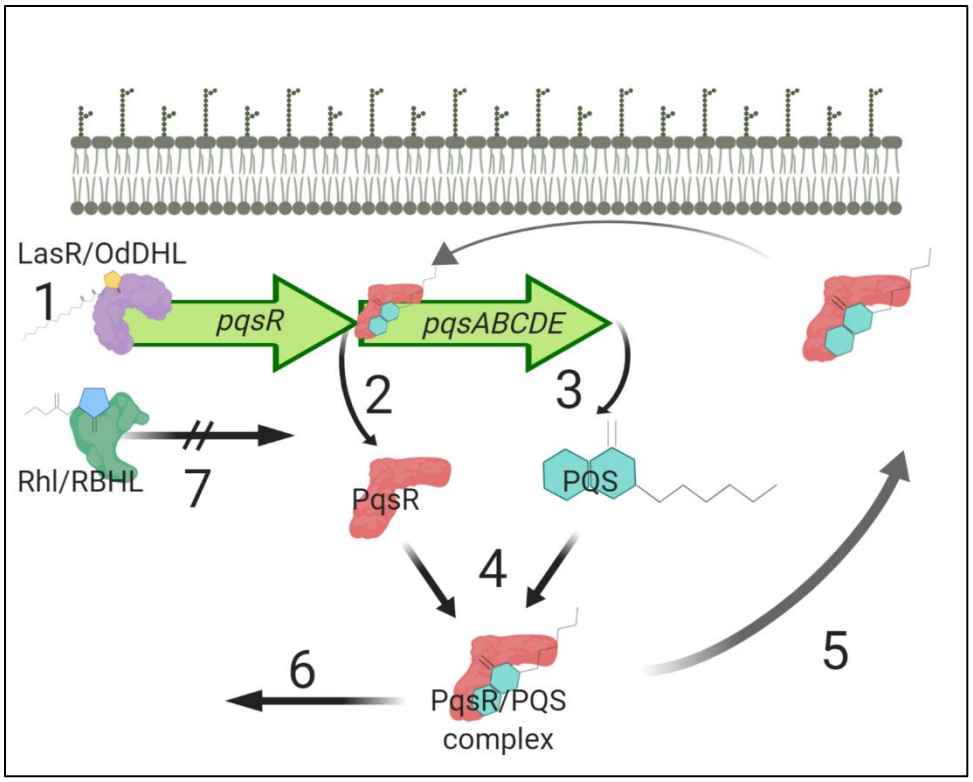

Figure 1.7 – The PQS quorum sensing system of *P. aeruginosa.*

(1-3) The transcription of pqsR and the pqsABCDE operon is positively regulated by the LasR/OdDHL complex resulting in the production of the PqsR receptor protein and the PQS autoinducer. (4) PqsR and PQS form a complex. (5) The PqsR/PQS complex then positively regulated the transcription of the pqsABCDE operon, thus, resulting in a positive feedback loop. (6) PqsR/PQS complex positively regulates the transcription of RhlI. (7) The RhlR/BHL complex negatively regulates the transcription of pqsR.

1.2.5 Integrated quorums sensing system

The integrated quorum sensing system (IQS) is a recently proposed *P. aeruginosa* communication pathway. The proposed IQS autoinducer has been identified as 2-(2-

hydroxyphenyl)-thiazole-carbaldehyde. As it is neither a quinolone or homoserine lactone it is structurally distinct from OdDHL, BHL and PQS (Lee *et al.*, 2013) (Figure 1.8).

Currently, the IQS quorum sensing system is not as well studied as other systems, however, in their seminal study on IQS, Lee *et al.* (2013) show that the IQS autoinducer may be important for the production of both the PQS and BHL signalling molecules.

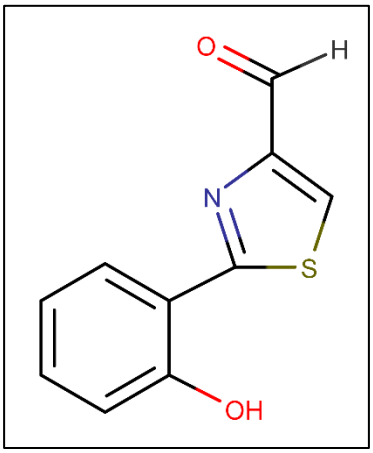

Figure 1.8 – Chemical structure of 2-(2-hydroxyphenyl)-thiazole-carbaldehyde.

This compound is the identified autoinducer for the proposed IQS quorum sensing system of P. aeruginosa.

The different QS systems and cognate autoinducers used by *P. aeruginosa* allow tighter control of the various virulence factors and phenotypes displayed during an infection. The interrelated nature of the three systems also facilitates an element of compensation if one system is not fully operational at any time. This is an important consideration when investigating QS inhibitors or antagonists against these

autoinducers. While it is likely that the elimination of one branch of the quorum sensing system will attenuate the organism's virulence, it may not remove virulence entirely as each of the systems play a unique role in pathogenicity and virulence.

1.3 The role of quorum sensing in *Pseudomonas aeruginosa*

QS has been shown to have a wide range of functions in *P. aeruginosa*. These functions are either vital for the organism's survival or provide a distinct advantage for the organism when infecting a host. These functions include the production of virulence factors, coordination of complex behaviours such as biofilm formation, and some types of cell motility.

1.3.1 Virulence factor production

Each of the QS systems described above control the production of a distinct set of secreted virulence factors which greatly increase the ability of *P. aeruginosa* to colonise and infect a host organism. The Las QS system controls the production of several important virulence factors including the degradative enzymes LasA protease, LasB elastase and Apr alkaline protease as well as other virulence factors such as exotoxin A (Gambello and Iglewski, 1991; Toder, Gambello and Iglewski, 1991; Gambello, Kaye and Iglewski, 1993). Similarly, the Rhl system is responsible for regulating the production of virulence factors, such as hydrogen cyanide and pyocyanin. It should also be noted that, similar to the activation of the QS systems there is a certain amount of overlap between the systems responsible for production of some virulence factors. It has been shown that the production of hydrogen cyanide, for example, can be stimulated by the action of both LasR-OdDHL and RhlR-BHL complexes (Pessi and Haas, 2000). The virulence factors employed by *P. aeruginosa*

are numerous and for a full review of *P. aeruginosa* virulence factors the reader is referred to Strateva and Mitov. (2011).

1.3.2 Biofilm formation

In addition to its role in secreted virulence factor production, QS is an integral part of biofilm formation, the process by which planktonic cells form organised communities encased in a polymeric substance often attached to a surface (Rasamiravaka *et al.*, 2015). Briefly, planktonic bacteria will attach to a surface (either biotic or abiotic in nature) first reversibly, then irreversibly. This first reversible attachment results in changes in the expression of multiple genes involved in the biofilm formation process, such as those involved in the production of the polymeric matrix which provides the biofilm structure. Bacterial cells then begin to aggregate and form microcolonies, encased in the extracellular polymeric substance. These polymers are continually produced and gradually accumulate while bacterial cells divide, providing much of the three-dimensional structure of the biofilm. Finally, once the biofilm has matured it can disperse, thus, returning some of its cells to the planktonic phase. These newly planktonic cells relocate and seed new biofilms, thus, beginning the process again (Figure 1.9). This dispersal may be brought about through the mature biofilm experiencing a damaging mechanical force or it may be triggered by environmental cues such as an abundance of nutrients (Kostakioti, Hadjifrangiskou and Hultgren, 2013).

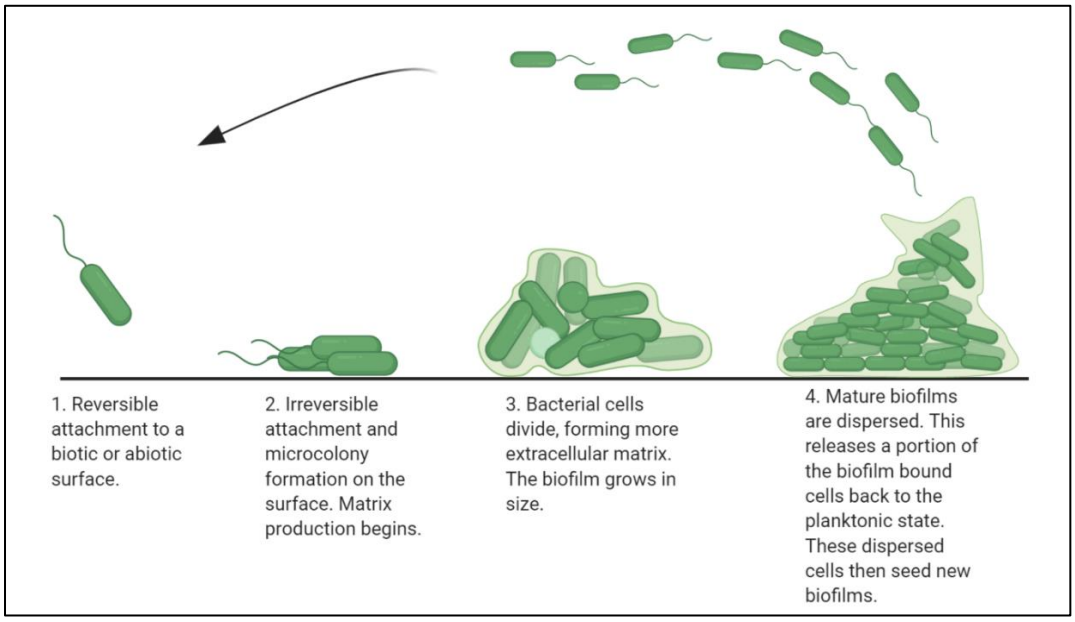

Figure 1.9 – The process of biofilm formation and dispersal.

Planktonic cells attach to a surface first reversibly then irreversibly. Cells begin to aggregate and form microcolonies on the surface. Cells then continue to divide and produce extracellular polymer further developing the three-dimensional structure of the biofilm. Mature biofilms then disperse retuning some of their cells back to the planktonic state. These planktonic cells then seed new biofilms.

The role of QS in biofilm formation has been debated for some time with many papers reporting contradictory findings. Despite this, QS has been implicated in almost all stages of biofilm development in *P. aeruginosa.* Although there is no evidence to suggest that quorum sensing plays a role in the initial attachment of *P. aeruginosa* to a surface, it has been shown that the Las and Rhl controlled process of twitching motility is required for the formation of microcolonies during the early stages of biofilm formation (O'Toole and Kolter, 1998). This work showed that the ability of *P. aeruginosa* to form a biofilm on an abiotic surface was significantly compromised when a mutation was present in the *pilBCD* genes. These pili biogenesis mutants were seen to grow and produce a monolayer on the surface as expected but did not form the

microcolonies which are characteristic of the early stages of biofilm formation. In addition, O'Toole and Kolter (1998) also showed that strains of *P. aeruginosa* defective in flagellum production were unable to effectively form a monolayer. While this data indicates that both pili mediated, and flagellar motility are vital for the formation of a biofilm Glessner *et al.* (1999) demonstrated that only the pili mediated twitching motility was dependent upon the Las and Rhl QS system. They showed that Δ*lasI* or Δ*rhlI P. aeruginosa* mutants exhibited highly diminished twitching motility. Furthermore, mutants deficient in both genes displayed no detectable twitching motility. Subsequently, motility was partially restored through the exogenous addition of each corresponding autoinducer (Glessner *et al.*, 1999). Importantly, these findings were later repeated with clinical isolates of *P. aeruginosa*, showing a significant positive correlation between twitching motility and the ability to form a biofilm (Otton *et al.*, 2017). This correlation was seen in a range of clinical strains including faecal, lung, urine and wound isolates. The knowledge that the ability of a strain to form a biofilm is related to its capacity for twitching motility is important. It clearly shows that QS is involved in the process of biofilm formation from the very early stages and may, in fact, be vital for the formation of the microcolonies which form the foundation on which the mature biofilm (Figure 1.10) is formed.

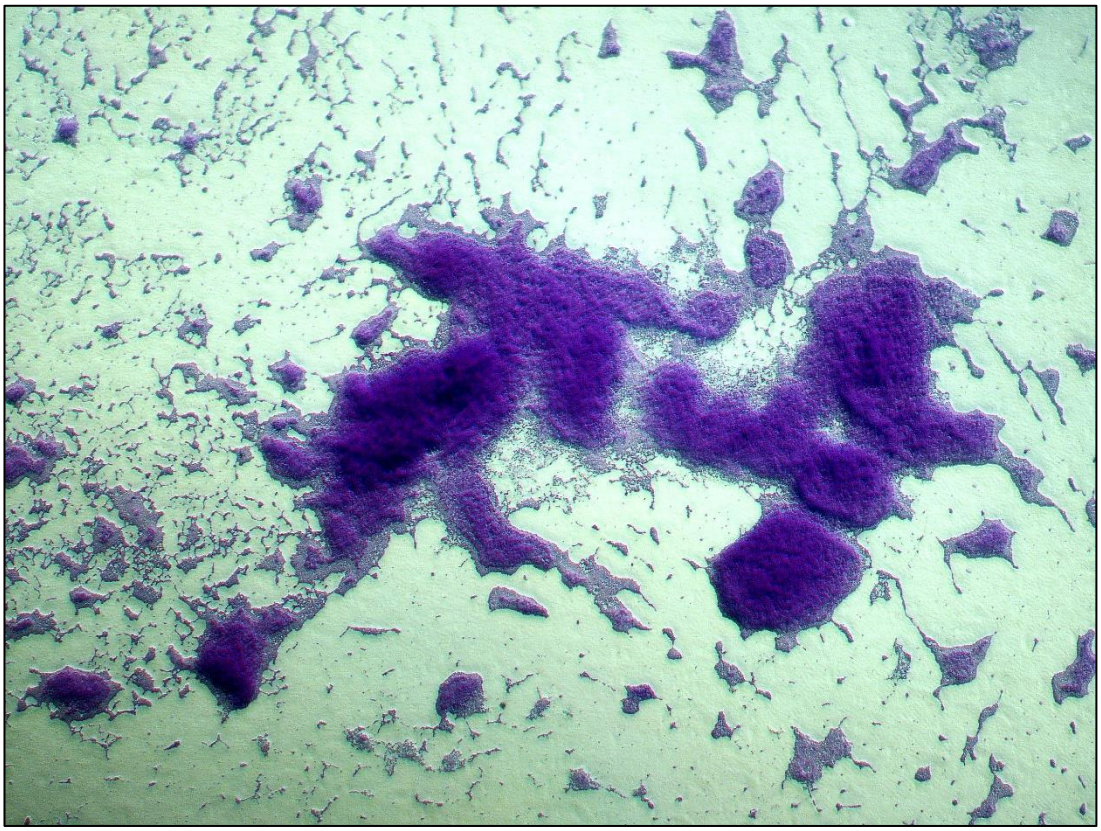

Figure 1.10 – Light micrograph of a mature *P. aeruginosa* DSM50071 biofilm grown on polycarbonate.

The sample was grown for 24 h and stained with crystal violet prior to visualisation. Image taken as 20x magnification using a Nikon ECLIPSE E400 microscope.

As well as having a role in microcolony formation through the regulation of twitching motility, QS has also been shown to be involved in the process of biofilm maturation and the formation of its three-dimensional structure. An early study by Davies *et al.* (1998) showed that *lasI* and *rhlI* deficient mutants of *P. aeruginosa* were significantly less able to form thick biofilms with a three-dimensional structure. Interestingly, single *lasI* mutants showed the same diminished biofilm thickness while single *rhlI* mutants showed no deficit (Davies *et al.*, 1998). Biofilms formed by the *lasI* mutants

appeared to have similar numbers of bacterial cells as the wild type, but the biofilms had approximately 75% less vertical height above the substratum. As with the twitching motility mutants, normal biofilm formation was restored in the *lasI* mutant following the addition of exogenous autoinducer. In addition to this, the authors tested the susceptibility of the abnormal biofilms to treatment with a chemical detergent. They found that the mutant biofilms were significantly more susceptible to sodium dodecyl sulfate treatment when compared to wild type biofilms and completely detached and dispersed after exposure. The results presented by Davies *et al.* (1998) demonstrate that not only is the Las QS system involved in the development of a biofilms vertical structure, but also plays a role in providing protection against detergents. However, it may be the case that the reduced thickness of the biofilm simply allowed for deeper penetration of the detergent rather that the mutant strains lacking a specific defence mechanism against it. It was later shown by Allesen-Holm *et al.* (2006) that, in addition to having a diminished biofilm thickness, *las* and *rhl* deficient mutants were significantly less capable of producing extracellular DNA (eDNA), an important structural component of biofilms (Allesen-Holm *et al.*, 2006). This study also showed that eDNA is localised primarily on the substratum and surface of early microcolonies, and later, in the stalks of the mushroom shaped portions of mature biofilms. Importantly, it is believed that these mushroom shaped formations are heavily involved in the maintenance of the biofilm, providing a route for nutrients to the deeper sub-populations and an efficient method of waste removal (Tolker-Nielsen, 2014). The reduced eDNA production reported by Allesen-Holm *et al.* (2006) may indicate that QS plays a regulatory role in the formation of these structures and, thus, has a role in biofilm maintenance systems. Both Davies *et al.* (1998) and Allesen-

Holm *et al.* (2006) suggest that QS is an important part of both the construction and maintenance of *P. aeruginosa* biofilms. This is important as it may mean that disruption of quorum sensing systems could effectively weaken biofilms making treating and eradicating them easier.

QS has been shown to play a key role in the dispersal of a mature biofilm and the subsequent spread of new biofilms. Originally, it was shown that the Las QS sensing system was responsible for positively regulating the transcription of a primary *P. aeruginosa* exopolysaccharide known as PEL. This was demonstrated through the use of *lasI/rhlI* mutants which showed a significant drop in *pel* transcription which could subsequently be restored through the addition of exogenous autoinducer (Sakuragi and Kolter, 2007). However, a later study claimed that QS may instead negatively regulate the formation of biofilms (Ueda and Wood, 2009). The authors of this study showed that the deletion of a gene known as *tpbA*, encoding for a tyrosine phosphate, resulted in an increased production of the PEL exopolysaccharide. It was also seen that the Las QS system appears to, at least partially, be responsible for the activation of *tpbA.* Interestingly, this would mean that the Las QS system negatively regulates the production of PEL and, therefore, may aid in the dispersal of cells back into a planktonic state.

Another class of molecule that has been shown to be important to the maintenance and dispersal of mature biofilms are the rhamnolipids. It was shown that these rhamnolipids, which are primarily produced in the mushroom like structures within the biofilm were vital for the maintenance of the biofilms three-dimensional structure. Without them, the channels required for nutrient and waste transport were not

effectively maintained (Davey, Caiazza and O'Toole, 2003; Lequette and Greenberg, 2005). As well as being required for biofilm maintenance Boles *et al.* (2005) showed that over expression of rhamnolipids was responsible for increased biofilm detachment and dispersal in a hyper-detaching variant of *P. aeruginosa* (Boles, Thoendel and Singh, 2005). Additionally, it was found that addition of exogenous rhamnolipid to wild type *P. aeruginosa* could bring about biofilm detachment. These findings indicate that rhamnolipid production, which is controlled by QS, is an important mechanism by which biofilms detach from a surface, disperse and subsequently seed new biofilms.

If QS is indeed involved in the maintenance and dispersal of mature biofilms as suggested by the above studies, inhibition of the QS system may be of significant clinical interest. If the maintenance of mature biofilms can be disrupted then they may be less likely to thrive and, perhaps, become simpler to treat. Similarly, if the dispersal of biofilms, and hence one of the main modes of persistence, is lessened, the duration and severity of infection may also be reduced.

1.4 The role of biofilms in human disease

Biofilms are known to be involved in a wide range of diseases in humans such as cystic fibrosis, conjunctivitis, endocarditis and persistent urinary tract infections. Indeed, in a public announcement in 2002 the National *i*nstitutes of Health stated that biofilms may account for up to 80% of all microbial infections in the body (National Institutes of Health, 2002).

While biofilms in conditions such as cystic fibrosis and endocarditis are well investigated areas of research and studies into novel treatments for these conditions are numerous, the treatment of biofilms in chronic wounds is severely under examined.

1.5 Biofilms and chronic wounds

It has been shown that almost 80% of chronic wounds have a bacterial biofilm present (Malone *et al.,* 2017). These wound biofilms can be caused by a wide range of organisms and are often polymicrobial in nature. *P. aeruginosa* is one of the most common causative organisms in wound infections. *P. aeruginosa* readily forms biofilms in a wound environment and, during such infections, it grows almost exclusively in this form (Brandenburg *et al.*, 2015; Neopane *et al.*, 2018).

When present in a wound, biofilms cause a prolonged inflammatory state which, in turn, delays the healing process. The presence of biofilms in a wound leads to inappropriately high numbers of neutrophils in the wound environment which then release continually large amounts of proinflammatory cytokines such as Interleukin-6 and tissue necrosis factor alpha (Fazli *et al.*, 2011). Due to the highly persistent nature of the biofilm this inflammatory state is maintained long-term and results in a significant delay of normal wound healing. This results in a wound which is unable to heal normally.

1.5.1 Biofilm development in wounds

There are numerous routes of infection for open wounds including foreign bodies such as dirt or gravel becoming embedded in the wound, infection introduced from the source of the wound such as animal and insect bites, and even infection from the

patient's own microbiome (including faecal bacteria and skin isolates) (Rothe, Tsokos and Handrick, 2015; Hirashima *et al.*, 2019). Following the introduction of bacteria to a wound, biofilms can begin to form very rapidly.

In 1996, Akiyama *et al.*, using a murine wound model, showed that just 6 hours after inoculation with *S. aureus,* small characteristic clusters of cells (micro colonies characteristic of a biofilm) had already begun to appear in a wound (Akiyama *et al.*, 1996). This was later shown also to be the case for *P. aeruginosa* when tested *in vitro*. Here, the authors showed that some characteristic traits of a biofilm (specifically exopolysaccharide production) was detectable within just 5 hours of inoculation (Harrison-Balestra *et al.*, 2003; Metcalf, Bowler and Parsons, 2016).

The rapid formation of a biofilm in a wound environment is highly problematic as it provides only a short time frame in which a wound must be disinfected. If effective disinfection is not achieved, the formation of a biofilm by the infecting organism may result in the prolonged inflammatory state that may result in a non-healing wound.

1.5.2 The role of biofilm in chronic wound development

Normal wound healing requires the seamless transition between several distinct physiological stages. First, during the haemostasis phase, blood vessels constrict, and a fibrinous blood clot is formed in order to prevent further bleeding (Zaidi and Green, 2019). This is followed by the inflammatory stage of wound healing. During this stage immune cells are drawn to the site of the wound and here they act as a primary defence against infection by phagocytosing any invading organisms. Other types of immune cells such as macrophages are also recruited to help prevent infection. A wide range

of other immune cells including dendritic cells and T-cells are also involved in this complex stage. After the inflammatory stage the proliferative phase begins. This stage involves the formation of new blood vessels at the injury site through a process known as angiogenesis. This is accompanied by the production of new connective tissues by dermal fibroblasts. This is followed by reepithelialisation in which new epithelial cells begin to form to replace the protective layer of skin which maintains barrier function (Rodrigues *et al.*, 2019). When these stages progress as described an acute wound will heal fully. However, many factors can interrupt the wound healing process causing failure to heal and a chronic wound will be formed.

The most common cause of failure to heal in wounds is bacterial infection (Leaper, Assadian and Edmiston, 2015) and it has been shown that the wound healing time of chronic wounds such as venous leg ulcers increases with each additional organism isolated from the wound (Kruszewska, Wesolowska-Gorniak and Czarkowska-Paczek, 2020). As previously stated, when bacteria are present in a wound they will grow primarily as a biofilm. This affords the bacteria high levels of protection against host immune defences such as opsonisation and subsequent phagocytosis (Pier *et al.*, 2001). Biofilms provoke an inflammatory response, but they cannot be cleared by the immune system. This means that a persistent inflammatory state is maintained within the wound. As the inflammatory stage of wound healing is not resolved the wound cannot progress to the proliferative phase and a chronic wound results (Schultz *et al.*, 2017). Due to the inherent resilience of biofilms, chronically infected wounds may persist for many months and in some cases will never heal. A simplified schematic of

the role of bacterial biofilm formation in the development of a chronic wound is shown in figure 1.11

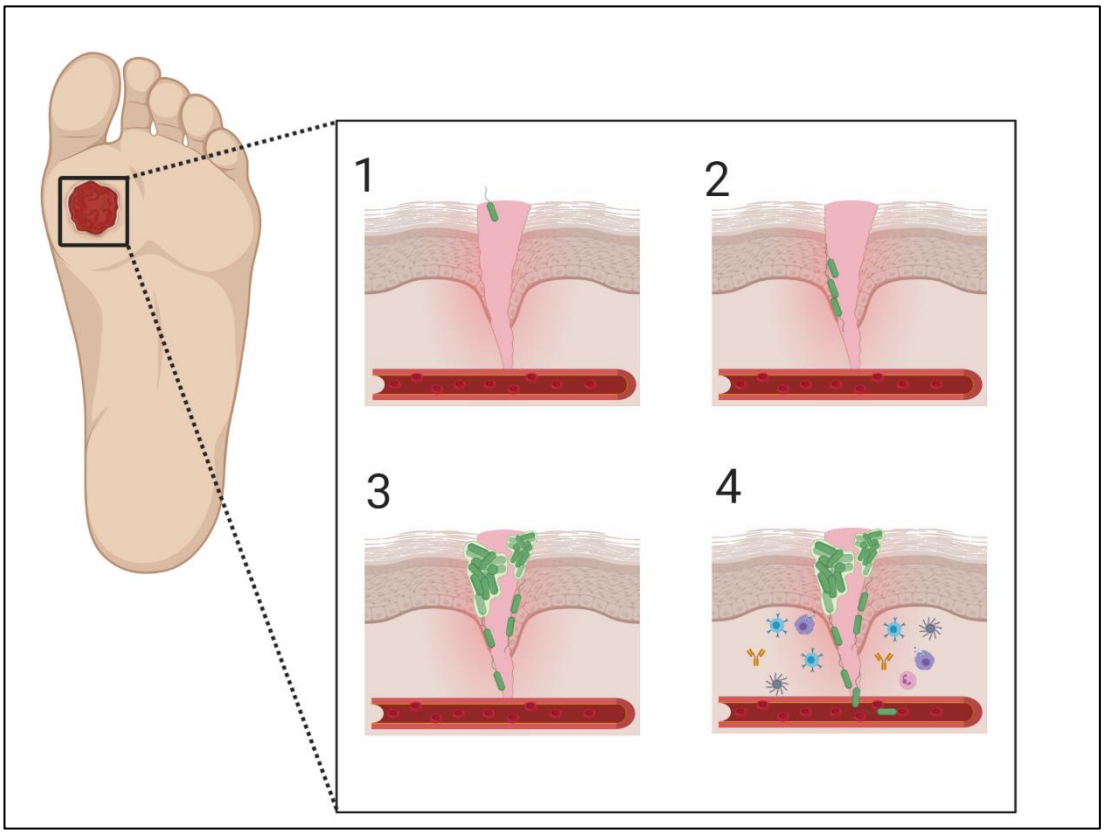

Figure 1.11 – The role of biofilms in the formation of a chronic wound.

(1) Bacteria are introduced to a wound either from the environment or the patient's own microbiome. (2) Within 6 h bacteria have proliferated and the early stages of a biofilm are formed. (3) Bacteria being to proliferate, and biofilms mature. (4) The inflammatory state is maintained in the wound environment. Many immune calls are continually present at the wound site. Biofilms continue to grow, and bacteria may penetrate deeper tissues or even the blood stream causing potentially fatal bacteraemia.

It is clear that bacterial biofilms are a significant problem in wounds. However, their treatment is often difficult, and many biofilms cannot be eradicated using traditional antimicrobials. Novel approaches are, therefore, needed. One approach which may

provide a means of treating these biofilms involves interfering with or inhibiting the QS communication systems that the bacteria use to coordinate the formation and maintenance of these biofilms.

1.6 Quorum sensing inhibitors

It has been known for some time that the virulence and pathogenicity of many bacteria can be attenuated through the inhibition of their QS systems. Early studies such as the work of Passador *et al.* (1996) showed that the cognate autoinducers in QS bacteria experienced competition when binding to their corresponding receptor if structural homologues of the autoinducer were introduced (Passador *et al.*, 1996). A study by McClean *et al.* (1997) showed that the production of the purple pigment violacein by *Chromobacterium violaceum* could be inhibited by the addition of homoserine lactones which were structurally similar to the *C. violaceum* cognate autoinducer, N-hexanoyl-L-homoserine lactone, but differed in the length on their acyl side chain (McClean *et al.*, 1997). While QS inhibition was possible through the use of other bacterial AHLs, Givskov *et al.* (1996) also showed that a species of marine algae, *Delisea pulchra*, produced a set of secondary metabolites called furanones which were capable of interfering with AHL mediated processes such as swarming motility in *Serratia liquefaciens* (Givskov *et al.*, 1996). These findings were important as they clearly showed that QS could be inhibited by molecules from natural sources and did not necessarily have to be other homoserine lactones. This realisation then prompted further research into other potential quorum sending inhibitors (QSIs) and an increase in research focused on discovering and characterising both furanone and non-furanone QSIs.

1.6.1 Non-furanone quorum sensing inhibitors

In recent years, a number of non-furanone compounds have been shown to have anti-quorum sensing, anti-biofilm or virulence attenuation capabilities. These compounds have ranged from enzymes which degrade the autoinducer molecules to currently used medicines such as aspirin (Lin *et al.*, 2003; El-Mowafy *et al.*, 2014).

1.6.1.1 Microorganism derived QSIs

In an early study, AHL acylase, a bacterially produced enzyme which actively degrades AHLs by separating the acyl chain from the lactone ring (LaSarre and Federle, 2013), was shown to be effective in reducing the levels of active autoinducer in the extracellular environment. It was also shown to effectively reducing swarming motility in *P. aeruginosa* (Lin *et al.*, 2003). Following the work of Lin *et al.* several studies aimed to characterise AHL acylases from different sources or to better understand the enzymes role in various biological processes (Sio *et al.*, 2006; Bokhove *et al.*, 2010; Kusada *et al.*, 2017). However, despite showing promise in *in vitro* work these acylase enzymes have not been extensively studied *in vivo*.

In addition to AHL degrading enzymes, it has been shown that other compounds produced by a range of microorganisms can be effective when used to disrupt QS. For example, one research group showed that several compounds isolated from the fungal genus *Penicillium* may have QSI properties (Rasmussen *et al.*, 2005). This study demonstrated how two compounds, penicillic acid and patulin, were able to effectively disrupt the transcription of quorum sensing controlled genes in *P. aeruginosa* indicating QSI effects. Additionally, patulin was shown to significantly decrease levels of the quorum sensing receptor protein detected in culture samples as well as

increasing *P. aeruginosa* biofilm sensitivity to treatment with the antibiotic tobramycin. Importantly, these effects were seen when patulin was added in concentration considerably below the lethal dose, significantly decreasing the possibility of introducing selection pressures and, therefore, resistance to the compound. In addition to this a 7-day course of intravenous patulin at 2.5 $\mu g\ g^{-1}$ was also shown to be effective in increasing the rate at which *P. aeruginosa* infection was cleared from the lungs in a murine respiratory infection model. While the difference in mortality between patulin and placebo treated mice was not significant, a clear trend was seen.

1.6.1.2 Plant-derived QSIs

Another common source of novel QSIs is plants, plant extracts and oils (from both marine and terrestrial plants). Several studies have characterised compounds with QSI activity from such sources. In 2006, it was shown that a crude extract of vanilla was capable of inhibiting the production of violacein by *C. violaceum* (Choo, Rukayadi and Hwang, 2006). The authors showed that the presence of 10 $\mu mol\ l^{-1}$ of exogenous autoinducer in cultures of *C. violaceum* resulted in significant production of the pigment. The addition of between 0.25% and 2.00% w/v of crude vanilla extract showed a dose dependent reduction in violacein up to an almost 100% reduction showing that the vanilla extract could effectively inhibit quorum sensing. Similarly, a 2009 study showed that a number of plant essential oils, including lavender, clove and peppermint, had anti-quorum sensing properties. The authors demonstrate that clove oil in particular was able to inhibit the production of QS controlled molecules in a dose dependent manner. This was also shown through the inhibition of violacein production

(Khan *et al.*, 2009). However, such studies often have the same fundamental limitation. Essential oils and plant extracts are typically a complex mix of a large number of compounds. While these two studies have shown that the various plant extracts do indeed have QSI activity the authors have not identified the active component. Kahn *et al.* (2009) were able to show that the main component of clove oil, Eugenol, was not responsible for its QSI activity but no further analysis was performed. This lack of identification of active compounds limits the applicability of these studies, and the potential for their findings to be translated into *in vivo* work and subsequently into clinical practice is significantly reduced.

One plant-derived QSI which has been relatively well characterised is cinnamaldehyde. This organic compound has been shown to significantly reduce AHL-mediated fluorescence in a reporter *E. coli* strain (Niu, Afre and Gilbert, 2006). It was demonstrated that a concentration of between 100 - 200 μmol l^{-1} of cinnamaldehyde was able to reduce fluorescence in an *E. coli* reporter strain by up to 70%. This effect was achieved without significantly inhibiting the growth of the organism meaning that cinnamaldehyde can be used to inhibit the action of two AHLs without introducing a significant selection pressure which may lead to the development of resistance. The use of this reporter strain demonstrated that cinnamaldehyde effectively reduced the action of both N-hexanoyl-L-homoserine lactone and 3-Hydroxy-C4-homoserine lactone. Similarly, a study in 2008 showed that cinnamaldehyde and its derivatives reduced autoinducer AI-2 mediated fluorescence in both wild type *V. harveyi* and several QS mutants by up to 65%. It was shown that the pure cinnamaldehyde was more effective in reducing biofilm formation across a

number of *Vibrio spp*. than numerous cinnamaldehyde derivatives (Brackman *et al.*, 2008). These effects were also achieved without inhibiting bacterial growth. Kalia *et al.* (2015) showed that the addition of cinnamon oil to cultures of *P. aeruginosa* PAO1 reduced levels of pyocyanin, alginate, and overall levels of the AHL, OdDHL. The addition of the cinnamon oil was also seen to reduce the swarming motility of PAO1 cells. While this data is promising it lacks clear identification of the active molecule in the cinnamon oil and the authors note that the effects they observed may be caused by the action of individual components of the oil or a synergistic effect from several components (Kalia *et al.*, 2015). However, further insight may be gained from a recent study by Ahmed *et al.* (2019). This study showed treatment specifically with trans-cinnamaldehyde significantly reduced transcription of QS regulatory and virulence genes in *P. aeruginosa*. This work showed a significant reduction in the expression of *lasR, rhlR, lasI* and *rhlI* as well as reducing the expression of several virulence associated genes those encoding for degradative enzymes and those involved in rhamnolipid synthesis (Ahmed *et al.*, 2019).

El-sayed *et al.* (2020) showed the efficacy of 8 separate plant extracts in inhibiting quorum sensing (as measured as a reduction in biofilm formation using a crystal violet assay) in two strains of *P. aeruginosa*; C21 and E81. With green tea and olive leaf extracts resulting in the largest reductions in biofilm formation, the authors showed that treatment with sub inhibitory concentrations of these extracts exerted their effects via disruption of gene transcription of QS related genes; *lasR, lasI, rhlR,* and *rhlI* (El-Sayed *et al.*, 2020).

Finally, recent work by Asensio *et al.* (2020) showed that a nano-emulsion of oregano oil was capable of inhibiting quorum sensing in *C. violaceum*. Treatment with nano emulsions containing the highest concentration of oregano oil (0.125 mg mL^{-1}) resulted in reductions of violacein production (and therefore QS) of 97.4%. Unlike many other studies this work showed that the three main compounds in the oregano essential oil were terpinolene, thymol, and γ-terpinene. However, the authors did not show the QSI effects of these compounds individually (Asensio *et al.*, 2020).

While these, and many other studies, have claimed anti-quorum sensing and even antibiofilm effects of plant extracts and essential oils, to date, none of these plant derived QSIs have progressed beyond *in vitro* testing and basic animal models (Kerekes *et al.*, 2013; Olivero-Verbel *et al.*, 2014)

1.6.1.3 Other non-furanone QSIs

In addition to the previously discussed compounds and extracts, several other compounds from a range of sources have been shown to have QSI properties. In 2014, El-Mowafy *et al.* showed that the commonly used medication aspirin was capable of inhibiting QS in *P. aeruginosa* PAO1 at sub-inhibitory concentrations. It was shown that addition of aspirin resulted in significantly decreased levels of both OdDHL and BHL autoinducers detected in culture supernatants by up to 70% and 80% respectively. This translated to a dose dependant reduction of numerous virulence factors such as elastase and protease as well as a reduction in the swarming and twitching motility of the bacteria. It was found that aspirin was affecting the expression of several important QS genes namely *lasR, lasI, rhlR* and *rhlI* as well as *pqsA and pqsR*. It was suggested by the authors that this change in expression was due

to a conformational change in the LasR protein meaning it was unable to effectively activate transcription of the Las QS system genes. As the Las QS system partially regulates both the Rhl and Pqs QS systems, a knock-on effect was seen (El-Mowafy *et al.*, 2014). These findings were later supported by Ahmed *et al.* in 2019 who showed decreased in relative expression of *lasR, lasI, rhlR* and *rhlI* in *P. aeruginosa* treated with salicylic acid, the primary metabolite of aspirin (Ahmed *et al.*, 2019).

Ouyang *et al.* (2016) examined the effect of the flavonoid polyphenol compound quercetin on quorum sensing in *P. aeruginosa.* They showed that quercetin, when added to cultures of PAO1, reduced adhesion of bacterial cells to surfaces and reduced biofilm biomass by up to approximately 50% without negatively impacting on bacterial growth. As with aspirin and salicylic acid a reduction was also seen in the production of three key virulence factors; protease, elastase and pyocyanin. This study showed quercetin to be equally, or more effective than azithromycin, a commonly prescribed antibiotic capable of inhibiting biofilm formation (Favre-Bonte *et al.*, 2003), in reducing biofilm formation and virulence factor production in *P. aeruginosa*.

Although many non-furanone QSIs have been shown to inhibit quorum sensing and attenuate the virulence of a range of microorganisms none have progressed beyond the preclinical stage. This may be the case for several reasons including safety concerns or poor characterisation of molecular mechanisms of action. Despite this apparent lack of progress for non-furanone QSIS, the furanones have been well studied since their discovery and continue to be examined closely today.

1.6.2 Furanones as quorum sensing inhibitors

Although furanone compounds have been known for some time, investigations into their anti-quorum sensing properties began following the discovery of the halogenated furanones in the marine alga *Delisea pulchra* (de Nys *et al.*, 1993). These halogenated furanones were structurally similar to the autoinducer molecules used by many gram-negative organisms for cell to cell signalling. This observation prompted the work of Givskov *et al.* (1996) who demonstrated that supplementing growth medium with up to 100 μg mL^{-1} of either of the two primary halogenated furanones from *D. pulchra* resulted in a significant reduction in the velocity of swarming motility of *S. liquefaciens*. Additionally, they showed that the presence of these furanones in the early log phase of growth reduced bioluminescence in both a bioluminescent reporter strain of *S. liquefaciens* and in the naturally bioluminescent marine organisms *V. fischeri* and *V. harveyi*. This reduction was particularly evident in the marine organisms with up to 100-fold reductions in luminescence. This early study provided strong evidence that the halogenated furanones found in *D. pulchra* interfered with AHL-mediated cell to cell communication systems (Givskov *et al.*, 1996).

Manefield *et al.* later demonstrated that the halogenated furanones did indeed interfere with AHL mediated processes and that this was achieved through the displacement of the AHL from its cognate receptor. They showed that the addition of two different unnamed furanones, previously shown to be highly inhibitory of bioluminescence in a reporter strain, reduced the total percentage of autoinducer bound to LuxR (overexpressed in an *E. coli* strain). They found that when the furanones were added to a culture saturated with exogenous autoinducer, at a concentration of 100 μM, that

autoinducer-LuxR binding was reduced from almost 100% to approximately 25% for one furanone and 50% for the other. Importantly, they also showed that that while furanones had a significant impact on autoinducer-receptor binding, they did not have any deleterious or unexpected off target effects on protein synthesis. This was shown through 2D gel electrophoresis and, while this method was not comprehensive, a comparison of around 400 individual proteins was possible. Interestingly, this analysis showed that the addition of exogenous autoinducer resulted in increased abundance of three proteins which were believed to be LuxA, LuxB and LuxD, all of which are involved in the Lux QS system. Conversely, the addition of furanone to the culture caused these same set of proteins to be down regulated. The addition of furanone also prompted the down regulation of three other proteins believed to be an outer membrane protein, a chaperone protein and a glutamine synthetase. Several proteins were also upregulated (Manefield *et al.*, 1999).

It is clear that the furanones from *D. pulchra* could impact several bacterial processes mediated by AHL signalling such as swarming motility and bioluminescence. In 2001 Manefield *et al.* investigated the effect of furanones on the production of extracellular virulence factors. To achieve this, they examined the production of the antibiotic carbapenem and the exoenzymes cellulase and protease in the plant pathogen *Erwinia carotovora*. When furanone was added to the culture medium a dose dependant reduction in carbapenem activity was seen. It was then confirmed that this reduction in carbapenem activity was due to a delay in the production of both CarA and CarC proteins which are involved in carbapenem synthesis. This data strongly suggests that the furanone acted by inhibiting gene expression rather than interfering with the action

of these proteins (Manefield *et al.*, 2001). This idea is further supported by the earlier findings of Welch *et al.* (2000) who showed that AHLs directly interact with the transcriptional activator protein CarR causing a fundamental change in the protein thereby allowing it to bind to, and activate the transcription of, its associated genes (Welch *et al.*, 2000). Considering this, it may be the case that the furanone is able to bind to the CarR protein (due to structural similarity to AHL) but is unable to cause the change in the protein into its active state. Additionally, Manfield *et al.* (2001) show that the presence of furanone reduced the levels of both protease and cellulase enzymes produced by *E. carotovora*. However, it must be noted that the degree to which the enzyme activity was reduced was quite variable. This study demonstrates that, in addition to impacting innocuous processes such as bioluminescence, furanones have the potential to impact the production of harmful virulence factors and, therefore, reduce their deleterious effects.

1.6.3 Effects of furanones on human pathogens

The apparent success of furanones in attenuating virulence factor production in both plant pathogens and marine microorganisms led to an increase in studies focusing on the effect of these compounds on human pathogens such as *S. aureus, E.coli* and, particularly, the strong biofilm forming pathogen *P. aeruginosa.*

In 2001, Ren *et al.* showed that a natural furanone from *D. pulchra,* known as (5Z)-4-bromo-5-(bromoethylene)-3-butyl-2(5H)-furanone, effectively attenuated the virulence of *E. coli* by reducing its capacity for swarming motility, decreasing overall biofilm thickness by 50% and affecting biofilm structure at sub-inhibitory concentrations. As well as this decrease in motility and biofilm formation the authors

found that this natural furanone was a non-specific antagonist. Using a bioluminescence assay, they showed that as well as inhibiting QS *via E. coli* autoinducer-2 (a furanone-like autoinducer) it also had antagonistic effects against AHLs and autoinducer-2 from the marine organism *V. harveyi* (Ren, Sims and Wood, 2001). This finding was important as it shows that, similarly to some antibiotics furanones may have a broad spectrum of efficacy and, therefore, may be used against many organisms.

In 2002, Hentzer *et al.* investigated the effect of a halogenated furanone derivative on *P. aeruginosa* biofilms. They found that a furanone compound, named C-56, was capable of interfering with the QS process in *P. aeruginosa*. Using a *PlasB-gfp* containing PAO-JP2 reporter strain the authors demonstrated that addition of C-56 at a concentration of 7.1 μM suppressed *lasB-gfp* expression despite addition of exogenous OdDHL of varying concentrations. This *lasB-gfp* expression was shown to be activated by OdDHL and, at high concentrations, OdDHL could activate this expression despite the presence of C-56. The authors suggested that this indicated a mechanism of action involving antagonistic activity against the OdDHL for C-56. To confirm that the action of C-56 was in fact against the OdDHL and its cognate receptor and not another part of the *P. aeruginosa* QS network, the above experiment was conducted in *E. coli* MT102 (which does not have any native AHL mediated QS system) mutant which contained the *PlasB-gfp* fusion. The QS inhibition was also seen in the *E. coli PlasB-gfp* strain. A variation of the *P. aeruginosa PlasB-gfp* reporter strain was also used to assess the effect of C-56 on QS in biofilms. It was found that the addition of OdDHL to established biofilms (24 h old) induced green fluorescence

whereas addition of OdDHL and furanone C-56 did not. This suggests that C-56 was able to inhibit QS in both biofilms and planktonic cultures. As well as being able to inhibit quorum sensing, the authors showed that C-56 was also able to reduce the production of two virulence factors namely protease and chitinase. Maximum levels of both virulence factors were achieved by the addition of exogenous OdDHL and BHL to a planktonic culture. Addition of C-56 at concentrations of 3 μg ml^{-1} or 5 μg ml^{-1} resulted in a significant, dose dependent, decrease in the levels of both chitinase and protease. Levels of these enzymes were reduced by approximately 70% and 50% respectively when treated with the higher concentration of furanone. Finally, Hentzer *et al.* (2002) demonstrated that C-56 was also capable of inhibiting QS in wild-type *P. aeruginosa* biofilms. They showed that when grown in the presence of 5 μg ml^{-1} of C-56 the early stages of biofilm formation were not affected. However, by day 7 of growth the biofilm was found to be significantly thinner than the control with less green fluorescence being seen (Hentzer *et al.*, 2002).

Following on from their 2002 study into furanone C-56, Hentzer *et al.* (2003) conducted a study examining the effects of quorum sensing inhibitors on *P. aeruginosa* PAO1. This study aimed to identify changes in gene transcription when another synthetic furanone derivative, named C-30, was introduced to the culture medium. It was shown that, in the presence of C-30, PAO1 was able to grow well with no apparent inhibition. Despite this, a reduction in virulence factor production was seen. This was demonstrated by a decrease in the specific activity of the virulence factors. Levels of protease, chitinase, and the siderophore pyoverdine were significantly decreased in the presence of both 1 μM and 10 μM of C-30 with a greater

reduction being seen at the higher concentration. Using microarray technology, the authors showed that after treatment with 10 μM concentrations of furanone C-30 a total of 93 genes were affected with 85 being downregulated and 9 being upregulated in response to the treatment. As expected, a large portion of the downregulated genes have been previously described as QS-controlled genes such as *lasA, lasB* and several other genes involved in virulence factor production. Interestingly, it was found that the *fabH1* and *fabH2* were highly repressed (Hentzer *et al.*, 2003). These genes encode for the 3-oxo-acyl carrier protein (ACP) synthase III enzyme which is thought to be involved in the production of AHLs (Parsek *et al.*, 1999). This may suggest that furanone C-30 inhibits quorum sensing and subsequently alters gene transcription by interrupting the production of ACP, resulting in a decrease in the production of AHLs. Similarly, a downregulation of *phnAB* was seen by Hentzer *et al.* (2003) suggesting a reduction in the production of the PQS signalling molecule. As there is a relationship between the Las and Rhl systems and the regulation of the PQS QS system this is not unexpected.

While less numerous, the upregulated genes identified in the work of Hentzer *et al.* (2003) also provided valuable information about the response of PAO1 to C-30. The multidrug efflux pump encoding gene *mexEF* was upregulated in the presence C-30 as well as genes involved in the ATP-binding cassette transporters and major facilitator superfamily transporters. However, one upregulated gene was found to be *mexR*, a repressor for the multidrug resistance operon. This may suggest that treatment with C-30 may sensitise PAO1 to some antibiotics by increasing the production of the repressor of MexAB, therefore, limiting the cells ability to efflux antibiotics. The

authors explored this possibility in bacterial PAO1 biofilms and the effect of C-30 on biofilm formation was assessed. It was found that while C-30 did not prevent biofilm formation there was a significant effect on the sensitivity of the biofilm to tobramycin, a commonly used antibiotic. After treatment with C-30 the antibiotic was able to penetrate the biofilm more effectively and kill a larger portion of the cells as demonstrated by a larger quantity of cells being stained with propidium iodide after staining with BacLight. Finally, the authors investigated the effect of C-30 on QS *in vivo* using a mouse model. A fluorescent reporter strain of *P. aeruginosa* (containing a *lasB-gfp* fusion) was introduced to the lungs and the mice were left for 48 h for the infection to become established. The C-30 was then administered intravenously and a reduction in the fluorescence, and, thus QS, was seen (Hentzer *et al.*, 2003). This work indicates that furanone C-30 was effectively carried to the lungs and retained its activity after administration. This inhibition of QS was not permanent and was seen to reduce after approximately 6 hours. Additionally, during another experiment, it was found that mice treated with subcutaneous C-30 were better able to clear PAO1 from the lungs during a similar infection an infection when compared to a placebo. These experiments clearly show that furanone C-30 may be highly beneficial in combatting *P. aeruginosa* lung infections *in vivo.*

Interestingly, the decrease in siderophore production seen by Hentzer *et al.* (2003) was later contradicted by Ren *et al.* in their 2005 study (Ren, Zuo and Wood, 2005). Ren *et al.* showed that *P. aeruginosa* PAO1 and JB2 both experience an increase in siderophore production when exposed to the natural furanone (5Z)-4-bromo-5-(bromoethylene)-3-butyl-2(5H)-furanone while Hentzer *et al.* (2003) saw a significant

decrease. This is an important contradiction as one of the primary differences between the studies were the difference in structure of the two furanones. While the natural furanone has a hydrocarbon chain bound to the furan ring this is replaced with a single bromine in the synthetic C-30 (Figure 1.12). The observed differences in effect between these two molecules may suggest that alterations in chemical structure of a furanone or furanone derivative could have a significant impact on its QSI activity.

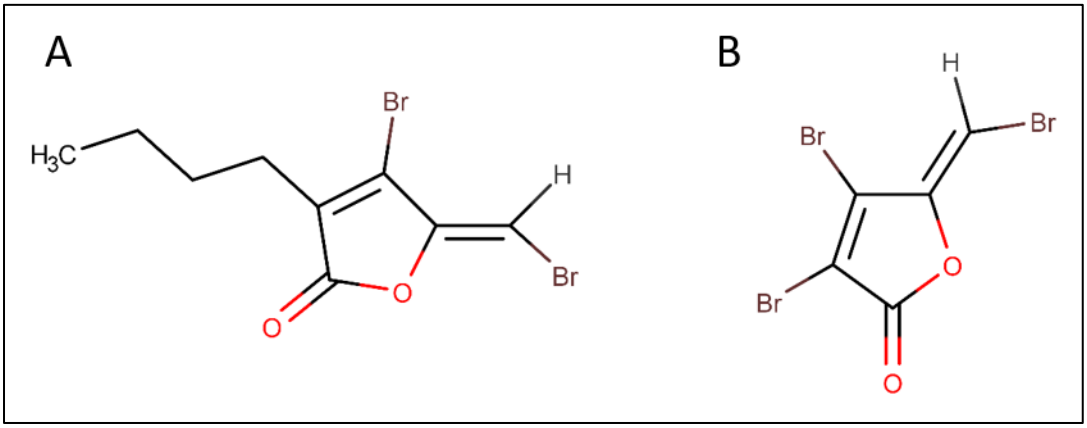

Figure 1.12 – Comparison of (a) the natural furanone (5Z)-4-bromo-5-(bromomethylene)-butyl-2(5H) furanone and (b) the synthetic furanone derivative known as C-30.

In a 2004 study by Wu *et al.*, the effect of both C-30 and C-56 on quorum sensing and bacterial clearance in a mouse model of lung infection was examined (Wu *et al.*, 2004). This study reinforced the findings of Hentzer *et al.* (2003) and confirmed that intravenous administration of C-30 resulted in a decrease in the expression of *lasR-PlasB-gfp* in PAO1 reporter strains. In addition to this, confirmation of previous work Wu *et al.* also showed that similar administration of furanone C-56 also resulted in a significant decrease in *lasR-PlasB-gfp* expression, although a much higher dose was required to do so (maximum 2 μg g^{-1} for C-30 and a maximum of 17 μg g^{-1} for C-56).

This indicates that C-30 may be a more effective QSI than C-56 when used *in vivo* although, no reason for this is suggested. The authors go on to describe the therapeutic effects of both C-30 and C-56 against lung infection. Oral administration of C-56 was found to decrease the death rate of mice infected with a lethal dose of *P. aeruginosa* PAO1 from 88% to 55%. It is unclear why the C-56 was administered orally rather than intravenously or subcutaneously. This may be due to the need for a larger dose of C-56 meaning the volume for injection was too large. It was also shown that oral administration of C-56 resulted in significantly better bacterial clearance from the lung in mice infected with sub-lethal doses of PAO1. Although no survival rate data is provided for C-30, it was shown to be more effective in assisting with bacterial lung clearance in infected mice when administered subcutaneously three times daily for three days. However, C-30 was only seen to significantly change bacterial clearance in the medium and high dose groups (0.5 μg g^{-1} and 0.75 μg g^{-1} respectively). In addition to these results, the authors found that furanone treated mice had less severe lung pathology with fewer abscesses forming in the C-30 group and a more restricted area of damage in the C-56 group (no abscesses formed in the C-56 group due to a shorter observation period during the experiment) (Wu *et al.*, 2004). As this was one of the first larger scale animal model studies into the effects of furanones on *P. aeruginosa* there are few other studies which can confirm these results, but the data provided by Wu *et al.* is encouraging.

Despite the success of C-30 both *in vitro* and *in vivo*, a 2015 study by Garcia-Contreras *et al.* claimed that the furanone derivative may not be an ideal QSI. It has been shown that C-30 is able to inhibit QS and virulence factor production in *P. aeruginosa* without

inhibiting growth (Hentzer *et al.*, 2003; Wu *et al.*, 2004). This is important as it means that no selection pressure is applied to the organism and the possibility of developing resistance to the furanone is greatly reduced. However, the work of Garcia-Contreras *et al.* (2015), assessed the effect C-30 on virulence factor production of 50 clinical strains of *P. aeruginosa* isolated from cystic fibrosis patients. They found that, while many clinical isolates responded to C-30 with reduced elastase and pyocyanin production, several strains showed either no decrease in virulence factor production or displayed an increase in production. It was then shown that these strains used several different resistance mechanisms. One strain, INP-42, was found to have significantly higher C-30 efflux capacity while two other strains were seen to have significantly decreased C-30 uptake. While the reason for this decreased uptake is not known the authors suggest a possible mutation in some unknown transporter protein. Despite many strains responding to the C-30 as expected, Garcia-Contreras *et al.* warn that furanones should be used with caution in the clinical setting as many resistant strains already exist and in extreme cases the furanone compound may worsen the infection (García-Contreras *et al.*, 2015).

Although much of the primary data on furanones as QSIs was obtained through studying C-30 and C-56, many other furanones have been studied. As is the case with C-30 and C-56 many of these furanones are synthetic halogenated furanones, primarily brominated furanones.

In 2013, Shetye *et al.* synthesised and tested four brominated furanone molecules for antibiofilm activity against *E. coli* and *P. aeruginosa.* They found that two of these furanone compounds, BF8 and BF15, were able to effectively reduce biofilm

formation in the wild type *E. coli* strain RP437. The effects of furanone treatment included reduced biomass, overall biofilm thickness and total biofilm surface coverage (Shetye *et al.*, 2013). This was achieved without negatively affecting bacterial growth. Compound BF8 also showed a similar decrease in biofilm production by *P. aeruginosa* PAO1 with an approximate decrease of 40% in biomass and surface coverage and a 30% decrease in biofilm thickness. It should also be noted that while BF15 was not capable of inhibiting biofilm production it reduced PAO1's production of elastase by 41%. Similarly, BF8 reduced elastase production by 43%. The observed difference in the inability of BF15 to inhibit biofilm formation and its ability to reduce elastase production may mean that brominated furanones are not global QSIs but may affect certain pathways and QS systems more strongly than others. Using a *lasI-gfp* reporter strain, it was seen that the application of both BF8 and BF15 to PAO1 cultures resulted in a decrease in *lasI* transcription. This reduction in *lasI* transcription indicates that the brominated furanones are antagonists of the transcriptional activator LasR. This experiment was repeated with a *rhlI-gfp* reporter strain and it was found that rather than displaying an antagonistic effect, both BF8 and BF15 had an agonistic effect on *rhlI* transcription with BF15 being a stronger agonist than BF8 (Shetye *et al.*, 2013). This result provides further evidence that the action of furanones upon QS systems is highly variable and may not always provide an antagonistic effect. As well as inhibiting biofilm formation and reducing elastase production, BF8 has also been shown to sensitise PAO1 persister cells, a type of cell found in biofilms which are largely dormant (Mulcahy *et al.*, 2010; Fauvart, De Groote and Michiels, 2011), to antibiotic treatment.

In 2012 Pan *et al.* showed that when treated with BF8 cultures of *P. aeruginosa* had reduced numbers of persister cells. Reductions in persister cell numbers occurred in a dose dependent manner between concentrations of 5 μg mL^{-1} and 100 μg mL^{-1} with reductions of approximately 3 log and 5 log respectively. Importantly, it was also shown that this reduction in persister cell numbers also occurred in surface attached biofilms as well as planktonic cultures with reductions of approximately 3 log at the highest tested dose of BF8 (60 μg mL^{-1}). It was also shown that a relatively low dose of BF8 (5 μg mL^{-1}) could be combined with standard antibiotic treatment to increase the efficacy of antibiotics such as tobramycin in killing persister cells (Pan *et al.*, 2012).

The idea that furanones could effectively supplement antibiotic treatment was further reinforced by Kim *et al.* (2012) who showed that, when combined with ciprofloxacin, 5-hydroxy-2(3H)-benzofuranone could prevent biofilms from forming on silicone tympanostomy tubes and significantly reduce the numbers of planktonic cells as demonstrated by SEM analysis. This study is of particular interest as it clearly demonstrates the potential for combined furanone/antibiotic therapies. While the combination therapy was able to prevent biofilm formation, the treatment with the furanone only treatment showed a reduced level of biofilm formation but no reduction in the planktonic cell numbers (Kim *et al.*, 2012). This is important as it is likely that when furanone treatment is stopped the planktonic cells will then begin to form biofilms once again.

In a later study, Pan and Ren (2013) identified a further two brominated furanone compounds which were capable of QS inhibition. These compounds, known as BF9

and BF11, could effectively sensitise persister cells to antibiotic treatment while others could inhibit QS but had no effect on the persister cells. As all these molecules are structurally related it seems likely that the differences in activity are dictated by the small changes in chemical structure. This idea is further reinforced as two compounds which were structurally similar but were non-brominated were found to have no QSI activity and no action against the persister cells (Pan and Ren, 2013).

The next set of synthetic brominated furanones to be tested were synthesised and studied by Yang *et al.* (2014). The so-called bicyclic brominated furanones (BBF) were designed around the brominated furanones produced by Pan *et al.* (2012) and were shown to retain the ability to inhibit biofilm formation resulting in significantly less biofilm mass when compared to furanone free controls. Furanones 5-BBF, 6-BBF, and 7-BBF showed reductions in biofilm of approximately 50%, 70% and 50% respectively when compared to an untreated control (Yang *et al.*, 2014). However, these 3 BBFs were still found to be considerably less effective that the BF4 compound produced by Pan *et al.* (2012). Despite the poorer performance of the BBFs Yang *et al.* state that they are considerably less cytotoxic to human cells than other furanones. They demonstrated that, when compared to the BF8 as used by Pan *et al.* (2012), BBFs showed reduced cell death when added to cultures of human neuroblastoma cells (SK-N-SH). Furanones 5-BBF, 6-BBF and 7-BBF showed immediate cell death of approximately 25%, 25% and 55% respectively. After 48 h incubation cell death was at 95%, 50% and 85% respectively. This was compared to BF which showed an immediate cell death of 70% increasing to almost 100% after 48 hours. However, the authors' choice of cell line (SK-N-SH) is unusual. Although SK-N-SH cells display

an epithelial cell morphology they are not epithelial cells (Biedler, Helson and Spengler, 1973). Testing furanones on a true epithelial cell line would likely be more relevant as furanones, if used in medical applications, are most likely to contact epithelial cells (e.g. airway epithelia). While the BBFs are undoubtedly better in terms of cytotoxicity further studies are needed. Currently, little data on furanone cytotoxicity is available so an accurate comparison cannot be made between the BBFs and BF8.

In addition to the work of Pan *et al.* and Yang *et al.*, there have been several other studies which have examined the effects of synthetic furanones and their derivatives. In 2008, Kim *et al.* showed that six separate furanone derivatives were effective in antagonising QS in cultures of a luminescent reporter strain of *E. coli.* With reductions of up to 90% in relative luminescence when compared to an untreated control. They also report that all of the tested furanone derivatives partially prevented the initial attachment of *P. aeruginosa* to a substrate and, thus, biofilm formation was significantly diminished (Kim *et al.*, 2008). This observation is in direct contradiction of Hentzer *et al.* (2002) who found that when grown in the presence of furanone C-56 the initial stages of biofilm formation were unaffected (Hentzer *et al.*, 2002). This discrepancy in the reported data clearly illustrates the wide range of effects that may be seen between two structurally distinct furanone derivatives and highlights the need for proper mechanistic studies of new candidate QSIs.

In 2012, Liu *et al.* found that, from a selection of 19 candidate molecules, many compounds showed biological activity. Three compounds, in particular, resulted in a reduction in biofilm formation between 58.7% and 71.8% when tested against *P.*

aeruginosa (ATCC 9027). A reduction in biofilm formation was also seen against two other strains of *P. aeruginosa* (ATC27853 and PAOA) (Liu *et al.*, 2012). No further information regarding the biological activity of these compounds was given as the study was focused primarily on compound synthesis and molecular docking studies.

In 2012, one study found that triazolyldihydrofuranones (AHLs in which the amide group has been replaced with a triazole group) displayed some antagonistic activity against LasR dependent QS in *P. aeruginosa* (Brackman *et al.*, 2012). Interestingly, while all triazolyldihydrofuranones tested were capable of inhibiting LuxR dependent QS (as tested using a *luxR-gfp* reporter strain of *E. coli*) it was found that only compounds with a side chain length of ten or twelve carbons could effectively inhibit the LasR dependant QS system. The authors found that the anti-QS ability of the compounds also translated to antibiofilm activity with the most active compounds decreasing both biofilm biomass and the number of viable cells present in the biofilm. It was also noted that many of the tested compounds acted agonistically upon either the LasR or LuxR dependant QS systems increasing their activity (Brackman *et al.*, 2012). The authors' data suggest that the closer a potential QSI is in structure to the organism's cognate autoinducer the better it will perform. However, there is a balance to be struck between finding a compound which inhibits QS and one which may activate QS, thus, worsening an infection.

Finally, in 2015 Goh *et al.* tested the QS inhibition capacity of furanone derivatives, known as 1,5-dihydropyrrol-2-ones. Their study showed that these furanone derivatives had a wide range of antagonistic activity against QS in a reporter strain of *E. coli* (Goh *et al.*, 2015). Like the work of Liu *et al.* (2012), this was primarily a

synthesis and docking study and so no further information regarding QSI inhibition is provided.

Another subset of furanones which have been reported to have anti-QS properties are the non-halogenated furanones which can be isolated from a number of natural sources. One non-halogenated furanone which has been of particular interest in recent years has been 4-hydroxy-2,5-dimethyl-3(2H)-furanone (HDMF) also known as furaneol, strawberry furanone or DMHF. It has been known for some time that HDMF is able to inhibit the growth of wild type *P. aeruginosa* at a concentration of 80 µg mL^{-1} and other gram-negative organisms at concentrations as low as 20 µg mL^{-1} (Sung *et al.*, 2007). However, until recently no studies had examined the compounds potential as a QSI. In 2014 Choi *et al.* provided evidence that HDMF is a potent QSI and has good biofilm inhibition activity. Using a crystal violet microtiter assay they showed that when cultured for 24 h with 0.1 µM and 1 µM of HDMF biofilm production was reduced by 27.8% and 42.6% respectively. Further, when cultured for up to 48 hours, additional loss of biofilm was seen indicating that HDMF may facilitate the detachment of established biofilms, although it is unclear how this might occur (Choi *et al.*, 2014). As well as reducing biofilm formation, the HDMF treated cells were found to form poorly constructed biofilms. These appeared as flat monolayers with sparsely distributed cells whereas untreated control cultures formed densely populated biofilms with good three-dimensional structure. This result, when considered alongside the detachment of preformed biofilms may suggest that HDMF impacts upon a process necessary for forming a good foundation for the biofilm on the substrate material. This puts the findings of Choi *et al.* against those of Hentzer *et al.*

(2002) who found that the early stages of biofilm formation were not significantly affected by furanone treatment. Choi *et al.* (2014) also tested the effects of HDMF on the motility of *P. aeruginosa* and found that when treated with 1.0µM of HDMF the swarming motility of *P. aeruginosa* was greatly reduced (as evidenced by a decrease in motility diameter – though no exact figures were reported) while twitching motility was unaffected. Again, this is an important finding as it has been shown that swarming motility is closely tied to biofilm formation (Verstraeten *et al.*, 2008). Lastly, it was shown that HDMF, when added to cultures of *P. aeruginosa* at a concentration of 1.0 µM, substantially reduced the production of three separate virulence factors; LasA protease, rhamnolipid and pyocyanin. The levels of these three virulence factors were reduced by 53.8%, 40.9%, and 51.4%, respectively. The decrease in virulence factors was accompanied by a corresponding decrease in the production of the two main autoinducer molecules used by *P. aeruginosa*, OdDHL and BHL. This may indicate that HDMF affects many QS controlled processes by interfering with the QS systems at a very early stage.

Unlike the previously discussed halogenated furanones, there is evidence that HDMF may be beneficial in a model of primary human airway epithelial cells. It was demonstrated by Ruffin *et al.* (2016) that *P. aerugnosa* secreted virulence factors such as LasA protease and LasB elastase impaired several important functions in airway epithelial cells including wound healing, cell proliferation, and cell migration (Ruffin *et al.*, 2016; Ruffin and Brochiero, 2019). This was achieved by treating cells with so-called *P. aeruginosa* diffusible materials (PsaDM). These are a collection of excreted molecules collected from bacterial culture supernatants. It was then shown the

deleterious effects caused by the presence of PsaDM could be prevented by deletion of the key genes involved in QS, specifically *lasR*. Treatment with PsaDM from these Las QS deficient mutants showed no apparent reduction in wound healing indicating that the negative effects of the PsaDM are at least partially due to the production of QS controlled molecules. The authors then demonstrated that treating *P. aeruginosa* PAO1 cultures with HDMF resulted in a significant decrease in elastase activity of approximately 70%, without affecting bacterial growth. It was also seen that, when exposed to PsaDM from HDMF treated PAO1 cultures, wound healing rates were significantly better than those exposed to PsaDM from untreated PAO1 (Ruffin *et al.*, 2016). A similar result was also seen in highly differentiated airway epithelial cell cultures. Importantly, it was also shown that exposure to HDMF alone did not have a negative impact on the wound healing capacity of airway epithelial cells. Unfortunately, no data were collected regarding the impact of HDMF on cell viability. However, it is reasonable to assume that because wound repair rates were not negatively affected by HDMF that cell viability and proliferation was not significantly reduced. However, despite this promising study further investigation into the cytotoxicity and safety of HDMF is needed.

The data presented by Choi *et al.* (2014) and Ruffin *et al.* (2016) are highly encouraging and provide evidence that the non-halogenated furanone HDMF may be a viable QSI candidate for use in medical applications, though considerably more research is needed.

Studies such as those detailed here show that natural furanones, halogenated furanones, and their synthetic derivatives can be highly effective QSIs. However, the

work published to date has focused primarily on furanones such as C-30, C-56 and HDMF. Due to the wide range of sources they can be isolated from there are hundreds of furanone compounds, such as 2-methyltetrahydrofuran-3-one (MTHF) from coffee and 4,5-dimethyl-3-hydroxy-2,5-dihydrofuran-2-one (Sotolon) from Fenugreek, that are yet to be investigated as QSI compounds.

In addition to the limited number of furanones that have been tested, those studies which have been published have failed to address some of the potential limitations that furanones may present.

1.7 Potential limitations of furanones

The studies discussed here provide good evidence that both halogenated and non-halogenated furanones can effectively inhibit QS and, therefore, reduce both biofilm formation and the production of numerous virulence factors *in vitro*. There have been a small number of studies showing that furanones are successful in animal and human cell models with results such as increased survival rates and improved bacterial clearance in murine lung infection models. This makes furanones apparently excellent candidates for use in medical applications such as wound dressings, medical implants/devices, and any other area in which biofilms and bacterial quorum sensing presents a problem. However, while there is considerable evidence that furanones are beneficial, some studies have noted that they may have a level of cytotoxicity, with some furanones being more harmful than others with one study found a reduction of cell viability of nearly 100% after treatment (Yang *et al.*, 2014). Unfortunately, these studies focused on different furanones under very different conditions and so a meaningful comparison cannot be made. It is clear, therefore, that more focused and

comprehensive safety studies are also required. However, this is not the only issue which needs to be addressed prior to using furanones in a medical setting.

As there has been no extended animal or human testing of any furanones to date, there are many aspects of these compounds which remain unknown. For example, both the pharmacokinetics and pharmacodynamics of furanones have not been reported. While the application of furanones to human cell cultures may not result in obvious negative effects, there may be a cumulative toxic effect when administered over a period of time. The inverse may also be true. When administered to a patient the furanone may be cleared from the system rapidly through channels such as first pass metabolism meaning that a therapeutic dose cannot be reached. While this did not appear to be the case in the work of Hentzer *et al.* (2003) who administered furanone C-30 intravenously to mice, further study is needed.

Another concern is that of potential drug interactions. It has been shown by several research groups that dual treatment of furanone and antibiotics is generally more efficacious than individual treatment with either component. This is important as it is likely that patients who have developed biofilm infections will be prescribed antibiotics in tandem. However, biofilms are also problematic in other patient groups such as those with diabetic wounds and post-surgical patients (Edmiston *et al.*, 2016; Di Domenico *et al.*, 2017). It is also likely that these patients will be on additional medications such as hypoglycaemic medications or analgesia so gaining information on drug-furanone interactions should be a priority. Similarly, information should be gathered on any contraindications for furanone treatment such as safety for patients with hepatic or renal failure.

Finally, and perhaps most importantly, is the issue of antimicrobial resistance. In the majority of studies concerning furanones, the authors report that the desired effects are seen at sub-inhibitory concentrations. This is important because, as stated previously, this limits the introduction of selection pressures and, thus, the chances of developing resistance are reduced. However, as Garcia Contreras *et al.* (2015) showed, furanone resistance has been seen in some clinical isolates. Therefore, it is crucial to further investigate the conditions under which such resistance might occur and methods for minimising this.

If all of the above knowledge gaps could be addressed, furanones may indeed be promising new tool in the treatment and control of biofilm-associated infections and their complications.

1.8 Aims and Objectives

The studies discussed in this chapter, when considered together, show that, due to their structural similarity to native QS signalling molecules, furanone compounds are potentially excellent candidates for QSI based treatments. The QSI activity of furanones allows them to inhibit biofilm formation both *in vitro* and *in vivo*. This thesis aims to use naturally occurring furanones to inhibit biofilm formation in chronic wounds. The work conducted here aims to develop novel a polymer system to deliver furanones to a chronic wound biofilm in a controlled manner, to demonstrate the *in vitro* efficacy of furanones delivered using the developed system, and to show efficacy of furanones against clinically representative biofilms using a novel *in vitro* chronic wound model.

1.9 References

Ahlgren, N. A. *et al.* (2011) 'Aryl-homoserine lactone quorum sensing in stem-nodulating photosynthetic bradyrhizobia', *Proceedings of the National Academy of Sciences*, 108(17), pp. 7183–7188. doi: 10.1073/pnas.1103821108.

Ahmed, S. A. K. S. *et al.* (2019) 'Natural quorum sensing inhibitors effectively downregulate gene expression of *Pseudomonas aeruginosa* virulence factors', *Applied Microbiology and Biotechnology*, 103(8), pp. 3521–3535. doi: 10.1007/s00253-019-09618-0.

Akiyama, H. *et al.* (1996) 'Staphylococcus aureus infection on cut wounds in the mouse skin: Experimental staphylococcal botryomycosis', *Journal of Dermatological Science*, 11(3), pp. 234–238. doi: 10.1016/0923-1811(95)00448-3.

Allesen-Holm, M. *et al.* (2006) 'A characterization of DNA release in *Pseudomonas aeruginosa* cultures and biofilms', *Molecular Microbiology*, 59(4), pp. 1114–1128. doi: 10.1111/j.1365-2958.2005.05008.x.

Arevalo-Ferro, C. *et al.* (2003) 'Identification of quorum-sensing regulated proteins in the opportunistic pathogen *Pseudomonas aeruginosa* by proteomics.', *Environmental microbiology*, 5(12), pp. 1350–69.

Asensio, C. M. *et al.* (2020) 'Rheological Behavior, Antimicrobial and Quorum Sensig Inhibition Study of an Argentinean Oregano Essential Oil Nanoemulsion', *Frontiers in Nutrition*, 7, p. 569913. doi: 10.3389/fnut.2020.569913.

Biedler, J. L., Helson, L. and Spengler, B. A. (1973) ‘Morphology and growth, tumorigenicity, and cytogenetics of human neuroblastoma cells in continuous culture.’, *Cancer research*, 33(11), pp. 2643–52.

Bokhove, M. *et al.* (2010) ‘The quorum-quenching N-acyl homoserine lactone acylase PvdQ is an Ntn-hydrolase with an unusual substrate-binding pocket.’, *Proceedings of the National Academy of Sciences*, 107(2), pp. 686–91. doi: 10.1073/pnas.0911839107.

Boles, B. R., Thoendel, M. and Singh, P. K. (2005) ‘Rhamnolipids mediate detachment of *Pseudomonas aeruginosa* from biofilms’, *Molecular Microbiology*, 57(5), pp. 1210–1223. doi: 10.1111/j.1365-2958.2005.04743.x.

Brackman, G. *et al.* (2008) ‘Cinnamaldehyde and cinnamaldehyde derivatives reduce virulence in Vibrio spp. by decreasing the DNA-binding activity of the quorum sensing response regulator LuxR’, *BMC Microbiology*, 8(1), p. 149. doi: 10.1186/1471-2180-8-149.

Brackman, G. *et al.* (2012) ‘Synthesis and evaluation of the quorum sensing inhibitory effect of substituted triazolyldihydrofuranones’, *Bioorganic and Medicinal Chemistry*, 20(15), pp. 4737–4743. doi: 10.1016/j.bmc.2012.06.009.

Brandenburg, K. S. *et al.* (2015) ‘Inhibition of *Pseudomonas aeruginosa* biofilm formation on wound dressings’, *Wound Repair and Regeneration*, 23, pp. 1–6. doi: 10.1111/wrr.12365.Inhibition.

Choi, S. C. *et al.* (2014) ‘Inhibitory effects of 4-hydroxy-2,5-dimethyl-3(2H)-furanone

(HDMF) on acyl-homoserine lactone-mediated virulence factor production and biofilm formation in *Pseudomonas aeruginosa* PAO1', *Journal of Microbiology*, 52(9), pp. 734–742. doi: 10.1007/s12275-014-4060-x.

Choo, J. H., Rukayadi, Y. and Hwang, J. K. (2006) 'Inhibition of bacterial quorum sensing by vanilla extract', *Letters in Applied Microbiology*, 42(6), pp. 637–641. doi: 10.1111/j.1472-765X.2006.01928.x.

Davey, M. E., Caiazza, N. C. and O'Toole, G. A. (2003) 'Rhamnolipid surfactant production affects biofilm architecture in *Pseudomonas aeruginosa* PAO1.', *Journal of bacteriology*, 185(3), pp. 1027–36. doi: 10.1128/JB.185.3.1027-1036.2003.

Davies, D. G. *et al.* (1998) 'The involvement of cell-to-cell signals in the development of a bacterial biofilm.', *Science*, 280(5361), pp. 295–8. doi: 10.1126/SCIENCE.280.5361.295.

Di Domenico, E. G. *et al.* (2017) 'Biofilm is a Major Virulence Determinant in Bacterial Colonization of Chronic Skin Ulcers Independently from the Multidrug Resistant Phenotype.', *International journal of molecular sciences*, 18(5). doi: 10.3390/ijms18051077.

Edmiston, C. E. *et al.* (2016) 'A narrative review of microbial biofilm in postoperative surgical site infections: clinical presentation and treatment', *Journal of Wound Care*, 25(12), pp. 693–702. doi: 10.12968/jowc.2016.25.12.693.

El-Mowafy, S. A. *et al.* (2014) 'Aspirin is an efficient inhibitor of quorum sensing, virulence and toxins in *Pseudomonas aeruginosa*', *Microbial Pathogenesis*, 74(1), pp.

25–32. doi: 10.1016/j.micpath.2014.07.008.

El-Sayed, N. R. *et al.* (2020) 'Olive leaf extract modulates quorum sensing genes and biofilm formation in multi-drug resistant *Pseudomonas aeruginosa*', *Antibiotics*, 9(9), pp. 1–19. doi: 10.3390/antibiotics9090526.

Fauvart, M., De Groote, V. N. and Michiels, J. (2011) 'Role of persister cells in chronic infections: clinical relevance and perspectives on anti-persister therapies', *Journal of Medical Microbiology*, 60(6), pp. 699–709. doi: 10.1099/jmm.0.030932-0.

Favre-Bonte, S. *et al.* (2003) 'Biofilm formation by *Pseudomonas aeruginosa*: Role of the C4-HSL cell-to-cell signal and inhibition by azithromycin', *Journal of Antimicrobial Chemotherapy*, 52(4), pp. 598–604. doi: 10.1093/jac/dkg397.

Fazli, M. *et al.* (2011) 'Quantitative analysis of the cellular inflammatory response against biofilm bacteria in chronic wounds', *Wound Repair and Regeneration*, 19(3), pp. 387–391. doi: 10.1111/j.1524-475X.2011.00681.x.

Fuqua, W. C., Winans, S. C. and Greenberg, E. P. (1994) 'Quorum sensing in bacteria: The LuxR-LuxI family of cell density- responsive transcriptional regulators', *Journal of Bacteriology*, 176(2), pp. 269–275. doi: 10.1128/jb.176.2.269-275.1994.

Gambello, M. J. and Iglewski, B. H. (1991) 'Cloning and characterization of the *Pseudomonas aeruginosa* lasR gene, a transcriptional activator of elastase expression.', *Journal of bacteriology*, 173(9), pp. 3000–9.

Gambello, M. J., Kaye, S. and Iglewski, B. H. (1993) 'LasR of *Pseudomonas*

aeruginosa is a transcriptional activator of the alkaline protease gene (apr) and an enhancer of exotoxin A expression.', *Infection and immunity*, 61(4), pp. 1180–4.

García-Contreras, R. *et al.* (2015) 'High variability in quorum quenching and growth inhibition by furanone C-30 in *Pseudomonas aeruginosa* clinical isolates from cystic fibrosis patients', *Pathogens and Disease*, 73(6), p. ftv040. doi: 10.1093/femspd/ftv040.

Givskov, M. *et al.* (1996) 'Eukaryotic interference with homoserine lactone-mediated prokaryotic signalling', *Journal of bacteriology*, 178(22). Available at: http://www.ncbi.nlm.nih.gov/pubmed/8932319.

Glessner, A. *et al.* (1999) 'Roles of *Pseudomonas aeruginosa* las and rhl quorum-sensing systems in control of twitching motility', *Journal of Bacteriology*, 181(5), pp. 1623–1629. doi: 10.1128/jb.181.5.1623-1629.1999.

Goh, W. K. *et al.* (2015) 'Synthesis, quorum sensing inhibition and docking studies of 1,5-dihydropyrrol-2-ones', *Bioorganic and Medicinal Chemistry*, 23(23), pp. 7366–7377. doi: 10.1016/j.bmc.2015.10.025.

Harrison-Balestra, C. *et al.* (2003) 'A wound-isolated *Pseudomonas aeruginosa* grows a biofilm in vitro within 10 hours and is visualized by light microscopy', *Dermatologic Surgery*, 29(6), pp. 631–635. doi: 10.1046/j.1524-4725.2003.29146.x.

Hentzer, M. *et al.* (2002) 'Inhibition of quorum sensing in *Pseudomonas aeruginosa* biofilm bacteria by a halogenated furanone compound', *Microbiology*, 148(1), pp. 87–102. doi: 10.1099/00221287-148-1-87.

Hentzer, M. *et al.* (2003) ‘Attenuation of *Pseudomonas aeruginosa* virulence by quorum-sensing inhibitors’, *Embo J.*, 22(15), p. 3803. doi: 10.1093/emboj/cdg366.

Hirashima, H. *et al.* (2019) ‘In vitro investigation of antibacterial activity against fecal bacteria infecting wounds’, *Wound Medicine*, 26(1), p. 100169. doi: 10.1016/j.wndm.2019.100169.

Jones, S. *et al.* (1993) ‘The lux autoinducer regulates the production of exoenzyme virulence determinants in Erwinia carotovora and *Pseudomonas aeruginosa*.’, *The EMBO Journal*. European Molecular Biology Organization, 12(6), pp. 2477–2482. doi: 10.1002/j.1460-2075.1993.tb05902.x.

Kalia, M. *et al.* (2015) ‘Effect of Cinnamon Oil on Quorum Sensing-Controlled Virulence Factors and Biofilm Formation in *Pseudomonas aeruginosa*’, *PLOS ONE*, 10(8), p. e0135495. doi: 10.1371/journal.pone.0135495.

Kerekes, E.-B. B. *et al.* (2013) ‘Anti-biofilm forming and anti-quorum sensing activity of selected essential oils and their main components on food-related micro-organisms’, *Journal of Applied Microbiology*, 115(4), pp. 933–942. doi: 10.1111/jam.12289.

Khan, M. S. A. *et al.* (2009) ‘Inhibition of quorum sensing regulated bacterial functions by plant essential oils with special reference to clove oil’, *Letters in Applied Microbiology*, 49(3), pp. 354–360. doi: 10.1111/j.1472-765X.2009.02666.x.

Kim, C. *et al.* (2008) ‘Furanone derivatives as quorum-sensing antagonists of *Pseudomonas aeruginosa*’, *Applied Microbiology and Biotechnology*, 80(1), pp. 37–

47. doi: 10.1007/s00253-008-1474-6.

Kim, S. G. *et al.* (2012) 'Effect of furanone on experimentally induced *Pseudomonas aeruginosa* biofilm formation: In vitro study', *International Journal of Pediatric Otorhinolaryngology*, 76(11), pp. 1575–1578. doi: 10.1016/j.ijporl.2012.07.015.

Kiratisin, P., Tucker, K. D. and Passador, L. (2002) 'LasR, a transcriptional activator of *Pseudomonas aeruginosa* virulence genes, functions as a multimer', *Journal of Bacteriology*, 184(17), pp. 4912–4919. doi: 10.1128/JB.184.17.4912-4919.2002.

Kostakioti, M., Hadjifrangiskou, M. and Hultgren, S. J. (2013) 'Bacterial biofilms: development, dispersal, and therapeutic strategies in the dawn of the postantibiotic era.', *Cold Spring Harbor perspectives in medicine*, 3(4), pp. 1–23. doi: 10.1101/cshperspect.a010306.

Kruszewska, K., Wesolowska-Gorniak, K. and Czarkowska-Paczek, B. (2020) 'Venous leg ulcer healing time is increased with each subsequent bacterial strain identified in the ulcer. A retrospective study', *Phlebology: The Journal of Venous Disease*, p. 026835552096194. doi: 10.1177/0268355520961945.

Kusada, H. *et al.* (2017) 'A novel quorum quenching N-Acylomoserine lactone acylase from Acidovorax sp. stain MR-S7 mediates antibiotic resistance', *Applied and Environmental Microbiology*, 83(13), pp. 1–9. doi: https://doi.org/10.1128/AEM .00080-17.

LaSarre, B. and Federle, M. J. (2013) 'Exploiting Quorum Sensing To Confuse Bacterial Pathogens', *Microbiology and Molecular Biology Reviews*, 77(1), pp. 73–

111. doi: 10.1128/mmbr.00046-12.

Leaper, D., Assadian, O. and Edmiston, C. E. (2015) 'Approach to chronic wound infections', *British Journal of Dermatology*, 173(2), pp. 351–358. doi: 10.1111/bjd.13677.

Lee, J. *et al.* (2013) 'A cell-cell communication signal integrates quorum sensing and stress response', *Nature Chemical Biology*, 9(5), pp. 339–343. doi: 10.1038/nchembio.1225.

Lee, J. and Zhang, L. (2014) 'The hierarchy quorum sensing network in *Pseudomonas aeruginosa*', *Protein and Cell*, 6(1), pp. 26–41. doi: 10.1007/s13238-014-0100-x.

Lequette, Y. and Greenberg, E. P. (2005) 'Timing and Localization of Rhamnolipid Synthesis Gene Expression in *Pseudomonas aeruginosa* Biofilms', *Journal of Bacteriology*, 187(1), pp. 37–44. doi: 10.1128/JB.187.1.37-44.2005.

Lin, Y. H. *et al.* (2003) 'Acyl-homoserine lactone acylase from Ralstonia strain XJ12B represents a novel and potent class of quorum-quenching enzymes', *Molecular Microbiology*, 47(3), pp. 849–860. doi: 10.1046/j.1365-2958.2003.03351.x.

Liu, G.-Y. Y. *et al.* (2012) 'Synthesis, Molecular Docking, and Biofilm Formation Inhibitory Activity of 5-Substituted 3,4-Dihalo-5H-furan-2-one Derivatives on *Pseudomonas aeruginosa*', *Chemical Biology and Drug Design*, 79(5), pp. 628–638. doi: 10.1111/j.1747-0285.2012.01342.x.

Malone, M. *et al.* (2017) 'The prevalence of biofilms in chronic wounds: a systematic

review and meta-analysis of published data.', *Journal of wound care*, 26(1), pp. 20–25. doi: 10.12968/jowc.2017.26.1.20.

Manefield, M. *et al.* (1999) 'Evidence that halogenated furanones from Delisea pulchra inhibit acylated homoserine lactone (AHL)-mediated gene expression by displacing the AHL signal from its receptor protein', *Microbiology*. Microbiology Society, 145(2), pp. 283–291. doi: 10.1099/13500872-145-2-283.

Manefield, M. *et al.* (2001) 'Halogenated furanones from the red alga, Delisea pulchra, inhibit carbapenem antibiotic synthesis and exoenzyme virulence factor production in the phytopathogen Erwinia carotovora', *FEMS Microbiology Letters*, 205(1), pp. 131–138. doi: 10.1016/S0378-1097(01)00460-8.

McClean, K. H. *et al.* (1997) 'Quorum sensing and Chromobacteriurn violaceurn : exploitation of violacein production and inhibition for the detection of N-acyl homoserine lactones', *Microbiology*, 143, pp. 3703–37.

Metcalf, D., Bowler, P. and Parsons, D. (2016) 'Wound Biofilm and Therapeutic Strategies', in *Microbial Biofilms - Importance and Applications*. InTech, pp. 271–298. doi: 10.5772/63238.

Mulcahy, L. R. *et al.* (2010) 'Emergence of *Pseudomonas aeruginosa* Strains Producing High Levels of Persister Cells in Patients with Cystic Fibrosis', *Journal of Bacteriology*, 192(23), pp. 6191–6199. doi: 10.1128/JB.01651-09.

National Institutes of Health (2002) *NIH Guide: RESEARCH ON MICROBIAL BIOFILMS, Public announcement*. Available at:

https://grants.nih.gov/grants/guide/pa-files/pa-03-047.html (Accessed: 26 April 2020).

Neopane, P. *et al.* (2018) 'In vitro biofilm formation by Staphylococcus aureus isolated from wounds of hospital-admitted patients and their association with antimicrobial resistance', *International Journal of General Medicine*, 11, pp. 25–32. doi: 10.2147/IJGM.S153268.

Niu, C., Afre, S. and Gilbert, E. S. S. (2006) 'Subinhibitory concentrations of cinnamaldehyde interfere with quorum sensing', *Letters in Applied Microbiology*, 43(5), pp. 489–494. doi: 10.1111/j.1472-765X.2006.02001.x.

de Nys, R. *et al.* (1993) 'New halogenated furanones from the marine alga delisea pulchra (cf. fimbriata)', *Tetrahedron*, 49(48), pp. 11213–11220. doi: 10.1016/S0040-4020(01)81808-1.

O'Toole, G. A. and Kolter, R. (1998) 'Flagellar and twitching motility are necessary for *Pseudomonas aeruginosa* biofilm development', *Molecular Microbiology*. Blackwell Science Ltd, UK, 30(2), pp. 295–304. doi: 10.1046/j.1365-2958.1998.01062.x.

Olivero-Verbel, J. *et al.* (2014) 'Composition, anti-quorum sensing and antimicrobial activity of essential oils from Lippia alba.', *Brazilian journal of microbiology*, 45(3), pp. 759–67.

Otton, L. M. *et al.* (2017) 'Influence of twitching and swarming motilities on biofilm formation in Pseudomonas strains', *Archives of Microbiology*, 199(5), pp. 677–682.

doi: 10.1007/s00203-017-1344-7.

Pan, J. *et al.* (2012) 'Reverting Antibiotic Tolerance of *Pseudomonas aeruginosa* PAO1 Persister Cells by (Z)-4-bromo-5-(bromomethylene)-3-methylfuran-2(5H)-one', *PLoS ONE*, 7(9), p. e45778. doi: 10.1371/journal.pone.0045778.

Pan, J. and Ren, D. (2013) 'Structural effects on persister control by brominated furanones', *Bioorganic and Medicinal Chemistry Letters*, 23(24), pp. 6559–6562. doi: 10.1016/j.bmcl.2013.10.070.

Papenfort, K. and Bassler, B. L. (2016) 'Quorum sensing signal–response systems in Gram-negative bacteria', *Nature Reviews Microbiology*, 14(9), pp. 576–588. doi: 10.1038/nrmicro.2016.89.

Parsek, M. R. *et al.* (1999) 'Acyl homoserine-lactone quorum-sensing signal generation.', *Proceedings of the National Academy of Sciences of the United States of America*, 96(8), pp. 4360–5. doi: 10.1073/PNAS.96.8.4360.

Passador, L. *et al.* (1996) 'Functional analysis of the *Pseudomonas aeruginosa* autoinducer PAI.', *Journal of bacteriology*, 178(20), pp. 5995–6000.

Pearson, J. P., Van Delden, C. and Iglewski, B. H. (1999) 'Active efflux and diffusion are involved in transport of *Pseudomonas aeruginosa* cell-to-cell signals.', *Journal of bacteriology*, 181(4), pp. 1203–10.

Pearson, J. P., Pesci, E. C. and Iglewski, B. H. (1997) 'Roles of *Pseudomonas aeruginosa* las and rhl quorum-sensing systems in control of elastase and rhamnolipid

biosynthesis genes.', *Journal of bacteriology*, 179(18), pp. 5756–67.

Pessi, G. and Haas, D. (2000) 'Transcriptional control of the hydrogen cyanide biosynthetic genes hcnABC by the anaerobic regulator ANR and the quorum-sensing regulators LasR and RhlR in *Pseudomonas aeruginosa*.', *Journal of bacteriology*, 182(24), pp. 6940–9.

Pier, G. B. *et al.* (2001) 'Role of alginate O acetylation in resistance of mucoid *Pseudomonas aeruginosa* to opsonic phagocytosis', *Infection and Immunity*, 69(3), pp. 1895–1901. doi: 10.1128/IAI.69.3.1895-1901.2001.

Rasamiravaka, T. *et al.* (2015) 'The Formation of Biofilms by *Pseudomonas aeruginosa* : A Review of the Natural and Synthetic Compounds Interfering with Control Mechanisms', *BioMed Research International*, 2015, pp. 1–17. doi: 10.1155/2015/759348.

Rasmussen, T. B. *et al.* (2005) 'Identity and effects of quorum-sensing inhibitors produced by Penicillium species', *Microbiology*, 151(5), pp. 1325–1340. doi: 10.1099/mic.0.27715-0.

Ren, D., Sims, J. J. and Wood, T. K. (2001) 'Inhibition of biofilm formation and swarming of Escherichia coli by (5Z)-4-bromo-5-(bromomethylene)-3-butyl-2(5H)-furanone', *Environmental Microbiology*, 3(11), pp. 731–736. doi: 10.1046/j.1462-2920.2001.00249.x.

Ren, D., Zuo, R. and Wood, T. K. (2005) 'Quorum-sensing antagonist (5Z)-4-bromo-5-(bromomethylene)-3-butyl-2(5H)- furanone influences siderophore biosynthesis in

Pseudomonas putida and *Pseudomonas aeruginosa*', *Applied Microbiology and Biotechnology*, 66(6), pp. 689–695. doi: 10.1007/s00253-004-1691-6.

Rodrigues, M. *et al.* (2019) 'Wound healing: A cellular perspective', *Physiological Reviews*, 99(1), pp. 665–706. doi: 10.1152/physrev.00067.2017.

Rothe, K., Tsokos, M. and Handrick, W. (2015) 'Animal and Human Bite Wounds', *Deutsches Arzteblatt international*, pp. 433–443. doi: 10.3238/arztebl.2015.0433.

Ruffin, M. *et al.* (2016) 'Quorum-sensing inhibition abrogates the deleterious impact of *Pseudomonas aeruginosa* on airway epithelial repair', *FASEB Journal*, 30(9), pp. 3011–3025. doi: 10.1096/fj.201500166R.

Ruffin, M. and Brochiero, E. (2019) 'Repair Process Impairment by *Pseudomonas aeruginosa* in Epithelial Tissues: Major Features and Potential Therapeutic Avenues', *Frontiers in Cellular and Infection Microbiology*. Frontiers, 9, p. 182. doi: 10.3389/fcimb.2019.00182.

Rybtke, M. *et al.* (2015) '*Pseudomonas aeruginosa* Biofilm Infections: Community Structure, Antimicrobial Tolerance and Immune Response', *Journal of Molecular Biology*. Academic Press, pp. 3628–3645. doi: 10.1016/j.jmb.2015.08.016.

Sakuragi, Y. and Kolter, R. (2007) 'Quorum-sensing regulation of the biofilm matrix genes (pel) of *Pseudomonas aeruginosa*.', *Journal of bacteriology*. American Society for Microbiology, 189(14), pp. 5383–6. doi: 10.1128/JB.00137-07.

Sappington, K. J. *et al.* (2011) 'Reversible signal binding by the *Pseudomonas*

aeruginosa quorum-sensing signal receptor LasR', *mBio,* 2(1). doi: 10.1128/mBio.00011-11.

Schultz, G. *et al.* (2017) 'Consensus guidelines for the identification and treatment of biofilms in chronic nonhealing wounds', *Wound Repair and Regeneration*, 25(5). doi: 10.1111/wrr.12590.

Schuster, M., Urbanowski, M. L. and Greenberg, E. P. (2004) 'Promoter specificity in *Pseudomonas aeruginosa* quorum sensing revealed by DNA binding of purified LasR', *Proceedings of the National Academy of Sciences of the United States of America,* 101(45), pp. 15833–15839. doi: 10.1073/pnas.0407229101.

Seed, P. C., Passador, L. and Iglewski, B. H. (1995) 'Activation of the *Pseudomonas aeruginosa* lasI gene by LasR and the Pseudomonas autoinducer PAI: An autoinduction regulatory hierarchy', *Journal of Bacteriology,* 177(3), pp. 654–659. doi: 10.1128/jb.177.3.654-659.1995.

Shetye, G. S. *et al.* (2013) 'Structures and biofilm inhibition activities of brominated furanones for Escherichia coli and *Pseudomonas aeruginosa*', *MedChemComm,* 4(7), p. 1079. doi: 10.1039/c3md00059a.

Sio, C. F. *et al.* (2006) 'Quorum Quenching by an N-Acyl-Homoserine Lactone Acylase from *Pseudomonas aeruginosa* PAO1', *Infection and immunity,* 74(3), pp. 1673–1682. doi: 10.1128/IAI.74.3.1673.

Streeter, K. and Katouli, M. (2016) '*Pseudomonas aeruginosa*: A review of their pathogenesis and prevalence in clinical settings and the environment.', *Infection,*

Epidemiology and Medicine, 2(1), pp. 25–32. doi: 10.7508/iem.2016.01.008.

Sung, W. S. *et al.* (2007) '2,5-dimethyl-4-hydroxy-3(2H)-furanone (DMHF); antimicrobial compound with cell cycle arrest in nosocomial pathogens', *Life Sciences*, 80(6), pp. 586–591. doi: 10.1016/j.lfs.2006.10.008.

Toder, D. S., Gambello, M. J. and Iglewski, B. H. (1991) '*Pseudomonas aeruginosa* LasA: a second elastase under the transcriptional control of lasR.', *Molecular microbiology*, 5(8), pp. 2003–10.

Tolker-Nielsen, T. (2014) '*Pseudomonas aeruginosa* biofilm infections: From molecular biofilm biology to new treatment possibilities', *Apmis*, 122(s138), pp. 1–51. doi: 10.1111/apm.12335.

Ueda, A. and Wood, T. K. (2009) 'Connecting quorum sensing, c-di-GMP, pel polysaccharide, and biofilm formation in *Pseudomonas aeruginosa* through tyrosine phosphatase TpbA (PA3885).', *PLoS pathogens*, 5(6), p. e1000483. doi: 10.1371/journal.ppat.1000483.

Ventre, I. *et al.* (2003) 'Dimerization of the quorum sensing regulator RhlR: Development of a method using EGFP fluorescence anisotropy', *Molecular Microbiology*, 48(1), pp. 187–198. doi: 10.1046/j.1365-2958.2003.03422.x.

Verstraeten, N. *et al.* (2008) 'Living on a surface: swarming and biofilm formation', *Trends in Microbiology*, 16(10), pp. 496–506. doi: 10.1016/J.TIM.2008.07.004.

Wade, D. S. *et al.* (2005) 'Regulation of Pseudomonas quinolone signal synthesis in

Pseudomonas aeruginosa.', *Journal of bacteriology*, 187(13), pp. 4372–80. doi: 10.1128/JB.187.13.4372-4380.2005.

Welch, M. *et al.* (2000) 'N-acyl homoserine lactone binding to the CarR receptor determines quorum-sensing specificity in Erwinia.', *The EMBO journal*, 19(4), pp. 631–41. doi: 10.1093/emboj/19.4.631.

Wu, H. *et al.* (2004) 'Synthetic furanones inhibit quorum-sensing and enhance bacterial clearance in *Pseudomonas aeruginosa* lung infection in mice', *Journal of Antimicrobial Chemotherapy*, 53(6), pp. 1054–1061. doi: 10.1093/jac/dkh223.

Yang, S. *et al.* (2014) 'Bicyclic brominated furanones: A new class of quorum sensing modulators that inhibit bacterial biofilm formation', *Bioorganic and Medicinal Chemistry*, 22(4), pp. 1313–1317. doi: 10.1016/j.bmc.2014.01.004.

Zaidi, A. and Green, L. (2019) 'Physiology of haemostasis', *Anaesthesia and Intensive Care Medicine*, pp. 152–158. doi: 10.1016/j.mpaic.2019.01.005.

Chapter 2

Formulation and characterisation of PVA borate hydrogels as furanone delivery systems

2.1 Introduction

Hydrogels can be broadly defined as hydrophilic, three dimensional, crosslinked polymer networks capable of absorbing and holding large amounts of fluid relative to their dry weight (Chai *et al.*, 2017). The first synthetic hydrogels were produced by Wichterle and Lim as an alternative to hard plastics for biomedical alloplastic and prosthetic applications (Wichterle and Lim, 1960). Since these early studies hydrogels, in various forms, have become more prevalent in a wide range of areas including cosmetics, biological and tissue engineering, as well as domestic and healthcare use (Masuda, 1994; Bae, Nam and Park, 2019; Gupta *et al.*, 2019; Nezhad-Mokhtari *et al.*, 2019). While polymer hydrogels all fall under the same broad definition, substantial variation in the properties and characteristics can be achieved by changing one or more aspects of a hydrogel's formulation. These changes can include polymer concentration and polymer type (i.e. natural, synthetic, or co-polymers), crosslinking concentration and crosslinking type (i.e. physical or chemical cross linking), gel formation method (e.g. *in-situ* forming or pre-formed) and the addition of rheology modifiers, such as plasticisers. This section will give a brief overview of the different types of polymers commonly used in the production of hydrogels, the different types of crosslinking used and some of the wider applications of hydrogels. Focus will then be placed on the use of hydrogels in wound healing and drug delivery.

2.1.1 Use of natural and synthetic polymers in the production of hydrogels

Hydrogels can be produced using a wide range of polymers including both naturally occurring and synthetically produced polymers. Each polymer type will produce a hydrogel with a distinct set of properties and potential uses.

Natural plant derived polymers, such as alginate or cellulose, and animal derived polymers such as silk, gelatin and chitosan have all been previously used to produce

hydrogels (Konishi *et al.*, 2003; Rammenssee *et al.*, 2005; Olaru *et al.*, 2018; Bae, Nam and Park, 2019; Fan *et al.*, 2019). These natural polymer hydrogels have proven useful in a wide range of areas but particularly in medicine. The extensive application of these polymers for biomedical purposes is often attributed to their high biocompatibility, low toxicity, and their biodegradability (Calvo Catoira *et al.*, 2019). Synthetic polymers are also often used in biomedical applications. However, while polymers, such as gelatin and alginate are naturally biocompatible, producing synthetic polymers from base components or monomers means that these materials are highly modifiable. This means that the biocompatibility and physical properties can be finely tuned to formulate a hydrogel tailored to serve a particular purpose. By exploiting the tunability of synthetically produced polymers, such as poly(vinyl alcohol) (PVA) and poly(propylene), highly complex gels can be produced. For example, hydrogels which are responsive to changes in local pH or fluctuations in environmental temperature are easily achieved (Hibbins *et al.*, 2017; Avais and Chattopadhyay, 2019). Similarly, hydrogels with a highly tuned rate of degradation are possible meaning that tightly controlled drug release can also be achieved (Ashley *et al.*, 2013).

2.1.2 Crosslinking types in hydrogels

In order for a hydrogel to form, the macromolecular polymer strands must be linked to form a three-dimensional network of interconnected polymer strands. This process begins with individual polymer strands in a solution (known as a sol) linking with other strands which are in close proximity. As this linking process progresses, a point is reached in which the linking is so extensive that the individual polymer strands can now be considered a single large macromolecule (known as a gel) (Ross-Murphy and McEvoy, 1986). The point at which a sol becomes a gel is known as the sol-gel

transition point. This process, known as gelation, can be achieved with a number of types of crosslinking. Polymer gels can be sub classified based on the mechanism of crosslinking used to form them. They can be classified as physically linked gels, chemically crosslinked gels, or entangled network gels.

Chemically crosslinked gels are hydrogels in which crosslinking is achieved through the addition of a chemical crosslinking agent. These chemically crosslinked hydrogels can be formed with a number of cross linking methods including free radical polymerisation (Jeong *et al.*, 2007), enzymatically mediated crosslinking (Lee, Bae and Kurisawa, 2015) and covalent bonding (Marco-Dufort and Tibbitt, 2019). The covalent bonds in these hydrogels are often strong and non-reversible due to high bond energy (Li *et al.*, 2018). This often means that covalently crosslinked hydrogels are more stable under a range of conditions and usually have tuneable physical properties (Hu *et al.*, 2019). As such, chemically crosslinked gels are often used in biomedical applications such as drug delivery systems (Larrañeta *et al.*, 2018) and the production of contact lenses (Rosa dos Santos *et al.*, 2009).

Physically crosslinked hydrogels are gels in which crosslinking is achieved without the use of a chemical crosslinking agent. These gels can be crosslinked through bonds such as electrostatic interactions, hydrophobic interactions, physical entanglement of the polymer network, and π-π stacking (H*u et al*, 2019). As these gels do not require additional chemicals to produce, they are often used to ameliorate issues which arise through the use of chemical crosslinking agents such as unwanted off target effects, leeching of the crosslinker from the hydrogel, impairment of biocompatibility, and interactions with any active compounds entrapped within the gel (Hennink and van Nostrum, 2012; Zhang, Zhang and Wu, 2013).

The effects of the chosen polymer, crosslinking agent, and choice of liquid phase of a hydrogel can interact in a number of ways to result in a wide range of potential properties. These properties can be altered and designed to give a hydrogel with particular characteristics such as elasticity, durability, flow and degradation. Due to their enormous versatility, hydrogels have found use in a wide range of fields.

2.1.3 Applications of hydrogels

Hydrogels have been used in a range of purposes in a variety of settings. These include use in personal care products, food science and bioremediation. In each of these uses the unique proprieties of hydrogels have made them superior to alternative methods.

The superabsorbent properties of hydrogels, particularly acrylamide, polyacrylate and PVA based hydrogels, have been used for many years in both infant and adult incontinence products such as nappies and pads. Here, the ability of hydrogels to absorb and retain large amounts of liquid offer a clear advantage over cloth only products by sequestering moisture and preventing moisture damage to the adjacent skin (Bashari, Rouhani Shirvan and Shakeri, 2018; Castrillon *et al.*, 2019).

In food technology, hydrogels are being used in numerous applications. Recently, hydrogels have shown to be highly effective in stabilising oil in water Pickering emulsions at low pH as well as allowing for controlled release of a payload at near neutral pH (Lim *et al.*, 2020). In this instance, the use of natural calcium alginate hydrogels is clearly advantageous due to their relative low cost to manufacture, high biocompatibility and food grade status (Ali and Ahmed, 2018). Combination natural and food grade synthetic polymer hydrogels have also been used to good effect for the oral co-delivery of vitamins and minerals. These pectin-polyethylene glycol (PEG) hydrogels showed excellent loading of vitamin D, calcium, vitamin C and iron. Loaded pectin-PEG hydrogels exhibited a controlled degradation in an intestinal pH indicating

that the vitamin and mineral payload would be released in this environment (Gautam and Santhiya, 2019). Again, the biocompatibility and pH responsive nature of these hydrogels is a clear advantage.

Hydrogels also show great utility in the field of bioremediation where they have been deployed in several ways. Firstly, hydrogels have been shown to be highly effective substrates for the removal of toxic impurities from aquatic environments (Shalla *et al.*, 2019). For example, in 2019, Lone *et al.* showed that composite gelatin-chitosan hydrogel particles could effectively remove 98% of mercury 2^+ ions and 34% of lead 2^+ from water samples (Lone *et al.*, 2019). This removal was attributed to the reactive sites on the polymer strands. Similarly, the work of Hui *et al.* showed the successful removal of approximately 11 mg of phosphate, a common pollutant of waterways, per gram of a novel PVA hydrogel bead (Hui, Zhang and Ye, 2014). These PVA hydrogel beads were functionalised with aluminium 3+ ions. The phosphate in contaminated water was removed via an ion exchange reaction and was held within the hydrogel resin. These studies show the utility of hydrogels with naturally occurring reactive sites but also those hydrogels which have been functionalised to contain non-native reactive groups.

The studies noted here clearly demonstrate that hydrogels are a highly versatile material and have a broad range of uses in many areas. One of the main sectors which has embraced the use of hydrogels is the biomedical sector. Hydrogels have been used in the biomedical field for the production of contact lenses and as scaffolds for tissue engineering. However, two applications for hydrogels which are of particular relevance to this work are their use as drug delivery vehicles and the use of hydrogels as wound therapeutics.

2.1.4 Hydrogels as wound therapeutics

There are a significant number of wound dressings currently in clinical use which incorporate hydrogels. These include both amorphous hydrogels, such as Askina Gel, and hydrogel sheet dressings such as Actiform Cool (Joint Formulary Comittee, 2019). Hydrogel dressings are primarily used in the treatment of dry and necrotic wounds. In such wounds, the high water content of hydrogels allows them to donate moisture to the dry wound bed effectively, thus assisting with debridement (Koehler, Brandl and Goepferich, 2018). Also, it has been known for nearly 60 years that maintaining a moist wound environment greatly reduces wound healing time (Winter, 1962) and therefore, by donating moisture and maintaining that moist environment, hydrogels assist wound healing on two fronts.

2.4.1.1 Non-medicated hydrogel wound dressings

Some hydrogel dressings are claimed to not only help reduce reported wound pain in patients but also helping to remove slough (the mass of loose dead tissue often found in wounds) and increasing wound granulation and epithelialisation (Holger Kapp, 2006; Zoellner, Kapp and Smola, 2007). While these particular studies were funded by the manufacturer of the dressing being tested, many independent studies have shown the benefits of hydrogel dressings in wound healing.

In a systematic review and meta-analysis of 43 studies conducted between 1998 and 2018, Zhang *et al.* (2019) found that the application of hydrogels was highly beneficial in a range of wound types including acute traumatic wounds such as animal bites, thermal injuries such as second-degree burns, and chronic wounds like diabetic foot ulcers. The application of a hydrogel dressing in these cases was found to not only reduce wound healing time but also to reduce the overall pain associated with the wound (Zhang *et al.*, 2019).

2.4.1.2 Antimicrobial hydrogels as wound dressings

Due to the compelling evidence that non-medicated hydrogels are highly beneficial in both reducing wound pain and expediting wound closure there has been much research into the development and assessment of antimicrobial hydrogel wound dressings. Infections, and, in particular, bacterial infections in the form of a biofilm, are the most common cause of delayed healing in wounds (Leaper, Assadian and Edmiston, 2015). Therefore, the development of an antimicrobial hydrogel that can both prevent, or eradicate, infections while simultaneously promoting wound closure and reducing pain is an obvious goal for clinicians. Such a therapy would also greatly improve clinical outcomes for patients.

There has been an abundance of research surrounding the development and assessment of antimicrobial hydrogels in recent years. These hydrogels have often been formulated from inherently antimicrobial polymers such as chitosan. Hydrogels have also been loaded with an antimicrobial compound such as silver, and with traditional antibiotics, antimicrobial peptides or natural phytochemicals (Boonkaew *et al.*, 2014; Annabi *et al.*, 2017; Kim *et al.*, 2020; Tamahkar *et al.*, 2020). Many of these antimicrobial hydrogels have been shown to be highly effective in reducing bacterial viability. In 2014, Boonkaew *et al.* showed that the a 2-acrylamido-2-methylpropane sulfonic acid (AMPS) based hydrogel loaded with *in situ* formed silver nanoparticles was effectively able to reduce numbers of viable cells of four bacterial strains; *Staphylococcus aureus* (both methicillin resistant and methicillin sensitive), vancomycin resistant *Enterococcus faecalis* and *Acinetobacter baumanii.* Reductions of 99%, 99%, 97.5% and approximately 90% were reported for these bacteria, respectively. Similarly, the work of Tsou *et al.* (2005) demonstrated that a ciprofloxacin-loaded, 2-hydroxymethacrylate hydrogel was capable of both releasing

the antimicrobial and inhibiting growth of *S. aureus* and *P. aeruginosa.* Interestingly, this work also showed that by increasing the amount of cross linking in the gel, the drug release and therefore the antimicrobial effects, could be significantly prolonged. This ability to modulate drug release from hydrogels also makes them an excellent candidate for drug delivery vehicles.

2.1.5 Hydrogels as drug delivery vehicles

It is clear that hydrogels are a highly versatile material with numerous applications across many fields of study. However, possibly the most widely investigated application is the use of hydrogels as drug delivery systems.

2.1.5.1 Hydrogels in drug delivery

Hydrogels, in many different forms, have been shown to be effective drug delivery mechanisms. For example, thin hydrogel films have been investigated for their potential in releasing several different active compounds. The work of El-Aassar *et al.* in 2015 showed up to 100% release of a model dipeptide, l-carnosine, from biopolymer hydrogel films made of κ-carageenan and hyaluronic acid (El-Aassar *et al.*, 2015). Similarly, dual polymer hydrogel films made of carboxymethylcellulose and PVA were reported to release the aminoglycoside antibiotic gentamicin sulphate effectively. Gentamicin was released in a controlled manner (showing first order kinetics) reaching a total release of up to 90% of the total loaded dose over 24 h (Ghorpade *et al.*, 2019). Hydrogel films have also been shown to be useful in the delivery of drugs to specific sites such as the buccal mucosa and have even been suggested as potential delivery mechanisms to the brain (Alopaeus *et al.*, 2020; Singh, Kumar and Rohit, 2020).

Other forms of hydrogel which have been used as drug delivery systems include nanogels, monolithic hydrogels (hydrogels consisting of one single piece, often cast

moulded) and injectable hydrogels (Chen *et al.*, 2019; Xing *et al.*, 2019; Bender *et al.*, 2020; García-Fernández *et al.*, 2020; Mandal *et al.*, 2020). All of these hydrogel forms have been shown to be acceptable for drug delivery in various medical conditions or delivery to specific sites. However, the use of PVA-borate hydrogels as drug delivery systems has not been so extensively studied.

2.1.5.2 PVA-borate hydrogels in drug delivery

PVA-borate hydrogels have been previously shown to be effective drug delivery systems for a range of compounds including vitamins, anaesthetics and antimicrobials (Loughlin *et al.*, 2008; Tang, Pang and Wang, 2017; Tavakoli and Tang, 2017). Tang *et al.* (2017) demonstrated that a PVA hydrogel, crosslinked with a combination of borate glass and freeze-thaw cycles, was able to release vitamin B12 into a phosphate buffered saline (PBS) receiver phase with a total drug release of up to 80% over 90 min. This indicated that borate crosslinked PVA hydrogels could be an excellent drug delivery vehicle for bioactive molecules (Tang, Pang and Wang, 2017). Similarly, a 2017 study by Tavakoli and Tang showed that a Manuka honey/PVA hydrogel crosslinked with borate was an effective delivery system for the release of the macrolide antibiotic erythromycin. While the exact total percentage release of the erythromycin achieved is unclear in their paper, the authors show a definite controlled release profile and demonstrate that the released antibiotic retained its bactericidal activity against *S. aureus* (Tavakoli and Tang, 2017). In 2009, Donnelly *et al.* showed that PVA-borate hydrogels could effectively release two photodynamic antimicrobial chemotherapy agents, namely methylene blue, and meso-tetra (N-methyl-4-pyridyl) porphine tetra tosylate, at volumes of 16.08% and 17.05% of the total loaded doses respectively over 6 h (Donnelly *et al.*, 2009). Loughlin *et al.* (2008) used PVA-borate hydrogels to good effect when delivering the local anaesthetic lidocaine, showing

release of approximately 75% of the total loaded drug at a physiologically relevant temperature and pH.

When the studies detailed here, and their previous successful use as drug delivery systems in our group are considered, it is clear that hydrogels are a remarkable material with a range of unique properties that make them highly useful in many areas. Although the use of borate crosslinked PVA hydrogels as drug delivery vehicles is not widely reported in the literature, they appear to have significant potential for the delivery of a number of different compounds.

2.1.6 Rheology of polymer hydrogels

Rheology is a branch of materials science focused on the deformation and flow of soft matter materials. More specifically, rheology deals with the characterisation of a material's time-dependent response to an applied stress or force (Struble and Ji, 2001). This response can be measured in several ways. These include measuring how the material flows in response to an applied stress or, in the case of non-Newtonian materials, how its viscosity changes in response to a force. This section will focus on the rheology of amorphous PVA-borate hydrogels for use in wound treatment and healing.

Whether intended for use as a drug delivery system or a wound therapeutic, the rheological properties of hydrogels are of great importance. For example, in the case of amorphous hydrogels the ability of the material to flow and conform to the shape of the wound allows for total contact between the wound bed and the hydrogel (Loughli*n et al*, 2008). Not only does rheology affect the use of hydrogels as a wound therapeutic but the rheology of materials has been shown to have a profound effect on their ability to release drugs (Martinez *et al.*, 2014).

PVA-borate hydrogels have a number of unique properties that make them excellent candidates for wound dressings. These materials display a unique property known as dilatancy (Murphy *et al*, 2012). These dilatant properties mean that the hydrogel material becomes more viscous when a high shear force is applied and is less viscous when no force is applied (Savins, 1968). These properties allow the PVA-borate hydrogels to flow into a wound without the requirement for external forces, therefore, minimising pain and trauma for the patient. Conversely, the application of a force, such as the removal of the gel from a wound, causes the material to increase in viscosity meaning that it may be removed from the wound simply and in one cohesive piece (McCarron *et al.*, 2011).

In this chapter the properties of the formulated hydrogels will be assessed using five measurements. These measurements include defining the linear viscoelastic region, assessing the viscoelastic profile of the material, confirmation of the viscoelastic profile by measuring phase angle shift, assessing changes in viscosity upon the application of a force and, finally, a measurement of the adhesiveness of the materials. Each measurement and the reason for its selection is detailed here.

2.1.6.1 Linear viscoelastic region

The linear viscoelastic region (LVR) is defined as the region in which the material's properties are independent of the magnitude of the stress being applied. This linear behaviour is due to the balancing of the destruction of the internal structure of the material (due to flow) being matched by the formation of new areas of structure due to Brownian motion (Koetting *et al*, 2015). Simply put, the LVR defines the range of shear forces that a material can experience without experiencing the destruction of the internal structure. This is an important measurement to make as it ensures that all

subsequent testing is conducted at a shear force that will not affect the internal structure of the gel and, therefore, not influence other measurements.

2.1.6.2 Viscoelasticity

In this work the viscoelastic properties of the gel will be assessed by measuring both the storage and loss moduli (G′ and G″ respectively) over a range of shear frequencies. G′ can be considered as the solid portion of the hydrogel and represents the elastic energy stored in the polymer network. G″, alternatively, can be considered to be the liquid portion of the gel and represents the energy lost from the system as heat due to material flow (Franck, 2004). Both moduli are measured over a range of shear frequencies and in instances where G′ is greater that G′′ the material is acting more like a solid material. The converse is also true. When G″ is dominant over G′ this indicates the material is behaving more like a liquid (Malvern Intruments Limited, 2016). When G′ and G″ profiles are plotted as a function of shear frequency a crossover point can be identified. The point at which this crossover occurs represents the force required to induce fluid-like flow in the material. This is an important measurement for an amorphous hydrogel wound dressing as the requirement for a high force to induce flow would be disadvantageous as the gel would not readily flow into the wound.

2.1.6.3 Phase angle shift

Phase angle shift (δ) is the observed lag between an applied sinusoidal stress and the deformation of the material being tested. For a completely solid material, such as concrete, no lag between the stress and the response would be observed and, thus, δ would be 0°. For samples which show viscoelastic properties there is a delay between the application of the shear force and the response of the material. This lag would be measured between 1 and 90° with more fluid like samples having a larger δ. For shear

sensitive PVA-borate hydrogels a shear frequency dependent change in δ should be apparent with lower angle shifts seen at higher shear frequencies (indicating solid like behaviour) and δ measurements tending towards 90° at low shear frequencies (indicating liquid like behaviour) (Malvern Intruments Limited, 2016). In this work, phase angle measurements will be used as a validation of the viscoelastic profile of the hydrogel.

2.1.6.4 Viscosity

Viscosity is a measure of the resistance of a fluid to deformation and it is caused by internal intermolecular forces within a material. As previously stated, PVA-borate hydrogels show a force-dependent increase in viscosity known as dilatancy (Murphy *et al.*, 2012). Several suggestions have been made as to why shear thickening occurs but the generally accepted explanation is that the application of shear causes local clustering of solid material in the gel structure, resulting in structural heterogeneity and a general increase in material viscosity (Braun and Rosen, 2000). Measuring the shear frequency-dependent change in viscosity of the PVA-borate hydrogels is crucial. The dilatant nature of the hydrogels is what will allow them to be removed from a wound in one piece (McCarron *et al.*, 2011) and, thus, demonstrating that the hydrogels possess this quality is essential.

2.1.6.5 Adhesiveness

It has been shown previously that the removal of adhesive wound dressings is not only a source of significant worry and pain for patients but that it is also a potential cause of so-called micro-traumas such as removal of the uppermost layers of the skin (Matsumur*a et al*, 2013; Charlesworth *et al*, 2014). Therefore, it is vital to ensure that the formulated hydrogels display as little adhesiveness as possible as the aim is to ensure minimisation of likelihood further damage to the wound area upon removal.

PVA-borate hydrogels will be produced and, using the rheological measurements detailed here, the formulations with the most appropriate physical properties will be selected for drug loading and further biological testing.

2.2 Aims and objectives

This experimental chapter will focus on the formulation and rheological characterisation of a PVA hydrogel which has been crosslinked with sodium tetraborate decahydrate (referred to as borate).

The primary aim of the work detailed in this chapter is to develop and characterise a novel PVA hydrogel for use as a mechanism to deliver furanone compounds to chronic wound biofilms. To achieve this, the following objectives will be addressed. First, a method for the production of PVA hydrogels will be developed. This will include identifying the best production method as well as the optimal grades of polymer to use. Second, an ideal hydrogel formulation will be identified. This will be achieved by rapidly characterising a range of hydrogel formulations using the shear modulus (G) as an indicator for the overall flow properties of the hydrogel. Once the most appropriate candidate formulations have been identified a full rheological characterisation will be undertaken so that an ideal formulation can be identified. Next, the ideal hydrogel formulation will be used to prepare furanone-loaded gels which will then be characterised rheologically to assess the impact of furanone loading on the physical properties of the hydrogel. Finally, the release kinetics of the furanone compounds from the hydrogels will be assessed.

2.3 Materials and methods

2.3.1 Materials and equipment

Poly(vinyl alcohol), molecular weight 31,000-50,000, 98-99% hydrolysed, Poly(vinyl alcohol, molecular weight 31,000-50,000, 87-89% hydrolysed, and sodium tetraborate decahydrate were purchased from Sigma Aldrich (Gillingham, Dorset, UK) and were used without further modification.

4-hydroxy-2,5-dimethyl-3(2H) furanone (HDMF), 2-methyltetrahydrfuran-3-one (MTHF), 5-(1,2-dihydroxyethyl)-3,4-dihydroxy-2(5H)-furanone (ascorbic acid) and 3-hydroxy-4,5-dimethyl-2(5H) furanone (sotolon) were all purchased from Sigma Aldrich (Gillingham, Dorset, UK) and used without further modification.

Poly(vinyl alcohol), 100% hydrolysed, was purchased from Spectrum Chemicals (Wallaston, UK) and used without further modification.

Cuprophan 150M dialysis membrane (MWCO 10,000Da) was purchased from Medicell Membranes (Liverpool, UK)

A Malvern Kinexus Pro Rheometer (Malvern, UK) was used with the included 20mm diameter parallel plate geometry for all rheological testing.

A Varian Cary 50 ultraviolet-visible spectrophotometer (Gatwick, UK) was used for all UV absorbance measurements.

A Jenway 351201 pH meter with integrated thermal probe (Jenway, UK) was used for all pH measurements.

2.3.2 Identification of an ideal hydrogel production method

2.3.2.1 Production of hydrogels from stock solutions

PVA hydrogels were produced using a simple thermal process. Hydrogels were first produced using liquid components (i.e. PVA and borate stock solutions). Following assessment of this method optimisation was performed. Appropriate amounts of a 30% w/w PVA solution and 5% w/w borate solution were weighed out according to the final polymer and crosslinker percentages required for the formulation (see Table 2.1). Solutions were added to a 100 mL beaker and deionised water was added to give a final weight of 50 g. The beaker and total contents were re-weighed, and the weight was recorded. This mixture was briefly stirred and then covered with aluminium foil and placed in a static water bath preheated to 90 °C. Gels were heated at 90 °C for 3 h and stirred using a glass rod every 30 min. Gels were removed from the water bath once a homogenous mixture had formed. Each beaker and contents were weighed, and any mass lost was presumed to be water lost through evaporation and was replaced with fresh deionised water (ensuring a final gel weight of 50 g). Gels were allowed to cool to room temperature and were then transferred to air-tight sample jars. Gel samples were then left at room temperature for a further 18 h prior to rheological testing.

Table 2.1 - A summary of each hydrogel formulation prepared using the liquid component method. Values given in the grey boxes are the required weight (g) of a 30% w/w PVA stock and values in white are the required volume of a 5% borate stock. The highlighted formulation (14% PVA and 3% borate) was not prepared as the required volumes of stock solution would have resulted in a gel of greater than 50g.

		% w/w PVA						
		6	8	9	10	11	12	14
% w/w Borate	1	10	13.3	15	16.6	18.3	20	23.3
		10	10	10	10	10	10	10
	2	10	13.3	15	16.6	18.3	20	23.3
		20	20	20	20	20	20	20
	3	10	13.3	15	16.6	18.3	20	23.3
		30	30	30	30	30	30	30

2.3.2.2 Preparation of hydrogels from dry components

Hydrogels were also prepared using dry powdered components in place of stock solutions. PVA and borate powders were weighed out in appropriate quantities into a beaker. Deionised water was added to give a final weight of 50 g. The beaker and contents were reweighed, and the weight was noted. This mixture was briefly stirred and then covered with aluminium foil and placed in a static water bath preheated to 90 °C. Gels were heated at 90 °C for 3 h and stirred using a glass rod every 30 min. Gels were removed from the water bath once a homogenous mixture had formed. Each beaker and contents were reweighed, and any lost mass was replaced with fresh deionised water to ensure a final gel weight of 50 g. Gels were allowed to cool to room temperature and were then transferred to air-tight sample jars. Gel samples were then left at room temperature for a further 18 h prior to rheological testing. For accurate comparison to the liquid method, an 8% PVA 2% borate gel was made using the powder method.

2.3.2.3 Preparation of varying PVA percentage hydrolysis gels

Gels were prepared using PVA of differing percentage hydrolysis. Gels were prepared using the dry component method outlined in section 2.3.2.2 using 87-89%, 98-99% and 100% hydrolysed PVA. For direct comparisons 8% w/w PVA and 2% w/w borate hydrogels were produced using the various percentage hydrolysis PVA.

2.3.2.4 Rheological assessment of each production method

Hydrogels produced using both the liquid and dry powder methods were assessed to establish their shear moduli using a Malvern Kinexus Pro Rheometer (Malvern, UK). The rheometer was used according to the manufacturer's guidelines. Briefly, a 20 mm diameter parallel plate geometry was used during all testing of hydrogels and a constant shear gap of 1 mm was used throughout all experiments. To measure shear

modulus of the hydrogels a frequency sweep with crossover analysis was performed. The sample was subjected to an increasing range of shear frequencies (0.1 Hz to 150 Hz) and both storage and loss moduli (G′ and G″ respectively) were measured at each shear frequency. Crossover analysis was undertaken to identify the shear modulus (G). The shear modulus can be defined as the point at which G′ is equal to G″.

2.3.3 Identification of an ideal gel formulation

Using the ideal gel production method identified in section 2.3.2.2 a range of hydrogel formulations were produced and compared to identify the ideal formulation for a PVA – borate hydrogel. The formulations prepared and the quantity of PVA and borate used to produce them are summarised in Table 2.2. Gels were compared in terms of shear moduli to identify four potential formulations. Each of these formulations was then subjected to full rheological testing. From this data, an optimal hydrogel formulation was identified. All rheological tests used a Kinexus Pro rheometer (Malvern, UK) and 20 mm diameter parallel plate geometry unless otherwise stated.

2.3.3.1 Production and assessment of PVA-borate hydrogel formulations

A range of hydrogel formulations (Table 2.2) were produced using the powder method described in section 2.3.2.2 and 98-99% hydrolysed PVA (Sigma Aldrich, Dorset UK) was used. Each hydrogel formulation was assessed rheologically to identify the shear modulus as described in section 2.3.2.4. Gels with a shear modulus in the range of 1.5 kPa – 5.5 kPa were considered for further characterisation.

Table 2.2 - A summary of each hydrogel formulation prepared using the powder component method. Values given in the grey boxes are the required weight (g) of PVA and values in white are the required weight of borate.

		% w/w PVA						
		6	8	9	10	11	12	14
% w/w Borate	1	3	4	4.5	5	5.5	6	7
		0.5	0.5	0.5	0.5	0.5	0.5	0.5
	2	3	4	4.5	5	5.5	6	7
		1	1	1	1	1	1	1
	3	3	4	4.5	5	5.5	6	7
		1.5	1.5	1.5	1.5	1.5	1.5	1.5

2.3.3.2 Full rheological characterisation of chosen hydrogel formulations

Hydrogels chosen for further characterisation in section 2.3.3 were fully characterised rheologically to identify their LVR, assess their overall viscoelastic profile, assess their viscosity profile, and finally, to assess their adhesiveness.

To identify the LVR of each gel, samples were subjected to an amplitude sweep. This placed the sample under increasing shear strains over time while measuring both G′ and G″. The amplitude sweep was conducted over a shear strain range of 0.01-200% at a frequency of 1 Hz and 10 samples per decade. Viscoelastic profiles of each gel were assessed by conducting a frequency sweep beginning at a force frequency at 0.01 Hz and ending at a force frequency of 150 Hz (these values representing the upper and lower frequency limit of the rheometer). Measurement of G′, G″ and the phase angle were taken at each frequency tested. The viscosity of the gels was measured at a range of shear frequencies from 50 Hz to 150 Hz using a frequency sweep test. Gel adhesiveness was measured using a pull away test. Normal force was measured over time as the rheometer geometry holding the gel was separated. A greater negative normal force measure on the spindle of the rheometer during the pull-away test indicated a more adhesive gel. These tests were then repeated for each of the chosen gel formulations.

2.3.4 Assessment of furanone release kinetics

Furanone-loaded PVA aerogels were then prepared and their drug release kinetics assessed.

2.3.4.1 Preparation of furanone-loaded hydrogels

Furanone-loaded hydrogels were prepared using a similar method to that detailed in section 2.3.2.2 with one amendment. PVA and borate powders were weighed out according to the quantities shown in Table 2.2 for desired hydrogel formulation. Both powders were added to a beaker that had been paced on a previously zeroed balance. The furanone to be loaded into the hydrogel, either HDMF, MTHF, ascorbic acid or sotolon (Figure 2.1) was weighed out and added to the beaker. A standardised concentration of 1% w/w of furanone was used so that initial testing of a loaded gel could be performed. Deionised water was added the powder components to give a final weight of 50 g. The protocol was completed and furanone-loaded hydrogels were stored as per section 2.3.2.2.

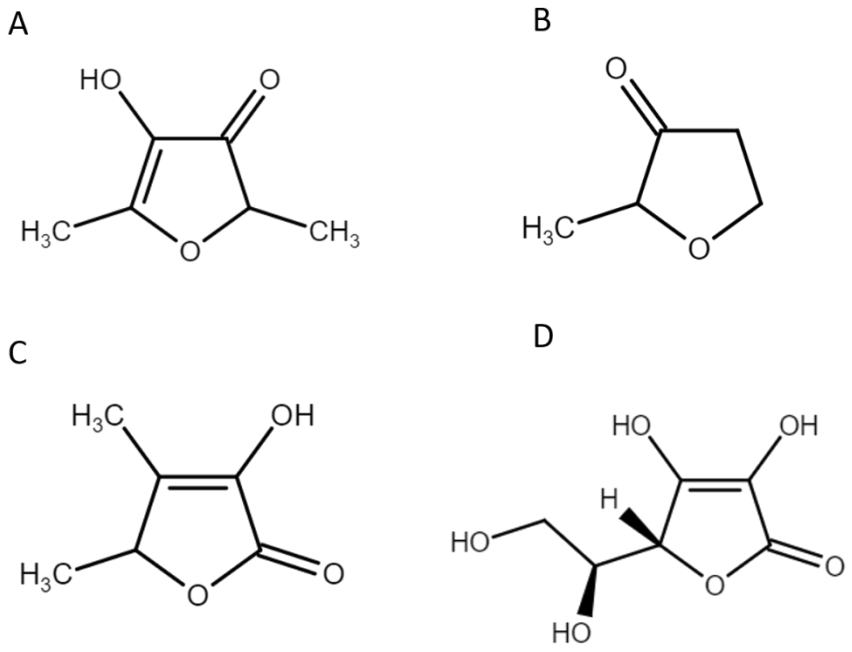

Figure 2.1 – The chemical structures of (a) HDMF, (b) MTHF, (c) sotolon, and (d) ascorbic acid show a high degree of similarity with each compound having a central lactone ring with varying side groups.

2.3.4.2 Assessment of furanone release kinetics

The release of furanone compounds from loaded hydrogels was assessed using a Franz diffusion cell (Figure 2.2 a). The diffusion apparatus was prepared as follows. Each cell was rinsed thoroughly with 100% ethanol followed by three deionised water rinses to ensure that no contaminants were present. Each cell was filled with 15 mL deionised water to act as receiver phase for the furanone ensuring that a slight meniscus was seen above the neck of the cell and that the sampling port was filled to the 500 µL mark (Figure 2.2 b). A 2 cm x 2 cm square of semi permeable Cuprophan 150M dialysis membrane (MWCO 10,000 Da) (Medicell Membranes, Liverpool, UK) was placed on top of the diffusion cell ensuring good contact between the membrane and the receiver phase and avoiding the introduction of bubbles into the system. The sample chamber was then placed on top of the diffusion cell and clamped to hold the membrane in place. The magnetic stirrers were started, the water pump was set to 37 °C and the

temperature was allowed to equilibrate for 60 min. Samples of loaded hydrogel were weighed out into 1 g amounts. Each sample was placed in the sample chamber of the diffusion cell ensuring good contact between the membrane and the sample. A 500 µL volume of the receiver phase was taken from the sampling port of the diffusion cell and 500 µL of fresh receiver phase was added to the diffusion cell ensuring the sample port was filled to the mark. Samples of receiver phase were then analysed via ultraviolet-visible spectroscopy over the full range of wavelengths (190 - 800 nm) to quantify furanone concentrations in the receiver phase. Furanone release was then calculated and plotted as a percentage release of the total furanone concentration in the hydrogel sample. Measurements of the furanone release were taken every 60 min for 8 h and then again after 24 h. All samples were tested in triplicate and data was reported as the mean ± S.D. An unloaded hydrogel was used as a negative control.

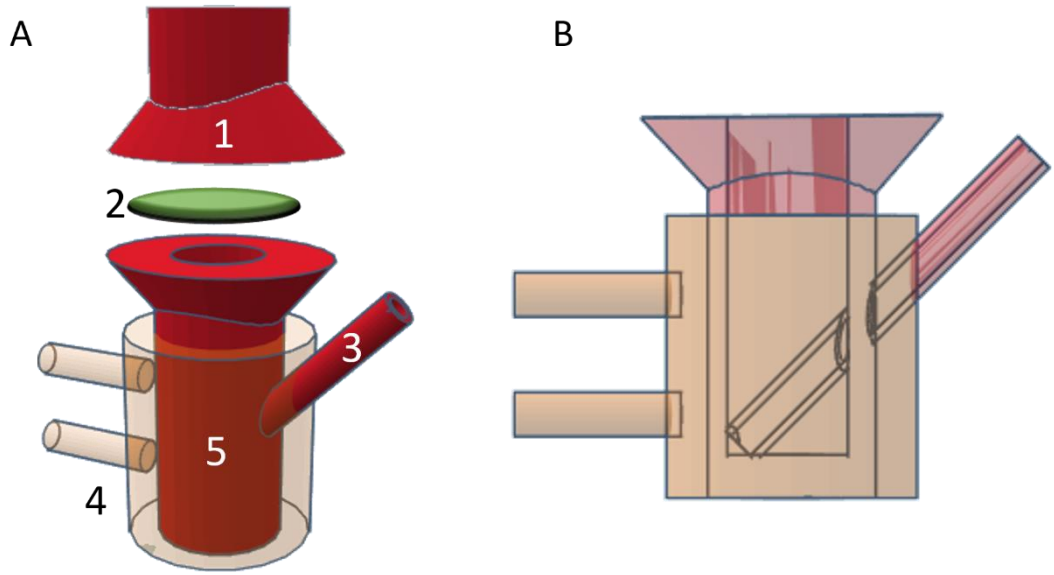

Figure 2.2 – (a) a three-dimensional schematic of a Franz diffusion cell and (b) an orthogonal view of a Franz diffusion cell.

(a) A sample is placed in the sample chamber [1] and drug is released through a semi permeable membrane [2]. Samples of receiver phase are removed from the sample port [3] for analysis. A water jacket [4] ensures that the receiver phase in the cell [5] is kept at a constant temperature. (b) An orthogonal view of a Franz diffusion cell.

2.3.5 Stability of furanone compounds

Furanone compounds were assessed for their stability under a range of conditions. Each furanone was tested in aqueous solution, in a solution of 1% sodium tetraborate and in pH adjusted solution with a pH similar to that of a 1% sodium tetraborate solution. Furanones were tested under these conditions at room temperature and 90 °C. These conditions were selected to mimic the conditions which the compounds would be exposed to during the formation of a hydrogel.

2.3.5.1 Assessment of furanone stability by UV spectrometry.

Furanones were dissolved into 50 mL deionised water to give a solution with a concentration of 1% furanone by weight. These stock solutions were then incubated under each of the different conditions noted above. Each furanone was tested for

degradation under each condition individually and in combination with other conditions. The conditions used were;

- Incubation in aqueous solution at room temperature
- Incubation in aqueous solution at 90 °C
- Incubation at room temperature in the presence of 1% borate
- Incubation at 90 °C in the presence of 1% borate
- Incubation at room temperature at pH 9.31 (equivalent to a 1% borate solution)
- Incubation at pH 9.31 at 90 °C.

These conditions represented the conditions under which the gels are formed. Tests performed at pH 9.31 served to establish if any observed degradation was caused by the borate and its associated chemistry specifically or if pH changes caused by borate was the cause. During the incubation of the furanone stock solutions 1 mL samples of furanone solution were removed every 5 min up to 30 min incubation then every 20 min up to 90 min incubation. Samples were analysed in a UV spectrophotometer (Varian, Gatwick, UK) over the full range of wavelengths (190 – 800 nm) to measure absorbance at the compounds corresponding λ_{max} and to assess any changes in the full absorbance spectrum. Any reduction or increase in the UV-Vis absorbance or change in λ_{max} over the 90 min incubation was assumed to be due to degradation or changes in the structure of the furanone compound.

2.3.5.2 Assessment of furanone pH under hydrogel forming conditions.

To assess the change in pH of each furanone during heating and identify the temperature at which pH changes may occur, solutions of 1% w/w borate and 1% w/w of a furanone were prepared in triplicate. The solutions were covered and placed on a hot plate and heated to 70 °C. The pH of the solution was recorded after every 5 °C

increase in solution temperature using a Jenway 351201 pH meter with integrated thermal probe (Jenway, UK). The temperature probe was used at all times throughout the experiment to ensure that the recorded pH was adjusted for the temperature of the solution. This method was used to assess each furanone and a borate only solution as a control. The pH was plotted as a function of temperature.

As the hot plate method described above was not suitable for assessing the long-term effects of heating a second method was used. Furanone/borate solutions were prepared as described above. These solutions were covered and placed in a water bath pre-heated to 90 °C for 3 h (representative of the average time to prepare a hydrogel). The pH of the solutions was measured every 30 min for the duration of the experiment and the solutions were removed from the water bath. Finally, the pH was measured again once the solutions had cooled to room temperature. The pH was then recorded as a function of time.

2.4 Results

2.4.1 Identification of an ideal hydrogel production method.

Investigation into the ideal production method for the PVA hydrogels showed that the liquid method showed high variability in the viscoelastic properties of the hydrogels. It was subsequently shown that a production method in which powder components were used in place of the stock solutions eliminated this issue.

2.4.1.1 Production of hydrogels using the liquid method

To identify the ideal formulation for a PVA-borate hydrogel a range of hydrogels were produced with varying concentration of both PVA and borate using the previously established liquid method. A summary of the formulations produced, including their concentrations of both polymer and cross linker can be seen in Table 2.1 in section 2.3.2.1. The shear modulus of each hydrogel formulation was measured and compared. No relationship between the concentration of PVA and shear modulus was observed at any concentration of borate (Figure 2.3 a-c). Similarly, no relationship between shear modulus and borate concentration was noted. Higher concentrations of borate generally resulted in higher shear moduli. However, there were several exceptions (Figure 2.3 a-c).

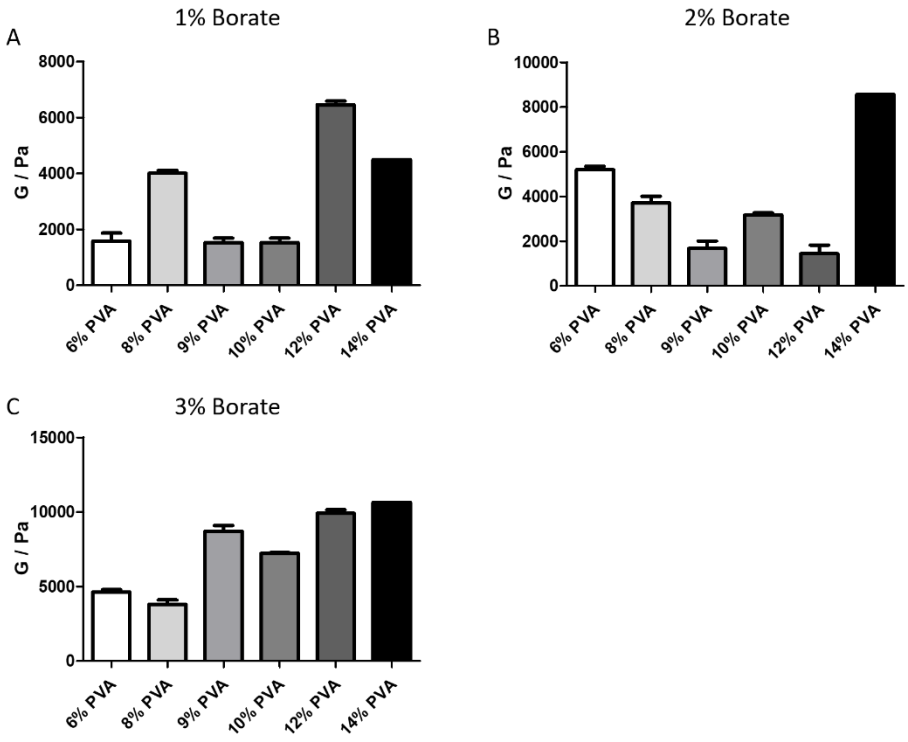

Figure 2.3 - A comparison of the shear moduli (G) of hydrogels with varying formulations.

Hydrogels were prepared with (a) 1% w/w borate, (b) 2% w/w borate and (c) 3% w/w borate. Hydrogel formulations where tested rheologically to measure the shear moduli. No relationship between shear modulus and PVA concentration was found when borate concentration remained the same. Similarly, no relationship between borate concentration and shear modulus was observed. All values represent mean values of independent triplicates (± SD).

2.4.1.2 Comparison of the liquid and powder methods of hydrogel production

A comparison of the shear moduli of hydrogels produced using liquid stocks of each component and those made using dry powder components was made. It was found that the hydrogels produced using the dry powder components had a lower overall lower standard deviation in the shear modulus between independent samples (Figure 2.4). It was discovered that hydrogels containing 8% w/w PVA and 2% w/w borate produced using powdered components had an average shear modulus of 3717 Pa ±238.7 Pa while hydrogels produced using liquid stocks of both components had an average shear modulus of 8592 Pa ± 1027.2 Pa.

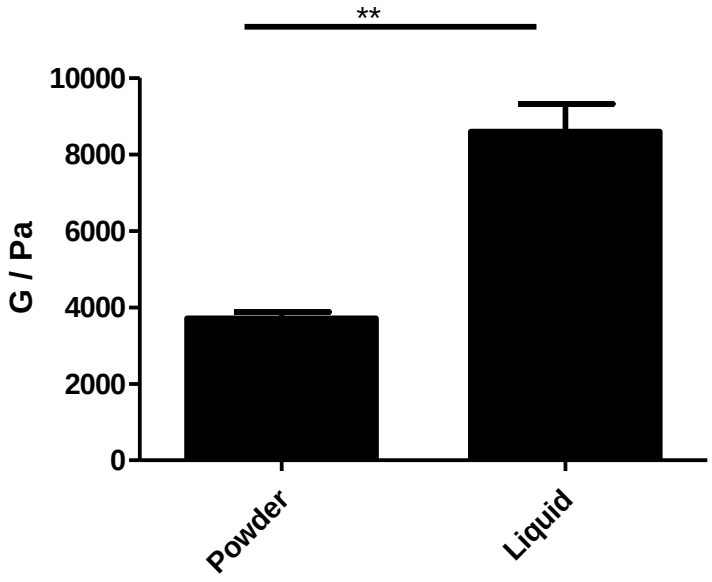

Figure 2.4 - A comparison of the mean shear modulus (G) of hydrogels produced by two distinct methods.

Powder hydrogels were produced using dry powder components and liquid hydrogels were produced using liquid stocks of component chemicals. Powder hydrogels had an average shear modulus of 3717 Pa ± 238.7 whereas hydrogels produced using the liquid stocks had an average shear modulus of 8592 Pa ± 1027.2. Values shown represent mean values of independent triplicates ± standard deviation (SD). Data analysed using a two-tailed t-test. P= 0.0028

Due to the lower standard deviation between samples and the consequent increase in consistency between batches, the dry powder method was carried forward and used in the production of all subsequent hydrogels.

2.4.1.3 Assessment of the impact of PVA type on hydrogel properties

Using the dry powder production method identified above, hydrogels were produced using a range of PVA types with varying hydrolysis percentages. All hydrogels contained 8% w/w PVA and 2% w/w borate. The PVA types tested were 87-89% hydrolysed, 98-99% hydrolysed and 100% hydrolysed. Comparison of the shear modulus of each hydrogel showed no significant difference between gels produced using the 87-88% hydrolysed and 98-99% hydrolysed PVA with an average shear

modulus of 3635 Pa ± 248.1 and 3717 Pa ± 238.7 respectively. A significant difference in shear modulus was seen in hydrogels produced using the 100% hydrolysed PVA with an average shear modulus of 8356 Pa ± 13.9 (Figure 2.5). It was decided that 98-99% hydrolysed PVA would be used in all future hydrogel formulation due to its low inter gel variation and the availability of the compound.

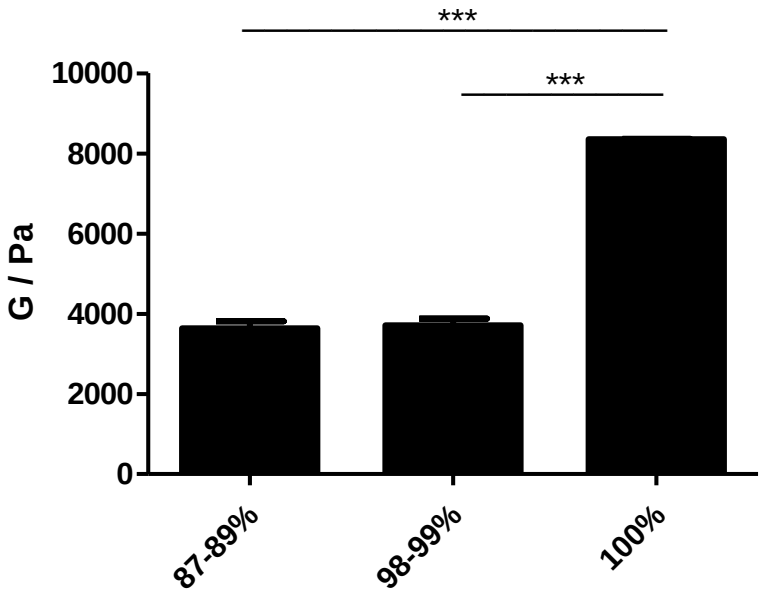

Figure 2.5 - A comparison of the mean shear modulus (G) of hydrogels produced using a range of PVA types with varying hydrolysis percentages.

*Hydrogels produced using 87-88% hydrolysed PVA had an average shear modulus of 3635 Pa ± 248.1 while gels produced using 98-99% hydrolysed PVA and 100% hydrolysed PVA had average shear moduli of 3717 Pa ± 238.7 and 8356 Pa ± 13.9 respectively. Statistical significance was calculated using a 1-way ANOVA with a post-hoc Tukey's multiple comparison test (*** $p<0.001$). All measurements represent mean values of independent triplicates (± SD).*

2.4.2 Identification of an ideal hydrogel formulation

Following the identification of an optimised hydrogel production method an ideal hydrogel formulation was identified. The same range of formulations prepared using the liquid method (Table 2.1) were prepared using the dry powder method and their shear moduli were measured.

2.4.2.1 Rapid assessment of hydrogel formulations produced using an optimised method

The dry powder method of producing hydrogels was shown to superior to the liquid component method. It was found that with the dry powder method there was a clear positive correlation between PVA concentration and hydrogel shear modulus (Figure 2.6 a-c). It was also shown that hydrogels with a higher concentration of crosslinker generally had a higher shear modulus. These correlations were expected when producing polymer hydrogels but was only apparent when using the dry powder method.

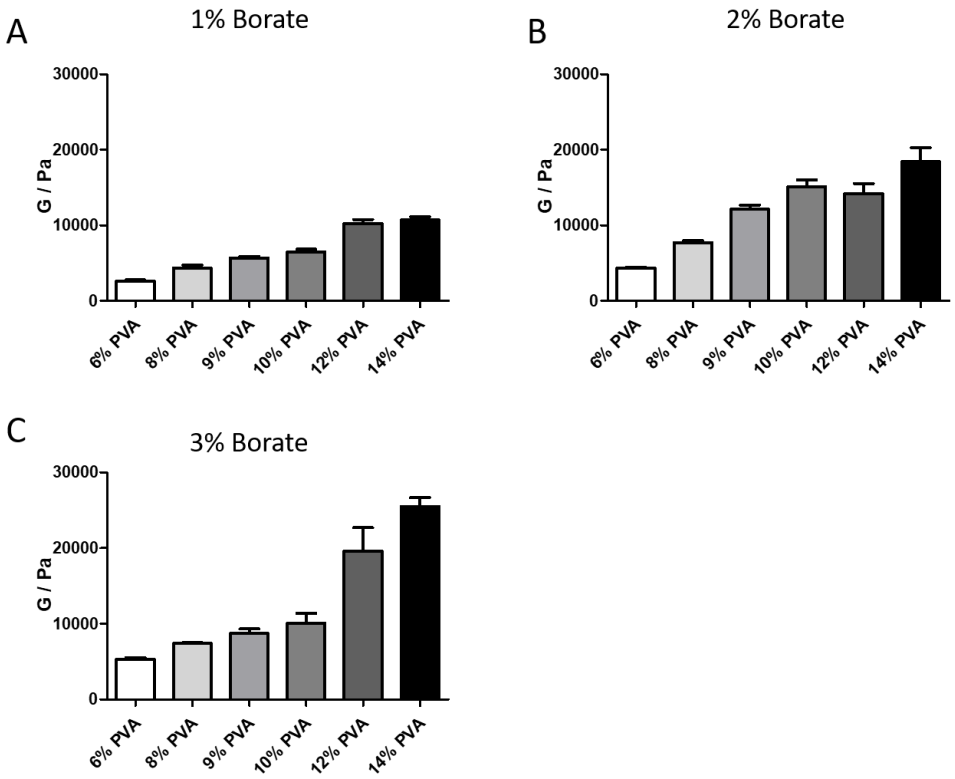

Figure 2.6 - A comparison of the shear moduli (G) of hydrogels with varying formulations produced using dry powder components.

Hydrogels were prepared with (a) 1% w/w borate, (b) 2% w/w borate and (c) 3% w/w borate. Hydrogel formulations where tested rheologically to measure the shear moduli. A clear correlation between shear modulus and PVA concentration was found when borate concentration remained the same. Similarly, a correlation between borate concentration and shear modulus was observed. All values represent mean values of independent triplicates (± SD).

2.4.2.2 Full rheological characterisation of selected formulations

Each of the four candidate hydrogels selected in section 2.3.3.1 were subjected to further rheological characterisation. This characterisation included establishing the LVR of the material, assessing their overall viscoelastic profile, characterising their viscosity and finally measuring the hydrogels adhesiveness or tackiness. All tests were conducted using the Malvern Kinexus Pro rheometer as detailed in section 2.3.3.2

6% w/w PVA, 1% w/w borate

Hydrogels containing 6% w/w PVA and 1% borate showed that both the storage and loss moduli were unaffected at shear strains below 6.3% (Figure 2.7 a). All future tests were carried out below this shear rate to ensure accurate results. Assessment of the viscoelastic profile of this hydrogel formulation showed that the elastic component of the gel was dominant ($G'>G''$) at shear frequencies greater than approximately 1.7 Hz while the viscous component of the gel was dominant ($G'<G''$) at lower shear rates (Figure 2.7 b). This indicates that the sample acts more like a solid when a force is applied rapidly and acts more like a viscous liquid when force is applied slowly. These findings were further confirmed by the measurement of the phase angle (θ) over the same shear frequency range. As shear frequency increased the phase angle tended towards 0° and tended towards 90° when a lower shear frequency was applied indicating more solid like and more fluid like behaviour respectively (Figure 2.6 b). The cross over point ($G'=G''$) was 2274 Pa, meaning that a force greater than 2274 Pa was required to initiate liquid-like flow in this gel. At high frequency shear forces (>50 Hz) the viscosity of this hydrogel increased with shear frequency indicating dilatant behaviour (Figure 2.7 c). This finding is in keeping with real world observations of the shear sensitive nature of the hydrogel. Finally, adhesiveness testing of this hydrogel formulation showed a peak normal force of -6.607 N. over 0.11 s indicating

some adhesiveness which is easily overcome with a small amount of force (Figure 2.7 d).

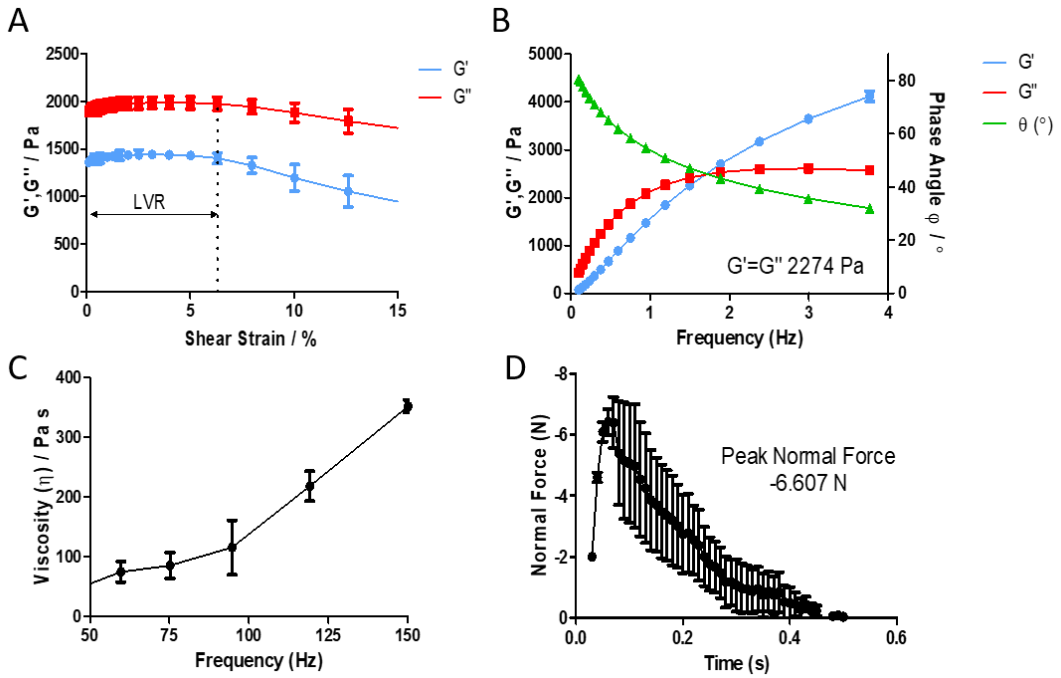

Figure 2.7 – A full rheological profile of a 6% PVA 1% borate hydrogel including measurement of the (a) LVE (b) viscoelastic profile (c) viscosity profile and (d) adhesiveness of the gel.

(a) Measurements of both the storage and loss moduli (G′ and G″ respectively) over a range of shear strains showed no change in either modulus below a shear strain of 6.3%. This indicated that no destruction of the polymer network has occurred below this shear strain. (b) At high shear frequencies the elastic component of the hydrogel is dominant (G′>G″) indicting solid-like behaviour. At low frequencies the liquid component of the hydrogel is dominant (G′<G″) indicating fluid-like behaviour. This is confirmed by phase angle measurement which tend towards 0° at higher frequencies indicating solid-like behaviour and tend towards 90° at lower frequencies indicating fluid-like behaviour. (c) This sample showed dilatant behaviour, increasing in viscosity with increased shear frequency. (d). Adhesiveness testing of this hydrogel showed a peak normal force of -6.607 N experienced over 0.11 s indicating that this hydrogel had a small amount of adhesiveness which released rapidly after the application of a pulling force. All values represent the mean of independent triplicates (± SD).

6% w/w PVA, 2% w/w borate

Rheological testing showed that the storage and loss moduli of a 6% w/w PVA and 2% w/w borate hydrogel were unchanged over the shear rate range of 0% to 7.9%.

This indicates that no destruction of the polymer network had occurred before this upper shear rate (Figure 2.8 a). A gel with a shear rate in this range was used for all further rheological testing. Characterisation of the viscoelastic profile of the hydrogel showed that the elastic component of the gel was dominant at higher shear frequencies ($G' > G''$) while the liquid component dominates at lower shear frequencies ($G' < G''$). This data was further confirmed with phase angle measurements that showed a phase angle that tended towards 0° at higher shear frequencies, typical of materials behaving more like solids and phase angle measurements that tend towards 90° at lower shear frequencies indicating fluid-like behaviour (Figure 2.8 b). Similar to the 6% PVA and 1% borate, this formulation showed dilatant behaviour with increasing viscosity at very high shear rates (Figure 2.8 c). Adhesiveness testing showed a peak normal force of -15.3667 N exerted over approximately 0.09 s indicating that this formulation is considerably more adhesive than the previously tested formulation (Figure 2.8 d).

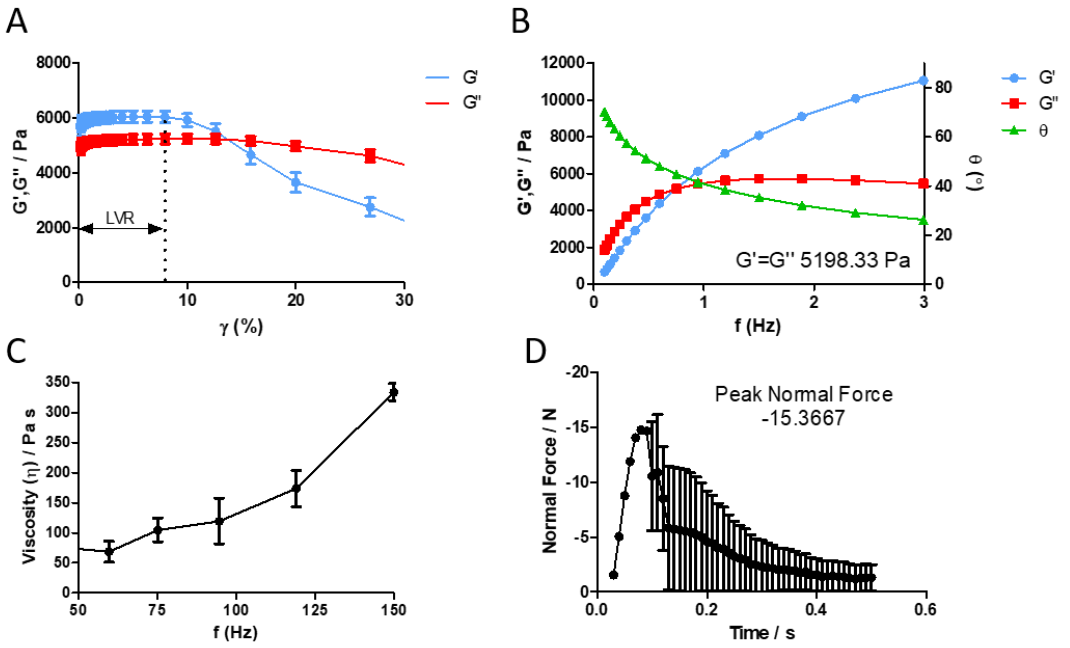

Figure 2.8 – Full rheological profile of a 6% w/w PVA, 2% w/w borate hydrogel including measurement of the (a) LVE (b) viscoelastic profile (c) viscosity profile and (d) adhesiveness of the gel.

(a) G′ and G″ were unchanged over a range of shear strains of 0% to 7.9%. This indicated that no destruction of the polymer network has occurred below this shear strain. (b) At high shear frequencies the elastic component of the hydrogel is dominant (G′>G″) indicting solid-like behaviour. At low frequencies the liquid component of the hydrogel is dominant (G′<G″) indicating fluid-like behaviour. This is confirmed by phase angle measurement which tend towards 0° at higher frequencies indicating solid-like behaviour and tend towards 90° at lower frequencies indicating fluid-like behaviour. (c) This hydrogel was found to show dilatant behaviour and increase in viscosity with increasing shear frequency. (d) Adhesiveness testing of this hydrogel showed a peak normal force of -15.3667 N experienced over 0.09 s. All values represent the mean of independent triplicates (± SD).

6% w/w PVA, 3% w/w borate

Rheological testing of a 6% w/w PVA and 3% sodium tetraborate hydrogel showed a stiffer gel overall. Assessment of the linear viscoelastic region showed no changes in the storage and loss moduli at shear rates below 7.9% (Figure 2.9 a). Assessment of the viscoelastic profile of this hydrogel showed a similar profile to those tested thus far with the storage modulus being dominant at high shear speeds and the loss modulus dominating at low shear speeds. This data was again confirmed with phase angle

measurements. The crossover point for this gel formulation was found to be 4770 Pa at a frequency of approximately 0.5 Hz (Figure 2.9 b). Viscosity measurements over a range of high frequency shear forces this gel formulations showed an increase in viscosity up indicating dilatant behaviour (Figure 2.9 c). Adhesiveness testing of the 6% w/w PVA and 3% w/w borate gel showed a maximum normal force of -19.5267 N exerted over approximately 0.07-0.09 s indicating that this formulation is highly adhesive when compared to previously tested formulations (Figure 2.9 d).

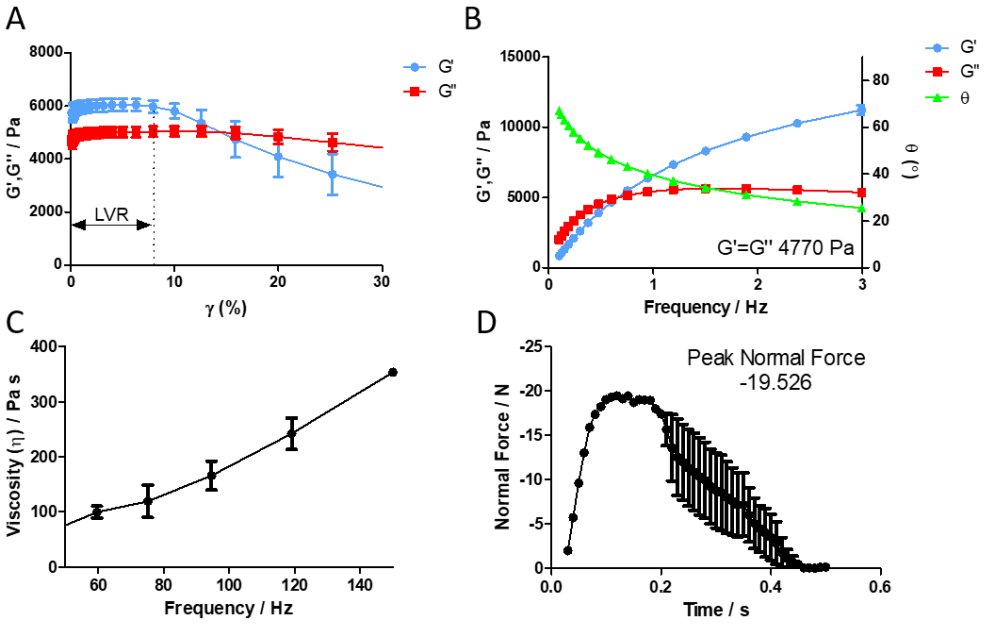

Figure 2.9 – Full rheological profile of a 6% w/w PVA, 3% w/w borate hydrogel including measurement of the (a) LVE (b) viscoelastic profile (c) viscosity profile and (d) adhesiveness of the gel.

(a) Measurements of both the storage and loss moduli (G' and G" respectively) over a range of shear strains showed no change in either moduli below a shear strain of 7.9%. This indicated that no destruction of the polymer network has occurred below this shear strain. (b) At high shear frequencies the elastic component of the hydrogel is dominant (G'>G") indicting solid-like behaviour. At low frequencies the liquid component of the hydrogel is dominant (G'<G") indicating fluid-like behaviour. This is confirmed by phase angle measurement which tend towards 0° at higher frequencies indicating solid-like behaviour and tend towards 90° at lower frequencies indicating fluid-like behaviour. (c) This hydrogel was found to show dilatant behaviour and increase in viscosity with increasing shear frequency. (d) Adhesiveness testing of this hydrogel showed a peak normal force of -19.526 N experienced over 0.09 s indicating that this hydrogel had a small amount of adhesiveness which released rapidly after

the application of a pulling force. All values represent the mean of independent triplicates (± SD).

8% w/w PVA, 1% w/w borate

Characterisation of the 8% w/w PVA and 1% w/w sodium tetraborate hydrogel showed a gel with similar properties to the previously tested gels. Investigation of the linear viscoelastic region showed that this gel formulation experienced no changes in storage or loss modulus at shear rates below 12.5% (Figure 2.10 a). Assessment of the viscoelastic profile showed a dominant storage modulus at high shear speeds and a dominant loss modulus at low shear speeds. This was confirmed by phase angle measurements showing a phase angle that tended towards 0° at higher shear rates. The crossover point for this gel formulation was found to be 6515 Pa at a frequency of approximately 2.5 Hz (Figure 2.10 b). Viscosity measurements showed an increase in gel viscosity with increasing shear frequency. This data shows that the 8% PVA and 1% sodium tetraborate displays shear thickening behaviour (Figure 2.10 c). Adhesiveness testing showed that the 8% w/w PVA 1% hydrogel was slightly adhesive to the steel rheometer geometry surface. A peak normal force of -18.80 N was exerted by the gel in 0.9s. The adhesion of the gel released rapidly once the pulling force was applied (Figure 2.10 d).

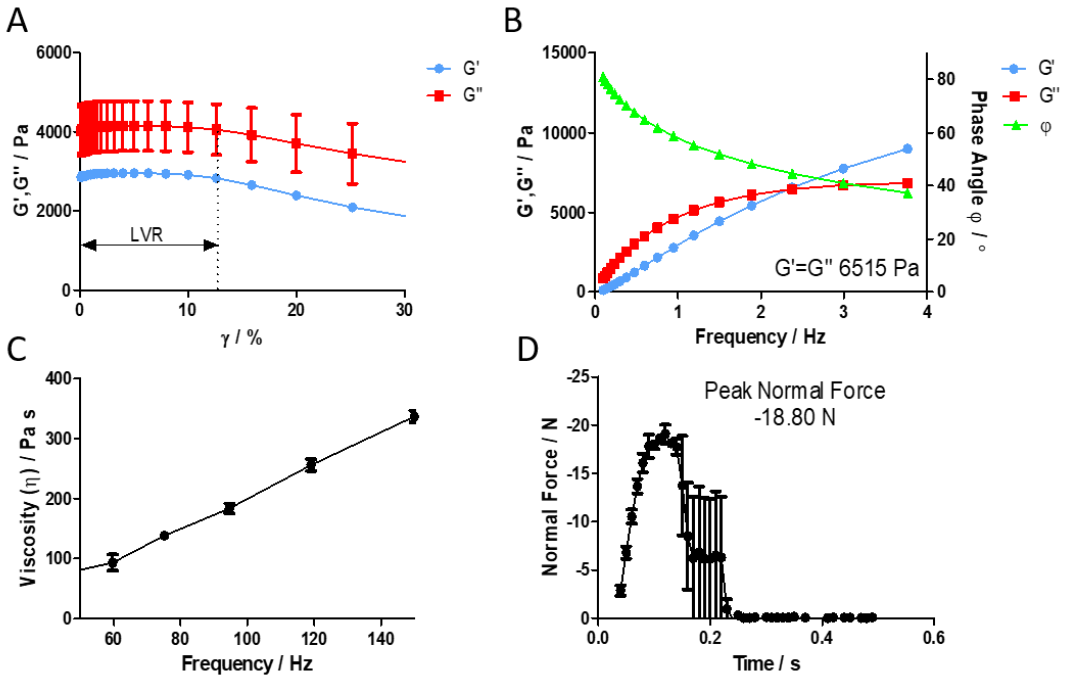

Figure 2.10 – Full rheological profile of an 8% w/w PVA, 1% w/w borate hydrogel including measurement of the (a) LVE (b) viscoelastic profile (c) viscosity profile and (d) adhesiveness of the gel.

(a) Measurements of both the storage and loss moduli (G' and G" respectively) over a range of shear strains clearly showed no change in either moduli below a shear strain of 12.5%. (b) At high shear frequencies the elastic component of the hydrogel is dominant (G'>G") indicting solid-like behaviour. At low frequencies the liquid component of the hydrogel is dominant (G'<G") indicating fluid-like behaviour. This is confirmed by phase angle measurement which tend towards 0° at higher frequencies towards 90° at lower frequencies (c) This formulation was found to show shear thickening behaviour and increase in viscosity with increasing shear frequency. (d) Adhesiveness testing of this hydrogel showed a peak normal force of -18.80 N experienced over 0.09 s indicating that this hydrogel had a small amount of adhesiveness which released soon after the application of a pulling force. All values represent the mean of independent triplicates (± SD).

2.4.3 Selection and drug loading of an ideal formulation

From the rheological characterisation of each hydrogel formulation, the 6% w/w PVA and 1% w/w borate formulation was chosen and carried forward for drug loading due to its low shear modulus and low adhesiveness and ease of handling. These characteristics ensured this formulation would flow easily into a wound and would not adhere to the wound bed, causing further trauma upon removal.

Drug-loaded hydrogels were prepared using the protocol outlined in section 2.3.4.1. All hydrogels were loaded with 1% w/w of each furanone so that direct comparisons could be made between loaded samples.

When loaded with 1% w/w of HDMF, the hydrogels shear modulus was significantly reduced resulting in a very soft gel that that did not hold its shape under gravity. This change in shear modulus was coupled with an obvious colour change from colourless to bright yellow (Figure 2.11 a). When initially mixed with the PVA and the borate solution the HDMF dissolved to form a colourless solution. Upon heating to produce the hydrogel a bright yellow colour was observed, indicating a possible reaction between the HDMF and one or more components of the hydrogel. When loaded with ascorbic acid the hydrogel did not form and the sample remained entirely liquid. A slight colour change was seen from colourless to a faint yellow (Figure 2.11 b). This colour change increased in intensity over a period of five days resulting in a dark brown/orange discoloration (Figure 2.11 b – inset). When the hydrogels were loaded with sotolon at a concentration of 1% w/w the samples did not gel and remained entirely liquid. A very slight pale-yellow colour was observed in the hydrogels (Figure 2.11 c). When hydrogels were loaded with 1% w/w MTHF a clear, homogenous gel was formed (Figure 2.11 d). No discolouration was noted during the production or storage of the MTHF-loaded hydrogels.

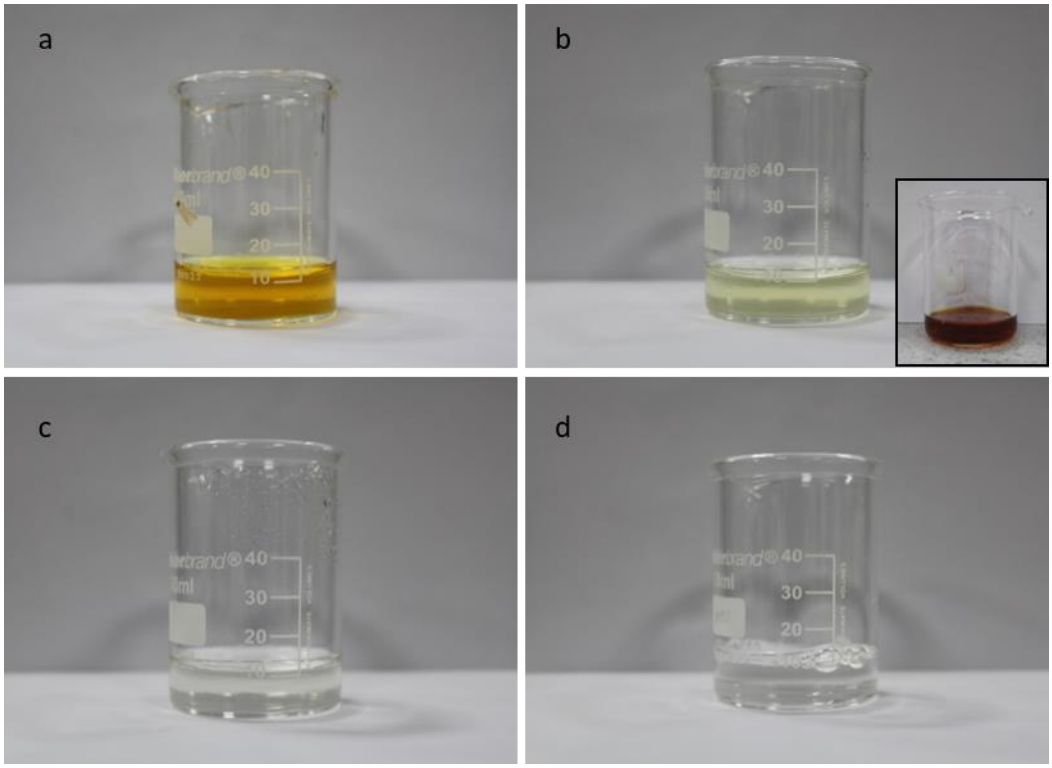

Figure 2.11 - Images of 6% w/w PVA and 1% w/w borate hydrogels loaded with 1% w/w furanone.

(a) HDMF-loaded hydrogel showed a stark colour change from colourless to bright yellow after the heating step of gel production. The hydrogel formed poorly resulting in a gel which did not hold shape well. (b) Ascorbic acid-loaded hydrogels did not form well and the sample was entirely liquid. A slight colour change from colourless to straw yellow was seen post heating that gradually darkened to a brown/orange over 5 days (inset). (c) Sotolon-loaded gels did not form and the sample remained entirely liquid. (d) MTHF-loaded hydrogel formed homogenous gels with an appropriate consistency and no colour change was observed.

2.4.4 Furanone release from loaded hydrogels

The release kinetics of both HDMF and MTHF from a 6% w/w PVA and 3% w/w borate hydrogel were assessed using the protocol outlined in section 2.3.4.2. Ascorbic acid and sotolon-loaded samples were unsuitable for testing due to their significantly altered viscosity.

HDMF was released in a steady manner over 24 h reaching a maximum release of 45% of the total loaded drug (Figure 2.12 a).

MTHF-loaded hydrogels also showed a steady release profile over 24 h. However, when cumulative release was calculated the apparent total release of MTHF was approximately 2000% of the total loaded drug volume (Figure 2.12 b).

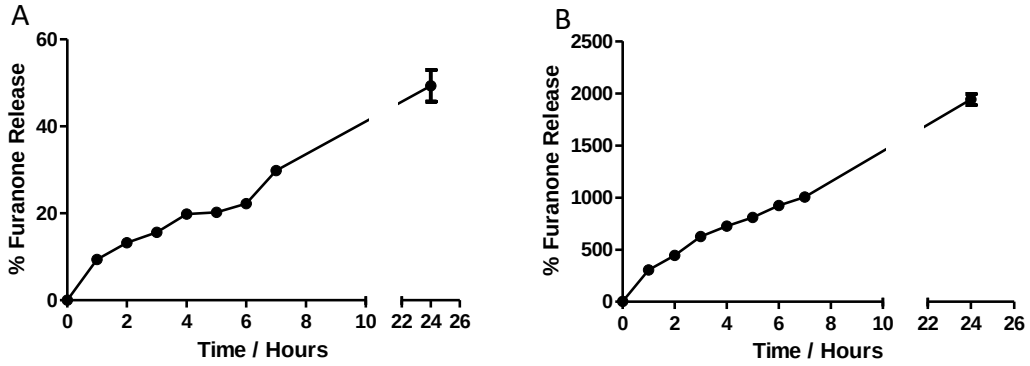

Figure 2.12– Drug release profiles of two furanones; HDMF (a) and MTHF (b) from a 6% w/w PVA and 1% w/w borate hydrogel.

The HDMF-loaded gel showed a steady release of compound over 24 h with a maximum release of 45% of the total loaded drug. The MTHF-loaded hydrogel also showed a steady release profile. However, the calculated release values were above 100% of the total loaded drug. Further investigations into the cause of this are needed.

It was suspected that although the MTHF hydrogels had formed well and no colour changes were observed the furanone had either degraded or reacted with a hydrogel component resulting in a product which was highly absorbent, thus, giving release readings of over 100% of the total loaded drug volume. This finding then prompted investigations into the stability of the furanones in both aqueous solution and under hydrogel forming conditions.

2.4.5 Stability of furanones under hydrogel forming conditions.

The discovery of possible degradation of MTHF during the production of an MTHF-loaded hydrogel prompted an investigation of the stability of all furanones used in this

work. Compounds were tested for their stability under a range of conditions. The conditions tested were representative of those present during the formation of the hydrogels namely; exposure to high temperatures, presence of borate and increased pH.

Furanones were subjected to a range of conditions both individually and in combination. The UV spectra of the furanones were measured to identify any loss of compound or possible changes in compound structures. An aqueous solution of each furanone was subjected to incubation at room temperature with and without 1% borate, incubation at 90 °C with and without 1% borate and finally exposure to a pH representative of that of 1% borate.

2.4.5.1 MTHF degradation

It was shown that when in aqueous solution at room temperature MTHF was apparently stable for the duration of the test with no changes in absorbance and no changes in the λ_{max} of the compound (Figure 2.13 a). This was also seen to be the case when the MTHF was exposed to 90 °C in aqueous solution (Figure 2.13 b). When exposed to 1% borate in aqueous solution at room temperature the absorbance of the MTHF showed some variability over time but this was attributed to variance in the UV-Vis spectrophotometer as no net increase or decrease in absorbance was observed over time (Figure 2.13 c). However, when exposed to a combination of 1% borate and 90 °C temperatures in aqueous solution an obvious increase in absorbance at 285 nm was observed during the experiment (Figure 2.13 d). Analysis of the full absorbance spectrum clearly showed that the entire absorbance spectrum of the compound was both flattening and increasing giving an apparent increase in concentration of MTHF. This finding clearly explains the unusual readings of a more than 100% release seen

in section 2.4.4 (Figure 2.13 e). As the above experiments clearly demonstrate the presence of the 1% borate and the 90 °C temperature appear to act synergistically to cause the changes in the absorbance of the MTHF. It was then necessary to identify if the degradation was due to the presence of borate specifically or, rather, due to the change in pH caused by the borate. MTHF was then exposed to a pH representative of that of 1% borate (pH 9.31). It was discovered that MTHF was stable in the presence of a pH altered solution at both room temperature (Figure 2.13 f) and at 90 °C (Figure 2.13 g). Therefore, it was concluded that the observed changes in the MTHF absorbance was caused specifically by the presence of borate and not simply due to the altered pH.

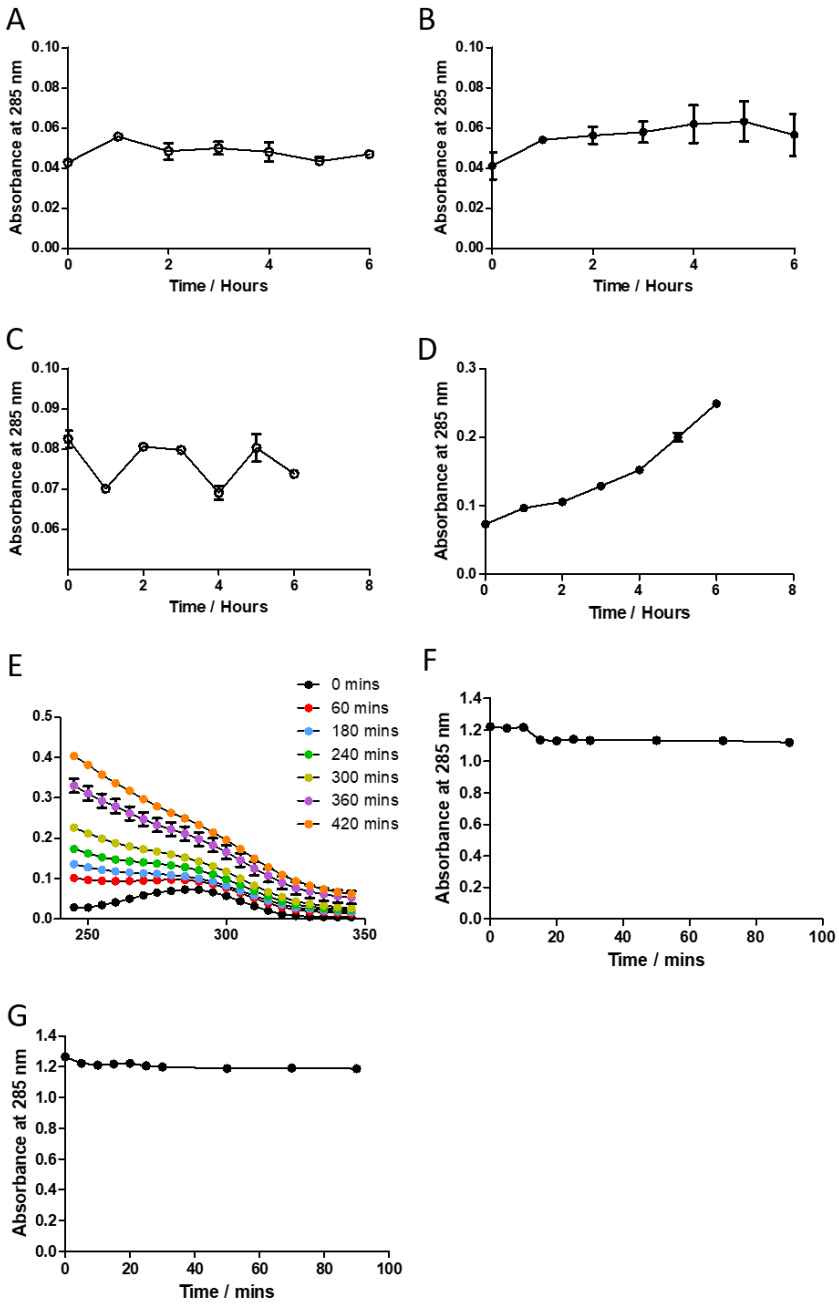

Figure 2.13 – Degradation profile of MTHF under hydrogel forming conditions including (a-b) aqueous environment at ambient temperature and 90°C, (c-e) in the presence of 1% borate at ambient temperature and 90°C, and (f-g) at pH 9.31 at ambient temperature and 90°C.

(a-c) MTHF was found to be stable in aqueous solution at both temperatures tested and in 1% borate at ambient temperature. (d) At 90°C in 1% borate a gradual increase in the absorptivity of an MTHF solution was seen. (e) This was caused by a gradual flattening of the UV absorbance spectrum throughout the test. (f-g) MTHF was found to be stable at a pH representative of a 1% borate solution. All values represent the mean of three independent replicates ± S.D.

2.4.5.2 HDMF degradation

Due to the stability issues observed with MTHF it was decided that similar stability studies should be undertaken for HDMF. It was found that HDMF was stable at room temperature in aqueous solution over the course of the experiment (Figure 2.14 a). When exposed to 90 °C in aqueous solution the absorbance of HDMF rapidly decreased over 90 min suggesting that the compound is heat labile (Figure 2.14 b). When exposed to a 1% borate solution a slight, immediate decrease in the absorbance was seen from 0.97 (as seen in Figure 2.14 a) to 0.69 as well as a change in the overall λ_{max} of the compound from 285 nm to 335 nm (Figure 2.14 c). There was no further change in the absorbance during the rest of the experiment. This suggested that there was an immediate reaction on exposure to borate possibly resulting in a product with a lower overall absorptivity as well as an altered λ_{max}. When exposed to 1% borate and 90 °C the same immediate changes in absorptivity and in λ_{max} were seen as well as a rapid reduction in the total absorbance of the solution with the absorbance reaching zero in just 70 min (Figure 2.14 d). The changes in the full absorbance spectrum of HDMF when exposed to 1% borate and 90 °C were investigated. It was found that when exposed to these conditions the shape of the HDMF UV-Vis absorbance spectrum shifted towards longer wavelengths (λ_{max} 335 nm) and became asymmetric. The total absorbance was reduced immediately (even prior to placing the sample in a 90 °C water bath) (figure 2.14 e). When exposed to the 1% borate and 90 °C, this 'new' absorbance spectrum did not change over time, but the total absorbance did gradually decrease over time. The role of pH in the observed changes in the absorbance properties of HDMF was investigated (Figure 2.14 f). It was shown that at room temperature an increase in pH did not have any effects on the absorbance or λ_{max} of HDMF (Figure 2.14 g) while a decrease in total absorbance was seen in on exposure

to 90 °C (figure 2.14 h). These data indicate that HDMF can be degraded by exposure to high temperatures and that exposure to 1% borate may cause a change in the structure of HDMF leading to a change in the λ_{max}. This change in λ_{max} is likely caused specifically by interactions with borate and is not due to the change in pH associated with the presence of borate.

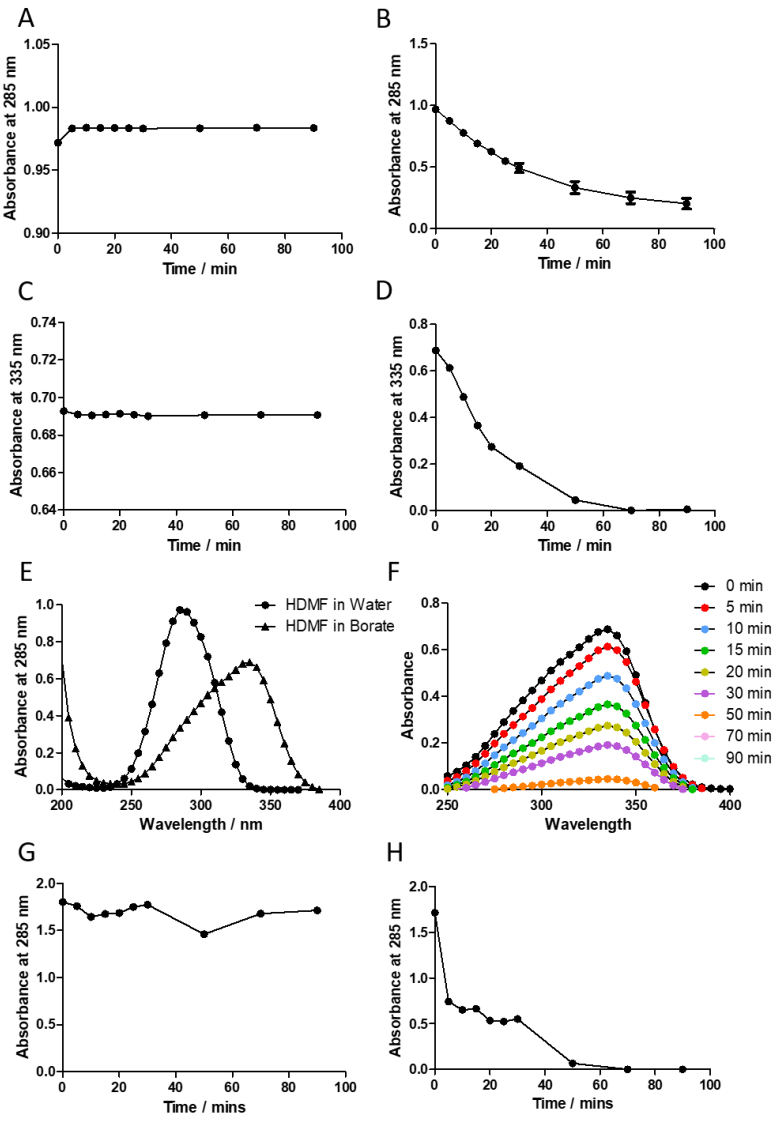

Figure 2.14 - Degradation profile of HDMF under hydrogel forming conditions including (a-b) aqueous environment at ambient temperature and 90°C, (c-e) in the presence of 1% borate at ambient temperature and 90°C, and (f-g) at pH 9.3 at ambient temperature and 90°C.

(a-b) HDMF was found to be stable in aqueous solution at ambient temperature. But unstable at 90°C in aqueous environment. (c) HDMF was stable in the presence of 1% borate at ambient temperature but a change in λmax from 285nm to 335nm was observed. (d) At 90°C in 1% borate HDMF underwent the same change in λmax as previously and the solution gradually decreased in absorptivity. (e) The change in absorbance spectrum between HDMF in water and HDMF exposed to 1% borate showed the maintenance of one absorbance peak but a shift in absorbance to longer wavelengths. (f) The absorbance spectrum of the borate exposed HDMF remained constant when exposed to 90°C but the sample gradually decreased in absorptivity. (g-h) HDMF was largely stable in a solution with a pH representative of 1% borate at ambient temperature but apparently unstable at 90°C. All values represent the mean of three independent replicates ± S.D.

2.4.5.3 Ascorbic acid degradation

The effects of hydrogel forming conditions on ascorbic acid were then investigated. In simple aqueous solution at room temperature, ascorbic acid was unstable and a gradual decrease in total absorbance over 90 min was seen (figure 2.15 a). This reduction in total absorbance was greatly accelerated by exposure to 90 °C temperatures (Figure 2.15 b). When exposed to 1% borate at room temperature the reduction in total absorbance was accelerated compared to that in water only. A change in λ_{max} from 250 nm to 265 nm was also seen (Figure 2.15 c). When exposed to 1% borate and 90 °C, a similar change in λ_{max} was seen and the decrease in total absorbance was rapid with absorbance readings reaching zero in under 5 min (Figure 2.15 d). The full absorbance spectrum of ascorbic acid under hydrogel forming conditions was investigated. It was shown that when exposed to 1% borate the UV absorbance spectrum shifted to the right, from 250 nm to 265 nm. The total absorbance also became highly variable (Figure 2.15 e). The role of pH in the above described absorbance changes was investigated. It was found that an increase in pH also caused a change in λ_{max} from 250 nm to 265 nm as was seen with exposure to 1% borate

(Figure 2.15 f). This change in λ_{max} was also seen in the pH altered solution at 90 °C (Figure 2.15 g). This suggests that the change in λ_{max} seen during the formation of an ascorbic acid hydrogel was mediated by changes in pH rather than by the presence of borate specifically.

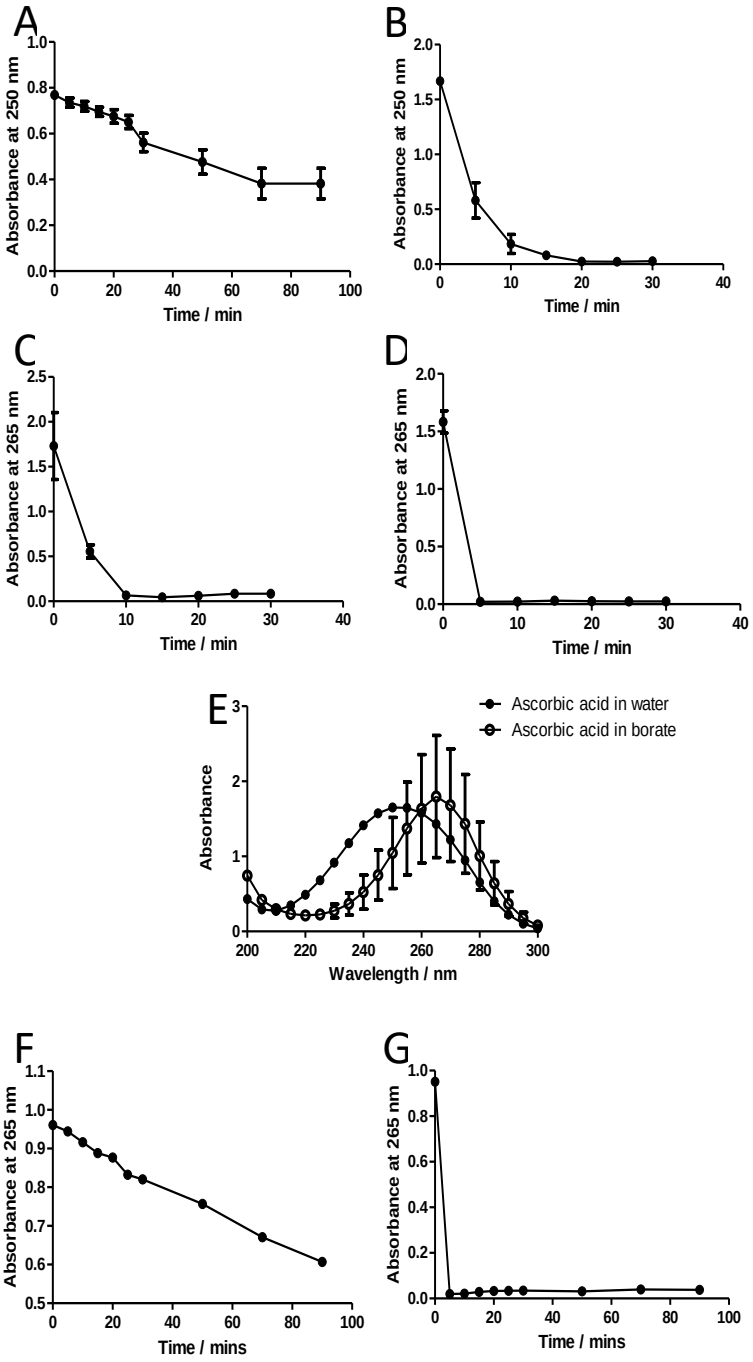

Figure 2.15 - Degradation profile of ascorbic acid under hydrogel forming conditions including (a-b) aqueous environment at ambient temperature and 90°C, (c-e) in the presence of 1% borate at ambient temperature and 90°C, and (f-g) at pH 9.3 at ambient temperature and 90°C.

(a-b) Ascorbic acid was found to be unstable in aqueous solution at ambient temperature and 90°C in aqueous environment showing a gradual and rapid decrease in absorptivity respectively. (c-d) Ascorbic acid was unstable in the presence of 1% borate at both ambient temperature and at 90°C rapidly decreasing in absorptivity in both conditions. Ascorbic acid displayed a change in λmax from 250nm to 265nm at both temperatures in the presence of borate. (e) The change in λmax showed the maintenance of one absorbance peak but a shift in absorbance to longer wavelengths and an increase in the variability of absorbance measurements. (f) Ascorbic acid underwent a similar change in λmax and was unstable in a solution with a pH representative of 1% borate at ambient temperature and very unstable at 90°C. All values represent the mean of three independent replicates ± S.D.

2.4.5.4 Sotolon degradation

The stability of sotolon under hydrogel forming conditions was investigated. In aqueous solution at room temperature sotolon was stable with no change in λ_{max} or total absorbance over 90 min (Figure 2.16 a). When exposed to 90 °C temperatures in aqueous solution sotolon showed no change in λ_{max} but a slight and gradual increase in total absorbance was seen over the 90 min (Figure 2.16 b). When exposed to 1% borate at room temperature a slight initial decrease in total absorbance was apparent and an obvious change in λ_{max} was seen from 230 nm to 265 nm. No further change in total absorbance was seen (Figure 2.16 c). When exposed to both 1% borate and 90 °C a similar change in λ_{max} was observed and a rapid decrease in total absorbance over 90 min was seen (Figure 2.16 d). This finding indicates that the change causing a shift in λ_{max} was a change from sotolon to a much less thermally stable compound. The effect of pH on the absorbance spectrum of sotolon was investigated. It was found that when exposed to pH 9.31 at room temperature a change in λ_{max} similar to that seen in the borate solution occurred but the total absorbance did not change significantly (Figure 2.15 e). When exposed to the altered pH at 90 °C a change in λ_{max} was also

seen and a rapid decline in total absorbance was apparent (figure 2.16 f). These data indicate that the change in λ_{max} was brought about by the change in pH.

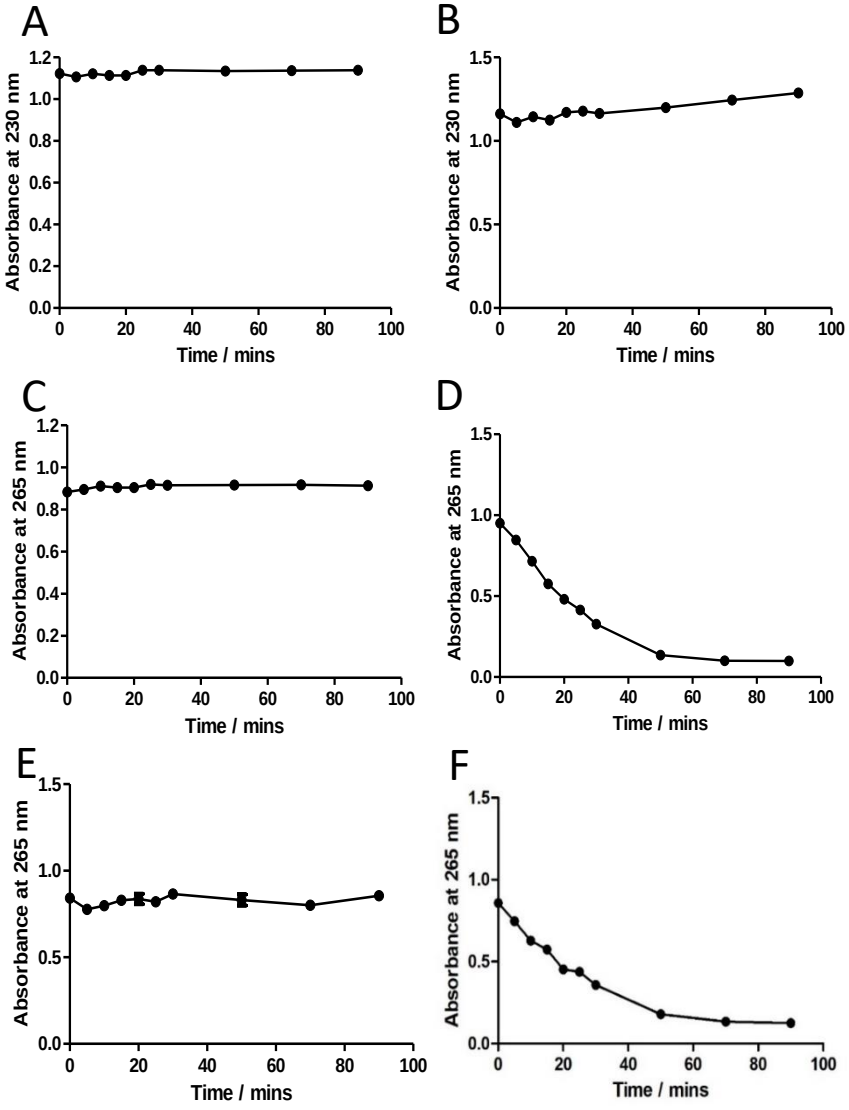

Figure 2.16 - Degradation profile of sotolon under hydrogel forming conditions including (a-b) aqueous environment at ambient temperature and 90°C, (c-d) in the presence of 1% borate at ambient temperature and 90°C, and (e-f) at pH 9.3 at ambient temperature and 90°C.

(a-b) Sotolon was found to be stable in aqueous solution at ambient temperature and at 90°C. (c-d) Sotolon was stable in the presence of 1% borate at ambient temperature and seemingly unstable at 90°C in a 1% borate solution, rapidly decreasing. Sotolon also displayed a change in λmax from 230nm to 265nm at both temperatures in the presence of borate. (e-f) Sotolon underwent a similar change in λmax and was stable in a solution with a pH representative of 1% borate at ambient temperature and was unstable at 90°C. All values represent the mean of three independent replicates ± S.D.

2.4.6 Assessment of furanone pH under hydrogel forming conditions

Changes in the pH of each furanone were assessed in order to identify any temperature threshold at which pH change, and so compound degradation, may occur. It was found that upon gradual heating from 20 °C to 70 °C the pH of a 1% borate solution decreased from 9.18 to 8.86. A similar change of 9.21 to 8.83 was seen in a 1% borate solution with MTHF indicating no effect of MTHF on the overall pH of the hydrogel system. The addition of both HDMF and ascorbic acid to the borate solution caused a reduction in pH to 8.61 and 8.58 respectively even before any heat was applied. During heating, the pH of the ascorbic acid and borate solution further decreased to 8.29 while the HDMF/borate solution reduced to a pH of 8.08. Finally, the addition of sotolon to the borate solution did not cause a significant initial reduction in pH but did result in a gradual decrease in pH to 8.45 over the course of the experiment (Figure 2.17).

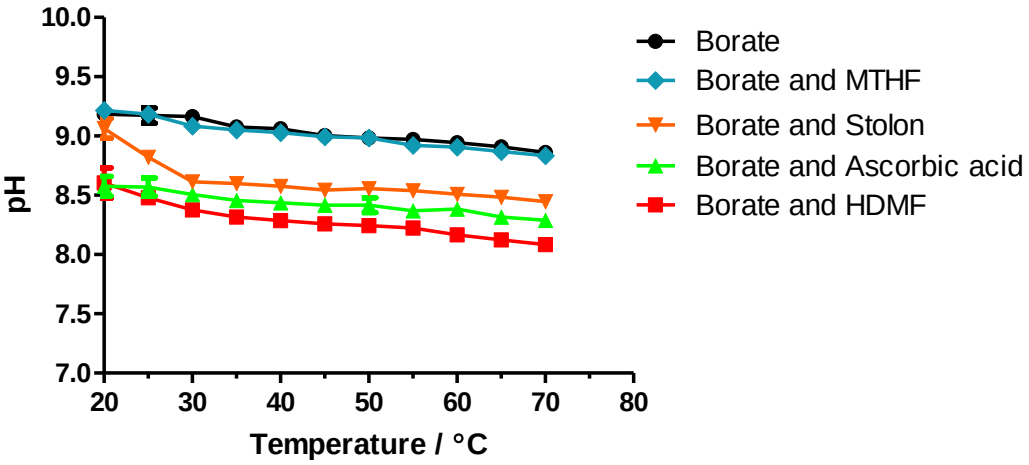

Figure 2.17 – Changes in pH of solutions of borate and each furanone when subjected to increasing temperatures up to 70 °C.

The pH of a borate only solution decreased slightly over the time course of the experiments. The addition of MTHF had no effect on this. The addition of sotolon to the solution resulted in a reduction in pH up to a temperature of 30°C then remaining stable. Both the addition of HDMF and ascorbic acid to the borate solution caused an initial decrease in a reduction in solution pH that was then exacerbated upon heating. All values represent the mean of three independent replicates ± S.D.

Similar furanone and borate solutions were then subjected to prolonged heating at 90 °C for 3 h to mimic the conditions used in hydrogel formation. As before the addition of MTHF and sotolon to the borate solution caused no initial decrease in pH. However, upon heating both the MTHF/borate and sotolon borate solutions decreased in pH (to 8.73 and 8.53 respectively) over the first 30 min and then remained stable for the remainder of the experiment. Both HDMF and ascorbic acid caused an initial drop in pH to 8.71 and 8.52 respectively. Both solutions then showed gradual decreased in pH up to 90 min of heating then remaining stable giving a final pH of 7.92 for HDMF and 7.51 for ascorbic acid (Figure 2.18).

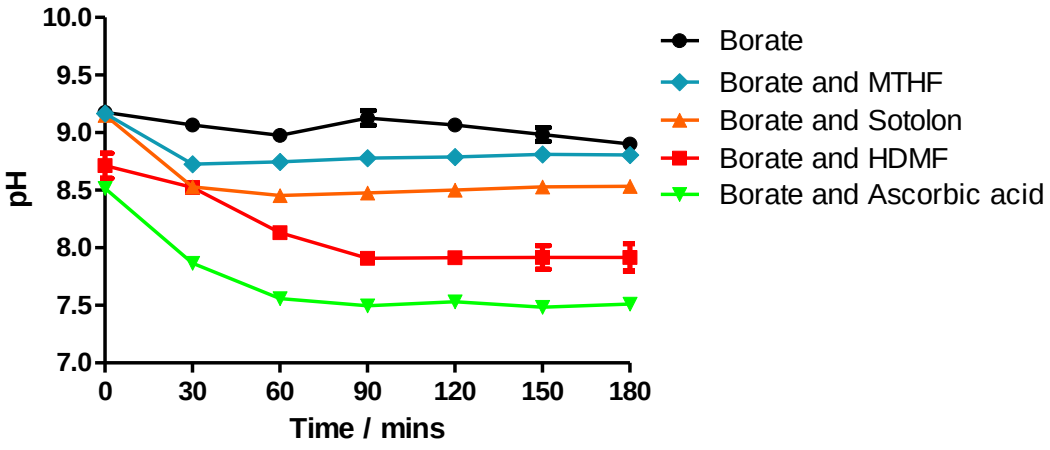

Figure 2.18 – Changes in the pH of borate and furanone solutions during prolonged heating at 90°C.

The presence of MTHF did not cause a significant decrease in the pH of the system over the time course of the experiment. A significant reduction in pH was observed in samples containing sotolon, HDMF and ascorbic acid. All values represent the mean of three independent replicates ± S.D.

Samples were also assessed for colour change before and after prolonged heating. It was found that HDMF, MTHF, ascorbic acid, and sotolon all showed a significant colour change from a colourless solution to a vibrant yellow (HDMF) and a straw

yellow (MTHF and ascorbic acid) and a very pale yellow (sotolon) when heated to 90 °C for 3 h in the presence of 1% borate. Borate only solutions showed no obvious colour change (Figure 2.19).

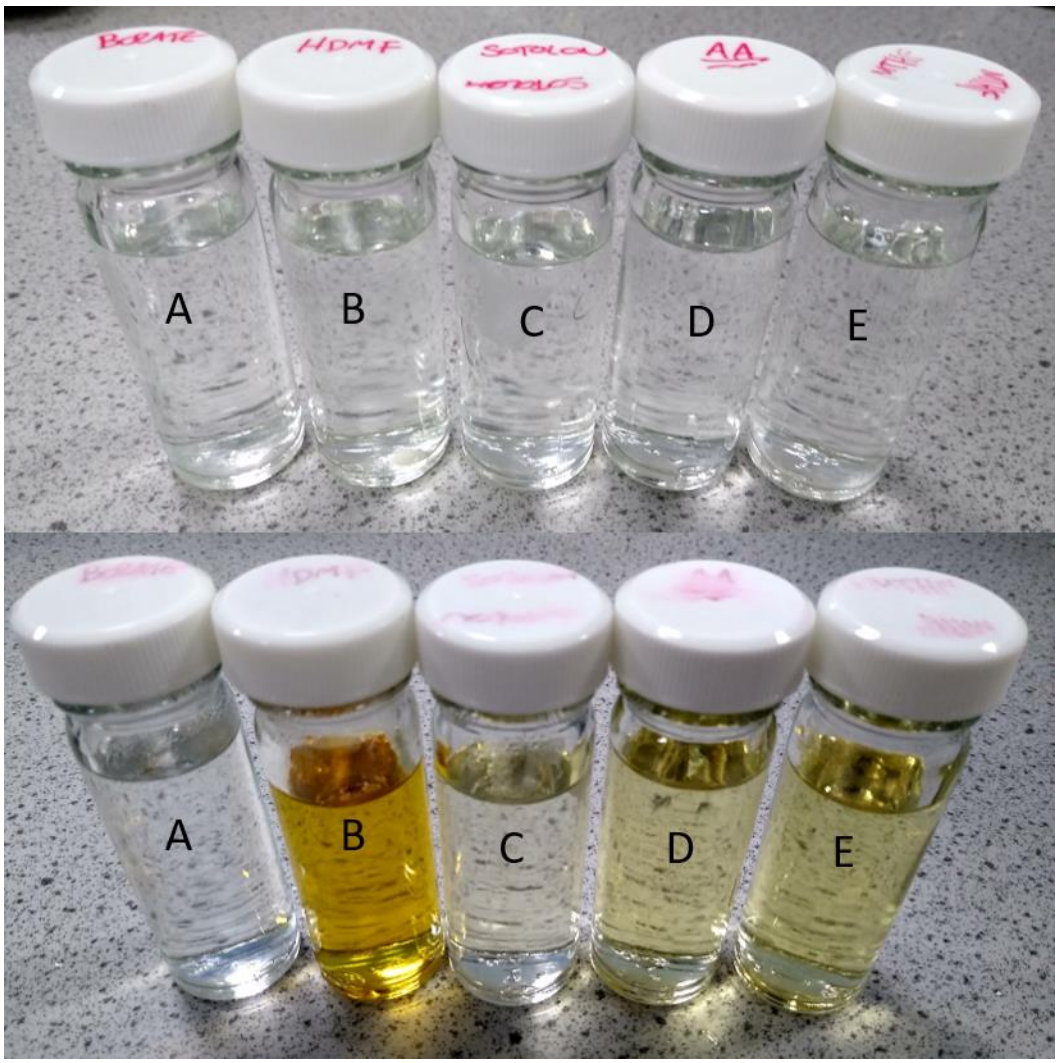

Figure 2.19 – A comparison of the colour of furanone solutions before (top) and after (bottom) heating to 90°C for 3 h in the presence of 1% w/v borate.

Solutions are (a) borate only, (b) HDMF, (c) sotolon, (d) ascorbic acid, and (e) MTHF. Samples were representative of three independent replicates.

2.5 Discussion

Semi-solid, PVA-borate, hydrogels are an ideal material for use as wound dressings. Due to their inherent viscoelastic and dilatant properties they can be placed in a wound and allowed to flow in order to fill the wound. This is important as flowing and filling of the wound environment ensures total contact of the gel with the wound bed (Murphy *et al.*, 2012). Upon the application of a rapid force (as would be experienced during wound dressing removal) these materials act as a more solid-like material, thus, facilitating their easy removal from the wound in one piece. Further, their non-adherent nature helps to minimise trauma and further damage to the epithelialising tissues found in healing wounds (McCarron *et al.*, 2011).

Not only do the viscoelastic properties of semi-solid PVA-borate hydrogels make them excellent candidates for basic wound dressings but the ability to load these formulations with high concentrations of hydrophilic drugs makes them potentially excellent dressing/drug delivery hybrid systems. Indeed, these hydrogels have previously been loaded with a range of compound for the improvement of wound healing or the treatment of wound infections (Donnelly *et al.*, 2009; Abdelkader *et al.*, 2016, 2018). While these formulations are easily loaded with various active compounds it should be noted that incorporation of a drug into a PVA-borate hydrogel has the potential to interfere with and disrupt the viscoelastic properties of the material (Loughlin *et al.*, 2008).

In this chapter, which aimed to formulate and characterise PVA-borate hydrogels for use as a drug delivery system capable of delivering furanones to bacterial biofilms, the method for the production of PVA-borate hydrogels was optimised in terms of polymer hydrolysis degree and starting gel component form (liquid components or dry powder components). A range of PVA-borate hydrogels were then formulated, and

their shear moduli measured using oscillatory rheometry. Several candidate formulations with appropriate shear moduli were then selected and subjected to in depth rheological characterisation to fully explore their viscoelastic properties and adhesiveness. Finally, one ideal hydrogel formulation was selected and was loaded with four naturally occurring furanone compounds. The impact of compound loading on the hydrogels was then investigated.

To begin, a range of hydrogel formulations with varying polymer and cross linker concentrations were produced using a liquid component method. The shear modulus of each formulation was then tested. Considering previous work, it was expected that hydrogels would generally become stiffer with increasing PVA concentration and increasing borate concentration due to increased formation of PVA-borate cross links (as shown in Figure 2.20) as previously reported by Murphy *et al.* (2012).

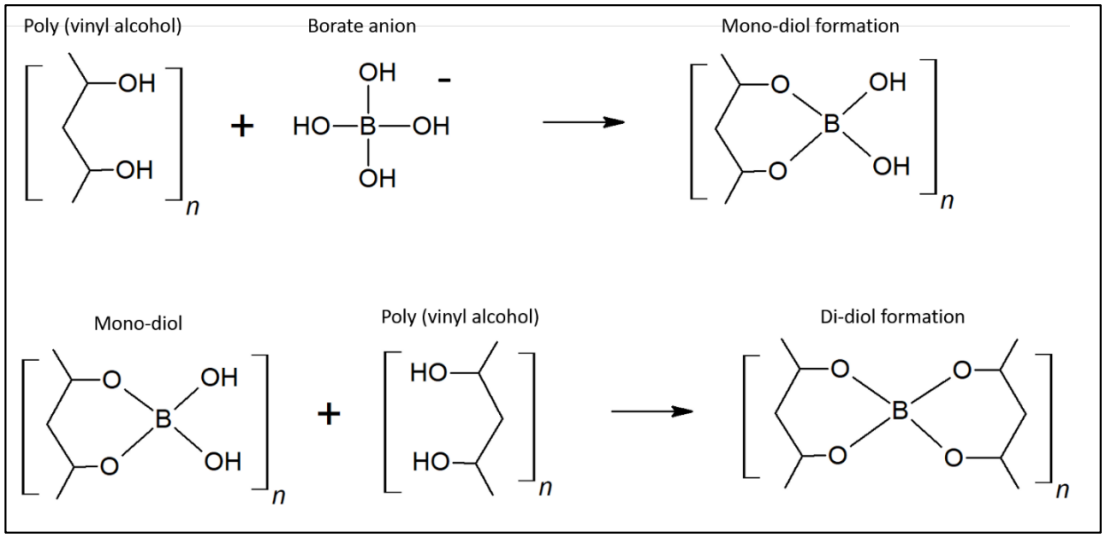

Figure 2.20 – The process of cross linking between PVA and borate.

The dissociation of boric acid in water yields the negatively charged borate anion. Borate ions then form a mono-diol complex with one PVA molecule. The borate then binds to the hydroxyl groups of an adjacent PVA molecule forming a link between the two PVA molecules.

However, unlike the work of Murphy *et al.*, the work detailed here did not show any linear relationship between either PVA concentration borate concentration and shear modulus in this work (Murphy *et al.*, 2012). It was found that, while hydrogels with high concentrations of PVA (14% w/w) had the highest shear modulus, the shear modulus in hydrogels with PVA concentrations between 6% and 12% w/w showed no obvious correlation. Due to this unexpected finding it was decided that optimisation of the hydrogel production method should be undertaken to identify and mitigate any potential reasons for the variability.

Changes in the starting component form between aqueous solutions of PVA and borate and dry powder PVA and borate were assessed. It was believed that the use of liquid components was causing variation in the concentrations of PVA added during production. The PVA stock solution used was a 30 % w/w solution and was solid at room temperature. This meant that melting of the stock prior to adding PVA to the formulation was required. This step may have introduced some variation due to incomplete melting of the PVA stock or improper mixing of the melted PVA stock before adding to the borate resulting in areas of high and low PVA concentration within the viscous stock solution. When dry powder components were used consistent concentrations of PVA during formulation were achieved and the variability in hydrogel properties was greatly reduced. In addition to this reduction in variability it was found that the overall stiffness of the gel (as indicated by a change in shear modulus) was significantly reduced from 8.5k Pa to 3.7k Pa. The increased shear modulus may be due to dehydration of the PVA stock over time. Loss of water from the PVA stock solution through evaporation during storage and rapid evaporation during exposure to 90 °C temperature required may have led to a gradual increase in the concentration of the stock solution. This would have meant that greater

concentrations of PVA were being added to the formulation than was expected. This idea is partially supported by the fact that increasing polymer concentrations in PVA borate hydrogels has been shown to result in a stiffer material. Murphy *et al.* (2012) showed that increasing PVA concentration (while maintaining borate concentration) resulted in increased hardness of a hydrogel sample. In this instance hardness was defined as the force necessary to produce a set deformation in the material. The measurement of hardness is largely comparable to shear modulus measurements used in this work which measure the force required to produce a deformation, in the form viscous flow, in the hydrogels. This indicates that the increased shear modulus between hydrogels produced using the liquid component method was likely due to an unintentional increase in PVA concentration.

The impact of differing degrees of PVA hydrolysis was then assessed. It was shown that PVA with 87-89% hydrolysis and 98-99% hydrolysis produced very similar hydrogels with shear moduli of 3.6k Pa and 3.7k Pa respectively with low variation between gels. Fully hydrolysed PVA (hydrolysis degree of 100%) produced a hydrogel with a significantly higher shear modulus. Despite the increased shear modulus, the fully hydrolysed PVA produced gels with very low variability between samples (30-40 Pa variation across three replicates). Although the variability between gels was low, the 100% hydrolysed PVA was not used for further experimentation as the high shear modulus led to poor flow properties. The 98-99% hydrolysed PVA was selected for all further hydrogels as it produced a softer gel and the relatively high percentage hydrolysis would mean the hydrogels had lower bio adhesion and lower rates of component dissolution (Murphy *et al.*, 2012).

Once the method of hydrogel production had been optimised the same set of formulations prepared using the liquid component method were prepared using the

now optimised method. When these samples were analysed rheologically it was found that there was a close relationship between both the concentration of the PVA used in the formulation and the shear modulus, with shear modulus increasing with PVA concentration. Similarly, a positive correlation between the concentration of the borate cross linker and the shear modulus was also seen. This was in keeping with previously published works (Murphy *et al.*, 2012; Abdelkader *et al.*, 2016).

Of the formulations tested, four were selected based on their shear modulus and their texture when handled. To be selected, hydrogels needed to have a shear modulus between 1.5 kPa and 5k Pa and were required to not be noticeably heterogeneous in texture and not excessively adhesive when handled. The four formulations chosen contained 6% PVA and 1%, 2% and 3% borate and also the formulation containing 8% PVA and 1% borate. The chosen formulations were then subjected to full rheological characterisation.

Prior to full characterisation the LVR of each formulation was identified using an amplitude sweep. It was found that as the LVR was increased with increased polymer concentration but not necessarily by cross linker concentration. The limit of the linear viscoelastic region for the 6% PVA gels were 6.3%, 7.9% and 7.9% (for 1%, 2%, and 3% borate respectively). This is in direct contradiction to the findings of Wong *et al.* (2015) who reported that the linear viscoelastic region of UV crosslinked polyethylene oxide/pentaerythritol tetra-acrylate hydrogels was extended with increasing crosslinking (as measured by an increase in the critical strain value) (Wong, Ashton and Dodou, 2015). Similarly, the work of Shengmao and Gu (2015) found that gel stiffness increased with crosslinking density in collagen. While these reports contradict the data described here, the mechanisms of cross linking are, however, very different, making direct comparisons difficult. When the PVA concentration in the

hydrogels was increased to 8% w/w, the upper limit of the LVR was increased to 12.5%. As the LVR denotes the range of shear strains that a material can withstand without experiencing internal structure compromise (Koetting *et al.*, 2015) this result suggests that the 8% w/w PVA hydrogel has greater integrity of the internal polymer network than hydrogel containing 6% PVA. A potential explanation for the increased internal structural integrity of the higher PVA concertation gels is noted by Zhang *et al.* (2019). This group suggested that increasing polymer concentration brings the polymer solution closer to the critical overlap concentration (COC). This COC is the concentration at which overlapping of polymer molecules begins to occur in dilute solutions (Skelland and Meng, 1996). Zhang *et al.* (2009) suggest that as this concentration is approached physical interactions between polymer strands also increases (Zhang, Wehrman and Schultz, 2019). If this is indeed the case, the increase of PVA concentration from 6% w/w to 8% w/w may cause an increase in physical interactions (e.g. polymer chain tangling) and this may give a higher degree of structural integrity, thus, increasing the upper limit of the LVR.

Assessment of the total viscoelastic profile of each hydrogel revealed that all hydrogels displayed dilatant behaviour, in which the material displays solid-like properties when a high frequency force is applied and a liquid or viscous-like properties when at rest or when a low frequency force is applied. These measurements were validated by measuring phase angle shift in the samples during the tests. These results are consistent with previous reports that have shown PVA-borate hydrogels to display obvious dilatancy (Savins, 1968; Murphy *et al.*, 2012). In addition to these measurements, the G′ G″ crossover point, also known as the shear modulus, was measured. This point (which denotes the force required to initiate liquid-like viscous flow) was found to increase with both borate concentration and PVA concentration

with 6% PVA hydrogels displaying a shear modulus of 2.27 kPa, 5.19 kPa, and 4.77 kPa when 1%, 2% and 3% w/w borate was added, respectively. This is in keeping with the results of Abdelkader *et al.* (2016), who showed that an increase in borate concentration resulted in an increase in the shear modulus of their PVA-borate gels, as assessed using oscillating rheometry (Abdelkader *et al.*, 2016). These authors also reported shear moduli in the range of 3.3 - 4.6 kPa for hydrogels consisting of 6% w/w PVA and containing between 1 % and 2.5% w/w borate. The observed shear modulus of an 8% PVA 1% borate hydrogel in the present experimental work was 6.515 kPa indicating a stiffer gel than the 6% PVA gels. This difference in shear moduli was also observed by Abdelkader *et al.* (2016).

Both the shear dependent viscosity and the adhesiveness of each of the four hydrogel formulations was assessed. The viscosity measurements of all formulations revealed obvious dilatant behaviour with viscosity increasing relative to the shear frequency. These observations are in keeping with the seminal work of Inoue and Osaki (1993) who were the first to demonstrate the shear thickening behaviour of PVA-borate gels. They reported that, at 25 °C, no apparent change in viscosity of a 1% PVA gel (containing an unspecified amount of borate) was seen until approximately 110 Hz at which point the viscosity rapidly increased (Inoue and Osaki, 1993). The gels in the present work showed an increase in viscosity above frequencies of 50 Hz. This is likely due to the increased polymer concentration in the formulations used compared to those of Inoue and Osaki (1993).

When formulation adhesiveness was assessed it was found that adhesiveness increased relative to both borate concentration and PVA concentration. Peak normal force, which was measured as the pulling force exerted on the rheometer geometry by the gel (giving rise a negative force values) increased from -6.6 N to -15.3 N to -19.5 N

for hydrogels containing 6% PVA and 1% 2% and 3% borate respectively. This finding is in direct contradiction to several other works who showed a borate dependent decrease in adhesiveness (Murphy *et al.*, 2012; Abdelkader *et al.*, 2016). However, it should be noted that both of these studies examined adhesiveness on porcine skin whereas this work examined adhesiveness using the stainless-steel surface of the rheometer geometry. The vast differences in the stainless-steel surface compared to a biotic surface such as skin is likely to have affected the adhesiveness test. Following full rheological testing the 6% PVA 1% borate formulation was selected for all further tests due to its low shear modulus (allowing for easier flow into a wound bed) and its low adhesiveness (which would minimise trauma to the wound bed upon removal).

Hydrogels were then loaded with 1% by weight of four furanone compounds (HDMF, MTHF, sotolon and ascorbic acid). Significant changes in both the texture and physical appearance of the hydrogels was observed. When loaded with HDMF the hydrogel failed to fully form a gel with the sample remaining very soft. This effect was also noted in hydrogels loaded with sotolon and ascorbic acid. It was hypothesised that the change in texture is due to a change in the overall pH of the system. It is known that the formation of a PVA-borate hydrogel is highly dependent on pH. This is due to the limited dissociation of boric acid in more acidic environments (Kochkodan, Darwish and Hilal, 2015). If boric acid does not dissociate, no borate ions are formed and thus crosslinking of PVA cannot take place efficiently. This means that a softer gel will be formed, or no gelation will occur. With a pK_a of 4.2, ascorbic acid is weakly acid and as such should be expected to interfere with the crosslinking process of PVA by borate. This was indeed the case in this work. However, with pK_a values of 8.56 (measured) and 9.28 (predicted) for HDMF and

sotolon, respectively, these compounds are weakly basic (Chen and Sidisky, 2011; Yeast Metabolome Database, 2020). As such, these compounds should not interfere with the dissociation of boric acid. It was hypothesised that, when exposed to the high temperatures required for hydrogel formation, the furanone compounds degraded and that it was the degradation products which resulted in a decrease in the pH of the system. Indeed, it has been shown previously that HDMF undergoes thermal degradation (at 160 °C) to products such as 2,3-pentanedione and acetoxy acetone, among others (Shu, Mookherjee and Ho, 1985). Unfortunately, neither of these compounds have reported pK_a values and consequently determining if their presence was the cause of gelation failure is not possible. As HDMF is heat labile, and considering similarities between the molecules, it is likely that sotolon experiences a degree of thermal degradation as well though there are no reports of this in the literature. The colour changes seen during the hydrogel forming process may also indicate a structural change in the furanone molecules as colour change is an indicator of compound degradation in many other instances, particularly in other phytochemicals such as betalains and xanthophylls (Chandran *et al.*, 2014; Dini *et al.*, 2019).

When MTHF was incorporated into the hydrogel formulation, no changes in hydrogel texture or colour were seen and it was, therefore, concluded that MTHF did not degrade under gel forming conditions. Considering this data, it was hypothesised that the degradation products being produced during hydrogel formation were decreasing the overall pH of the system. As stated previously, a more acidic environment would limit the dissociation of boric acid, leading to formation of fewer borate ions and, subsequently, less cross linking and poorer gelation.

Despite the observed changes in hydrogel texture and colour, the release of HDMF and MTHF from a PVA hydrogel were assessed. These furanones were tested as MTHF formed a suitable hydrogel and HDMF formed a very soft but still slightly workable hydrogel when incorporated into a 6% PVA 1% borate formulation. It was found that an HDMF-loaded hydrogel released a maximum of 45% of the total loaded compound over 24 h. The efficiency of drug delivery from PVA-borate hydrogels reported in the literature varies widely. Reports range from approximately 16 % total release for methylene blue to almost 80% for lidocaine hydrochloride (Loughlin *et al.*, 2008; Donnelly *et al.*, 2009). This variation may be due to a number of factors including differences in the polymer and crosslinking concentrations (Censi *et al.*, 2009; Martinez *et al.*, 2014) or differences in the loaded drugs themselves such as polarity, molecular mass or interaction with the hydrogel matrix (Li and Mooney, 2016). The release profile of MTHF from the hydrogel formulation was also assessed. When total drug release was calculated it was noted that maximum release was nearly 2000% of the total loaded drug. As this is not possible, and, following the elimination of any calculation and measurement errors as causes, it was hypothesised that while the there was no effect on hydrogel texture and no observed colour change, MTHF was also being degraded during the hydrogel production process.

Due to the changes in hydrogel properties, obvious colour changes and unexpected drug release profiles, further investigations into the stability of furanone compounds during hydrogel production were planned. Aspects to be investigated included; elevated temperature, exposure to borate and general stability in aqueous environments.

Degradation and loss of active compounds in pharmaceutical formulation is a significant problem for several reasons. Primarily, with a reduction in active

compound comes a reduction or total loss of efficacy of the formulation. Drug degradation in pharmaceutical formulation can occur for a number of reasons including interactions with one or more excipients, conditions required to make the formulation (e.g. heat or mixing), or simply time (Snape, Astles and Davies, 2010).

The stability of each of the four furanone compounds, MTHF, HDMF, ascorbic acid and sotolon, under hydrogel-forming conditions was examined. The effect of elevated temperature, presence of water, presence of borate, and altered pH were individually assessed. The presence of borate and altered pH were then assessed in combination with elevated temperature to accurately represent the conditions present when forming a hydrogel.

Due to the anomalous release profile of MTHF in which data suggested that maximum drug release was in excess of 1500% of the total loaded dose this compound was examined first. Exposure of MTHF to an aqueous environment at ambient temperature or at 90 °C for 6 h showed no obvious changes in UV absorbance or the λ_{max} which remained at 285 nm. However, when the MTHF was exposed to both 90 °C and the presence of 1% borate a gradual increase in the absorbance of the sample was seen. This increase in absorbance was identified as the cause of the over estimation of released MTHF in section 2.4.4. When the full UV absorbance spectrum of MTHF over the course of the experiment was examined it was found that the absorbance spectrum was becoming flatter and absorbance at shorter wavelengths was increasing over time. This suggests that the degradation products produced by exposing MTHF to elevated temperature and borate were more broadly absorptive than the original compound. Finally, the experiment was repeated with one amendment. The MTHF was exposed to 90 °C in a buffer adjusted to a pH equivalent of that of a 1% borate solution and it was found that no changes in the absorbance of MTHF occurred. This

indicates that the reaction leading to degradation of the compound was due to the neither the presence of borate or altered pH alone but caused by a synergy between the borate and the elevated temperature. It is possible that the presence of borate at ambient temperature would have caused the same degradation if left for an extended period of time, but the addition of heat catalysed the reaction. Stability issues have been reported for several compounds similar to MTHF in the literature. For example, it has been shown that several furan-based compounds found in coffee (as MTHF is) undergo significant degradation after heat treatment. In 2003 Kumazawa and Masuda found that autoclaving at 121 °C for 10 min effectively reduced the concentration of 2-furfurylthiol (a benzylic thiol consisting of furanone ring with an attached sufanylmethyl group). Furthermore, these authors showed that this reduction in 2-furfurylthiol was exacerbated by increasing pH. Compounds in lower pH (pH 3-5) solutions degraded significantly less than those in less acidic solutions (pH 6-7). Interestingly, the converse was true for 3 other furanone compounds; furfural, furfuryl alcohol and difurfuryl disulphide which appeared to be more stable at higher pH (Kumazawa and Masuda, 2003). Similarly, the work of Charles-Bernard *et al.* (2005) showed that the degradation of 2-furfurylthiol was dependent upon two factors namely; electrophilic addition and the presence of radical species. This was concluded as the addition of a nucleophile and an inert atmosphere had a stabilising effect on the compound (Charles-Bernard *et al.*, 2005). These data, when taken together, show that the degradation of these compounds, and likely other furanones, is a complex and multifaceted process with many contributing factors. This supports the hypothesis that the degradation of MTHF in hydrogels results from a synergistic process between borate and temperature.

The stability of HDMF was then investigated and it was found that HDMF was stable at room temperature in aqueous solution but rapidly degraded at 90 °C. This data strongly supports previous reports that HDMF (also known as DMHF in some reports) is unstable in a range of aqueous buffer solutions. For example, at pH values close to neutral the half-life of HDMF was only 10 days (Roscher, Schwab and Schreier, 1997). Additionally the work of Shu *et al.* (1985) showed that, at pH 7.1, HDMF was extensively degraded at 160 °C into a wide range of degradation products including other furanones (Shu, Mookherjee and Ho, 1985). It is, therefore, unsurprising that the addition of excessive heat would accelerate the degradation of HDMF in this work. It was also discovered that although the levels of absorbance of HDMF remained stable when exposed to borate the λ_{max} was changed, shifting from 285 nm to 335 nm. This shift occurred rapidly upon addition of HDMF to the borate solution with the change being observed in less than 10 s. When the full absorbance spectrum was investigated it was noted that a slight decrease in the overall level of absorbance occurred in addition to the λ_{max} shift. In contrast to the changed spectrum of MTHF, when the absorbance spectrum of HDMF was altered, a clear, single, absorbance peak was still present. Although no reports of HDMF degradation in the presence of borate has been reported in the literature, it seems likely that, due to the maintenance of a single peak in the UV absorbance spectrum that the HDMF is not being degraded to a range of degradation products but, rather, to a single product. This hypothesis is further supported when the effect of altered pH on HDMF is considered. It was shown that exposure to a pH representative of that of a 1% borate solution at ambient temperature did not have a significant effect on HDMF stability and no change in λ_{max} was observed. Further, at 90 °C and pH 9.31 the degradation of HDMF was similar to that in pure deionised water at elevated temperature. This led to the hypothesis that, while

the degradation of HDMF (as measured by a loss of absorptivity) was caused solely by exposure to elevated temperature, the change in λ_{max} was mediated by the presence of borate and not simply by the change in pH the presence of borate would have caused.

Degradation of ascorbic acid occurred under all conditions tested. Loss of approximately 50% of the loaded volume occurred over 90 min in aqueous solution at ambient temperature was observed. At 90 °C, total degradation was apparent in just 10 min. In the presence of 1% borate, rapid degradation also occurred with total loss of drug being seen in 20 min and 5 min for ambient temperature and 90 °C respectively. However, similarly to HDMF, a shift in λ_{max} was seen. The shift from 250 nm to 265 nm occurred upon exposure to borate and, again, this shift was seen immediately after adding ascorbic acid to the borate solution. Further, when exposed to a solution of pH 9.31, the degradation rate of ascorbic acid remained similar to that seen when exposed to borate at both ambient and elevated temperature. At altered pH, the shift in λ_{max} was again seen suggesting that this change was in fact due to the pH change caused by borate rather than by the presence of borate itself. Degradation of ascorbic acid in an aqueous environment is well reported in the literature. In 1998, Yuan and Chen showed that, in aqueous solution under heating, ascorbic acid degrades into four primary products dependent upon pH. At acidic pH ascorbic acid degraded preferentially to either furfural, 3-hydroxy-2-pyrone or 2-furoic acid whereas at a more alkaline pH ascorbic acid appeared to degrade to an unknown compound. The authors suggest several possible pathways for the degradation of ascorbic acid in aqueous solution each of which involves opening of the furan ring structure (Yuan and Chen, 1998). However, degradation via these pathways to furfural, 3-hydroxy-2-pyrone likely does not explain the observed degradation of the ascorbic acid in this work. In

their study Yuan and Chen also show that the three degradation products have very distinct absorbance profiles with furfural, 2-furoic acid, 3-hydroxy-2-pyrone having λ_{max} values of 277 nm, 252.3 nm and 294.8 nm respectively. If the ascorbic acid in this work had degraded to any of these products, they would have been clearly visible during UV absorbance readings. Similarly, the unknown compound showed a λ_{max} of 287.7 nm and so it is unlikely that the ascorbic acid had degraded to that product either. It remains unclear exactly how the ascorbic acid used in the work described here was degrading in pure aqueous solution. However, the change in λ_{max} observed with ascorbic acid in the presence of borate or altered pH may be easily explained. In 1970, Ogata and Kosugi showed that the negatively charged ascorbate monoion has a λ_{max} of 265.5 nm (Ogata and Kosugi, 1970). This is in keeping with our observations of maximal absorbance at 265 nm in borate and high pH exposed samples. When these studies are considered it can be suggested that in pure aqueous solution ascorbic acid is degrading *via* an unknown pathway to products which do not readily absorb light in the UV-visible range. Furthermore, the observed shift in λ_{max} when ascorbic acid is exposed to conditions similar to those found in a forming hydrogel (namely high pH and 1% borate) are likely due to dissociation of the compound to form the ascorbate monoion.

The stability of sotolon was also assessed. Sotolon was found to be stable in aqueous solution at both ambient temperature and 90 °C. However, as with ascorbic acid a change in λ_{max} occurred upon addition of sotolon to a 1% borate solution. This was a change from 230 nm to 265 nm and, while the altered form of sotolon was stable at ambient temperature, it steadily degraded at 90 °C. When exposed to pH 9.31 the same change in λ_{max} occurred. Interestingly, while the altered form of sotolon produced by exposure to borate was stable at ambient temperature, the altered form obtained by

exposure to pH 9.31 in the absence of borate was not. This may suggest that, although the change in λ_{max} was identical between the borate and the altered pH exposed samples, the final product was not the same. The altered λ_{max} was the same as that of the presumed ascorbate ion discussed above. This similarity may be due to the inherent structural similarities between ascorbic acid and sotolon. Indeed, there have been several chemical pathways suggested in which several isotopomers of sotolon can be synthesised using ascorbic acid as a precursor (Konig *et al.*, 1999; Pons *et al.*, 2010). It may be that the structures of the ascorbate monoion responsible for the absorbance peak at 265 nm is also present in the altered form of sotolon. This possibility is represented in Figure 2.21 where it can be seen that both sotolon ascorbic acid and sotolon share a central structure consisting of a heterocyclic furan ring with an oxygen side group at position two on the ring and a double bond between position three and four in the ring.

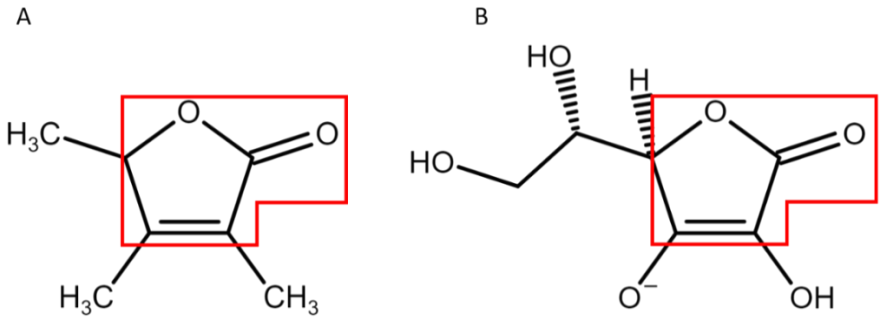

Figure 2.21 – A comparison of the structures of a) sotolon and b) the ascorbate mono ion.

These two compounds share a structural similarity in the furan ring and oxygen at position C1. It is likely that this structure or a portion of this structure is the cause of the observed UV absorbance at 265nm in both samples.

It is hypothesised that the presence of borate causes a change in the structure of sotolon resulting in a product that is stable in aqueous solution at ambient temperature but heat

labile. Further, this work suggests that exposure to pH 9.31 causes a different change in the structure of sotolon to yield a product which is unstable in aqueous solution independent of temperature.

Finally, the effect of furanone degradation on hydrogel system pH was examined. To assess the effect of hydrogel forming conditions on the pH, solutions of furanone and borate were subjected to two methods of heating. Firstly, the solution was heated slowly to identify a temperature at which a reduction in pH occurred. Secondly, solutions were incubated under hydrogel forming conditions (90 °C for 3 h). It was shown that when gradually heated to 70 °C there was no single temperature at which decreases in pH occurred. Instead the decrease was gradual. When heated at 90 °C for 3 h the change in pH was more pronounced and all furanones showed an initial decrease in pH and a lower final pH when compared to the borate only solution. It should be noted that the decrease brought about by the addition of MTHF was considerably less than the other furanones. This is also noteworthy as when loaded hydrogels were prepared the samples loaded with MTHF were able to gel appropriately while all other did not. This data strongly supports the hypothesis that furanone degradation caused a decrease in the pH of the hydrogel system, causing a reduction in boric acid dissociation, limiting the crosslinking in the gel.

While the mechanism of degradation for the compounds in this work is unknown it is likely very similar due to the similar structure that the furanones share. A potential mechanism of degradation may be found in the work of Bombarelli *et al* 2013, who showed that, in neutral and alkaline solutions (as 1% borate is) lactone compounds such as furanones degrade through the hydrolysis and opening of the lactone ring structure (Gómez-Bombarelli, Calle and Casado, 2013). This would mean that each of the furanone compounds use din this work may be degrading in this manner, yielding

a range of linear molecules such as succinic acid (Hashem and Senning, 1999). While this mechanism of degradation is supported by the literature there may be one or more other mechanisms occurring simultaneously in this work. However, further investigation into these mechanisms is beyond the scope of this project.

Due to the obvious impact the process of forming a loaded hydrogel has on the furanone compounds an alternative method of loading furanones into hydrogels is needed. If this is not possible a new drug delivery system for the application of furanones to chronic wounds may be required.

2.6 Conclusion

An optimal method for the repeatable production of PVA borate hydrogels was developed. It was found that repeatable hydrogels could be produced using dry powder components instead of liquid stock solutions as starting materials and that using 100% hydrolysed PVA yielded the least variation in gel stiffness but that over all stiffness was significantly higher. Therefore, as 98-99% hydrolysed PVA yielded softer gels yet still exhibited relatively low variation in stiffness, this polymer was selected for production of hydrogels. The hydrogels formed using the optimised method were assessed rheologically and several candidate formulations selected. Following full rheological characterisation, a hydrogel formulation containing 6% w/w PVA and 1% w/w borate was selected as the optimal formulation for the delivery of furanones to wounds due to its low shear modulus and low adhesiveness. This formulation was loaded with four furanone compounds, all of which resulted in significant changes in hydrogel textural properties, with some furanones (sotolon and ascorbic acid) causing complete failure of gelation and causing samples to remain entirely liquid. Additionally, one furanone (HDMF) significantly reduced gel stiffness giving a very soft and sticky gel. Significant colour changes were also noted in three furanones (HDMF sotolon and ascorbic acid). Investigation of the release profiles of HDMF and MTHF from the hydrogels revealed a total release percentage of approximately 2000% of the total loaded drug for MTHF, whereupon it was concluded that the changes in hydrogel texture, colour and anomalous release profiles were due to furanone degradation under hydrogel forming conditions. Upon investigation it was found that the conditions present during the formation of a hydrogel including elevated temperature, presence of borate and elevated pH exerted a significant effect on the

stability of each of the 4 furanones tested. It was therefore decided that either an alternative method of hydrogel loading or of compound delivery was needed.

2.7 References

Abdelkader, D. H. *et al.* (2016) 'Characterisation and in vitro stability of low-dose, lidocaine-loaded poly(vinyl alcohol)-tetrahydroxyborate hydrogels', *International Journal of Pharmaceutics*, 500(1–2), pp. 326–335. doi: 10.1016/J.IJPHARM.2016.01.046.

Abdelkader, D. H. *et al.* (2018) 'Enhanced cutaneous wound healing in rats following topical delivery of insulin-loaded nanoparticles embedded in poly(vinyl alcohol)-borate hydrogels', *Drug Delivery and Translational Research*. doi: 10.1007/s13346-018-0554-0.

Ali, A. and Ahmed, S. (2018) 'Recent Advances in Edible Polymer Based Hydrogels as a Sustainable Alternative to Conventional Polymers', *Journal of Agricultural and Food Chemistry*, pp. 6940–6967. doi: 10.1021/acs.jafc.8b01052.

Alopaeus, J. F. *et al.* (2020) 'Mucoadhesive buccal films based on a graft co-polymer – A mucin-retentive hydrogel scaffold', *European Journal of Pharmaceutical Sciences*, 142, p. 105142. doi: 10.1016/j.ejps.2019.105142.

Annabi, N. *et al.* (2017) 'Engineering a sprayable and elastic hydrogel adhesive with antimicrobial properties for wound healing', *Biomaterials*, 139, pp. 229–243. doi: 10.1016/J.BIOMATERIALS.2017.05.011.

Ashley, G. W. *et al.* (2013) 'Hydrogel drug delivery system with predictable and tunable drug release and degradation rates', *Proceedings of the National Academy of Sciences of the United States of America*, 110(6), pp. 2318–2323. doi: 10.1073/pnas.1215498110.

Avais, M. and Chattopadhyay, S. (2019) 'Waterborne pH responsive hydrogels:

Synthesis, characterization and selective pH responsive behavior around physiological pH', *Polymer*, 180, p. 121701. doi: 10.1016/j.polymer.2019.121701.

Bae, S. Bin, Nam, H. C. and Park, W. H. (2019) 'Electrospraying of environmentally sustainable alginate microbeads for cosmetic additives', *International Journal of Biological Macromolecules*, 133, pp. 278–283. doi: 10.1016/J.IJBIOMAC.2019.04.058.

Bashari, A., Rouhani Shirvan, A. and Shakeri, M. (2018) 'Cellulose-based hydrogels for personal care products', *Polymers for Advanced Technologies*, 29(12), pp. 2853–2867. doi: 10.1002/pat.4290.

Bender, L. *et al.* (2020) 'A novel dual action monolithic thermosetting hydrogel loaded with lidocaine and metronidazole as a potential treatment for alveolar osteitis', *European Journal of Pharmaceutics and Biopharmaceutics*, 149, pp. 85–94. doi: 10.1016/j.ejpb.2020.01.007.

Boonkaew, B. *et al.* (2014) 'Antimicrobial efficacy of a novel silver hydrogel dressing compared to two common silver burn wound dressings: Acticoat^{TM} and PolyMem Silver ®', *Burns*, 40(1), pp. 89–96. doi: 10.1016/j.burns.2013.05.011.

Braun, D. B. and Rosen, M. R. (2000) *Rheology Modifiers Handbook: Practical Use and Application*. doi: 10.1017/S0017383509990313.

Calvo Catoira, M. *et al.* (2019) 'Overview of natural hydrogels for regenerative medicine applications', *Journal of Materials Science: Materials in Medicine*. doi: 10.1007/s10856-019-6318-7.

Castrillon, N. *et al.* (2019) 'Super absorbent polymer replacement for disposable baby diapers', (October). doi: 10.13140/RG.2.2.15095.98720.

Censi, R. *et al.* (2009) 'Photopolymerized thermosensitive hydrogels for tailorable diffusion-controlled protein delivery', *Journal of Controlled Release*, 140(3), pp. 230–236. doi: 10.1016/j.jconrel.2009.06.003.

Chai, Q. *et al.* (2017) 'Hydrogels for Biomedical Applications: Their Characteristics and the Mechanisms behind Them', *Gels*, 3(1), p. 6. doi: 10.3390/gels3010006.

Chandran, J. *et al.* (2014) 'Degradation of colour in beetroot (Beta vulgaris L.): A kinetics study', *Journal of Food Science and Technology*. Springer India, 51(10), pp. 2678–2684. doi: 10.1007/s13197-012-0741-9.

Charles-Bernard, M. *et al.* (2005) 'Interactions between volatile and nonvolatile coffee components. 1. Screening of nonvolatile components', *Journal of Agricultural and Food Chemistry*, 53(11), pp. 4417–4425. doi: 10.1021/jf048021q.

Charlesworth, B. *et al.* (2014) 'Dressing-related trauma: Clinical sequelae and resource utilization in a UK setting', *ClinicoEconomics and Outcomes Research*, 6(1), pp. 227–239. doi: 10.2147/CEOR.S59005.

Chen, N. *et al.* (2019) 'Cellulose-based injectable hydrogel composite for pH-responsive and controllable drug delivery', *Carbohydrate Polymers*, 225, p. 115207. doi: 10.1016/j.carbpol.2019.115207.

Chen, Y. and Sidisky, L. M. (2011) 'Quantification of 4-hydroxy-2,5-dimethyl-3-furanone in fruit samples using solid phase microextraction coupled with gas chromatography-mass spectrometry', *Journal of Chromatography A*, 1218(38), pp. 6817–6822. doi: 10.1016/j.chroma.2011.07.103.

Dini, A. *et al.* (2019) 'The kinetics of colour degradation, chlorophylls and xanthophylls loss in pistachio nuts during roasting process', *Food Quality and Safety*,

3(4), pp. 251–263. doi: 10.1093/fqsafe/fyz020.

Donnelly, R. F. *et al.* (2009) 'Delivery of Methylene Blue and meso-tetra (N-methyl-4-pyridyl) porphine tetra tosylate from cross-linked poly(vinyl alcohol) hydrogels: A potential means of photodynamic therapy of infected wounds', *Journal of Photochemistry and Photobiology B: Biology*, 96(3), pp. 223–231. doi: 10.1016/J.JPHOTOBIOL.2009.06.010.

El-Aassar, M. R. *et al.* (2015) 'Controlled drug release from cross-linked κ-carrageenan/hyaluronic acid membranes', *International Journal of Biological Macromolecules*, 77, pp. 322–329. doi: 10.1016/j.ijbiomac.2015.03.055.

Fan, X. *et al.* (2019) 'pH-responsive cellulose-based dual drug-loaded hydrogel for wound dressing', *European Polymer Journal*. Elsevier Ltd, 121, p. 109290. doi: 10.1016/j.eurpolymj.2019.109290.

Franck, A. (2004) 'Understanding rheology of structured fluids'. TA Instruments, pp. 1–11. Available at: http://www.tainstruments.com/pdf/literature/AAN016_V1_U_StructFluids.pdf.

García-Fernández, L. *et al.* (2020) 'Injectable hydrogel-based drug delivery system for cartilage regeneration', *Materials Science and Engineering C*, 110, p. 110702. doi: 10.1016/j.msec.2020.110702.

Gautam, M. and Santhiya, D. (2019) 'Pectin/PEG food grade hydrogel blend for the targeted oral co-delivery of nutrients', *Colloids and Surfaces A: Physicochemical and Engineering Aspects*, 577, pp. 637–644. doi: 10.1016/j.colsurfa.2019.06.027.

Ghorpade, V. S. *et al.* (2019) 'Citric acid crosslinked carboxymethylcellulose-polyvinyl alcohol hydrogel films for extended release of water soluble basic drugs',

Journal of Drug Delivery Science and Technology, 52, pp. 421–430. doi: 10.1016/j.jddst.2019.05.013.

Gómez-Bombarelli, R., Calle, E. and Casado, J. (2013) 'Mechanisms of lactone hydrolysis in acidic conditions', *Journal of Organic Chemistry*, 78(14), pp. 6880–6889. doi: 10.1021/jo4002596.

Gupta, A. *et al.* (2019) 'The production and application of hydrogels for wound management: A review', *European Polymer Journal*. Pergamon, 111, pp. 134–151. doi: 10.1016/J.EURPOLYMJ.2018.12.019.

Hashem, A. and Senning, A. (1999) '2(3H)-Furanones', in *Advances in Heterocyclic Chemistry*.

Hennink, W. E. and van Nostrum, C. F. (2012) 'Novel crosslinking methods to design hydrogels', *Advanced Drug Delivery Reviews*, 64, pp. 223–236. doi: 10.1016/J.ADDR.2012.09.009.

Hibbins, A. R. *et al.* (2017) 'Design of a Versatile pH-Responsive Hydrogel for Potential Oral Delivery of Gastric-Sensitive Bioactives', *Polymers*, 9(12), p. 474. doi: 10.3390/polym9100474.

Holger Kapp (2006) *Clinical performance of a hydrogel dressing in the management of chronic wounds – a prospective application study in 81 patients*. Hartmann Group, Germany.

Hu, W. *et al.* (2019) 'Advances in crosslinking strategies of biomedical hydrogels', *Biomaterials Science*, 7, p. 843. doi: 10.1039/c8bm01246f.

Hui, B., Zhang, Y. and Ye, L. (2014) 'Preparation of PVA hydrogel beads and adsorption mechanism for advanced phosphate removal', *Chemical Engineering*

Journal, 235, pp. 207–214. doi: 10.1016/j.cej.2013.09.045.

Inoue, T. and Osaki, K. (1993) 'Rheological properties of poly(vinyl alcohol)/sodium borate aqueous solution.', *Rheologica Acta*, 32, pp. 550–555.

Jeong, G.-T. *et al.* (2007) 'Synthesis of poly(sorbitan methacrylate) hydrogel by free-radical polymerization', *Applied Biochemistry and Biotechnology*, 137–140(1–12), pp. 935–946. doi: 10.1007/s12010-007-9109-4.

Joint Formulary Comittee (2019) *British National Formulary 78: Sept 2019 - March 2020*. London: Pharmaceutical Press. Available at: www.bnf.nice.org.uk (Accessed: 28 March 2020).

Kim, M. S. *et al.* (2020) 'Antimicrobial hydrogels based on PVA and diphlorethohydroxycarmalol (DPHC) derived from brown alga Ishige okamurae: An in vitro and in vivo study for wound dressing application', *Materials Science and Engineering C*, 107, p. 110352. doi: 10.1016/j.msec.2019.110352.

Kochkodan, V., Darwish, N. Bin and Hilal, N. (2015) 'The Chemistry of Boron in Water', in *Boron Separation Processes*, pp. 35–63. doi: 10.1016/B978-0-444-63454-2.00002-2.

Koehler, J., Brandl, F. P. and Goepferich, A. M. (2018) 'Hydrogel wound dressings for bioactive treatment of acute and chronic wounds', *European Polymer Journal*, 100, pp. 1–11. doi: 10.1016/j.eurpolymj.2017.12.046.

Koetting, M. C. *et al.* (2015) 'Stimulus-responsive hydrogels: Theory, modern advances, and applications', *Materials Science and Engineering R: Reports*, pp. 1–49. doi: 10.1016/j.mser.2015.04.001.

Konig, T. *et al.* (1999) 'Flavor: Elucidation of Its Formation Pathways during Storage

of Citrus', *J. Agric. Food Chem.,* 2(888), pp. 3288–3291.

Konishi, M. *et al.* (2003) 'In vivo anti-tumor effect through the controlled release of cisplatin from biodegradable gelatin hydrogel', *Journal of Controlled Release*, 92(3), pp. 301–313. doi: 10.1016/S0168-3659(03)00364-X.

Kumazawa, K. and Masuda, H. (2003) 'Investigation of the change in the flavour of a coffee drink during heat processing', *Agricultural and Food Chemistry*, 51, pp. 2674–2678.

Larrañeta, E. *et al.* (2018) 'Hydrogels based on poly(methyl vinyl ether-co-maleic acid) and Tween 85 for sustained delivery of hydrophobic drugs', *International Journal of Pharmaceutics*, 538(1–2), pp. 147–158. doi: 10.1016/J.IJPHARM.2018.01.025.

Leaper, D., Assadian, O. and Edmiston, C. E. (2015) 'Approach to chronic wound infections', *British Journal of Dermatology*, 173(2), pp. 351–358. doi: 10.1111/bjd.13677.

Lee, F., Bae, K. H. and Kurisawa, M. (2015) 'Injectable hydrogel systems crosslinked by horseradish peroxidase', *Biomedical Materials*, 11(1), p. 014101. doi: 10.1088/1748-6041/11/1/014101.

Li, J. and Mooney, D. J. (2016) 'Designing hydrogels for controlled drug delivery', *Nature Reviews Materials*. doi: 10.1038/natrevmats.2016.71.

Li, X. *et al.* (2018) 'Functional Hydrogels With Tunable Structures and Properties for Tissue Engineering Applications', *Frontiers in Chemistry*. Frontiers, 6, p. 499. doi: 10.3389/fchem.2018.00499.

Lim, H. P. *et al.* (2020) 'Pickering emulsion hydrogel as a promising food delivery

system: Synergistic effects of chitosan Pickering emulsifier and alginate matrix on hydrogel stability and emulsion delivery', *Food Hydrocolloids*, 103, p. 105659. doi: 10.1016/j.foodhyd.2020.105659.

Lone, S. *et al.* (2019) 'Gelatin-chitosan hydrogel particles for efficient removal of Hg(ii) from wastewater', *Environmental Science: Water Research and Technology*, 5(1), pp. 83–90. doi: 10.1039/c8ew00678d.

Loughlin, R. G. *et al.* (2008) 'Modulation of gel formation and drug-release characteristics of lidocaine-loaded poly(vinyl alcohol)-tetraborate hydrogel systems using scavenger polyol sugars', *European Journal of Pharmaceutics and Biopharmaceutics*, 69(3), pp. 1135–1146. doi: 10.1016/J.EJPB.2008.01.033.

Malvern Intruments Limited (2016) 'A Basic Introduction to Rheology'. Available at: https://cdn.technologynetworks.com/TN/Resources/PDF/WP160620BasicIntroRheology.pdf.

Mandal, P. *et al.* (2020) 'Magnetic Particle Anchored Reduction and pH Responsive Nanogel for Enhanced Intracellular Drug Delivery', *European Polymer Journal*, p. 109638. doi: 10.1016/j.eurpolymj.2020.109638.

Marco-Dufort, B. and Tibbitt, M. W. (2019) 'Design of moldable hydrogels for biomedical applications using dynamic covalent boronic esters', *Materials Today Chemistry*, 12, pp. 16–33. doi: 10.1016/J.MTCHEM.2018.12.001.

Martinez, A. W. *et al.* (2014) 'Effects of crosslinking on the mechanical properties, drug release and cytocompatibility of protein polymers', *Acta Biomaterialia*, 10(1), pp. 26–33. doi: 10.1016/j.actbio.2013.08.029.

Masuda, F. (1994) 'Trends in the Development of Superabsorbent Polymers for

Diapers', in *Superabsorbent Polymers*, pp. 88–98. doi: 10.1021/bk-1994-0573.ch007.

Matsumura, H. *et al.* (2013) 'A model for quantitative evaluation of skin damage at adhesive wound dressing removal', *International Wound Journal*, 10(3), pp. 291–294. doi: 10.1111/j.1742-481X.2012.00975.x.

McCarron, P. A. *et al.* (2011) 'Preliminary Clinical Assessment of Polyvinyl Alcohol-Tetrahydroxyborate Hydrogels as Potential Topical Formulations for Local Anesthesia of Lacerations', *Academic Emergency Medicine*, 18(4), pp. 333–339. doi: 10.1111/j.1553-2712.2011.01032.x.

Murphy, D. J. *et al.* (2012) 'Physical characterisation and component release of poly(vinyl alcohol)–tetrahydroxyborate hydrogels and their applicability as potential topical drug delivery systems', *International Journal of Pharmaceutics*, 423(2), pp. 326–334. doi: 10.1016/J.IJPHARM.2011.11.018.

Nezhad-Mokhtari, P. *et al.* (2019) 'A review on the construction of hydrogel scaffolds by various chemically techniques for tissue engineering', *European Polymer Journal*, 117, pp. 64–76. doi: 10.1016/J.EURPOLYMJ.2019.05.004.

Ogata, Y. and Kosugi, Y. (1970) 'Ultraviolet spectra of l-ascorbic acid and cupric ascorbate complex', *Tetrahedron*, 26(20), pp. 4711–4716. doi: 10.1016/S0040-4020(01)93122-9.

Olaru, A.-M. *et al.* (2018) 'Biocompatible chitosan based hydrogels for potential application in local tumour therapy', *Carbohydrate Polymers*, 179, pp. 59–70. doi: 10.1016/J.CARBPOL.2017.09.066.

Pons, A. *et al.* (2010) 'Identification of a sotolon pathway in dry white wines', *Journal of Agricultural and Food Chemistry*, 58(12), pp. 7273–7279. doi: 10.1021/jf100150q.

Rammenssee, S. *et al.* (2005) 'Rheological characterization of hydrogels formed by recombinantly produced spider silk', *Appl. Phys A*. doi: 10.1007/s00339-005-3431-x.

Rosa dos Santos, J.-F. *et al.* (2009) 'Soft contact lenses functionalized with pendant cyclodextrins for controlled drug delivery', *Biomaterials*, 30(7), pp. 1348–1355. doi: 10.1016/J.BIOMATERIALS.2008.11.016.

Roscher, R., Schwab, W. and Schreier, P. (1997) 'Stability of naturally occurring 2,5-dimethyl-4-hydroxy-3[2H]-furanone derivatives', *European Food Research and Technology*, 204(6), pp. 438–441. doi: 10.1007/s002170050109.

Ross-Murphy, S. B. and McEvoy, H. (1986) 'Fundamentals of Hydrogels and Gelation.', *British Polymer Journal*, 18(1), pp. 2–7. doi: 10.1002/pi.4980180103.

Savins, J. G. (1968) 'Shear thickening phenomena in poly(vinyl)alcohol-borate complexes', *Rheologica Acta*, 7(1), pp. 87–93. doi: 10.1007/BF01970320.

Shalla, A. H. *et al.* (2019) 'Recent review for removal of metal ions by hydrogels', *Separation Science and Technology (Philadelphia)*, 54(1), pp. 89–100. doi: 10.1080/01496395.2018.1503307.

Shu, C.-K., Mookherjee, B. and Ho, C.-T. (1985) 'Volatile Components of the Thermal Degradation of 2,5 - dimethyl-4-hydroxy-3(2H)-furanone', *Journal of Agricultural and Food Chemistry*, 07735, pp. 446–448.

Singh, B., Kumar, A. and Rohit (2020) 'Synthesis and characterization of alginate and sterculia gum based hydrogel for brain drug delivery applications', *International Journal of Biological Macromolecules*, 148, pp. 248–257. doi: 10.1016/j.ijbiomac.2020.01.147.

Skelland, A. H. P. and Meng, X. (1996) 'The critical concentration at which interaction

between polymer molecules begins in dilute solutions', *Polymer - Plastics Technology and Engineering*, 35(6), pp. 935–945. doi: 10.1080/03602559608000608.

Snape, T., Astles, A. and Davies, J. (2010) 'Understanding the chemical basis of drug stability and degradation', *The Pharmaceutical Journal*, 285, p. 416.

Struble, L. J. and Ji, X. (2001) 'Rheology', in *Handbook of Analytical Techniques in Concrete Science and Technology*, pp. 333–367. doi: 10.1016/B978-081551437-4.50012-6.

Tamahkar, E. *et al.* (2020) 'A novel multilayer hydrogel wound dressing for antibiotic release', *Journal of Drug Delivery Science and Technology*, p. 101536. doi: 10.1016/j.jddst.2020.101536.

Tang, Y., Pang, L. and Wang, D. (2017) 'Preparation and characterization of borate bioactive glass cross-linked PVA hydrogel', *Journal of Non-Crystalline Solids*, 476, pp. 25–29. doi: 10.1016/j.jnoncrysol.2017.07.017.

Tavakoli, J. and Tang, Y. (2017) 'Honey/PVA hybrid wound dressings with controlled release of antibioticsStructural, physico-mechanical and in-vitro biomedical studies', *Materials Science and Engineering C*, 77, pp. 318–325. doi: 10.1016/j.msec.2017.03.272.

Wichterle, O. and Lim, D. (1960) 'Hydrophillic gels for biological use', *Nature*, 185, pp. 117–118. doi: 10.1038/scientificamerican0268-74.

Winter, G. D. (1962) 'Formation of the scab and the rate of epithelization of superficial wounds in the skin of the young domestic pig', *Nature*, 193(4812), pp. 293–294. doi: 10.1038/193293a0.

Wong, R. S. H., Ashton, M. and Dodou, K. (2015) 'Effect of crosslinking agent

concentration on the properties of unmedicated hydrogels', *Pharmaceutics*, 7(3), pp. 305–319. doi: 10.3390/pharmaceutics7030305.

Xing, L. *et al.* (2019) 'pH-sensitive and specific ligand-conjugated chitosan nanogels for efficient drug delivery', *International Journal of Biological Macromolecules*. ., pp. 85–97. doi: 10.1016/j.ijbiomac.2019.08.237.

Yeast Metabolome Database (2020) *Sotolon (YMDB01572) - Yeast Metabolome Database*, *Yeast Metabolome Database 2.0*. Available at: http://www.ymdb.ca/compounds/YMDB01572 (Accessed: 21 April 2020).

Yuan, J. P. and Chen, F. (1998) 'Degradation of Ascorbic Acid in Aqueous Solution', *Journal of Agricultural and Food Chemistry*, 46(12), pp. 5078–5082. doi: 10.1021/jf9805404.

Zhang, H., Wehrman, M. D. and Schultz, K. M. (2019) 'Structural Changes in Polymeric Gel Scaffolds Around the Overlap Concentration', *Frontiers in Chemistry*, 7(MAY), p. 317. doi: 10.3389/fchem.2019.00317.

Zhang, H., Zhang, F. and Wu, J. (2013) 'Physically crosslinked hydrogels from polysaccharides prepared by freeze–thaw technique', *Reactive and Functional Polymers*, 73(7), pp. 923–928. doi: 10.1016/J.REACTFUNCTPOLYM.2012.12.014.

Zhang, L. *et al.* (2019) 'A Systematic Review and Meta-Analysis of Clinical Effectiveness and Safety of Hydrogel Dressings in the Management of Skin Wounds', *Frontiers in Bioengineering and Biotechnology*. Frontiers Media S.A., 7. doi: 10.3389/fbioe.2019.00342.

Zoellner, P., Kapp, H. and Smola, H. (2007) 'Clinical performance of a hydrogel dressing in chronic wounds: a prospective observational study.', *Journal of wound*

care, 16(3), pp. 133–136. doi: 10.12968/jowc.2007.16.3.27019.

Chapter 3

Formulation and characterisation of a novel PVA aerogel for the delivery of furanones to wound biofilms

3.1 Introduction

The stability of active ingredients used in pharmaceutical formulations is of the utmost importance. Degradation of the active ingredients in a formulation can not only affect the efficacy of a product, but can also impact upon formulation safety and physical properties (Blessy *et al.*, 2014). Avoiding these unwanted effects is the primary reason stability studies must be carried out when formulating a new drug product. The production of PVA-borate hydrogels, while simple, has many aspects which may have led to the degradation of the four furanone compounds which are the focus of this work. As such, an alternative method of preparing furanone-loaded hydrogels is required. However, prior to developing a novel method for loading furanones into hydrogels while avoiding degradation, the possible sources of degradation must be understood.

3.1.1 Drug degradation in PVA-borate hydrogels

When considering the production and use of PVA-borate hydrogels as a drug delivery mechanism there are three possible causes of compound degradation; thermal degradation, pH and borate mediated degradation, and hydrolytic degradation. Thermal degradation may be caused by the requirement for temperatures of 90 °C when forming the hydrogel. This stage is likely unavoidable as, without the elevated temperature, PVA would not dissolve to form the sol phase.

The requirement for borate as a crosslinking agent results in the system having an alkaline pH. Due to its relatively high pK_a value (9.2) boric acid does not readily dissociate in an acidic environment. This means that, under acidic conditions, the borate anion required for mono- and di-diol formation (see figure 2.20 in chapter 2) is

not present (Kochkodan, Darwish and Hilal, 2015). Therefore, attempts to reduce the pH of the hydrogel system will result in incomplete gel formation.

Finally, hydrolytic degradation may occur due to the aqueous environment required for the successful formation of a hydrogel. Indeed, regarding drug stability, hydrogels and other semi-solid formulations with a high percentage water content are often considered in the same way as single-phase liquids (Loftsson, 2014). However, hydrolysis in this aqueous environment may also be encouraged by the elevated temperature, and the increased pH in the system. These potential mechanisms of degradation will be discussed in the context of furanones.

3.1.2 Degradation of furanones

Furanones are most commonly associated with various terrestrial and marine plants. It has been previously noted, in fields such as nutraceutical manufacture, that the formulation factors affecting the stability and degradation of botanical compounds remain largely unknown (Hoag, 2001). As such, the incorporation of phytochemicals such as furanones into pharmaceutical products is likely to be highly complex. As stated previously, during the formation of PVA-borate hydrogels the furanone compounds would experience a range of harsh conditions, including elevated temperatures, elevated pH and a potentially hydrolytic environment. The stability of furanones under each of these conditions is considered. Unfortunately, due to the limited use of furanones in pharmaceutical products, reports of the stability of these compounds in this context are extremely limited.

3.1.2.1 Thermal stability of furanones

Furanones have previously been shown to be heat labile. Shu *et al.* (1985) showed that when subjected to high temperatures (160 °C) for 30 minutes in aqueous solution, the

furanone HDMF (also known as DMHF) is readily degraded to produce a wide range of products such as 2,3-entanedione and acetoxy acetone. The authors suggest that the degradation process begins with the opening of the furan ring followed by further degradation of the resultant linear molecule (Shu, Mookherjee and Ho, 1985). Interestingly, in this study, Shue *et al*. found the extent of thermal degradation and the products formed was found to be largely dependent on pH.

3.1.2.2 pH mediated degradation of furanones

Shu *et al.* (1985) showed that the thermal degradation of HDMF was significantly influenced by the environmental pH. The furanone displayed higher rates of degradation (i.e. greater mass of degradation products was detected) at lower pH but furanone degradation resulting in a wider range of degradation products was noted at a higher pH. These high pH degradation products included 3 separate furanone derivatives; 2,4,5-trimethyl-furanone, 2-ethyl-5-methyl-furanone, and 2,4-dimethyl-5-ethyl-3(2H)-furanone. This is not the only report of pH mediated structural changes in furanone compounds. A study by Raab *et al.* in 2003 showed that HDMF underwent rapid change from a mono-enantiomeric sample to a racemic mixture as pH increased. Conversely, HDMF was found to undergo minimal racemisation at a pH of between 3.8 and 5 (Raa*b et al*, 2003). This indicates that in aqueous solution pH can have a profound effect on the structure of this furanone. Finally, the work of Roscher *et al.* (1997) demonstrated that HDMF was unstable in an aqueous environment over a range of pH (2.0-8.0). The authors showed that, at the upper and lower pH values tested, the half-life of HDMF was 4 days and 7 days, respectively. It was found that the optimal pH to maintain HDMF stability was 3.5, with a reported half-life of 141 days (Roscher, Schwab and Schreier, 1997). Again, this work clearly demonstrates the effects of pH, particularly in the alkaline range, can have a significant effect on furanone stability.

Similarly, the stability of ascorbic acid has been shown to be closely related to the pH of the solution. Bandelin *et al.* (1955) showed that at concentrations of 1 mg mL^{-1} or 5 mg mL^{-1} in aqueous solution ascorbic acid was degraded by 100% and 94% respectively over 24 hours at pH 6. This degradation was significantly reduced as the pH of the solution was reduced (Bandelin and Tuschhoff, 1955). The authors also note that ascorbic acid is merely oxidised at a pH of less than 7.2 but truly decomposed at a pH of 7.2 and above. This is significant as the pH of PVA-borate hydrogels, while variable depending on the ratio of PVA and borate, is universally above pH 7.2.

These data on the pH dependent degradation of ascorbic acid supports the idea that it is not just the stability of HDMF that is affected by varying pH but a wider range of furanones.

In order to ameliorate any potential furanone degradation due to increased temperature and raised pH in the hydrogel production process, a cold loading method that did not expose furanones to heat or free borate was trialled. This method aimed to eliminate the two main factors causing degradation in the hydrogels which are elevated temperature, and the presence of free borate ions. The development and use of a novel, minimally crosslinked, polymer aerogel, in place of hydrogels, was also investigated as a potential solution furanone degradation.

3.1.3 Polymer aerogels

There has been much debate in recent years surrounding the definition of an aerogel. Often these definitions are based on the properties of the produced material, and the effect of the drying process on the polymer network (Vareda, Lamy-Mendes and Durães, 2018). Depending on the drying process used and the degree of shrinkage in the polymer network during drying, similar materials may also be classed as a cryogel

or a xerogel (Maleki, Durães and Portugal, 2014). However, for the purposes of this work the original definition of an aerogel will be used. Kistler defined a aerogels as "a gel in which the liquid phase has been replaced with a gas phase" (Kistler, 1931; Vareda, Lamy-Mendes and Durães, 2018).

Aerogels often have a low density, high levels of internal structure, and high porosity (García-González *et al*, 2019). Due to these properties, aerogels have been primarily used in fields such as engineering and aerospace but their use in the biomedical sciences is gaining popularity.

3.1.3.1 Aerogel production

Aerogels can be produced using a number of different methods including supercritical drying, ambient temperature and pressure drying, and lyophilisation. While these methods vary significantly, the main mechanism of replacing a gel's liquid phase with a gas phase remains constant (Figure 3.1).

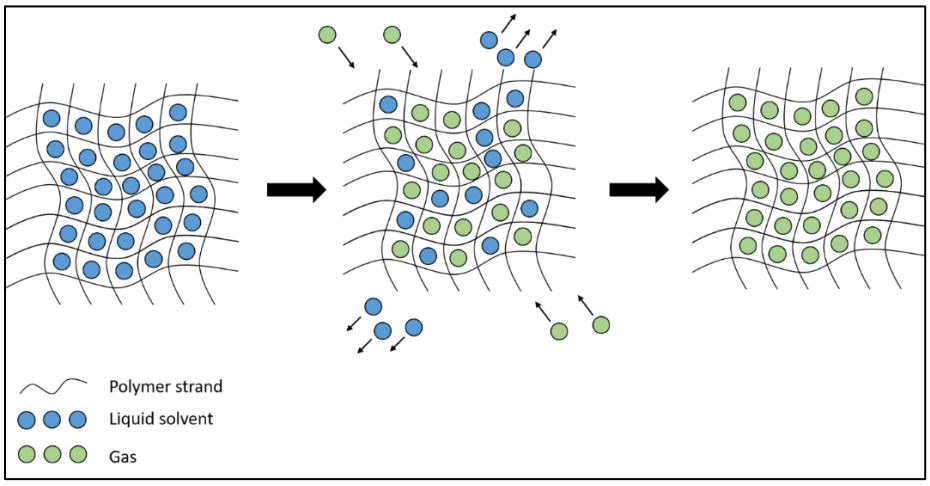

Figure 3.1 – A schematic of the general mechanism of aerogel formation.

A polymer network swollen with a liquid phase (gel) undergoes a process in which the liquid phase is removed either by simple evaporation, freezing and subsequent sublimation, or replacement with a supercritical fluid such as super critical CO_2. This liquid phase is then replaced with a gas, resulting in a three dimensional, highly porous, polymer network with very low density and very high surface area.

The main method for aerogel production reported in the literature is supercritical CO_2 drying, and this method is used primarily to make silica aerogels. The process involves preparing a tetramethyl orthosilicate (TMOS) gel followed by several solvent exchange steps. The TMOS gel, swollen with an organic solvent such as methanol, is then subjected to solvent exchange with supercritical CO_2. The supercritical CO_2 is then evaporated off as CO_2 gas (García-González *et al*, 2012). This method, while effective, is time consuming and expensive due to the solvent exchange steps, the cost of TMOS, and the equipment required to produce and maintain supercritical CO_2. In addition to these limitations, because of the requirement for incredibly high pressures, the process is not without risk. To address these limitations other materials and other methods of drying aerogels have been used.

Ambient temperature and pressure drying has been used to good effect to produce aerogels from a range of materials including graphene, carbon spheres, and silica (Bhagat *et al.*, 2007; Kanamori *et al.*, 2007; Shao *et al.*, 2010; Dubey *et al.*, 2014). These methods have exploited the volatility of the solvents used to form the gel. Primarily, organic solvents such as methanol, methylnonafluorobutylether and hexane are used. The use of ambient pressure and temperature drying addresses the safety issues with supercritical drying but remains a lengthy process due to the numerous solvent exchange steps, and the time required to properly air dry the gel. It should be noted that in the literature an aerogel produced under ambient temperature and pressure may often be referred to a xerogel.

Finally, the process of lyophilisation can also be used. A freeze drying process has been previously used to produce a range of aerogel types including silica aerogels, polymer composite aerogels, and graphene aerogels (Pei, Zhai and Zheng, 2014, 2015;

Li *et al*, 2016). This process is advantageous over the previous methods as the lyophilisation process is often more rapid than ambient drying. While freeze-dry prepared gels often still require a solvent exchange step in their production these steps appear to be shorter than their air-dried counterparts.

With the numerous methods of production and the multiple variations in properties aerogels have been suggested as potential materials for a diverse range of applications such as domestic insulation, electrodes in next generation electronics, and as particle collectors for use in space missions (Jones, 2006; Luo *et al.*, 2020; Yuan *et al.*, 2020). However, one application which is gaining popularity is the use of aerogels as drug delivery systems.

3.1.3.2 Polymer aerogels in drug delivery

Aerogels have been used to good effect in the delivery of several classes of drug. For example, Lovskoya and Menshutina (2020) showed that alginate aerogel particles loaded by drug adsorption, were effectively able to hold and release two non-steroidal anti-inflammatory drugs and a common antihistamine, namely ketoprofen, nimesulide, and loratadine respectively. The authors reported release of 100% of all three active compounds within 50 minutes when tested *in vitro*, with aerogels displaying a rapid burst release of each drug ($T_{1/2}$ of 1.2, 25, and 0.5 minutes, respectively) (Lovskaya and Menshutina, 2020). Similarly, the work of Li *et al.* (2019) demonstrated the use of a halloysite nanoclay aerogel for the dual controlled release of ibuprofen and dexamethasone. They showed total release percentages of approximately 70% and 80%, respectively, at a gastric pH (1.2), and 80% and 90% at pH7.4. Furthermore, the authors showed that these aerogel particles did not significantly inhibit the proliferation of murine intestinal epithelia (Li *et al.*, 2019)

suggesting a level of biocompatibility. This study clearly displays the potential utility of aerogels as drug delivery systems. In addition to these particular studies, success in drug delivery has been shown with silica aerogels, starch aerogels and alginate aerogels among others (García-González *et al.*, 2015; Gonçalves *et al.*, 2016; Follmann *et al.*, 2018).

3.1.3.3 Antimicrobial aerogels

With their proven ability to deliver a range of drugs in a controlled manner, the use of aerogels to deliver antimicrobials is an area of research that is gaining popularity. For example, in 2019 Afrashi *et al.* showed that a novel, fluconazole-loaded, multilayer composite aerogel could effectively release the drug with a total release of approximately 80% over 300 minutes. Further, the loaded aerogel was shown to effectively inhibit the growth of *Candida albicans* as demonstrated by a standard agar diffusion assay (Afrashi *et al*, 2019). Similarly, chitosan aerogel particles were shown to effectively release the glycopeptide antibiotic vancomycin (López-Iglesias *et al.*, 2019). These particles released bactericidal quantities of the drug and, indeed, treatment with vancomycin-loaded particles showed a 1.5-log decrease in viable *S. aureus* bacteria after 6 hours, a 4-log reduction in viable cells at 24 hours post-treatment, and total bacterial killing after 48 hours in a suspension test. The authors also demonstrate that the vancomycin-loaded aerogel particles showed good biocompatibility with a fibroblast cell line that exhibited >80 % total cell viability after treatment (López-Iglesias *et al.*, 2019). Finally, in 2019 Ma *et al.* reported an antimicrobial effect with a PVA-alginate composite aerogel loaded with the nanomaterial graphene oxide, and the fluoroquinolone antibiotic norfloxacin. The authors showed an increase in the zone of inhibition against both *E. coli* and *S. aureus* in a standard agar diffusion assay(Ma *et al.*, 2019). However, the results showed a

maximum increase in zone diameter of 0.5 mm. A more conclusive result could have been obtained if the authors had used a suspension test and quantified loss of viable CFU mL^{-1}.

It is noteworthy that aerogels, loaded with traditional antimicrobials and antimicrobial materials, are not the only form of antimicrobial aerogel that have been tested. For example, the work of Jing *et al.* (2018) demonstrated the efficacy of a novel aerogel material made entirely of titanium dioxide and silver. This material was able to kill up to 100% of *E. coli* growing on agar plates and 99.86% of *S. aureus* in the same assay. This killing was found to be directly correlated with the concentration of silver in the material, with higher concentrations of silver showing a greater percentage killing (Jing *et al.*, 2018).

3.1.3.4 Aerogels as wound dressings

Several studies have suggested aerogels as potential candidates for use in wound dressings. As well as their documented ability to deliver antimicrobials and analgesic drugs, aerogels have been used in a range of other capacities for the improvement of wound healing. In 2016 Vincent-Edwards *et al.* showed that a cellulosic composite aerogel material, functionalised with a fluorescent peptide, could effectively detect as little as 0.13 units mL^{-1} of human neutrophil elastase (Vincent Edwards *et al.*, 2016). This enzyme, which is usually present in chronic wounds at concentrations of 20-30 units mL^{-1} (Ferreira *et al.*, 2017), is important in the wound healing process as it aids in the destruction of bacteria in the wound bed. However, it also destroys host tissue which may lead to the inhibition of epithelialisation and, thus, lead to the deterioration of the wound (Briggaman *et al.*, 1984). Therefore, detection of very low levels of this enzyme could facilitate early treatment for chronic wounds. Alternatively,

Govindarajan *et al.* (2017) showed that a hybrid aerogel material consisting of collagen and wheat grass showed the ability to promote angiogenesis in an embryonic chicken model versus an untreated control. Although limited improvement over a control was seen in *in vivo* wound healing experiments, the authors suggest that this material may make for an excellent wound therapeutic which can mimic the natural extracellular matrix (Govindarajan *et al.*, 2017). While this study showed only a small effect of aerogel treatment on *in vivo* models, a more recent study by Concha *et al.* showed a significantly more rapid wound closure with chitosan/chondroitin sulphate aerogel treatments up to 8 days post wounding in rabbits (Concha *et al.*, 2018). Finally, the previously discussed work of Ma *et al.* showed that treatment of dorsal wounds in mice with their PVA-alginate-graphene oxide aerogel material resulted in a 15% increase in wound closure versus treatment with gauze only, after 14 days. Wound closure was further improved after treatment with PVA/alginate/graphene oxide aerogels loaded with norfloxacin. A wound closure of 90% after 14 days was seen compared to gauze only, which yielded only 65% closure (Ma *et al.*, 2019).

When considered together these studies clearly demonstrate the potential of aerogels as wound dressings. These materials have been demonstrated as effective drug delivery systems as well as potential biocompatible wound healing scaffolds and biosensors for the diagnosis of wound inflammation. As such, this chapter aims to develop a polymer aerogel material to deliver furanones to chronic wound biofilms.

3.2 Aims and Objectives

The work described here aims, firstly, to develop a cold loading method for producing furanone-loaded hydrogels, while eliminating the exposure of furanones to high temperatures and free borate ions. Second, this chapter will develop and characterise a novel, minimally crosslinked PVA aerogels for the delivery of furanones to chronic wound biofilms. Finally, furanone release from the developed delivery mechanisms will be characterised.

3.3 Materials and Methods

3.3.1 Materials and equipment

Poly(vinyl alcohol), molecular weight 31,000-50,000, 98-99% hydrolysed, sodium tetraborate decahydrate, 4-hydroxy-2,5-dimethyl-3(2H)-furanone ≥98%, FG (HDMF), 2-methyltetrahydrofuran-3-one ≥ 97% FG (MTHF), L-ascorbic acid 99% and 4,5-Dimethyl-3-hydroxy-2,5-dihydrofuran-2-one ≥97% FG (Sotolon) were purchased from Sigma Aldrich (Gillingham, Dorset, UK) and used without further modification.

A Labconco FreeZone 4.5 bench top freeze dryer was used to perform drying of all samples (Labconco, Kansas, USA)

A Malvern Mastersizer 2000 was used with a Scirocco dry sampler for the determination of powder particle sizes (Malvern, UK).

3.3.2 Formulation and characterisation of a freeze-dried hydrogel

To overcome the compound degradation issues a new method of loading the hydrogels was required. A cold loading method involving the rehydration of a freeze-dried unloaded hydrogel in a furanone solution was developed.

3.3.2.1 Determination of optimal freeze-drying time

A PVA-borate hydrogel containing 8% PVA and 2% borate was prepared using the method developed in section 2.3.2.2, chapter 2. This gel was then divided in to either 5 g or 10 g samples. These samples were then placed in a 6 well uncoated, tissue culture plate and then stored at -30 °C for 6 hours to ensure the samples were completely frozen. The 6 well plate was then transferred to a freeze drier and hydrogel samples were lyophilised, uncovered for 36 hours at -80 °C and 0.04 mBar pressure. The samples were periodically removed from the freeze drier to be weighed so that

water loss could be assessed. Percentage water loss was calculated using the following equation 1. Where T_{wc} is the total water content of the sample (g) and W_l is the weight lost from sample at time point (g).

$$\left(\frac{W_l}{T_{wc}}\right) x\ 100 \qquad \text{Equation 1.}$$

3.3.2.2 Preparation and characterisation of a rehydratable freeze-dried hydrogel powder

A standard PVA-borate hydrogel containing 8% PVA and 2% sodium tetraborate was prepared using the method developed in section 2.3.2.2. An 8% PVA and 2% borate hydrogels were used so that comparisons could be made to earlier experiments. The gel was divided into 5 g samples which were then lyophilised as outlined in section 3.3.2.1. Once the hydrogel was completely dry the samples were weighed, and the exact volume of water lost was calculated. The samples were crushed to a coarse powder using a pestle and mortar, and then further processed using a standard domestic spice grinder (Kenwood, UK) to give a fine, free-flowing powder. This powder was then assessed for average particle size and particle size distribution using a Malvern Mastersizer. Briefly, 5 g of powdered freeze-dried material was loaded into the Scirocco 2000 dry sampler and samples were assessed for particle size with a run time of 10.5 s. The powder was then passed through a fine fabric mesh to separate the fine particulate that would rehydrate more quickly and evenly. Both the pass-through and the size excluded material were sized using the above described protocol.

3.3.2.3 Comparison of freeze-dried hydrogels to standard hydrogels

To ensure the freeze drying and rehydration process did not negatively affect the properties of the hydrogels, the similarity of a standard PVA-borate hydrogel to a freeze dried and fully rehydrated hydrogel was assessed rheologically.

A standard PVA-borate hydrogel containing 8% PVA and 2% sodium tetraborate was prepared using the method developed in section 2.3.2.2. The shear modulus of this gel was measured as per section 2.3.2.4. The gel was divided into 5 g samples which were then lyophilised as outlined in section 3.3.2.1. Once the hydrogel was completely dry, they were weighed, and the exact volume of water lost was calculated. The samples were powdered as per section 3.3.2.2.

To rehydrate the hydrogel, the powdered gel was placed in a beaker and deionised water was added at a volume equivalent to the volume of water lost in lyophilisation. The sample was stirred and mixed thoroughly and then incubated at room temperature for 24 hours to allow for complete rehydration. The rehydrated gel was then assessed for any changes in the shear modulus and a full rheological characterisation was performed as per section 2.3.2.4.

3.3.2.4 Further characterisation of freeze-dried hydrogel

The tunability of the shear modulus of a freeze-dried hydrogel was investigated. To assess this, samples of dried and powdered hydrogel were rehydrated with 100%, 110%, 120%, 130%, 140% and 150% of the total water lost during lyophilisation. Briefly 0.2 g of powdered hydrogel was weighed out and deionised water was added in an appropriate volume (Table 3.1). This was then mixed and incubated at room temperature for 24 hours to allow complete rehydration to occur. Rehydrated samples then had their shear moduli measured as detailed in section 2.3.2.4

Table 3.1 – Target percentage rehydration and the volumes of water required to rehydrate 0.2 g of freeze-dried hydrogel powder.

Target Rehydration Percentage	Volume of water added (g)
Control	-
100%	1.8
110%	1.98
120%	2.16
130%	2.34
140%	2.52
150%	2.7

3.3.2.5 Preparation of a furanone-loaded freeze dried hydrogel

To load a hydrogel without causing compound degradation, the following cold loading method was developed.

A hydrogel of the previously identified ideal formulation (6% PVA and 1% borate) was prepared using the method outlined described in section 2.3.2.2. The hydrogel was then frozen and processed to give a fine free flowing powder as detailed in section 3.3.2.2.

All drug-loaded hydrogels were made up to give a final gel weight of 10 g. First, 0.8 g of powered hydrogel was weighed out into a glass scintillation vial. A furanone solution of a suitable concentration was made so that the fully rehydrated gel would

contain 1% furanone by weight. The concentration of furanone solution required was calculated using the following equation.

$$\frac{C_{RH}\, x\, W_{RH}}{H} \qquad \text{Equation 2}$$

Where C_{RH} is the desired concentration of furanone in the final rehydrated gel (mg g^{-1}), W_{RH} is the final weight of the fully rehydrated gel (g) and H is the weight of water to be added to fully rehydrate the gel (g). Once an appropriate furanone stock solution was prepared 9.2 g of furanone stock solution was added to the 0.8 g of hydrogel powder. This was then thoroughly mixed and incubated at room temperature for 24 hours to allow complete rehydration to occur.

3.3.3 Formulation of an aerogel drug delivery system

In order to overcome the poor rehydration time, poor gelation and apparent degradation of the furanones that was observed in the freeze-dried and rehydrated hydrogel, a minimally crosslinked PVA aerogel delivery system was developed.

3.3.3.1 Preparation of PVA aerogels

PVA aerogels were prepared using PVA solutions of varying concentrations and a simple lyophilisation method. A 10% PVA solution was prepared using Mw 31,000-50,000, 98-99% hydrolysed PVA (Sigma Aldrich, Gillingham, UK). The solution was placed in a water bath preheated to 90 °C for 2 hours with intermittent stirring to completely dissolve the PVA. The PVA solution was then removed from the water bath and allowed to cool to room temperature. Once cooled, 2 g of PVA solution was pipetted into each well of a 12 well tissue culture plate. The tissue culture plate was then placed in a -30 °C freezer for 6 hours to ensure all samples were frozen. The frozen samples were then removed from the freezer and placed, uncovered in a freeze

dryer at 0.04 mBar of pressure and a temperature of -80 °C for 24 hours. Once dry, samples were removed from the 12 well plate and stored in an airtight container. This process was then repeated for PVA solutions containing 7.5%, 5% and 1% PVA.

3.3.4 Structural characterisation of PVA aerogels

The structure of the developed aerogels was assessed using three techniques. Firstly, stereo zoom microscopy was used to assess the macro scale internal structure of the aerogels. Secondly, scanning electron microscopy was used in order to assess both the surface morphology and internal structure of the aerogels. Finally, X-ray micro computerised tomography was used to assess the internal structure and homogeneity of the aerogels.

3.3.4.1 Stereo zoom microscopy of aerogels

The general morphology of the developed aerogels was images using stereo zoom microscopy. Samples were prepared as per section 3.3.2.1. Once the aerogels were dry, they were divided in two so that the outer surface and the inner aerogel structure could be viewed simultaneously. Aerogels were then visualised at a magnification of 10x using a Nikon SMZ1500 stereo zoom microscope. Images were captured using the native Nis-Elements software (version 3.2).

3.3.4.2 Scanning electron microscopy of aerogel surface and internal structure

The structure of the aerogels was assessed using scanning electron microscopy. To prepare aerogels for SEM analysis samples were prepped as per section 3.3.2.1. Once aerogels were dry, they were removed from the 12 well plate and divided into quarters. This division of the samples allowed for SEM analysis of both the surface morphology and the internal structure simultaneously. Samples were then affixed to a metal SEM stub using adhesive carbon pads and sputter coated in a gold / palladium alloy to ensure

the aerogels had a conductive surface. Samples were then imaged with a beam acceleration of 30 kV using a Quanta 200 Environmental SEM system.

3.3.4.3 X-ray micro computerised tomography of aerogel internal structure

In order to assess and characterise the internal microstructure of the developed aerogels it was decided that micro X-ray computerised tomography (micro CT) would be used. For this project the micro CT analysis of the novel aerogels was performed in conjunction with the Henry Moseley X-ray imaging facility in Manchester University using a Zeiss Xradia 520 Versa Micro CT scanner.

Aerogel samples were prepared as per section 3.3.2.1 with the following amendments. Aerogels were prepared in a 96 well plate. A 100 µL sample of either 10%, 7.5%, 5% or 1% PVA solution was pipetted into a 96 well plate and frozen at -30 °C for 6 hours. Frozen samples were then transferred to a freeze drier and dried at -80 °C and 0.04 mBar for 48 hours to ensure gels were completely dry. This method produced aerogel samples with an approximate diameter of 5 mm.

To prepare aerogel samples for micro CT analysis samples were fixed to the top of a metal spindle using 3M super 77 spray adhesive (3M, Bracknell, UK). So that images could be taken in triplicate, 3 aerogel samples were stacked on each spindle as shown in Figure 3.2 a. The sample spindle was then placed in a chuck grip positioned between the x-ray detector and x-ray source (Figure 3.2 b)

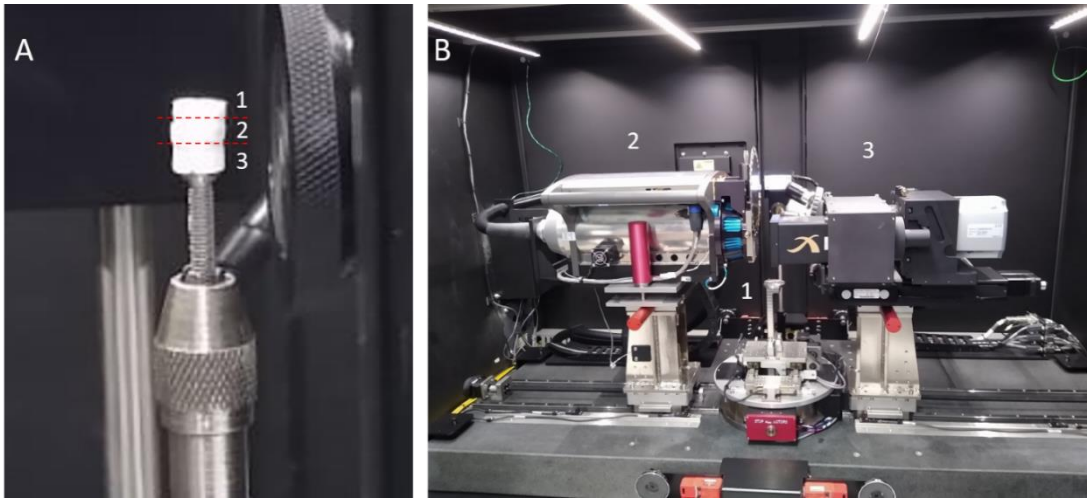

Figure 3.2 – (a) 10% PVA aerogels prepared for Micro CT analysis.

A small aerogel disc was affixed to the sample spindle head using 3M super 77 spray adhesive. In order for samples to be imaged in triplicate, 2 more aerogels were stacked on top of the initial sample. b) The sample spindle was then placed in a chuck grip [1] between the x-ray detector [2] and the x-ray source [3].

To minimise the scan time a 1 mm^3 section in the centre of each aerogel was imaged rather than scan the entire sample. This approach also allowed images to be taken without interference from the outer surface of the gel and from any excess adhesive used to mount the samples.

Samples were imaged using an x-ray source with a power of 70 kV at 71 µA. The sample was positioned 11.55 mm from the x-ray source and 9.55 mm from the x-ray detector. Each 1 mm^3 area within the samples had 1600 individual projections taken. These projections were then stacked using ImageJ (v1.52). ImageJ was then used to compile a 3-dimensional projection of the scan. Due to limitations in processing power that was available only a representative 3D projection of each 1mm^3 sample could be complied.

3.3.5 Preparation and optimisation of furanone-loaded aerogels

In order to assess the suitability of PVA aerogels to deliver furanones to chronic wounds furanone aerogels were prepared and drug release profiles were measured.

3.3.5.1 Preparation of a furanone-loaded aerogel

Furanone-loaded aerogels were prepared as follows. A 10% PVA solution was prepared. Once cooled to room temperature 10 mL of PVA solution was transferred to a glass vial. A furanone was then added to the 10 mL of PVA solution to give the desired final concentration per millilitre of PVA solution. A 1 g amount of the PVA furanone mixture was pipetted into each well of a 12 well tissue culture plate. The samples were then placed in a -30 °C freezer for 6 hours to ensure that all samples were frozen. Once frozen samples were placed, uncovered in a freeze drier for 48 hours to ensure all water was removed. Once dry, aerogels were transferred to an airtight container for storage. This process was repeated to make furanone-loaded 5% and 1% PVA aerogels.

3.3.5.2 Assessment of drug loss during aerogel formation

As the furanone compounds had previously been shown to be unstable when being loaded into PV-borate hydrogels the levels of furanone in loaded aerogels were assessed.

To assess the levels of furanone in loaded aerogels, the aerogels were prepared as per the protocol detailed above. Once furanone-loaded aerogels had been prepared the aerogels were placed in 50 mL of deionised water and vortexed until the aerogel had been completely dissolved. Samples of this solution were then analysed using the UV-Vis spectrophotometer. The values obtained were then converted to concentrations of

furanones using pre-prepared calibration plots and the levels of furanone in the aerogel were calculated using the following formula:

$$F_{RP} \times V_{RP} = F_{AER} \qquad \text{Equation 3}$$

Where F_{RP} is the concentration of furanone measured in the deionised water receiver phase (mg mL^{-1}), V_{RP} is the volume of the receiver phase (mL) and F_{AER} is the concentration of furanone in the aerogel. From this, the percentage drug loss was then calculated. Each loaded aerogel formulation was tested in triplicate.

3.3.5.3 Drug loss during pre-freezing

To assess the effect of pre-freezing on furanone concentration, a stock furanone solution of known concentration was prepared using deionised water as a solvent. The UV absorbance of this stock solution was measured using a UV spectrophotometer. A full scan of all wavelengths was performed to obtain a full absorbance spectrum for the sample. The stock solution was then placed in a -30 °C freezer for 6 hours to allow for ensure complete freezing of the sample. Once completely frozen the stock solution was removed from the freezer and allowed to thaw completely at room temperature. Once the sample was thawed and had come up to room temperature again the UV absorbance of the stock solution was measured a second time, and the furanone concentration was interpolated from the calibration plot. The furanone concentration of the non-frozen sample was taken to be 100% drug concentration and of the freeze thawed sample was reported as a percentage of the non-frozen sample. Each furanone was tested in triplicate.

3.3.5.4 Identification of optimal aerogel drying time

Unloaded PVA aerogels were produced from a 10% PVA solution as detailed in section 3.3.3.1 and furanone-loaded aerogels were prepared as per the protocol detailed in section 3.3.5.1. To identify optimal drying time, samples were removed from the freeze dryer and weighed intermittently to assess percentage water loss. Percentage water loss was calculated similarly to before using the equation in section 3.3.2.5. Each aerogel was tested in triplicate. The optimal drying time was taken to be the earliest time point after which the weight of the aerogel did not reduce further (indicating no further loss of water).

3.3.6 Characterising furanone release from PVA aerogels

Furanone release from PVA aerogels was characterised. Furanone-loaded aerogels containing 10%, 5% and 1% PVA aerogels were prepared as previously described. Due to the rigid nature of the aerogels the use of a Franz diffusion cell was not appropriate as total contact between the aerogel and the semi-permeable membrane could not be guaranteed. An alternative dissolution method was used. Briefly, deionised water was added to a beaker to a volume of 30 mL. This was placed on a magnetic stirrer and kept stirring at a constant speed. A furanone-loaded aerogel was added to the beaker and a 100 µL of receiver phase was removed and diluted appropriately. The absorbance of the diluted sample was read in a UV-Vis spectrophotometer. A full scan of the sample absorbance at all wavelengths was used so that changes in the λ_{max} or the UV absorbance spectrum could be identified. Percentage drug release over time was then calculated.

3.4 Results

3.4.1 Development and assessment of a cold loading technique for the preparation of furanone-loaded hydrogels

As the requirement for high temperatures and the presence of borate caused significant changes in the absorbance spectra of the furanone compounds, it was decided that a method of loading the hydrogel in which temperature and quantity of free, unbound, borate should be kept to a minimum was needed. Thus, the rehydration of a lyophilised PVA-borate hydrogel using a furanone solution was tested.

3.4.1.1 Optimisation of the hydrogel lyophilisation time

The time required to completely lyophilise PVA-borate hydrogel was assessed. It was found that 5 g hydrogels were totally dried after 18 hours and 10 g hydrogels took approximately 24 hours to become totally dried (Figure 3.3 a-b). A gel was defined as totally dry when there was no mass loss between two consecutive time points.

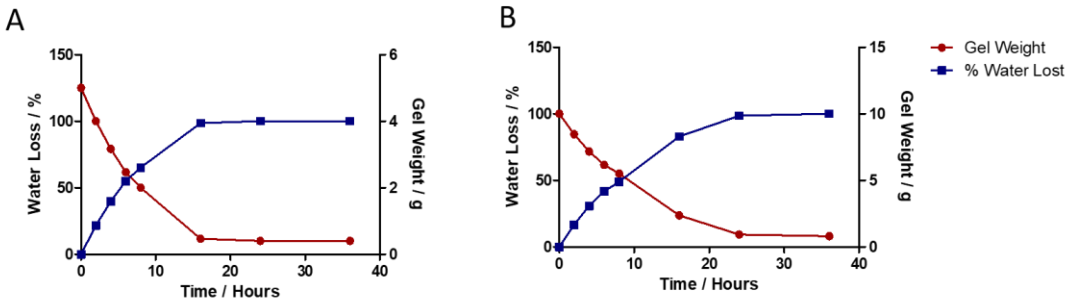

Figure 3.3 – Hydrogel weight and water content measured against lyophilisation time.

(a) When freeze dried in 5g amounts hydrogels were totally dried within 18 hours. (b) When dried in 10 g amounts hydrogels took approximately 24hours to become completely dry. Data points represent the mean of 3 independent replicates ± S.D.

3.4.1.2 Characterisation of a freeze-dried hydrogel powder

As monolithic gels were found to rehydrate poorly and unevenly, dried hydrogels were powdered prior to rehydration. It was hypothesised that a powdered dried hydrogel, having greater surface area, would rehydrate more rapidly and evenly than a monolithic gel. This would give a more homogenous final gel with more even distribution of furanone. Therefore, the freeze-dried hydrogel was powdered using a commercial spice grinder. The powder obtained using this method was assessed for average particle size and particle size distribution. It was found that when processed using only a commercial spice grinder the hydrogel powder had an average particle size of 487 µm. This powder was then passed through a fabric mesh in order to exclude the larger pieces of gel and it was found that this method of processing reduced the average particle size of the powder to 181 µm (Figure 3.4). This process was then used for the production of all future lyophilised gel powders.

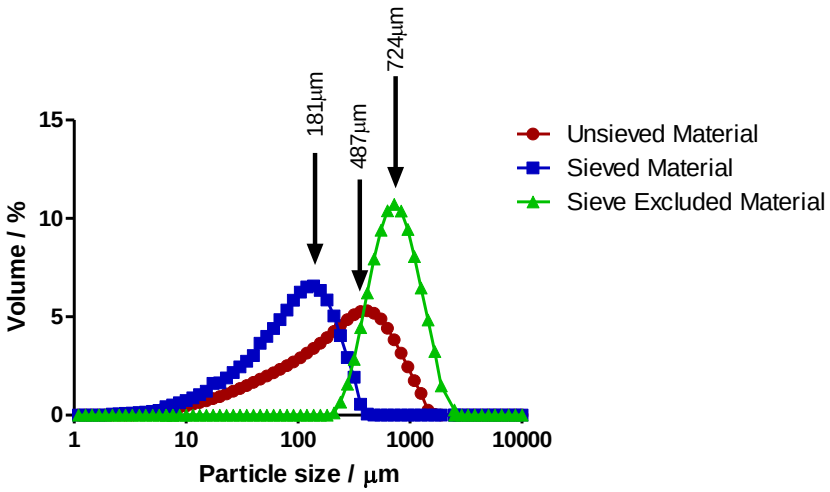

Figure 3.4 – Average particle sizes of freshly powdered dry hydrogel and hydrogel powder processed using a size exclusion mesh.

When processed using just the commercial spice grinder the hydrogel powder had an average particle size of 487µm. When passed through a fabric size exclusion mesh the average particle size was reduced to 181µm. Data points represent the mean of 3 independent replicates ± S.D.

3.4.1.3 Comparison of standard and rehydrated hydrogels

To ensure that the freeze drying, and rehydration process did not negatively affect the rheological properties of the hydrogel, a dried and rehydrated gel was compared to a portion of the same gel which had not been subjected to lyophilisation. It was found that in terms of the shear modulus of the hydrogel there was no significant difference between the standard hydrogel and the freeze dried gel indicating that drying and rehydrating had no negative impact on the rheology of gel and, thus, this method of cold loading could be used to produce a viable loaded gel (Figure 3.5).

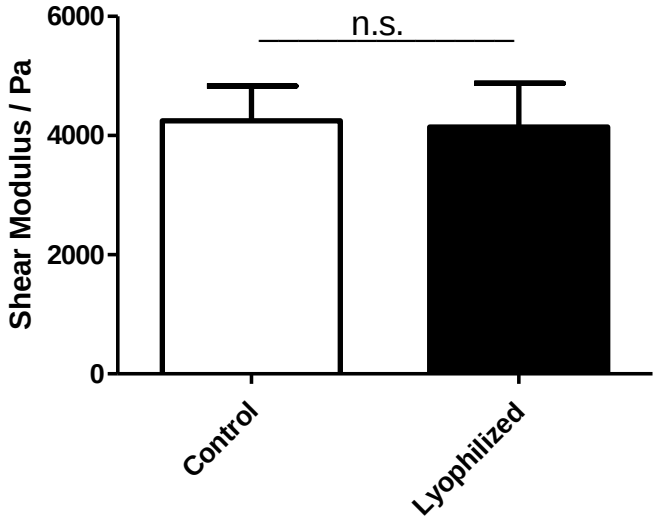

Figure 3.5 – A comparison of the shear moduli of a standard hydrogel and a freeze dried and rehydrated hydrogel.

The standard hydrogel has an average shear modulus of 4245 Pa ± 830.94 while the freeze dried and rehydrated hydrogel had an average shear modulus of 4140.67 PA ± 1043.50. Data was compared using a paired t-test. Data represent the mean of 3 independent replicates ± S.D. n.s. = not significant.

3.4.1.4 Full rheological characterisation of a rehydrated hydrogel

To ensure that the freeze drying, and rehydration process did not significantly impact the rheological profile of the hydrogel, a full rheological characterisation of a dried and rehydrated gel was performed. It was found that the linear viscoelastic region

extended to 100% shear strain before a reduction in G′ and G″ was seen (Figure 3.6 a). The viscoelastic profile showed a gel in which G′ dominated at high shear frequencies and G″ was dominant at low shear frequencies indicating a shear thickening gel. These measurements were confirmed by phase angle measurements which tended towards 0° at higher shear frequencies. The crossover point between G′ and G″ was 3060 Pa at a shear frequency of approximately 1 Hz (Figure 3.6 b). Viscosity measurements showed an increase in the viscosity of the rehydrated gel with increasing shear frequency above 50 Hz and up to 150 Hz (Figure 3.6 c). Adhesiveness testing indicated a gel with very low adhesiveness with a peak normal force of -1.24 N exerted over approximately 0.1 s (Figure 3.16 d).

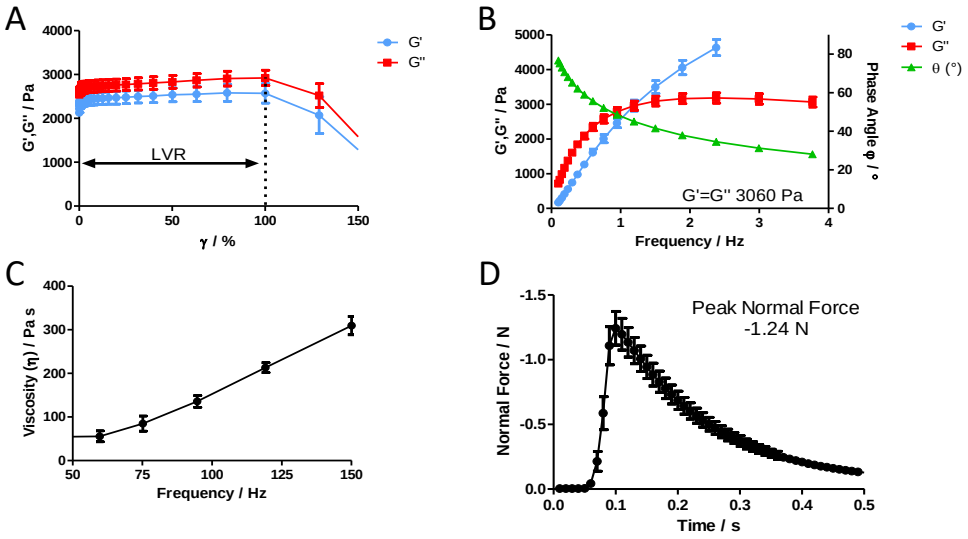

Figure 3.6 – A full rheological characterisation of a freeze dried and rehydrated 6% PVA and 1% borate hydrogels.

(a) Assessment of the linear viscoelastic region of the gel showed that both G′and G" were largely unchanged up to a shear strain of 100%. (b) The viscoelastic profile of the gel showed that G' was dominant at high shear frequencies and G" was dominant at lower shear frequencies indicating a gel which displayed more solid like behaviour at high shear frequencies. This finding was confirmed by phase angle measurements. (c) Assessment of the viscosity profile of the gel showed a steady increase in viscosity as shear frequency increased indicating shear thickening behaviour. (d) Adhesiveness testing showed the gel could exert a peak force of -1.24N over 0.1 s. Data represent the mean of 3 independent replicates ± S.D.

3.4.1.5 Tunability of the shear modulus of rehydrated hydrogels

The extent to which the shear modulus of a freeze dried and rehydrated hydrogel could be modulated using variable rehydration percentages was investigated. It was found that, when freeze dried hydrogels were rehydrated with volumes of water greater than 100% of the water removed during freeze drying, the shear modulus decreased (Figure 3.7 a). The correlation between rehydration percentage and shear modulus was assessed and it was found that the relationship was indeed linear (Figure 3.7 b) and, therefore, an approximate final shear modulus for any given rehydration percentage could be calculated. Conversely, if the shear modulus of the hydrogel prior to freeze drying was known, the volume of water of rehydration required to give a rehydrated gel with a specific shear modulus can be calculated.

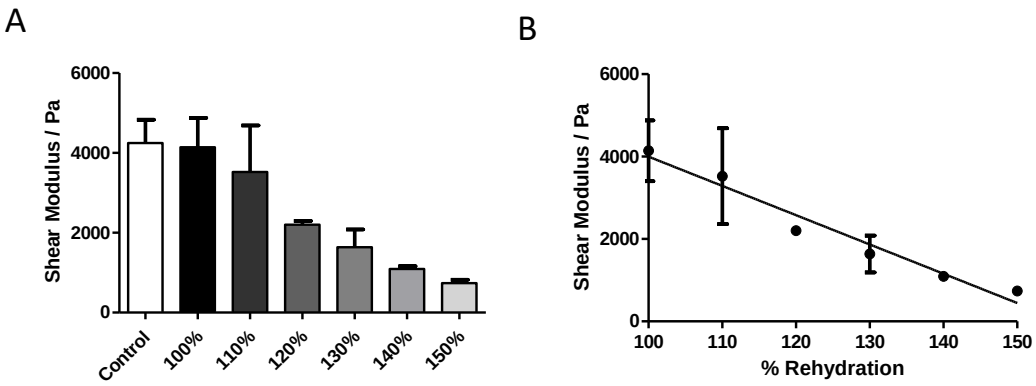

Figure 3.7 – An assessment of the tunability of a rehydrated hydrogels shear modulus.

(a) When freeze dried hydrogels were rehydrated with greater than 100% of the weight of water lost the shear modulus of the rehydrated gel was reduced. (b) The relationship between the rehydration volume and the final shear modulus was shown to be linear (Pearson's coefficient -0.9802, R^2 0.9607 p-value =0.0006). Data represent the mean of 3 independent replicates ± S.D.

3.4.2 Cold loading of hydrogels with furanone compounds

It was found that when loaded with HDMF, the rehydrated hydrogel became significantly softer (reduced shear modulus) and became discoloured with a clouded white appearance (Figure 3.8 a). When loaded with sotolon, the gel did not form, and the sample became entirely liquid. No discoloration of the sample was observed (Figure 3.8 b). When loaded with MTHF the hydrogel formed well and no discolouration or changes in the hydrogels texture was observed (Figure 3.8 c). When loaded with ascorbic acid the gel formed poorly and the sample remained largely liquid. An obvious orange/brown discolouration was seen which darkened in the days following the drug loading (Figure 3.8 d). The image shown in Figure 3.9 d shows an ascorbic acid-loaded sample 48 hours post drug loading.

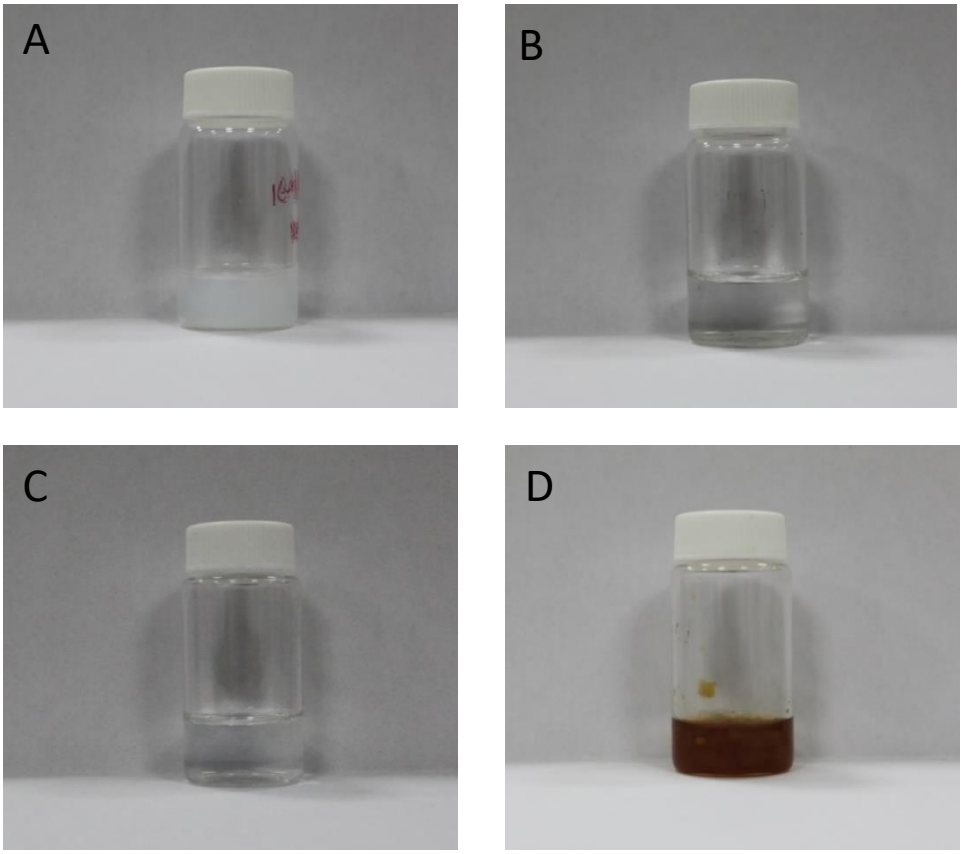

Figure 3.8 - Samples of freeze-dried hydrogel loaded with furanone using a cold loading method.

(a) HDMF-loaded hydrogels were softer than unloaded gels and became cloudy and discoloured. (b) Sotolon-loaded hydrogels formed poorly with samples being entirely liquid. (c) MTHF-loaded hydrogels formed well with no obvious changes in hydrogel texture and no discolouration. (d) Ascorbic acid-loaded hydrogels formed poorly remaining entirely liquid with heavy brown/orange discoloration which worsened over 48 hours

3.4.3 Preparation and characterisation of PVA aerogels

As issues were still being encountered when cold loading the furanones into freeze dried PVA hydrogels, it was hypothesised that the main contributing factor was the continued presence of borate ions in any form (free borate and borate bound in crosslinks). To overcome these issues borate was removed from the PVA hydrogel formulation and a novel minimally crosslinked PVA aerogel was developed and characterised.

3.4.3.1 Formulation and production of PVA aerogels

Several formulations of PVA aerogel were tested and the final products had a wide range of appearance and texture. A PVA aerogel prepared from both 10% and 7.5% PVA solutions produced a firm but slightly pliable aerogel coupons which displayed minimal shrinkage in volume after freeze drying. Aerogels produced using 5% PVA solution resulted in a soft product that held its shape and displayed minimal shrinkage in volume. Finally, aerogels produced using a 1% PVA solution yielded a product with a very soft texture similar to that of cotton wool. This formulation was very fragile and had reduced in volume slightly after freeze drying. The 10% PVA aerogel was selected to be taken forward for drug loading.

3.4.3.2 Structural characterisation of PVA aerogels

PVA aerogels were structurally characterised first by examining their macro structure under stereo zoom microscopy. This was followed by scanning electron microscopy to assess the micro-scale physical structure of the aerogels. Finally, to assess the structure homogeneity the aerogels were imaged using micro CT scanning.

When viewed under stereo zoom microscopy a level of organisation was seen in the internal structure of the aerogels. This took the form of apparent fibres in the gel. This organisation of the internal structure of the gel was most apparent in the 10% PVA aerogels with the majority of fibres being aligned along the vertical axis (perpendicular to the upper and lower surfaces of the gel). This structure was also apparent in the 7.5% PVA aerogel. In the 5% PVA aerogel some apparent organisation remained in the structure of the gel. However, the organisation in the 5% PVA aerogel took the form of distinct areas of fibre organisation. Each area was highly organised within itself, but each area was disorganised compared to the others. Finally, the 1% PVA

aerogel showed no organisation in internal structure with the fibres appearing loosely packed and resembling fibreglass (Figure 3.9 a-d).

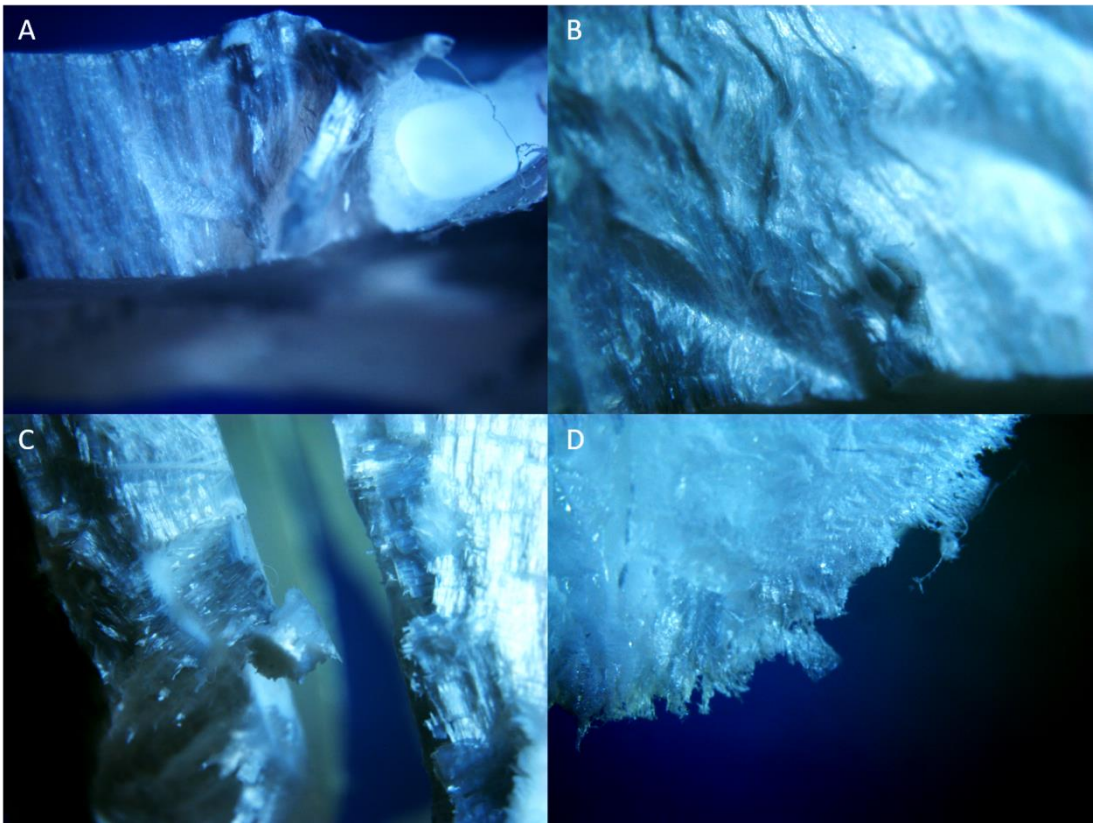

Figure 3.9 – Stereo zoom images of the internal structure of a (a) 10%, (b) 7.5%, (c) 5% and (d) 1% PVA aerogels under 10x magnification.

High levels of organisation can be seen in the 10% aerogel with fibres running vertically. The same order can be seen in the 7.5% aerogel. In the 5% aerogel the organisation is less obvious but small localised areas of organisation of fibres can be seen. No apparent organisation can be seen in the 1% PVA aerogels.

When viewed under SEM, the findings of the stereo zoom imaging were confirmed. The 10% PVA aerogel was found to have a high level of fibre organisation. Again, fibres were organised along one axis. The 7.5% PVA gel showed the same level of organisation along a single axis. The 5% PVA aerogel showed distinct areas of high

fibre organisation. Under SEM the 1% PVA aerogel showed structure that was loosely packed and largely disordered (Figure 3.10 a-h).

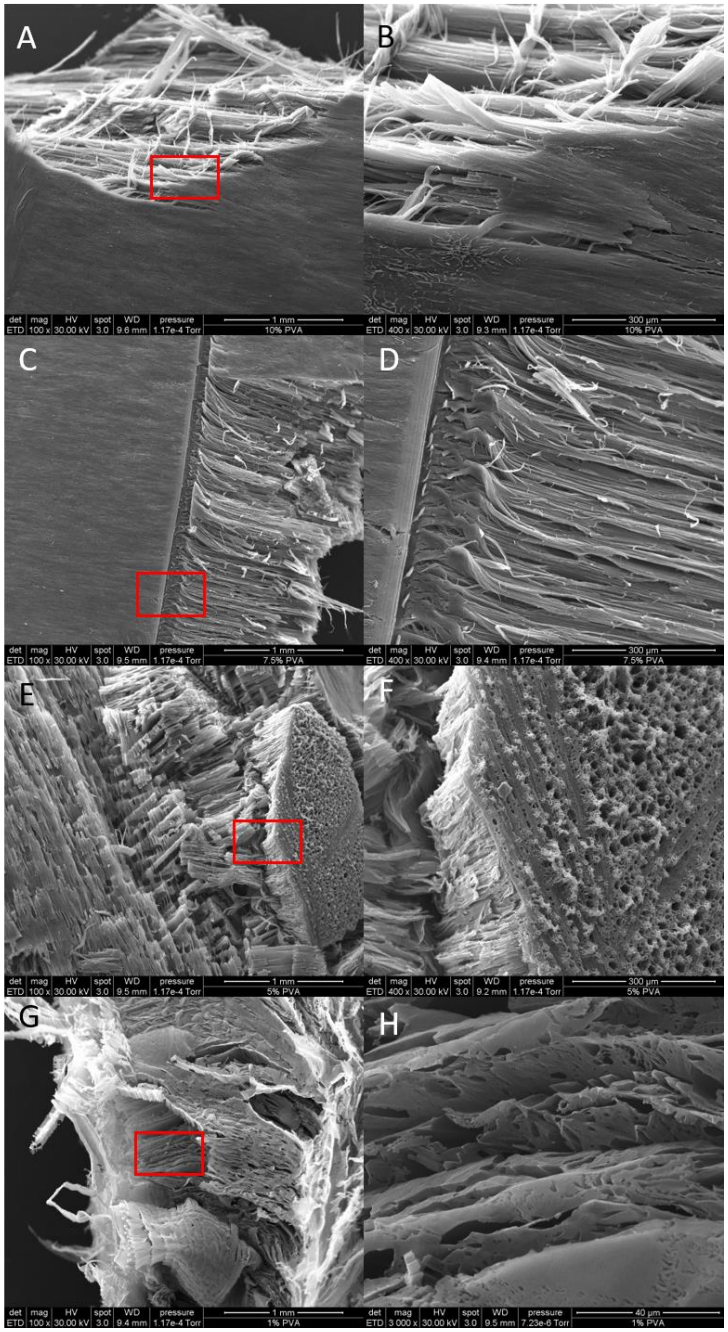

Figure 3.10 – SEM analysis of a (a-b) 10%, (c-d) 7.5%, (e-f) 5% and (g-h) 1% aerogels.

SEM analysis of the internal structure of the aerogels confirmed the findings of the stereo zoom microscopy with high levels of fibre organisation seen in the higher concentration PVA gels and less organisation in the lower concentration PVA gels.

Finally, samples of each aerogel were imaged using micro CT scanning. This allowed for the assessment of the homogeneity of the internal structure of each aerogel formulation. It was found that the 10% aerogel was partially homogeneous but had veins of material with differing density throughout the structure. These areas of altered density suggested that the packing of the fibre strands in the gel was less ordered here (Figure 3.11 a-c).

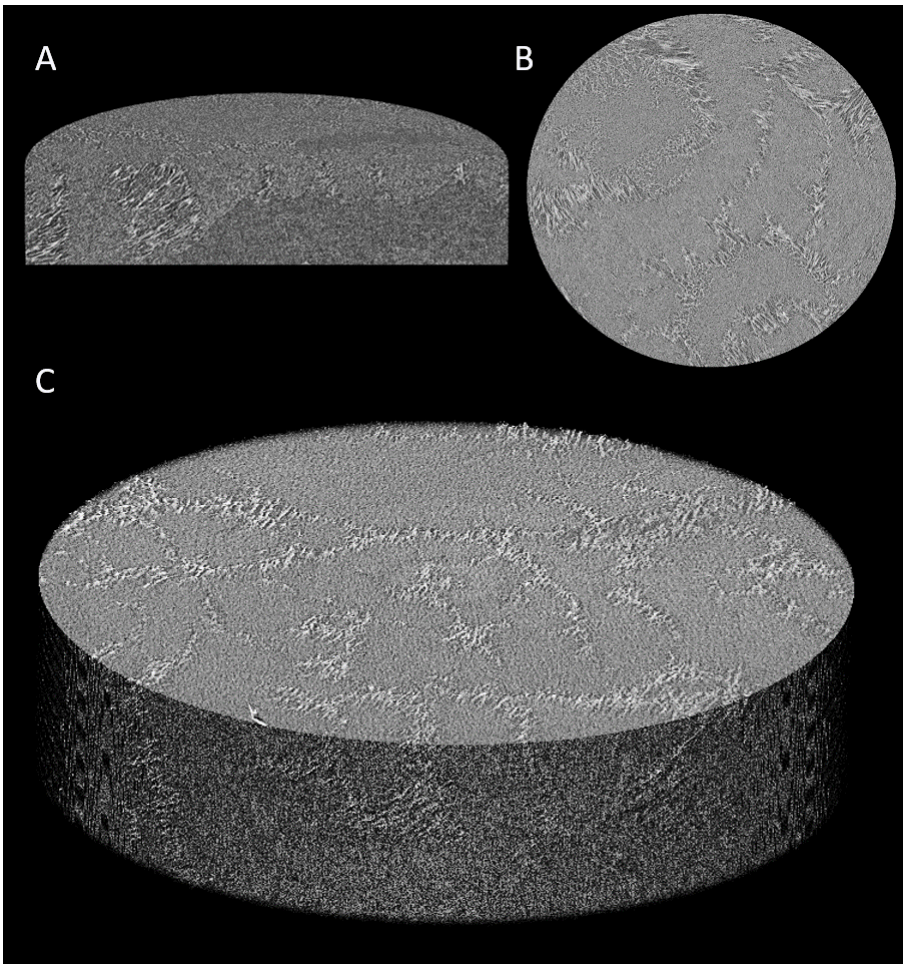

Figure 3.11 – Micro CT scans of a 10% PVA aerogel showing (a) a three-dimensional representation of an orthogonal slice through the scanned section (b) a cross section of the scanned section of the gel and (c) a full three-dimensional representation of the scanned portion of the gel.

Darker regions indicate areas of lower density. Veins of lighter material can be seen throughout the internal structure of the gel. This indicates areas of more tightly packed fibres and therefore a degree of structural heterogeneity within the gel. Images shown are representative images selected from 3 independent replicates.

When imaged using micro CT the 7.5% aerogel appeared similar to the 10% PVA gel with areas of homogenous density and areas of differing density. The areas of heterogeneity were less numerous than those found in the 10% PVA aerogel but were larger in area (Figure 3.12 a-c).

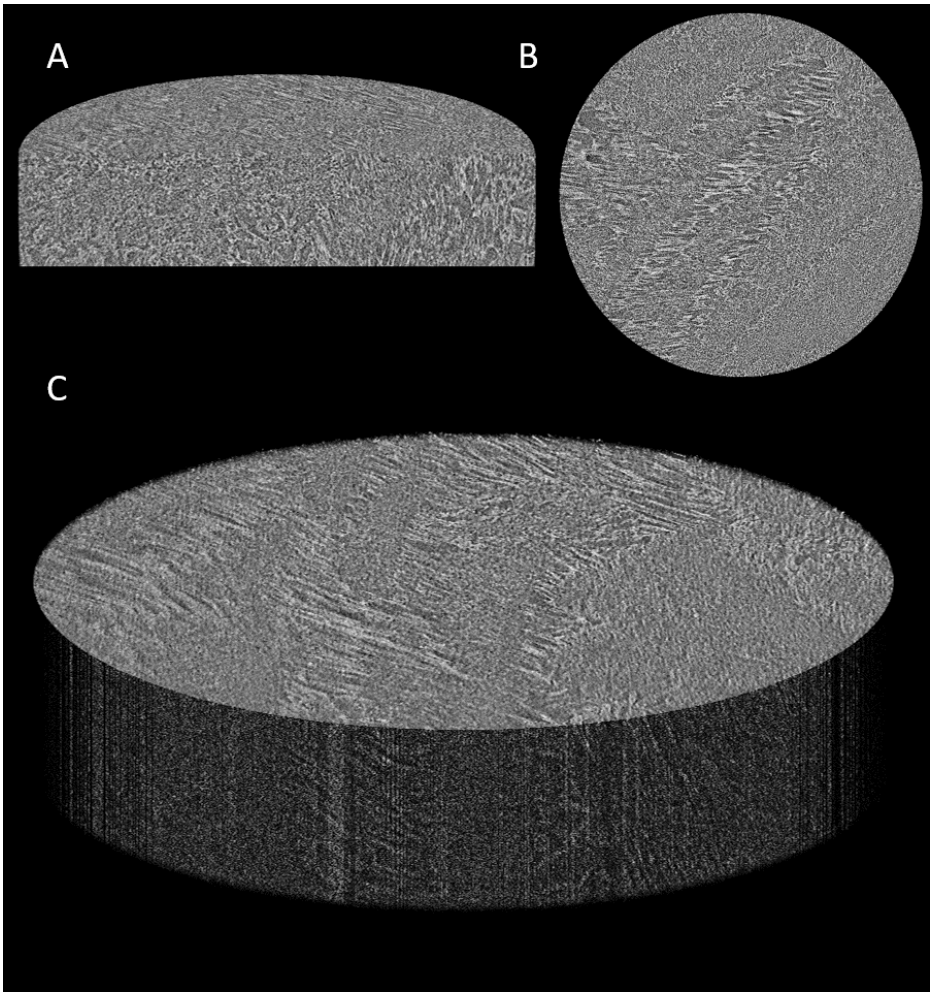

Figure 3.12 -Micro CT scans of a 7.5% PVA aerogel showing (a) a three-dimensional representation of an orthogonal slice through the scanned section (b) a cross section of the scanned section of the gel and (c) a full three-dimensional representation of the scanned portion of the gel.

Darker regions indicate areas of lower density. Veins of lighter material can be seen throughout the internal structure of the gel. Greater homogeneity is seen in the 7.5% PVA aerogel compared to the 10% PVA gel. Images shown are representative images selected from 3 independent replicates.

The 5% PVA aerogel showed significantly more heterogeneity in density with the areas of higher density, and, therefore, tightly packed fibres, being considerably smaller and more evenly distributed throughout the sample than were seen in the 10% and 7.5% PVA aerogels (Figure 3.13 a-c). However, although regions of higher density were more numerous, they were evenly distributed and so the density of the sample is likely more even.

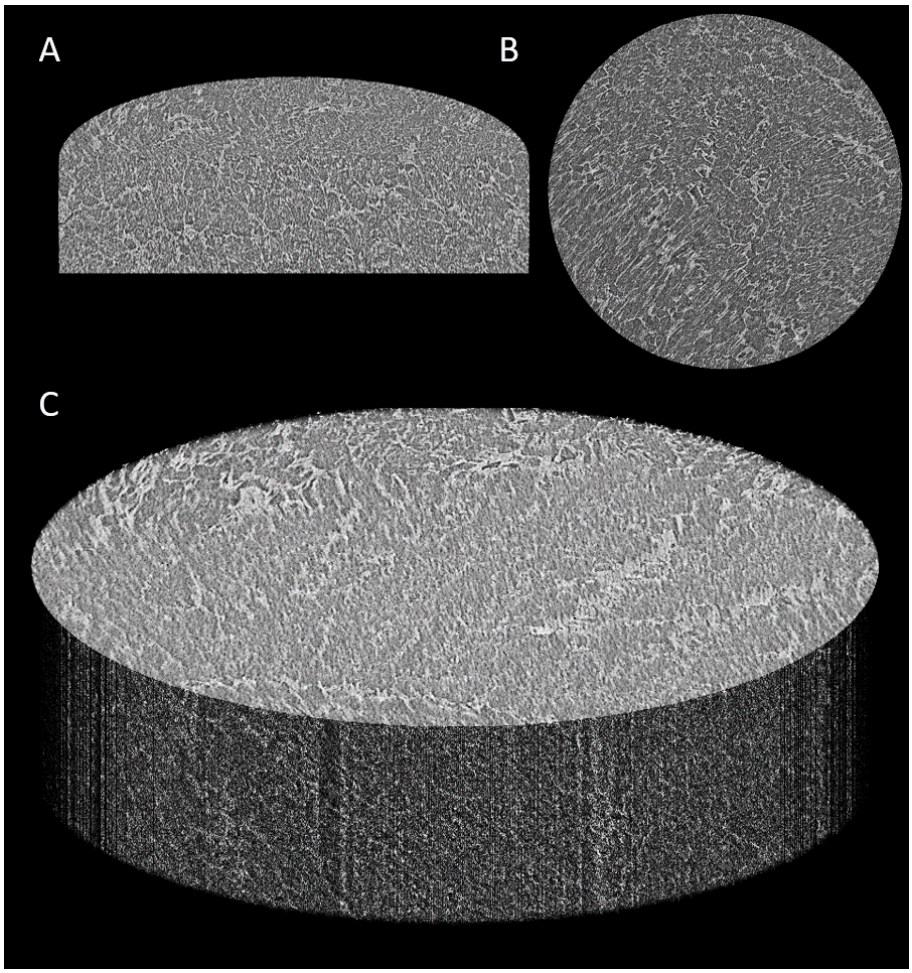

Figure 3.13 - Micro CT scans of a 5% PVA aerogel showing (a) a three-dimensional representation of an orthogonal slice through the scanned section (b) a cross section of the scanned section of the gel and (c) a full three-dimensional representation of the scanned portion of the gel.

Lighter regions indicate areas of higher density. Areas of lighter, and therefore more densely packed material, are more evenly distributed in this sample. This suggests a higher degree of homogeneity in the samples internal structure. Images shown are representative images selected from 3 independent replicates.

Finally, the 1% PVA aerogel appeared to be significantly less dense than the previous samples when viewed under micro CT with areas of higher density materials being less prominent in the sample. Areas of higher density were smaller in size and evenly distributed (Figure 3.14 a-c).

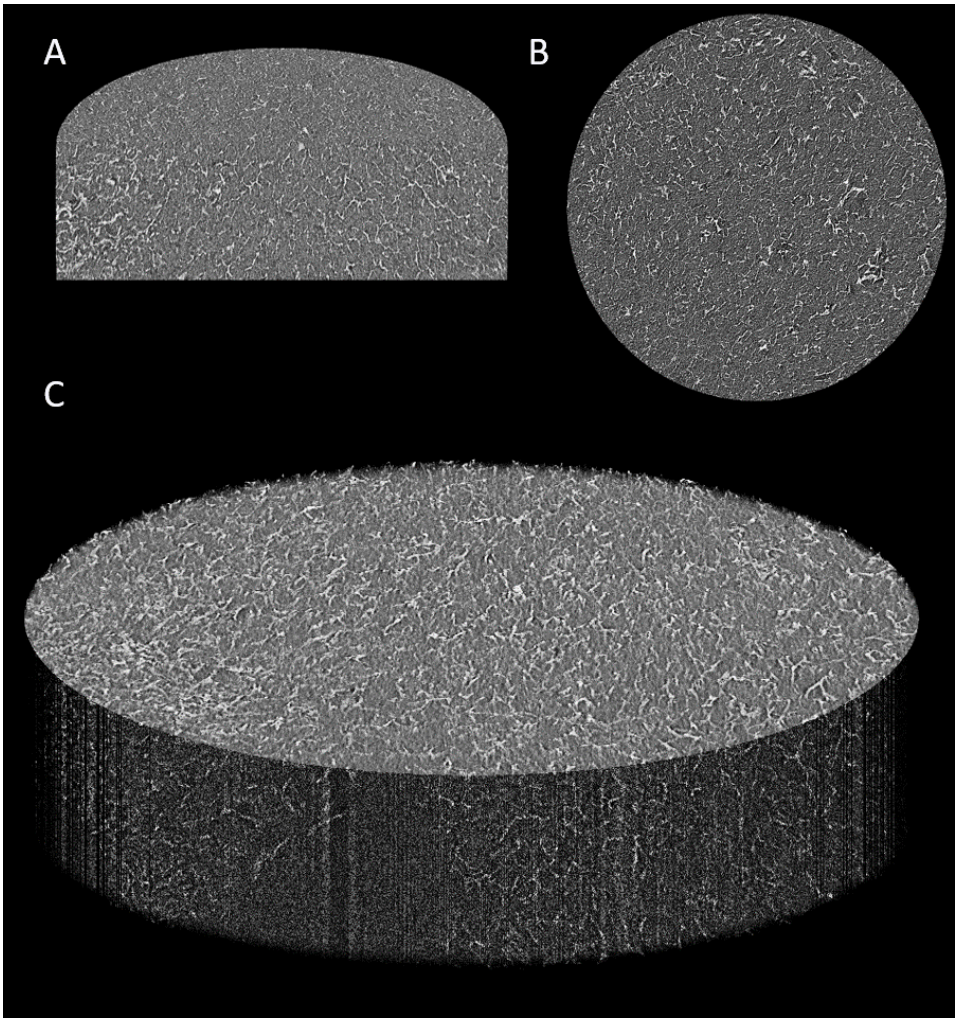

Figure 3.14 - Micro CT scans of a 1% PVA aerogel showing (a) a three-dimensional representation of an orthogonal slice through the scanned section (b) a cross section of the scanned section of the gel and (c) a full three-dimensional representation of the scanned portion of the gel.

Darker regions indicate areas of lower density. This sample appears to be very low density with areas of tightly packed material being smaller in size and more evenly distributed throughout the sample compared to aerogels with higher concentrations of PVA. Images shown are representative images selected from 3 independent replicates.

When the homogeneity and distribution of density of each aerogel was examined it was found that the 10% PVA aerogel was the least homogenous in structure with areas of higher density material (highlighted in red) irregularly distributed throughout the aerogel. The homogeneity increases as PVA concentration decreased (Figure 3.15 a-d).

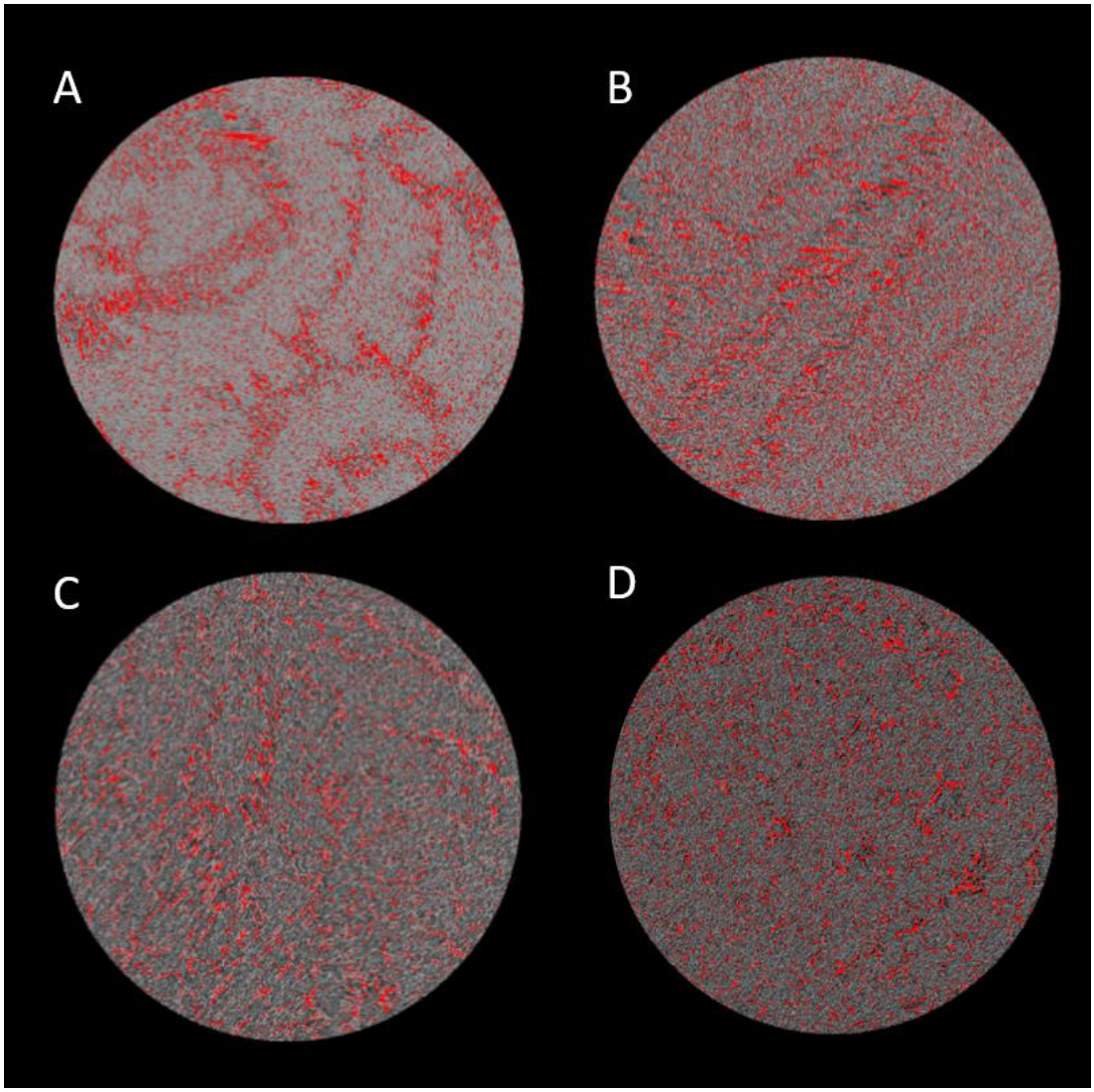

Figure 3.15 – Cross sectional images of (a) 10%, (b) 7.5%, (c) 5% and (d) 1% PVA aerogels with areas of higher density highlighted in red.

The 10% PVA aerogel showed the least structural homogeneity with areas of denser materials being irregularly distributed throughout the gel. Homogeneity of the materials increased as PVA concentration was reduced. Images shown are representative images selected from 3 independent replicates.

3.4.3.3 Stability of furanone compounds during aerogel production

Due to the problems encountered during the loading of furanones into both hydrogels and freeze-dried hydrogels the stability of furanones during the PVA aerogel production process was investigated. It was found that the concentration of HDMF present in the aerogel after it was produced was reduced by 47.68% of the total loaded volume while sotolon concentrations were reduced by 100%. Similar to the hydrogels, the concentration of MTHF was seen to increase significantly by 9591.79%. Ascorbic acid concentrations also appeared to increase by 37.14% (Figure 3.16).

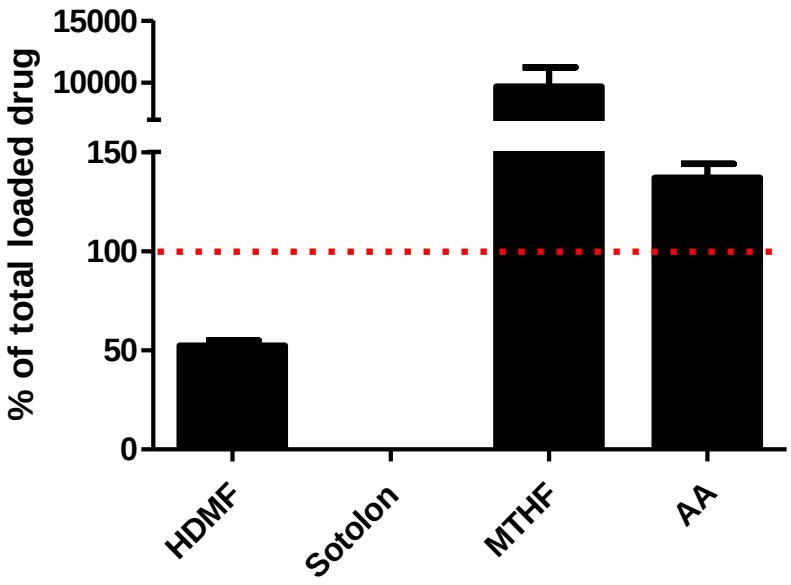

Figure 3.16 – Relative concentrations of furanone present in a loaded 10% PVA aerogel following preparation using a lyophilisation method.

HDMF concentrations decreased by 47.68 % and sotolon concentrations were reduced by 100%. Both MTHF and ascorbic acid concentrations showed an apparent increase of 9591.79% and 37.14% respectively. Data represent the mean of 3 independent replicates ± S.D.

3.4.3.4 Impact of freeze-drying process on furanone concentrations

To identify the cause of the observed loss of furanone the effect of the lyophilisation process on the concentration of furanones in loaded aerogels was explored. Firstly, the impact of the pre-freezing step in the aerogel production method on furanone concentrations in the final aerogel product was investigated. It was shown that undergoing a freeze-thaw cycle had little impact on the overall concentrations of furanone stock solutions with HDMF, Sotolon, MTHF and ascorbic acid showing a 3.45%, 2.40%, 1.66% and 6.02% decrease respectively (Figure 3.17).

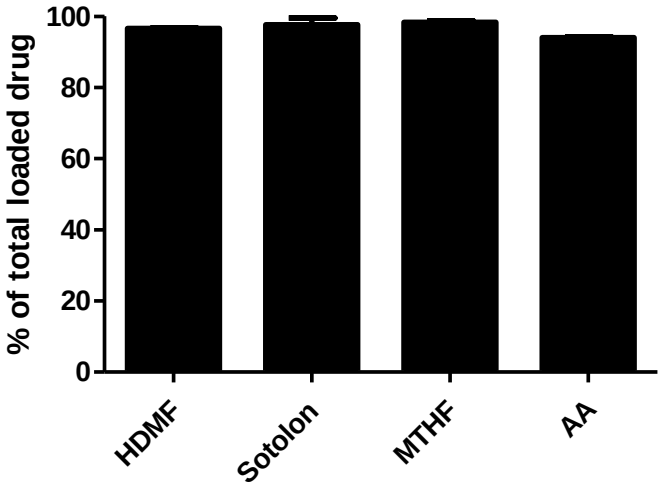

Figure 3.17 – The effect of the pre-freezing step of lyophilisation on the stability of furanones in aqueous solution.

Furanone stock solutions that were prepared and frozen at -30°C and thawed showed no significant reduction in furanone concentrations with HDMF, Sotolon, MTHF and ascorbic acid showed reductions of 3.45%, 2.40%, 1.66% and 6.02% of the total loaded drug volume. Data represents the mean of three independent replicates ± S.D.

3.4.3.5 Optimisation of the freeze-drying process.

It was hypothesised that the volatile furanone compounds were being lost during the freeze-drying process. The freeze-drying protocol was therefore carefully optimised in order to minimise the loss of furanone as far as possible. It was found that both

blank and loaded aerogel formulations were totally dry within 20 hours (Figure 3.18 a). This represented a 28 hours reduction in drying time compared to what had previously been used in this work when preparing the aerogels. Once an optimised freeze-drying process had been identified loaded aerogels were prepared and the concentrations of each furanone post freeze drying were measured. It was found that, after drying under optimised conditions, HDMF concentrations were reduced by only 1.64% and sotolon concentrations were reduced by only 6.15%. However, MTHF and ascorbic acid still showed apparent increased in concentrations of 7192.37% and 110.92% respectively (Figure 3.18 b).

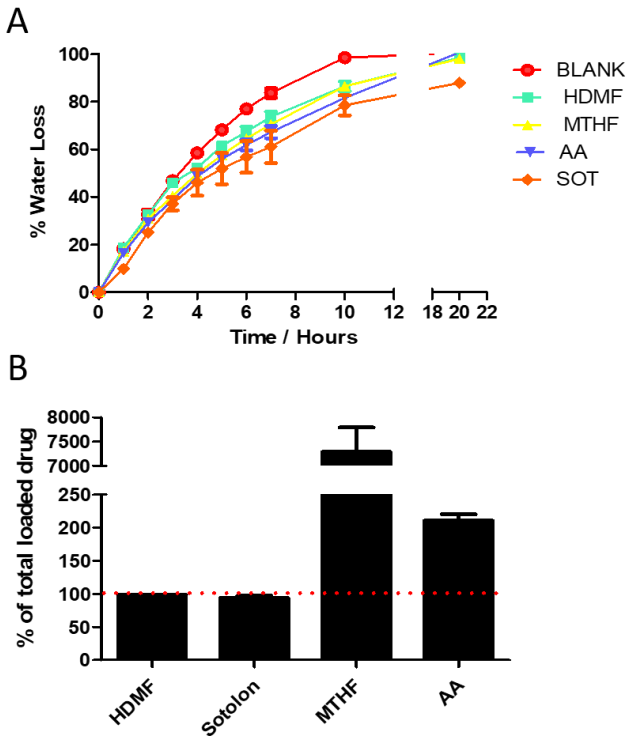

Figure 3.18 - The development and confirmation of an optimised 10% PVA, furanone-loaded aerogel production method.

(a) Water loss during freeze drying was measured and it was shown that all loaded 10% PVA aerogel formulations were dry after 20 hours. (b) Aerogels produced using the optimised method were assessed for drug concentrations post freeze drying. HDMF and sotolon concentrations were reduced by 1.64% and 6.15% respectively while MTHF and ascorbic acid concentrations shoed and apparent increase of 7192.37% and 110.92% respectively. Data represent the mean of 3 independent replicates ± S.D

3.4.5 Furanone release kinetics from PVA aerogels

The release kinetics of furanone compounds from 10%, 5% and 1% PVA aerogels. Both ascorbic acid and MTHF had poor release profiles. No aerogel formulation showed significant release of ascorbic acid (Figure 3.19 a). Those formulations loaded with MTHF showed greater than 100% release from a 1% and 10% PVA aerogels and no significant release from a 5% aerogel (Figure 3.19 b). HDMF showed no significant release from a 1% PVA aerogel but showed a rapid burst release from a 5% PVA aerogel releasing 84% of the total loaded drug in 30 minutes with a total drug release of 90% of the total loaded volume over the full 5 hours. HDMF also showed a more controlled initial release from a 10% PVA aerogel which resulted in a total release of 70% of the total loaded drug (Figure 3.19 c). The release of sotolon from a 1% PVA aerogel was not tested as the aerogel did not form appropriately. However, sotolon showed a rapid burst release from a 5% PVA aerogel over 10 minutes with a final release of 85% of the total loaded drug. Sotolon showed a rapid initial burst release from a 10% PVA aerogel, releasing 65% of the total loaded drug in 30 minutes and reaching a final release of 92% of the total loaded drug (Figure 3.19 d).

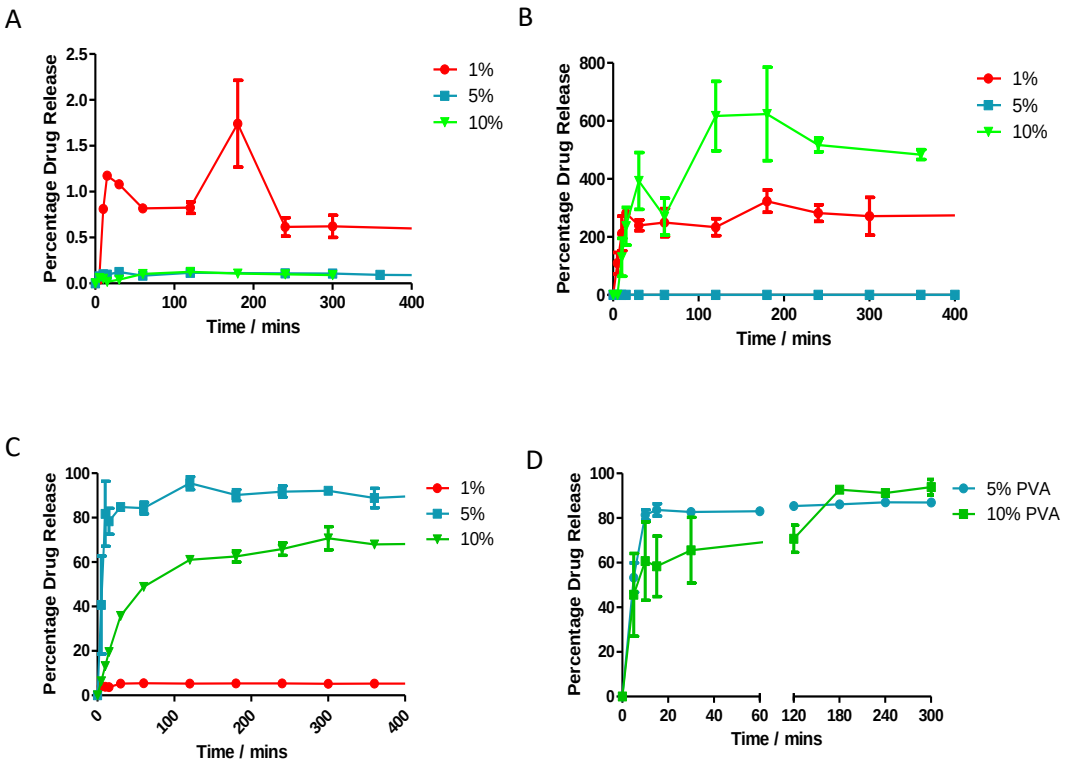

Figure 3.19– Release kinetics of each furanone from a 1%, 5% and 10% PVA aerogel.

(a) Ascorbic acid showed no significant release from any of the three aerogel formulations. (b) MTHF showed greater than 100% release from both the 1% and 10% PVA aerogel formulations and no significant release from the 5% PVA formulation. (c) HDMF showed no significant release from the1% PVA formulation but showed rapid burst release from the 5% PVA formulation and a more controlled release from the 10% PVA formulation. (d) Release of sotolon from a 1% PVA aerogel formulation was not tested. Sotolon showed initial burst release from both the 5% and 10% PVA aerogel formulations.

3.5 Discussion

As no single aspect of the hydrogel production process (i.e. elevated temperature, free borate or altered pH) was found to be universally responsible for the degradation of the four furanones (as shown in chapter 2), a method of cold loading the hydrogels in the absence of free borate was developed. This method involved total dehydration of an unloaded hydrogel, and rehydration of the resultant dry gel in a furanone solution. The hydrogels were originally dried in a standard oven at 40 °C or air dried at ambient temperature for 24 hours to 48 hours but it was found that this produced a compact, highly brittle, glass-like material which did not fully rehydrate when placed in a furanone solution. This was likely due to the nature of the drying process resulting in the formation of a material known as a xerogel. These materials are hydrogels which have been dried with no restrictions on network shrinkage. As the liquid phase leaves the gel by evaporation, high capillary pressure is introduced to the pores of the polymer network causing these pores to collapse (Duräes *et al.*, 2012; Rodríguez-Dorado *et al.*, 2019). The result is a material with a highly compacted and tight network of polymers which cannot easily take up liquid during rehydration. To solve this issue, a method of drying the hydrogels based on lyophilisation was investigated. It was hypothesised that the lyophilisation process would result in a dried hydrogel with a fully open pore structure as reported by Hou *et al.* in 2003. This study showed that lyophilisation could produce highly porous materials with porosities of up to 98% (Hou, Grijpma and Feijen, 2003). It was hypothesised that maintaining a high porosity in the in the dried gels used here would facilitate rapid rehydration in furanone solution. This method of furanone loading also avoided exposing the furanones to excessive heat and it was believed that as the hydrogel was cross linked before drying that the free borate ions would be at a minimum, thus, reducing their interaction with the furanone compounds.

Hydrogels were found to take between 18 to 24 hours to be completely dehydrated in a freeze dryer and, once submerged in a liquid phase, were largely rehydrated after 24 hours. However, it was observed that monolithic dried gels (i.e. a dried gel which remained as one piece after drying) often had areas near the centre of the gels which were poorly rehydrated while the edges were fully, or even over hydrated. It was decided that the rehydration process could be improved by increasing the surface area of the dried gel and minimising the total distance which liquid had to penetrate into the dried gel. To achieve this, dried gels were processed and powdered using a commercial spice grinder. Dried and powdered gel was then passed through a fine cloth mesh to remove any large pieces. This resulted in a dry gel powder with an average particle size of 181 μm. This powder was found to be easily rehydrated within 24 hours and the smaller particle size reduced the uneven rehydration, resulting in a homogeneous hydrogel. This is significant as extended rehydration times would not be suitable for the large scale, commercial preparation of these hydrogels.

The effect of lyophilisation and rehydration on the rheological properties of the hydrogel were assessed as significant changes in rheological properties may have meant that this method of cold loading of furanones was unsuitable. It was found that lyophilisation and rehydration had no effect on the overall shear modulus of the hydrogel. Further, the full viscoelastic profile and viscosity profile remained suitable for use in chronic wounds. It was shown that hydrogels retained their dilatant nature following the lyophilisation process. However, two primary changes in rheological properties were observed. First was the change in adhesiveness of the lyophilised and rehydrated gel. The normal 8% PVA, 2% borate hydrogel showed a peak normal force of -6.607 N while the lyophilised and rehydrated gel of the same formulation showed a peak normal force of -1.24N. This reduction in adhesiveness is both interesting and

potentially beneficial in the production of a wound dressing. This lower adhesiveness would likely result in a reduction in trauma to a wound bed upon dressing removal (McCarron *et al.*, 2011; Murphy *et al.*, 2012). A possible explanation for the reduction in adhesiveness is suggested by McCarron *et al.* (2011) who found that the adhesiveness of PVA-borate hydrogels to skin was dependent on the concentration of crosslinker in the formulation. While the concentration of crosslinker in the standard and lyophilised samples tested in this work were the same, the degree of crosslinking in the gel may have increased. It has been noted that PVA solutions subjected to freeze thaw cycles formed so-called supermolecular particles (Peppas, 1975). It is now known that when exposed to freeze thaw cycles PVA forms physical crosslinks due to the development of regions of high crystallinity within the gel network. When a hydrogel sample is cooled, the water in the gel network forms ice, swelling in volume and forcing PVA polymer strands together. This results in areas of high PVA concentration and, thus, areas of high crystallinity. In these areas of high crystallinity PVA strands form hydrogen bonds with adjacent polymer strands. When the ice in the structure thaws and shrinks in volume, these polymer areas remain crosslinked (Peppas, 1975; Hassan and Peppas, 2000; Holloway, Lowman and Palmese, 2013). These areas of high crystallinity are known as crystallites. It is likely that, during the pre-freezing stage of the lyophilisation process used in this work, the formation of crystallites in the hydrogel's polymer network occurred. This would have meant a higher degree of crosslinking in the gel and, potentially, a lower adhesiveness. The formation of these crystallites may also explain the second observed change in the rheological properties of the hydrogel post lyophilisation. It was observed that the linear viscoelastic region measured in the lyophilised gel was significantly greater than that of the standard hydrogel with the upper limits of the region being measured at 6%

for the standard gel and 100% for the lyophilised and rehydrated sample. If the hypothesis posited above is correct with crystallites forming in the hydrogel, and therefore, increasing crosslink density in the sample, an increase in the linear viscoelastic region would be expected. As the linear viscoelastic region represents the amount of force a system can be subjected to without experiencing destruction of the internal structure, an increase in crosslink density would have meant that any experienced force would be spread among a greater number of crosslinks. This would likely result in a network that could withstand greater pressure before yielding.

The minimal of impact of drying and rehydration on the shear modulus of the hydrogels then prompted investigations into the use of excess hydration to tune the rheological properties of the gels. It was found that hydration of the lyophilised hydrogels, with more than 100% of the water lost during drying, was effectively able to reduce the shear modulus. This was expected as it has been shown several times that decreasing the total mass of PVA and borate results in a softer, more fluid like gel (Loughlin *et al.*, 2008; McCarron *et al.*, 2011; Murphy *et al.*, 2012). As over hydration of the lyophilised gel effectively decreases the percentage of both polymer and cross linker by weight, a reduction in shear modulus is to be expected. This decrease in shear modulus was also demonstrated to be linear, suggesting that even hydrogels with non-ideal shear moduli could be lyophilised and rehydrated sufficiently to give a final product with the desired consistency, if the shear modulus of the original gel is known.

The data presented in this thesis, taken together in light of published work indicates that rehydrating a lyophilised hydrogel with a furanone solution presented a potentially useful method for preparing furanone-loaded hydrogels without exposing the compound to heat or free borate. As such, lyophilised gels were rehydrated with a

volume of furanone solution that would give a 100% rehydrated gel. After 24 hours rehydrating in a furanone solution, hydrogels were not suitable for use. HDMF-loaded gels became turbid in appearance and had a significantly softer texture. Sotolon and ascorbic acid caused the rehydrated hydrogels to become entirely liquid with a dark orange/brown discoloration observed in the ascorbic acid-loaded sample. As with the standard hydrogels, the MTHF-loaded samples formed well with no change in rheological properties or colour. The changes in the hydrogels after furanone loading were similar to those seen in the standard hydrogel production method. As temperature had been eliminated in this method, it was hypothesised that either some excess borate remained in the system after cross linking, the borate that was bound to PVA strands was still able to interact with the furanone compounds causing degradation, or, in the case of ascorbic acid, simply the presence of water resulted in compound degradation. If free borate does indeed remain in the system following cross linking the addition of a polyol sugar such as mannitol may help to ameliorate the borates negative effects. The addition of mannitol to a PVA borate hydrogel formulation was shown to effectively bind to free borate ions in a system just making them unavailable for cross linking (Loughlin *et al.*, 2008). If the same principal could be applied to the lyophilised gels the changes in texture and colour upon loading with furanone might be avoided. Overall, it was decided that due to the requirement for high temperatures, the presence of free borate and the inherently aqueous environment meant that hydrogels, in any form, could not be used to deliver furanones to chronic wounds.

In order to overcome the issues faced in the production of furanone-loaded hydrogels it was decided that the possible formation of crystallites (as discussed previously) during the pre-freezing stage of lyophilisation could be exploited in order to produce a completely dry, borate-free, furanone delivery system. The developed material

consisted of a polymer solution (of varying concentration) that was frozen to cause the formation of crystallites in the network structure giving a small degree of crosslinking. The frozen solution was then lyophilised to result in a low density, highly porous, completely dry aerogel–like material. The internal structure of this aerogel material was then characterised. The macro structure of the aerogel was examined under stereo zoom microscopy. Interestingly, a degree of regularity in the internal structure was apparent. This regularity was also seen to decrease, giving a more disordered internal structure, as polymer concentration decreased. In 2005, a similar alignment was observed in freeze dried PVA solutions that were subjected to highly controlled directional freezing (Zhang *et al.*, 2005). Here, the authors suggest that the uniaxial alignment of the PVA strands was caused by phase separation during the freezing process. Indeed, the authors showed that the formation of ice crystals in the sample occurred in a single direction and that this freezing likely forced the alignment of polymer strands. The reduction in order, seen in the aerogels produced in this work, as polymer concentration decreases may be explained by the occurrence of a phenomenon known as freeze concentration. Briefly, on cooling, as solvent crystals form, a solute may be forced out of the freezing solvent (phase separation). This results in a higher concentration of solute at the boundary between the frozen solvent and the non-frozen solvent (the interface). This effectively concentrates the solute in the non-frozen liquid phase (Butler, 2001, 2002). It is hypothesised that, in the work presented in this thesis, freeze concentration of the 10% polymer solution resulted in greater concentration of PVA at the interface, forcing the strands into alignment. Conversely, freeze concentration of the 5% and 1% polymer solutions resulted in comparatively lower concentrations of polymer strands at the interface, thus, allowing greater disorder between ice crystals. This process is illustrated in Figure 3.20.

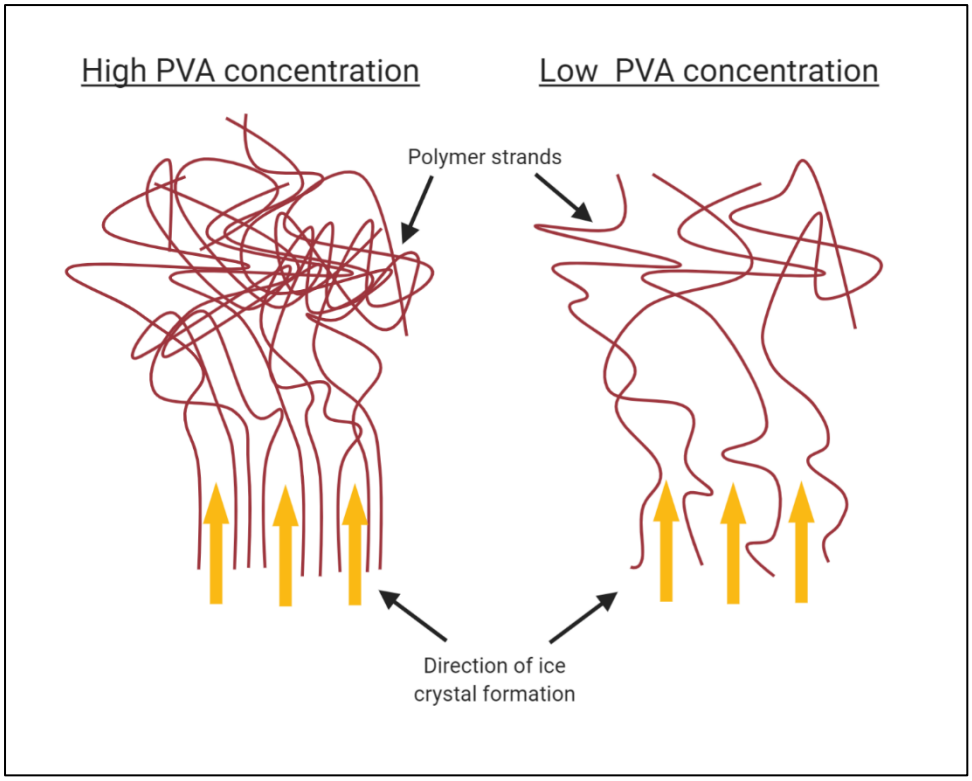

Figure 3.20 – A representation of freeze concentration of a high polymer concentration solution and a low polymer concentration solution.

Upon freezing of the polymer solutions, the polymer strands are separated from the liquid phase causing them to concentrate between ice crystals. In solutions with higher concentrations of polymer a greater concentration of polymer strands is present between ice crystals thus forcing them into alignment. For low concentration polymer solution, a lower number of polymer strands would be present between ice crystals thus allowing for a greater level of strand disorder in these samples.

The polymer strand alignment and gradual reduction in structure with decreasing polymer concentration was subsequently confirmed by SEM imaging of the microstructure of the gels. This imaging showed tightly packed unidirectional fibres in the aerogel made from a 10% PVA solution. These fibres remained unidirectional but appeared less tightly packed in the 7.5% PVA aerogel. Interestingly, under SEM, the 5% PVA aerogel showed localised areas of ordered fibres which were loosely packed. Finally, the 1% PVA aerogel showed no obvious fibres in the internal structure instead being ordered into a loosely packed, flat layers. The reason for this change in

structure from bundled fibres to flat lamellar sheets is unclear but it may be that the structure of the low-density, cotton-like, gel structure was compacted during sample preparation leading to a flattened lamellar appearance. Finally, the homogeneity of the aerogel internal structure was assessed by micro CT. It was found that the 10% PVA aerogel had the least homogeneous internal structure of all formulations tested with large areas of significantly more dense material throughout its internal structure. Structural homogeneity increased with decreasing polymer concentration. This was unexpected as the higher polymer concentrations showed greater structural order. This phenomenon has not been reported previously in the literature and so determining the cause is difficult. However, it is currently thought to be due to the uncontrolled freezing of the polymer solutions prior to drying. Unlike the work of Zhang *et al.* (2005), the polymer solutions used in this work were allowed to freeze with no defined directionality. As previously stated, the formation of ice crystals in the solution will likely have led to freeze concentration. With unidirectional freezing the ice crystals form in a regular pattern, leaving the areas of concentrated solute in a regular pattern or structure. However, as this work used non-regulated freezing ice crystals will have formed throughout the solution giving rise to irregular areas of solute concentration.

Following assessment of the internal structure of the aerogels, the stability of the furanone compounds during aerogel formation was assessed. It was discovered that the concentration of furanones in an aerogel was indeed affected by the process of aerogel formation. It was found that the concentration of HDMF was reduced by 48%, sotolon was reduced by 100% and both MTHF and ascorbic acid were apparently increased in concentration by 9500% and 37%, respectively. This was highly unexpected as the three primary sources of compound degradation in hydrogel formation (temperature, borate and altered pH) had now been eliminated. It was

thought that the pre-freezing step required for lyophilisation was causing degradation of the furanone compounds. This effect has been reported for other drug compounds including biological drugs such as proteins and antibodies (Authelin *et al.*, 2020). While furanones are biological compounds, their different chemistries mean that their stability profiles are likely very different from complex molecules such as proteins. Despite this, the process of freezing could potentially degrade the furanones. As such, the extent of furanone loss after a freeze thaw cycle was investigated. However, it was found that the process of freezing and thawing a stock solution of furanone did not cause the loss (or apparent increase) of any of the four compounds. This is in keeping with several previous reports which have shown that freeze thaw cycles often do not have an effect on the stability of a range of active compounds (Kozikowski *et al.*, 2003; Rayfield *et al.*, 2017; Lai *et al.*, 2019). The discovery that pre-freezing had no effect on compound degradation suggested that the freeze-drying process itself was the cause of the altered compound concentrations. It was hypothesised that due to the high volatility of the some of the furanone compounds (as evidenced by their strong aroma), they may have been volatilised under the vacuum required for the freeze-drying process. This would have resulted in a loss of furanone compounds which would have been seen after drying the aerogels. While this explanation is suitable for changes in HDMF and sotolon concentration it does not explain the apparent increase in MTHF and ascorbic acid concentrations. Nevertheless, the freeze-drying process was optimised in order to minimise the amount of time aerogels were under vacuum, with the aim of minimising the loss of volatile furanones. It was found that blank and furanone-loaded gels reached a constant mass (indicating they were completely dry) within approximately 20 hours. After undergoing optimised drying, the HDMF and sotolon aerogels lost only 1.64% and 6.15 % of the total loaded drug respectively.

MTHF and ascorbic acid aerogels showed apparent increased in drug concentration of approximately 7100 % and 110 % respectively. As these gels are novel, particularly when loaded with active compounds, there are no previous reports surrounding drug stability during production. However, as discussed in chapter 2 it is likely that the degradation of the compounds to more absorptive products (giving rise to apparent increases in drug concentrations) is due to the inherently hydrolytic aqueous environment that the compounds are exposed to. As HDMF and sotolon are not degraded by loading into the aerogels it might be that these compounds can withstand the aqueous environment until the water is removed by freeze drying. Conversely both MTHF and ascorbic acid appear to be unable to tolerate the aqueous environment even for a short time.

However, based on the data in this work it was concluded that, due to their inherent instability, MTHF and ascorbic acid were not viable for loading into PVA based hydrogel or aerogel drug delivery systems. HDMF and sotolon were both successfully loaded into PVA aerogels at high concentrations.

Finally, the release of each of the four compounds from the aerogels was examined. It was found that ascorbic acid, despite increasing in apparent concentration after drying, released less than 2% of the total loaded drug. This is contradictory to reports of ascorbic acid release from other polymeric carriers. For example, in 2016 Mangir *et al.* showed that ascorbic acid was effectively released from electrospun poly (lactic acid) fibres at concentrations of between 50 and 90% of the total loaded drug volume (Mangir *et al.*, 2016). Similarly, Voss *et al.* (2018) showed between 60% and 90% release of ascorbic acid from a newly developed PVA/polysaccharide film wound dressing (Voss *et al.*, 2018). The success of these studies in releasing ascorbic acid

further reinforces the hypothesis that one or more aspects of the aerogel production process have resulted in the poor stability and release of this compounds. As with the hydrogels, the release of MTHF remained highly anomalous with total release percentages of up to 600% being observed. This also suggests that the stability and absorptivity MTHF is negatively affected by the lyophilisation process. Despite the failure of ascorbic acid and MTHF-loaded aerogels, both HDMF and sotolon showed favourable drug release profiles with HDMF releasing up to 90% and sotolon also releasing up to 90% of the total loaded drug volume. When released from a 5% PVA aerogel both HDMF and sotolon showed a rapid burst release with 80% of the total loaded drug volume being released. This is similar to previous reports of drug release from aerogel materials many of which show rapid burst release effects of drugs such as triflusal, paracetamol, nicotinic acid, and ketoprofen (Mehling *et al.*, 2009; Veronovski, Novak and Knez, 2012; Murillo-Cremaes *et al.*, 2013; Goimil *et al.*, 2017). These burst release effects were reduced when HDMF and sotolon were released from an aerogel with a higher concentration of polymer. This is not unexpected as it has been shown that an increase in polymer concentration can slow the release of drugs from a polymeric system (Erös *et al.*, 2003). These data suggested that 10% PVA aerogels could be used to deliver furanones to wound biofilms as while avoiding burst release. These properties make PVA aerogels potentially excellent candidate materials for delivering antimicrobials to chronic wound infections.

3.6 Conclusion

A method of cold loading lyophilised hydrogels, with the aim of producing a furanone-loaded gel in which the furanone compounds did not degrade was developed. This was shown to be an unsuitable method for the production of furanone-loaded gels due to likely interactions between the active compounds and borate causing significant degradation of the furanones. To overcome these issues a novel, minimally crosslinked, PVA aerogel was developed and characterised. It was shown that aerogels, made using a high polymer concentration PVA solution, displayed unidirectional fibres in its internal structure. It was suggested that this structure was caused by ice crystals forming within the sample freezing causing a phenomenon known as freeze concentration. This observed structure decreased as the concentration of polymer in the aerogel was reduced. Upon further investigation it was discovered that the high degree of internal structure seen in high polymer concentration aerogel was not consistent throughout the aerogel structure with some areas consisting of much denser material. It was hypothesised that this was due to the lack of controlled directionality of the freezing of the samples causing irregular freeze concentration within the sample. The homogeneity of the internal structure of the aerogel was increased as polymer concentration decreased. It was discovered that during the production of furanone-loaded aerogel a significant percentage of HDMF and sotolon were lost. The impact of the pre-freezing step on furanone concentration was investigated and shown to have minimal effects. The lyophilisation process was then optimised and losses of HDMF and sotolon were significantly reduced. Due to continued degradation it was decided that MTHF and ascorbic acid were not suitable for use in the aerogel delivery system. Finally, the release kinetics of each of the furanones from several aerogel formulations was examined. It was demonstrated that

both HDMF and sotolon exhibited favourable release profiles from 10% PVA aerogels and, thus, this furanone delivery formulation was carried forward for testing against bacterial biofilms.

3.7 References

Afrashi, M. *et al.* (2019) 'Novel multi-layer silica aerogel/PVA composite for controlled drug delivery', *Materials Research Express*, 6(9). doi: 10.1088/2053-1591/ab3097.

Authelin, J. R. *et al.* (2020) 'Freezing of Biologicals Revisited: Scale, Stability, Excipients, and Degradation Stresses', *Journal of Pharmaceutical Sciences*, pp. 44–61. doi: 10.1016/j.xphs.2019.10.062.

Bandelin, J. and Tuschhoff, J. V. (1955) 'The stability of ascorbic acid in various liquid media.', *Journal of the American Pharmaceutical Association. American Pharmaceutical Association*, 44(4), pp. 241–244. doi: 10.1002/jps.3030440419.

Bhagat, S. D. *et al.* (2007) 'Methyltrimethoxysilane based monolithic silica aerogels via ambient pressure drying', *Microporous and Mesoporous Materials*, 100(1–3), pp. 350–355. doi: 10.1016/j.micromeso.2006.10.026.

Blessy, M. *et al.* (2014) 'Development of forced degradation and stability indicating studies of drugs - A review', *Journal of Pharmaceutical Analysis*, pp. 159–165. doi: 10.1016/j.jpha.2013.09.003.

Briggaman, R. A. *et al.* (1984) 'Degradation of the epidermal-dermal junction by proteolytic enzymes from human skin and human polymorphonuclear leukocytes', *Journal of Experimental Medicine*, 160(4), pp. 1027–1042. doi: 10.1084/jem.160.4.1027.

Butler, M. F. (2001) 'Instability Formation and Directional Dendritic Growth of Ice Studied by Optical Interferometry', *Crystal Growth and Design*, 1(3), pp. 213–223.

Butler, M. F. (2002) ‘Freeze Concentration of Solutes at the Ice/Solution Interface Studied by Optical Interferometry’, *Crystal Growth and Design*, 2(6), pp. 541–548. doi: 10.1021/cg025591e.

Concha, M. *et al.* (2018) ‘Aerogels made of chitosan and chondroitin sulfate at high degree of neutralization: Biological properties toward wound healing’, *Journal of Biomedical Materials Research Part B: Applied Biomaterials*, 106(6), pp. 2464–2471. doi: 10.1002/jbm.b.34038.

Dubey, S. P. *et al.* (2014) ‘Synthesis of graphene-carbon sphere hybrid aerogel with silver nanoparticles and its catalytic and adsorption applications’, *Chemical Engineering Journal*, 244, pp. 160–167. doi: 10.1016/j.cej.2014.01.042.

Duräes, L. *et al.* (2012) ‘Effect of the drying conditions on the microstructure of silica based xerogels and aerogels’, *Journal of Nanoscience and Nanotechnology*, 12(8), pp. 6828–6834. doi: 10.1166/jnn.2012.4560.

Erös, I. *et al.* (2003) ‘Examination of drug release from hydrogels’, *Polymers for Advanced Technologies*, 14(11–12), pp. 847–853. doi: 10.1002/pat.405.

Ferreira, A. V. *et al.* (2017) ‘Detection of human neutrophil elastase (HNE) on wound dressings as marker of inflammation’, *Applied Microbiology and Biotechnology*. Applied Microbiology and Biotechnology, 101(4), pp. 1443–1454. doi: 10.1007/s00253-016-7889-6.

Follmann, H. D. M. *et al.* (2018) ‘Multifunctional hybrid aerogels: Hyperbranched polymer-trapped mesoporous silica nanoparticles for sustained and prolonged drug release’, *Nanoscale*, 10(4), pp. 1704–1715. doi: 10.1039/c7nr08464a.

García-González, C. A. *et al.* (2012) 'Supercritical drying of aerogels using CO 2: Effect of extraction time on the end material textural properties', *Journal of Supercritical Fluids*. Elsevier, 66, pp. 297–306. doi: 10.1016/j.supflu.2012.02.026.

García-González, C. A. *et al.* (2015) 'Polysaccharide-based aerogel microspheres for oral drug delivery', *Carbohydrate Polymers*, 117, pp. 797–806. doi: 10.1016/j.carbpol.2014.10.045.

García-González, C. A. *et al.* (2019) *An opinion paper on aerogels for biomedical and environmental applications.*, *Molecules*. doi: 10.3390/molecules24091815.

Goimil, L. *et al.* (2017) 'Supercritical processing of starch aerogels and aerogel-loaded poly(ε-caprolactone) scaffolds for sustained release of ketoprofen for bone regeneration', *Journal of CO2 Utilization*, 18, pp. 237–249. doi: 10.1016/j.jcou.2017.01.028.

Gonçalves, V. S. S. *et al.* (2016) 'Alginate-based hybrid aerogel microparticles for mucosal drug delivery', *European Journal of Pharmaceutics and Biopharmaceutics*, 107, pp. 160–170. doi: 10.1016/j.ejpb.2016.07.003.

Govindarajan, D. *et al.* (2017) 'Fabrication of Hybrid Collagen Aerogels Reinforced with Wheat Grass Bioactives as Instructive Scaffolds for Collagen Turnover and Angiogenesis for Wound Healing Applications', *ACS Applied Materials and Interfaces*, 9(20), pp. 16939–16950. doi: 10.1021/acsami.7b05842.

Hassan, C. M. and Peppas, N. A. (2000) 'Structure and morphology of freeze/thawed PVA hydrogels', *Macromolecules*, 33(7), pp. 2472–2479. doi: 10.1021/ma9907587.

Hoag, S. (2001) 'Bioavailability of Nutrients and Other Bioactive Components from

Dietary Supplements What Do We Need to Know about Active Ingredients in Dietary Supplements ? Summary of Workshop Discussion 1', *The Journal of Nutrition*, 131, pp. 1387–1388.

Holloway, J. L., Lowman, A. M. and Palmese, G. R. (2013) 'The role of crystallization and phase separation in the formation of physically cross-linked PVA hydrogels', *Soft Matter*, 9(3), pp. 826–833. doi: 10.1039/c2sm26763b.

Hou, Q., Grijpma, D. W. and Feijen, J. (2003) 'Preparation of Interconnected Highly Porous Polymeric Structures by a Replication and Freeze-Drying Process', *Journal of Biomedical Materials Research - Part B Applied Biomaterials*, 67(2), pp. 732–740. doi: 10.1002/jbm.b.10066.

Jing, F. *et al.* (2018) 'Facile synthesis of TiO2/Ag composite aerogel with excellent antibacterial properties', *Journal of Sol-Gel Science and Technology*, 86(3), pp. 590–598. doi: 10.1007/s10971-018-4659-1.

Jones, S. M. (2006) 'Aerogel: Space exploration applications', *Journal of Sol-Gel Science and Technology*, 40(2–3), pp. 351–357. doi: 10.1007/s10971-006-7762-7.

Kanamori, K. *et al.* (2007) 'New transparent methylsilsesquioxane aerogels and xerogels with improved mechanical properties', *Advanced Materials*, 19(12), pp. 1589–1593. doi: 10.1002/adma.200602457.

Kistler, S. (1931) 'Coherent expanded aerogels and jellies', *Nature*, 127(3211), p. 741.

Kochkodan, V., Darwish, N. Bin and Hilal, N. (2015) 'The Chemistry of Boron in Water', in *Boron Separation Processes*, pp. 35–63. doi: 10.1016/B978-0-444-63454-2.00002-2.

Kozikowski, B. A. *et al.* (2003) 'The effect of freeze/thaw cycles on the stability of compounds in DMSO', *Journal of Biomolecular Screening*, 8(2), pp. 210–215. doi: 10.1177/1087057103252618.

Lai, D. *et al.* (2019) 'The effects of heat and freeze-thaw cycling on naloxone stability', *Harm Reduction Journal*, 16(1), p. 17. doi: 10.1186/s12954-019-0288-4.

Li, C. *et al.* (2016) 'Robust Vacuum-/Air-Dried Graphene Aerogels and Fast Recoverable Shape-Memory Hybrid Foams', *Advanced Materials*, 28(7), pp. 1510–1516. doi: 10.1002/adma.201504317.

Li, H. *et al.* (2019) 'Aerogel fabricated with halloysite nanoclay as ibuprofen and dexamrthasone carrier for dual drugs release', *Materials Rese*, 6(10).

Loftsson, T. (2014) *Drug Stability for Pharmaceutical Scientists*, *Drug Stability for Pharmaceutical Scientists*. Elsevier. doi: 10.1016/C2012-0-07703-4.

López-Iglesias, C. *et al.* (2019) 'Vancomycin-loaded chitosan aerogel particles for chronic wound applications', *Carbohydrate Polymers*, 204, pp. 223–231. doi: 10.1016/j.carbpol.2018.10.012.

Loughlin, R. G. *et al.* (2008) 'Modulation of gel formation and drug-release characteristics of lidocaine-loaded poly(vinyl alcohol)-tetraborate hydrogel systems using scavenger polyol sugars', *European Journal of Pharmaceutics and Biopharmaceutics*, 69(3), pp. 1135–1146. doi: 10.1016/J.EJPB.2008.01.033.

Lovskaya, D. and Menshutina, N. (2020) 'Alginate-based aerogel particles as drug delivery systems: Investigation of the supercritical adsorption and in vitro evaluations', *Materials*, 13(2). doi: 10.3390/ma13020329.

Luo, X. *et al.* (2020) 'Robust, sustainable cellulose composite aerogels with outstanding flame retardancy and thermal insulation', *Carbohydrate Polymers*, 230, p. 115623. doi: 10.1016/j.carbpol.2019.115623.

Ma, R. *et al.* (2019) 'Nanocomposite sponges of sodium alginate/graphene oxide/polyvinyl alcohol as potential wound dressing: In vitro and in vivo evaluation', *Composites Part B: Engineering*, 167, pp. 396–405. doi: 10.1016/j.compositesb.2019.03.006.

Maleki, H., Durães, L. and Portugal, A. (2014) 'An overview on silica aerogels synthesis and different mechanical reinforcing strategies', *Journal of Non-Crystalline Solids*, 385, pp. 55–74. doi: 10.1016/j.jnoncrysol.2013.10.017.

Mangir, N. *et al.* (2016) 'Production of ascorbic acid releasing biomaterials for pelvic floor repair', *Acta Biomaterialia*, 29(May 2016), pp. 188–197. doi: 10.1016/j.actbio.2015.10.019.

McCarron, P. A. *et al.* (2011) 'Preliminary Clinical Assessment of Polyvinyl Alcohol-Tetrahydroxyborate Hydrogels as Potential Topical Formulations for Local Anesthesia of Lacerations', *Academic Emergency Medicine*, 18(4), pp. 333–339. doi: 10.1111/j.1553-2712.2011.01032.x.

Mehling, T. *et al.* (2009) 'Polysaccharide-based aerogels as drug carriers', *Journal of Non-Crystalline Solids*, 355(50–51), pp. 2472–2479. doi: 10.1016/j.jnoncrysol.2009.08.038.

Murillo-Cremaes, N. *et al.* (2013) 'Nanostructured silica-based drug delivery vehicles for hydrophobic and moisture sensitive drugs', *Journal of Supercritical Fluids*, 73, pp. 34–42. doi: 10.1016/j.supflu.2012.11.006.

Murphy, D. J. *et al.* (2012) 'Physical characterisation and component release of poly(vinyl alcohol)–tetrahydroxyborate hydrogels and their applicability as potential topical drug delivery systems', *International Journal of Pharmaceutics*, 423(2), pp. 326–334. doi: 10.1016/J.IJPHARM.2011.11.018.

Pei, X., Zhai, W. and Zheng, W. (2014) 'Preparation and characterization of highly cross-linked polyimide aerogels based on polyimide containing trimethoxysilane side groups', *Langmuir*, 30(44), pp. 13375–13383. doi: 10.1021/la5026735.

Pei, X., Zhai, W. and Zheng, W. (2015) 'Preparation of poly(aryl ether ketone ketone)–silica composite aerogel for thermal insulation application', *Journal of Sol-Gel Science and Technology*, 76(1), pp. 98–109. doi: 10.1007/s10971-015-3756-7.

Peppas, N. A. (1975) 'Turbidimetric studies of aqueous poly(vinyl alcohol) solutions', *Die Makromolekulare Chemie*, 176(11), pp. 3433–3440. doi: 10.1002/macp.1975.021761125.

Raab, T. *et al.* (2003) 'Tautomerism of 4-hydroxy-2,5-dimethyl-3(2H)-furanone: Evidence for its enantioselective biosynthesis', *Chirality*, 15(7), pp. 573–578. doi: 10.1002/chir.10247.

Rayfield, W. J. *et al.* (2017) 'Impact of Freeze/Thaw Process on Drug Substance Storage of Therapeutics', *Journal of Pharmaceutical Sciences*, 106(8), pp. 1944–1951. doi: 10.1016/j.xphs.2017.03.019.

Rodríguez-Dorado, R. *et al.* (2019) 'Design of aerogels, cryogels and xerogels of alginate: Effect of molecular weight, gelation conditions and drying method on particles' micromeritics', *Molecules*, 24(6). doi: 10.3390/molecules24061049.

Roscher, R., Schwab, W. and Schreier, P. (1997) ‘Stability of naturally occurring 2,5-dimethyl-4-hydroxy-3[2H]-furanone derivatives’, *European Food Research and Technology*, 204(6), pp. 438–441. doi: 10.1007/s002170050109.

Shao, Z. *et al.* (2010) ‘Rapid synthesis of amine cross-linked epoxy and methyl co-modified silica aerogels by ambient pressure drying’, *Journal of Non-Crystalline Solids*, 358, pp. 2612–2615.

Shu, C.-K., Mookherjee, B. and Ho, C.-T. (1985) ‘Volatile Components of the Thermal Degradation of 2,5 - Dime t h’, *Journal of Agricultural and Food Chemistry*, 07735, pp. 446–448.

Vareda, J. P., Lamy-Mendes, A. and Durães, L. (2018) ‘A reconsideration on the definition of the term aerogel based on current drying trends’, *Microporous and Mesoporous Materials*, 258, pp. 211–216. doi: 10.1016/j.micromeso.2017.09.016.

Veronovski, A., Novak, Z. and Knez, Ž. (2012) ‘Synthesis and use of organic biodegradable aerogels as drug carriers’, *Journal of Biomaterials Science, Polymer Edition*, 23(7), pp. 873–886. doi: 10.1163/092050611X566126.

Vincent Edwards, J. *et al.* (2016) ‘Preparation, characterization and activity of a peptide-cellulosic aerogel protease sensor from cotton’, *Sensors*, 16(11), pp. 1–19. doi: 10.3390/s16111789.

Voss, G. T. *et al.* (2018) ‘Polysaccharide-based film loaded with vitamin C and propolis: A promising device to accelerate diabetic wound healing’, *International Journal of Pharmaceutics*, 552(1–2), pp. 340–351. doi: 10.1016/j.ijpharm.2018.10.009.

Yuan, S. *et al.* (2020) ‘Free-standing flexible graphene-based aerogel film with high energy density as an electrode for supercapacitors’, *Nano Materials Science*. doi: 10.1016/j.nanoms.2020.03.003.

Zhang, H. *et al.* (2005) ‘Aligned two- and three-dimensional structures by directional freezing of polymers and nanoparticles’, *Nature Materials*, 4(10), pp. 787–793. doi: 10.1038/nmat1487.

Chapter 4

Furanones as antibiofilm molecules against Pseudomonas aeruginosa

4.1 Introduction

P. aeruginosa is a ubiquitous gram-negative pathogen. It is present in a wide range of environmental niches including plants, soil, water, and farm animals (Mushin and Ziv, 1973; Green *et al.*, 1974). In recent years *P. aeruginosa* has become one of the most prevalent nosocomial infections in the developed world, making up 10.1% of reported hospital acquired infections in the United States in 1990. While this percentage has remained stable over time the prevalence of multidrug resistance in *P. aeruginosa* isolates has increased greatly. Indeed, imipenem, quinolone, and third generation cephalosporin resistance has increased in hospital *P. aeruginosa* isolates by 15%, 9% and 20% respectively between 2002 and 2003. (National Nosocomial Infection Surveillance System, 2004; Hirsch and Tam, 2010). Additionally, it was estimated that multi-drug resistant *P. aeruginosa* caused over 32,000 infections in hospitalised patients in 2017 leading to 2,700 deaths in the US alone (CDC, 2019). As well as the high levels of antimicrobial resistance seen in this organism, *P. aeruginosa* has the ability to form biofilms on a range of biotic and abiotic surfaces (Rasamiravaka *et al.*, 2015). These biofilms, which consist of a collection of bacterial cells encased in a self-produced polymer matrix, provide several advantages for *P. aeruginosa* including protection from physical stresses, such as mechanical force and desiccation, as well as protection from the host organism's own immune system, as well as classical antibiotic treatments (Limoli, Jones and Wozniak, 2015). The regulation of bacterial biofilm formation is governed by a process known as quorum sensing (QS) and, by understanding the mechanism of QS, new biofilm inhibitory strategies may be developed.

4.1.1 Quorum sensing

QS is a cell density dependant method of bacterial communication used by many different organisms to coordinate complex behaviours and to respond to various external stimuli or stresses (Abisado *et al.*, 2018). Although the signalling molecules used by gram-negative and gram-positive organisms for QS often differ significantly, the general mechanism remains the same. Briefly, bacterial cells constitutively express one or more signalling molecules, which exits the cell either by active transport or simple diffusion. These molecules then accumulate in the extra cellular environment (Ng and Bassler, 2009). This signalling molecule is detected by a recipient cell and this detection cause changes in the gene expression of the detecting cell. This process occurs simultaneously throughout large communities of organisms. By regulating population-wide gene expression, bacterial communities are able to coordinate complex behaviours such as the production of secreted virulence factors, swarming motility, and biofilm formation (Andersson *et al.*, 2000; Cvitkovitch, Li and Ellen, 2003; Hammer and Bassler, 2003; Brackman *et al.*, 2012). The coordination of these behaviours gives the bacteria a distinct advantage during the infection of a host or when living in close proximity to other bacterial species (Koutsoudis *et al.*, 2006; An *et al.*, 2014).

4.1.1.1 Quorum sensing in *Pseudomonas aeruginosa*

QS in *P. aeruginosa* has been well studied and the organism is often used as a model to study various aspects of gram-negative QS. This organism does not utilise a single QS system but rather three interconnected, yet completely distinct, systems. The QS systems of *P. aeruginosa* are the Las system, Rhl system, PQS system. A fourth QS system known as the IQS system has been recently proposed but has not been extensively characterised (Lee *et al.*, 2013). This section will discuss the Las, Rhl and

PQS system as they have been well studied. These QS systems are associated with the regulation of processes such as biofilm formation and virulence associated gene expression. They do not function in isolation as activation of one system leads to the activation or suppression of another (Pesc*i et al*, 1997; McKnight, Iglewski and Pesci, 2000; Welsh *et al*, 2015) and, as such, QS in *P. aeruginosa* is a complex process. In brief, *P. aeruginosa* constitutively expresses low molecular weight signalling molecules known as autoinducers (AI). In *P. aeruginosa* these molecules are known as N-(3-oxo-dodecanoyl)-homoserine lactone (OdDHL), N-(butyryl)-homoserine lactone (BHL) and the Pseudomonas quinolone signal (PQS). Both OdDHL and BHL are from a group of molecules known as the N-Acyl homoserine lactones (AHLs) while PQS is from a group of molecules known as quinolones. These signalling molecules are the cognate AI for the Las, Rhl and PQS systems respectively. These AHLs are produced and released by the bacteria accumulating in the extracelluar environment. Once a critical environmental AI concentration is reached the signalling molecules will interact with their cognate receptors and induce the expression of their target genes. The regulation of these target genes can result in the production of molecules such as endotoxins and enzymes (Lee and Zhang, 2014) or down regulation of surface antigens such as OprH (Arevalo-Ferro *et al.*, 2003) to avoid detection by a host's immune system.

While the Las QS system is not the only QS system used by *P. aeruginosa* it is regarded as the top of the QS hierarchy. This is due to the fact that the action of the Las system can result in the activation of both the Rhl system and the PQS systems. As well as the regulation of the Rhl and PQS systems, the Las system has been shown to be responsible for the production of many virulence factors including the LasA,

LasB, and Apr protease enzymes (Toder, Gambello and Iglewski, 1991; Gambello, Kaye and Iglewski, 1993; Pearson, Pesci and Iglewski, 1997).

Activation of the Rhl QS system controls the transcription and subsequent expression of distinct virulence associated genes including those involved in rhamnolipid, pyocyanin, and hydrogen cyanide production (Pearson, Pesci and Iglewski, 1997; Pessi and Haas, 2000). As with the Las QS system, the Rhl QS system does not act independently. As previously stated the Rhl system can be activated by the Las system but it can also supress the activation of the PQS QS system (Wade *et al.*, 2005). In turn the PQS system can activate the Rhl system (McKnight, Iglewski and Pesci, 2000; Mukherjee *et al.*, 2018). This interrelation of the various QS systems allows *P. aeruginosa* to compensate for the loss or inhibition of one QS system and still remain virulent. Figure 4.1 shows the interrelated nature of the Las, Rhl and PQS systems in *P. aeruginosa*. The complexity of bacterial QS and the ability of many species to compensate for the loss of one or more QS systems makes exploiting the inhibition of QS a particularly challenging task.

While inhibiting QS in *P. aeruginosa* can be very complex, it is a highly attractive target and the subject of much research. The successful inhibition of *P. aeruginosa* QS would mean the reduction of the majority of the organisms' virulence factor production, possible re-sensitisation of the organism to classical antibiotics and, perhaps most importantly, the inhibition of biofilm formation.

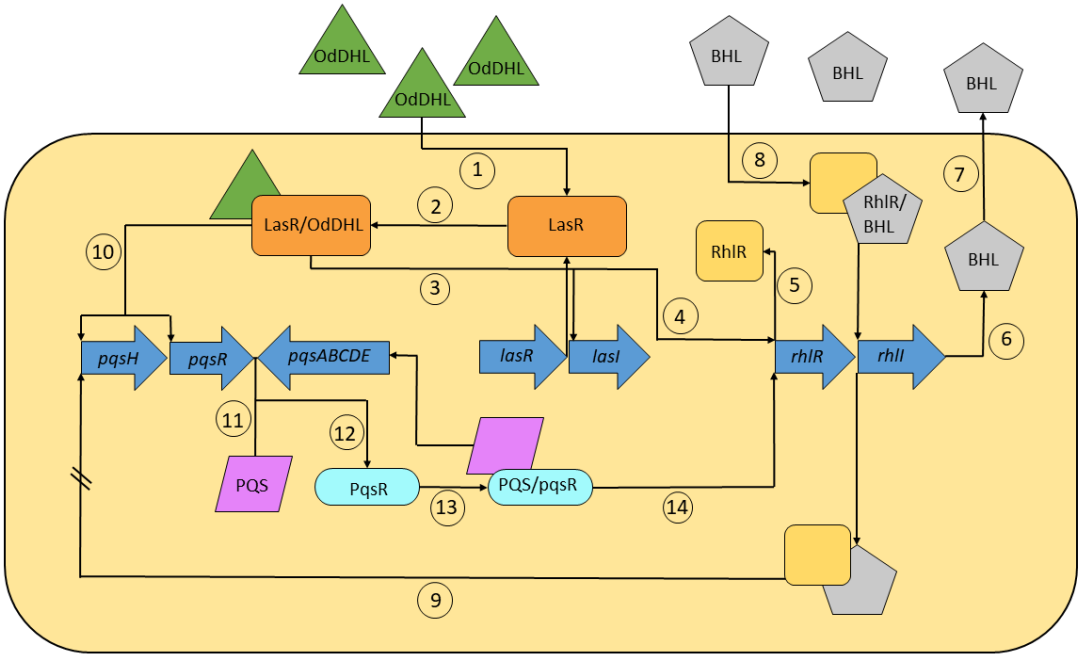

Figure 4.1 - A schematic diagram of the known quorum sensing systems of *P. aeruginosa.*

[1] OdDHL is produced by the organism and accumulates in the extracellular environment. [2] OdDHL enters the cell and interacts with the LasR transcriptional regulator. [3] The LasR/OdDHL complex initiates the transcription of genes such as lasI resulting in further production of OdDHL. [4] LasR/OdDHL also activates the trascrition of another QS system known as the Rhl system.[5] The transcription of rhlR results in the production of another transcriptional regulator (RhlR). [6] The transcription of rhlI results in the production of a second autoinducer molecule known as BHL. [7] BHL then diffuses out of the cell and begins to accumulate in the extracellular environment. [8] BHL then enters the cell and binds to RhlR and further activates the transcription of rhlI (and thus promotes the production of BHL and compounds such as pyocyanin and ramnolipids). [9] The RhlR/BHL complex also acts to negatively regulate the PQS system. [10-12] The PQS system is activated by the Las/OdDHL complex which causes the transcription of pqsH resulting in the production of the Pseudomonas Quinolone Signal (PQS). [13-14] As with the previous systems PQS then binds to PqsR and initiates transcription of the PQS operon which then positively regulates RhlR production and the production of virulence factors such as hydrogen cyanide. Figure from Proctor, McCarron and Ternan (2020).

4.1.1.2 Biofilm formation

Biofilms are groups of sessile cells attached to a biotic or abiotic surface by means of a self-produced polymer matrix. These biofilms have been implicated in a number of human diseases including cystic fibrosis (Lam *et al.*, 1980; Singh *et al.*, 2000),

infective endocarditis (Di Domenico *et al.*, 2019), periodontal disease (Sanz *et al.*, 2017) and colonisation of indwelling medical devices such as urinary catheters (Trautner and Darouiche, 2004). The ubiquity of biofilms in human disease has made them a primary target for the development of new anti-infective therapeutics. However, in order to develop novel therapies against biofilms the mechanisms surrounding their development must be understood.

The formation of a biofilm is a complex process governed, at each stage, by QS (Rasamiravak*a et al*, 2015). Briefly, planktonic bacteria will attach, first reversibly then irreversibly, to a surface. This attachment results in changes in the expression of multiple genes involved in the biofilm formation process, such as the genes involved in the production of the polymeric matrix which provides the biofilm structure. Bacterial cells begin to aggregate to form microcolonies, encased in the extracellular polymeric substance. These polymers accumulate while bacterial cells continually divide. This provides much of the three-dimensional structure of the biofilm. Finally, once the biofilm has matured, large quantities of surfactants such as rhamnolipid are produced. These surfactants allow the biofilm to disperse, returning some of its cells to a planktonic state. Cells which have become planktonic again are then free to relocate and seed new biofilms. (Kostakioti, Hadjifrangiskou and Hultgren, 2013).

The role of QS in biofilm formation has been debated for some time with many papers providing contradictory reports. Despite this, QS has been implicated in many stages of biofilm development by *P. aeruginosa*. QS controlled twitching motility has been shown to be involved in the formation of the microcolonies in the early stages of biofilm formation. As well as having a role in microcolony formation through the regulation of twitching motility, QS has also been shown to be involved in the process

of biofilm maturation and the formation and maintenance of its three-dimensional structure (Davies *et al.*, 1998).

As QS is indeed involved in the formation and maintenance of biofilms, the inhibition of the various QS systems in *P. aeruginosa* is of significant clinical interest. If the early stages of biofilm formation can be disrupted a weaker more treatable biofilm may be formed or there may be total prevention of biofilm formation. Similarly, if the maintenance of mature biofilms can be disrupted then it may be less likely to thrive and become less complex to eradicate. The potential for attenuating the impact of biofilms in human disease makes bacterial QS systems and their disruption a promising target for new therapeutics.

Preventing biofilm formation in human disease by inhibiting QS as well as the development of novel QS inhibitors (QSI) molecules has been the subject of much research in recent years.

4.1.2 Inhibition of quorum sensing

The inhibition of QS can be achieved in a number of ways. These include the enzymatic degradation of the signalling molecules in the extracellular environment. This approach is known as quorum quenching. Quorum quenching has been shown to be effective in the past in reducing the virulence factor production by various plant pathogens such as *Pectobacterium carotovorum* (previously known as *Erwinia carotovora*) (D*ong et al*, 2001; Kusada *et a*l, 2017). Efficacy has also been shown in human pathogens such as *P. aeruginosa* (Lin *et al.*, 2003). However, this chapter will focus on the use of AHL structural analogues for the inhibition of QS. In particular, the use of furanones for the inhibition of QS will be discussed.

4.1.2.1 AHL structural homologues for quorum sensing inhibition

Many studies have shown efficacy of various AHL analogues in inhibiting QS in a range of pathogens. These studies most often develop compounds in which one part of the AHL molecule (either the acyl side chain or the lactone ring) have been replaced or modified. Examples of these include the work of Morohoshi *et al.*(2007) and Ishida *et al.*(2007) and who showed that structural analogues of AHL, in which the lactone ring was replaced with a cyclopentane and the acyl side chain length varied from 4 carbons to 12 carbons, were effectively able to inhibit virulence factor production in *Serratia marcescens* and *P. aeruginosa* respectively (Ishida *et al.*, 2007; Morohoshi *et al.*, 2007).

As well as the synthesis of novel AHL analogues several naturally occurring compounds have been shown to be equally effective in attenuating virulence in a range of organisms. The natural aldehyde compound cinnamaldehyde has repeatedly been shown to be an effective QSI both downregulating the expression of key virulence factors in *P. aeruginosa* and potentiating the killing of *Burkholderia* biofilms by traditional antibiotics (Brackman *et al.*, 2008, 2011; Ahmed *et al.*, 2019). Further, even crude extracts of plants such as garlic have been shown to be highly effective in improving bacterial clearance in a mouse model of *P. aeruginosa* lung infection (Bjarnsholt *et al.*, 2005).

However, one family of natural compound that have shown promise as AHL analogues are furanones.

4.1.2.2 Furanones as quorum sensing inhibitors

The furanones are a class of natural molecules that are primarily found in marine and terrestrial plants where they often act as flavour and aroma compounds. They can be

extracted from a range of sources including seaweeds, strawberries, pineapple, coffee, herbs and spices (de Nys *et al.*, 1993; Slaughter, 1999). These compounds are not exclusive to plants and some fungal species also produce the compounds (Bao *et al.*, 2017; Phainuphong *et al.*, 2017; Zhou *et al.*, 2018). It is also possible to produce furanones in a number of ways including direct chemical synthesis from simple precursors such as ketones and acetals (Caine and Ukachukwu, 1985; Tanabe and Ohno, 1988). Furanones are also produced as a by-product of processes such as the Maillard reaction which occurs during the browning of cooked foods (Wang and Ho, 2008; Arihara, Yokoyama and Ohata, 2019). Although the structure of furanones had been tentatively characterised as early as the mid 1960's their similarity to bacterial signalling molecules would not be noted until the discovery of autoinduction in 1970 and the characterisation of the first AI in 1981 (Rodin *et al.*, 1965; Nealson, Platt and Hastings, 1970; Eberhard *et al.*, 1981). Indeed, the first characterised bacterial AI was named as N-(3-oxo-hexanoyl)-3-aminodihydro-2(3H)-furanone.

The first investigations into the QS inhibition potential of furanones showed that a natural furanone from the red seaweed, *D. pulchra*, could attenuate QS mediated behaviours such as the swarming motility of *S. liquifaciens* and the bioluminescence of some *Vibrio* species (Givskov *et al.*, 1996). Since this early study furanones have been shown to inhibit QS in a range of non-human pathogens such as *S. liquifaciens*, *V. harveyi.* and *P. carotovorum*. The utility of furanones against these pathogens lead to an interest in their utility against human pathogens.

Both synthetic and natural furanones have been shown to be effective in inhibiting QS controlled behaviours in both *E. coli* and *P. aeruginosa*. The natural furanone (5Z)-4-bromo-5-(bromomethylene)-3-butyl-2(5H)-furanone has been shown to effectively

inhibit biofilm formation by up to 87% in *E.coli* (Ren *et al.*, 2001). Similarly, a large number of natural furanones have been shown to inhibit not only biofilm formation but also virulence factor production and antibiotic resistance *in vitro* (Hentzer *et al.*, 2002, 2003; Pan *et al.*, 2012).

Furanones have also shown efficacy in *in vivo* models of *Pseudomonas* infections. Treatment with a furanone known as C-30 showed reduced QS by *P. aeruginosa* in the murine lung and that a 3-day treatment regime with C-30 allowed mice to better clear *P. aeruginosa* from the lungs. (Hentzer *et al.*, 2003; Wu *et al.*, 2004)

For a comprehensive overview of the use of furanones as QSI the reader is referred to a recent review, published as part of this work (Proctor, McCarron and Ternan, 2020).

4.2 Aims and objectives

The aim of the work described in this chapter is to characterise the antibiofilm effects of furanone compounds against the wound pathogen *P. aeruginosa* PAO1. This will be achieved by first characterising PAO1 growth and biofilm formation kinetics under ideal growth conditions. The minimum bactericidal concentration of each furanone will then be determined and validated. The biofilm formation kinetics of PAO1 will then be investigated under conditions of exogenous furanone treatment including treatment at the time of inoculation and, more realistically, a delayed biofilm treatment protocol. All furanone treatments will be conducted at sub-inhibitory concentrations to be determined in this chapter. Once the efficacy of each furanone has been assessed, biofilms will be treated using aerogels loaded with the most effective furanones. This will ensure the compounds' efficacy is retained when loaded into the novel polymer aerogel delivery system. To assess the effect of furanone treatment on bacterial cell viability within biofilms fluorescence microscopy techniques will be used.

4.3 Methods

4.3.1 Materials and equipment

All chemicals used were purchased from Sigma Aldrich (Poole, UK) and used without further modification unless otherwise stated.

All bacterial culture media was purchased from Oxoid (Basingstoke, UK) and used as per the manufacturers guidelines unless otherwise stated

BacLight cell viability stain was purchased from Thermo Fisher (Milton Keynes, UK) and used as per the manufacturer's guidance

4.3.2 Bacterial strain

Bacterial strain DSM50071 was purchased from Deutchse Sammlung von Mikrooganismen und Zellkulturen (DSMZ) (Braunschweig Germany) as a lyophilised culture. Strain DSM50071 is identified by DSMZ as *Pseudomonas aeruginosa* (Schroeter 1897) Migula 1900, a PAO1 type strain. DSM50071 was selected for this project as a full genome sequence has recently been deposited in GenBank under accession number CP012001 (Nakano *et al.*, 2015).

4.3.3 Biochemical characterisation

The purchased bacterial strain DSM50071 was verified as *Pseudomonas aeruginosa* PAO1 using several methods. DSM50071 was tested using a Gram stain, catalase test, oxidase test, and genetic identification.

4.3.3.1 Gram stain

A bacterial smear was prepared by placing 10 µL of sterile deionised water on a clean microscope slide. Using a sterile inoculation loop an individual colony was collected from a previously prepared streak plate of DSM50071 and mixed thoroughly with the

water. The suspended bacteria were then spread thinly across the glass slide and the slide was then passed rapidly through a flame to heat fix the smear. The heat fixed smear of was covered with 3-5 drops of Gram's crystal violet solution (Sigma-Aldrich, Poole UK) and left for 60 s. The crystal violet was rinsed of using an indirect stream of deionised water. The bacterial smear was then covered with 3-5 drops of Gram's iodine (Sigma-Aldrich, Poole UK) and left for 60 s. Gram's iodine was washed off the smear using 95% ethanol solution until the ethanol ran clear (approximately 15 s). The smear was then covered with 3-5 drops of Gram's safranin solution (Sigma-Aldrich, Poole UK) and left for 60 s. Safranin solution was washed off using an indirect stream of deionised water until the water ran clear. The bacterial smear was then visualised with a light microscope using oil immersion.

4.3.3.2 Cytochrome C oxidase test

Cytochrome c oxidase test was conducted using oxidase detection strips (Oxoid, Basingstoke UK). Using a sterile plastic inoculation loop an individual colony from a previously prepared streak plate was transferred to an oxidase detection strip and left for 5-10 s. As per the manufacturer's guidance the use of a nichrome inoculation loop was avoided as this may have produced a false positive result. The oxidase test strip was observed for a colour change from white to blue/violet which would indicate a positive result.

4.3.3.3 Catalase test

Catalase test was conducted using the slide drop method. Using a sterile inoculation loop an individual colony was transferred from a previously prepared streak plate to a clean glass microscope slide. The use of a platinum wire inoculation loop was avoided as this may have produced a false positive result. One drop of 3% hydrogen peroxide

solution (Sigma-Aldrich, Poole UK) was added and observed for effervescence, indicative of a positive result.

4.3.4 Genetic characterisation of DSM50071

The purchased strain was confirmed as *P. aeruginosa* PAO1 DSM50071 using next generation Illumina sequencing. Sequencing and genome assembly were conducted through MicrobesNG. The purchased strain was grown on nutrient agar as per the MicrobesNG guidance and all biomass was removed from the plate and transferred to the provided sample tube.

4.3.5 Microbiological characterisation of DSM50071

A number of baseline microbiological experiments were performed to characterise the behaviour of PAO1 DMS50071 under ideal growth conditions. This was to allow for better design future experiments in which furanone treatment would be used. The baseline experiments undertaken were a standard growth curve, and a biofilm formation assay including CFU mL^{-1} measurements of viable cells in biofilm culture supernatants.

4.3.5.1 Growth curve

The growth kinetics of DMS50071 were characterised using a standard growth curve protocol. Overnight cultures of DSM50071 were prepared by transferring an individual colony from a previously prepared streak plate to 10 mL of sterile tryptone soy broth (TSB) (Oxoid, Basingstoke UK). Cultures were incubated at 37 °C with shaking at 200 rpm for 18 hours. A 1 mL aliquot of each overnight was transferred to 99 mL of fresh, sterile, TSB in a sterile 250 mL Erlenmeyer flask giving a final dilution of 1:100. The optical density of the culture was then read at 600 nm (OD_{600}) using a benchtop UV spectrophotometer. The OD_{600} was measured every 60 minutes for 8

hours and a final reading was taken after 24 hours. Growth curves were performed in independent, biological triplicates.

4.3.5.2 Biofilm formation kinetics

Biofilm assays were conducted using a standard crystal violet biofilm biomass assay (O'Toole, 2011) which was adapted for use in a 12 well tissue culture plate. Overnight cultures (three biological replicates) were prepared as described in section 4.3.5.1. From each biological replicate an aliquot of 600 µL was added to 59.4 mL of fresh, sterile TSB giving a final dilution of 1:100. Each plate was inoculated with 2 mL of the 1:100 overnight dilution. Each 12-well plate had three technical replicates of each biological replicate as well as three uninnoculated control wells containing sterile broth only as shown below in Figure 4.2. Plates were incubated at 37 °C in a static incubator for 4 hours, 6 hours, 8 hours, 12 hours, 18 hours, 24 hours, 36 hours, 48 hours, and 72 hours. At each time point one plate was sacrificed. Prior to processing plates for assessment of biofilm biomass plates were gently shaken to resuspend planktonic cells. From each biological replicate an aliquot of 100 µL of culture supernatant was transferred to a sterile micro centrifuge tube. This aliquot was stored at 4 °C for later assessment of CFU mL^{-1}. Plates were sacrificed for assessment of biofilm biomass by emptying out both the media and planktonic cells and rinsing the wells by rinsing the wells with clean deionised water from a squirt bottle. Plates were then blotted dry on clean tissue paper. Each well of the plate then had 2 mL of a 0.1% crystal violet solution added and was incubated for 10 minutes at room temperature on a plate rocker. After 10 minutes incubation, crystal violet was emptied out of each plate and plates were submerged in clean deionised water 3 times and blotted dry on clean tissue. Stained and rinsed plates were left in an inverted position and allowed to air dry overnight. After overnight drying, the biofilm bound crystal violet stain was

solubilised using 30% acetic acid in water solution. Each well had 2 mL of 30% acetic acid solution added to it and plates were incubated for 10 minutes at room temperature on a plate rocker. After 10 minutes of incubation, 100 µL of solubilised crystal violet in acetic acid was transferred to a new 96-well plate and absorbance at 550 nm was read using 30% acetic acid in water as a blank using a FluoStar Omega plate reader (BMG Labtech, Aylesbury, UK).

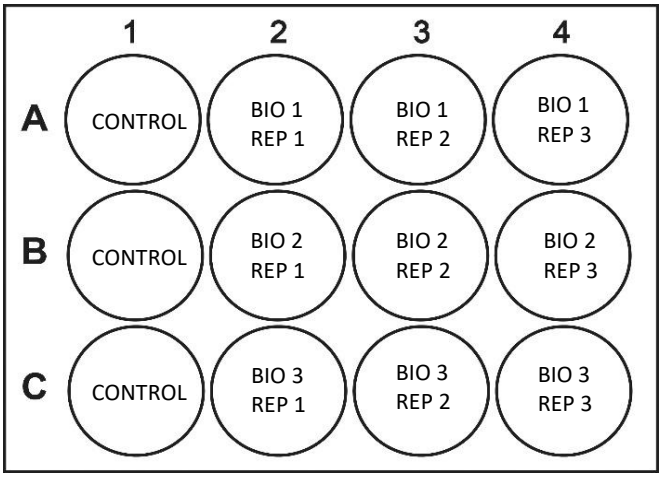

Figure 4.2 - A schematic showing the set up used for in vitro biofilm experiments.

Well A-C 1 are uninnoculated broth. Wells A 2-4 contain three technical replicated of the first biological replicate. Similarly, wells B 2-4 and C 2-4 contain technical replicates of the second and third biological replicates respectively.

4.3.5.3 Assessment of CFU mL^{-1}

Aliquots of culture supernatants were collected from biofilm assay plates as previously described. CFU mL^{-1} values were assessed by serially diluting a 100 µL sample of biofilm supernatant in sterile PBS (Oxoid, Basingstoke UK). Each 100 µL of culture supernatant was briefly vortexed to break up any bacterial aggregates then added to 900 µL of sterile PBS and mixed thoroughly to give a 10^{-2} dilution. A further 100 µL of this dilution was transferred to a fresh micro centrifuge tube containing 900 µL of sterile PBS and mixed thoroughly. This process was repeated to give a range of

concentrations from10^{-2} to 10^{-8}. Finally, a 100 µL volume of each dilution was plated on nutrient agar and incubated overnight at 37 °C. After incubation colonies were counted and average CFU mL^{-1} was calculated. This process was repeated for each time point.

4.3.6 Assessment of minimum bactericidal concentration of furanone compounds

To ensure that the concentrations of all furanone compounds tested in this project were the highest possible concentration without imposing a significant selection pressure on the bacterial cells minimum bactericidal concentrations (MBC) were measured for each compound. The MBC of each furanone compound was assessed using a broth dilution method and was confirmed using a streak plate method and a 2,3,5 triphenyl tetrazolium chloride (TTC) colorimetric assay.

Overnight cultures of DSM50071 were prepared as described in section 4.3.5.1. After 18 hours growth the overnight cultures were then diluted to a 1:50 dilution in fresh Meuller Hinton Broth (MHB) (Oxoid, Basingstoke, UK). Broth dilution plates were prepared by adding 1 mL of fresh sterile TSB aseptically to each well. A stock solution of the compound to be tested was prepared. For all four furanones tested stock solutions were prepared by making a saturated solution (according to the reported solubility of each compound) of the furanone in TSB. This stock solution was then filter sterilised using a 0.45µm syringe filter. For MTHF, which is a liquid at room temperature, a 500 µg mL^{-1} w/v stock solution was prepared in TSB and filter sterilised using a 0.45µm syringe filter. A 1 mL volume of a the furanone stock solution was added to the first well (A1) of the tissue culture plate and was mixed thoroughly by repeated gentle pipetting giving a 1:2 dilution of the furanone stock solution. Then 1 mL of the contents of well A1 were removed and transferred to well A2. This was then

thoroughly mixed with repeated gentle pipetting to give a 1:4 dilution of the furanone stock solution. This was repeated for all wells up to and including well C2. After mixing the contents of well C2 thoroughly a 1 mL volume was removed from this well and discarded. Well C3 contained TSB only. Once the tissue culture plates were prepared with the furanone 1 mL of the 1:50 overnight dilution was added to each well to give a final dilution of 1:100 of the overnight culture and further diluting the furanone solution by 50%. The tissue culture plate was then incubated for 18 hours at 37 °C with shaking. After 18 hours of incubation the tissue culture plate was removed from the incubator. Each well of the plate was gently pipetted several times to resuspend any settled cells. A 100 μL volume of culture was removed from each well and transferred to a fresh sterile 96-well tissue culture plate. To each well 100 μL of sterile 0.1% TTC in deionised water solution was added. Each well was thoroughly mixed by repeated pipetting. The plate was then wrapped in aluminium foil and incubated at 37 °C for 30 minutes. After 30 minutes, plates were assessed for a colour change with a red colour indicating the presence of metabolically active cells at that concertation of furanone.

To confirm the results of the TTC assay a streak plate method was also used. A sterile inoculation loop was dipped into each well of the 12-well tissue culture plate and then streaked onto nutrient agar plates. These plates were incubated for 18 hours at 37 °C. After 18 hours of incubation, plates were inspected for bacterial growth. Absence of growth indicated a lack of viable cells at that concentration of furanone and so a minimum bactericidal concentration could be established.

4.3.7 Biofilm inhibitory effects of furanone compounds

4.3.7.1 Biofilm inhibition of sub-inhibitory concentrations of furanones

Experiments were undertaken to assess the efficacy of furanone compounds at sub-MBC levels. *P. aeruginosa* PAO1 DSM50071 biofilms were grown in the presence of each furanone at half the previously measured MIC, one quarter, one eighth, one sixteenth and one thirty second of the previously measured MIC. Concentrations of furanone used are shown in Table 4.1. Biofilm plates were prepared as follows. Three biological replicate overnight cultures of PAO1 DSM50071 were diluted 1:100 into fresh TSB containing the concentration of furanone to be tested. A 2 mL volume of this overnight culture dilution was then pipetted into wells of a 12 well tissue culture plate as shown previously in Figure 4.2. This was repeated for each of the 5 concentrations for each furanone. Tissue culture plates were then incubated for 24 hours in a static incubator. After 24 hours incubation tissue culture plates were removed and biofilms were stained, destained and quantified as per section 4.3.5.2.

Table 1 – A summary of the concentrations of each furanone investigated for antibiofilm effects against Pseudomonas aeruginosa PAO1.

MBC Fraction	HDMF	MTHF	Sotolon	Ascorbic acid
1/2	4 mg mL^{-1}	1.95 µL mL^{-1}	4.33 mg mL^{-1}	5.50 mg mL^{-1}
1/4	2 mg mL^{-1}	0.98 µL mL^{-1}	2.16 mg mL^{-1}	2.75 mg mL^{-1}
1/8	1 mg mL^{-1}	0.49 µL mL^{-1}	1.08 mg mL^{-1}	1.38 mg mL^{-1}
1/16	0.5 mg mL^{-1}	0.25 µL mL^{-1}	0.54 mg mL^{-1}	0.69 mg mL^{-1}
1/32	0.25 mg mL^{-1}	0.12 µL mL^{-1}	0.27 mg mL^{-1}	0.34 mg mL^{-1}

4.3.7.2 Biofilm inhibition assay

The effect of furanone treatment on bacterial biofilms was assessed by assessing changes in biofilm biomass using a standard crystal violet assay. Overnight cultures of DSM50071 were prepared as described in section 4.3.5.1. Overnight cultures were diluted 1:100 into fresh, sterile TSB supplemented with a sub inhibitory dose of the compound to be tested. Sterile 12-well tissue culture plates were inoculated with 2 mL of 1:100 diluted overnight culture. Plates were incubated for 24 hours, 48 hours and 72 hours at 37 °C. At each time point plates were sacrificed and stained with crystal violet, dried, destained and quantified as per section 4.3.5.2.

4.3.7.3 Delayed treatment experiment

To assess the impact of delayed treatment on the antibiofilm effects of the furanones a range of delayed treatment experiments were conducted. In these experiments PAO1 DMS50071 biofilms were allowed to grow and become established for 24 hours or 48 hours prior to treatment. Biofilm plates were prepared as previously described and biofilms were incubated for an appropriate amount of time. After incubation plates were removed from the incubator and a sub MBC (MBC/2) concentration of furanone (in 100 µL sterile deionised water) was added to each well. Plates were then returned to the incubator for a further 24 or 48 hours. Post treatment incubation plates were removed from the incubator and were stained, destained and quantified.

4.3.8 Cell viability fluorescence imaging

To assess the impact of furanone treatment on bacterial cell viability within the biofilm Live/Dead fluorescence staining was used. BacLight Live/Dead stain was used for the differentiation of cell viability based on cell wall permeability. This stain uses SYTO9 to stain live cells green and propidium iodide (PI) to stain non-viable cells red.

4.3.8.1 Preparation of biofilms for BacLight staining

Biofilms were prepared for BacLight staining using several substrates to identify an optimal method for growing a *P. aeruginosa* biofilm for Live/Dead staining. Biofilms were grown on 1cm x 1cm glass coverslips, polycarbonate chips and polycarbonate membranes (0.2 µm cut off) (Merck Millipore, UK). The protocol was similar for each substrate.

Overnight cultures of *P. aeruginosa* PAO1 DSM50071 were grown in TSB for 18 hours at 37 °C shaking at 200 rpm. The overnight culture was then diluted 1:100 in fresh TSB or TSB supplemented with sub-MBC concentrations of furanone to prepare the inoculum. To seed the biofilm plates, 2 mL volumes of the inoculum were pipetted aseptically into the wells of a 12 well plate.

4.3.8.2 Preparation and application of the growth substrate

Each of the substrates were sterilised by soaking in 70% ethanol and air drying in a laminar flow hood. A representative sample of each substrate was sterilised and placed in fresh TSB an incubated at 37 °C with 200 rpm shaking for 24 hours to confirm sterility. Once sterile, one type of substrate (glass, polycarbonate chip or membrane) was placed in each of the inoculated wells and pushed to the bottom of the well using a sterile plastic inoculation loop. This ensured that the substrate stuck to the bottom of the plate minimising the amount of biofilm that would form on the underside of the substrate. Inoculated plates with the growth substrates were then incubated in a static incubator at 37 °C for 24 hours or 48 hours. Following incubation, the substrates were carefully removed from the 12-well plates and rinsed by gentle submerging in sterile deionised water to remove any remaining planktonic cells and unbound biofilm matrix. Rinsed substrates were then then transferred to a fresh 12 well tissue culture plate for BacLight staining.

4.3.8.3 BacLight staining

Bacterial biofilm in treated and untreated biofilms was assessed using a BacLight Bacterial Cell viability Kit (ThermoFisher, UK). A working BacLight reagent was prepared by mixing 4 µL of component A (1.67 mM SYTO9 and 1.67 mM PI) and 6 µL of component B (1.67 mM SYTO9 and 18.3 mM PI) and 1.5 mL of sterile deionised water. Once prepared the working solution was protected from light whenever possible. Cleaned and rinsed substrates were stained with the BacLight working solution by adding sufficient volumes of the working solution for that the entire surface of the substrate was covered. Stained substrates were incubated for 30 minutes in the dark at room temperature. Following the staining step, substrates were then removed from the 12-well plate and rinsed by gentle submerging in sterile deionised water to ensure any excess BacLight reagent had been removed. Substrates were then mounted on glass microscope slides. Biofilms were visualised at x40 magnification using a Nikon ECLPISE E400 microscope with a dual band emission filter (450-490 nm and 510-560 nm. Images were captured using the Nikon NIS-Elements BR software version 3.22.09.

4.3.9 Efficacy of aerogel delivered furanones

Once the antibiofilm activity of the furanone compounds had been established as described above the efficacy of furanones delivered using a novel polymer aerogel was assessed. Aerogel delivered furanones were tested when applied at the point of inoculation and using the more realistic delayed treatment protocol.

4.3.9.1 Early application of furanone-loaded aerogels

Furanone-loaded aerogels were prepared as per section 3.3.5.1 with one amendment. Furanones were loaded with sufficient concentrations of furanone so that the released portion of the total loaded drug (as identified in section 3.3.6) was equivalent to a sub-

MBC dose. Biofilm plates were prepared an inoculated as per section 4.3.5.2. Once biofilm plates were prepared a furanone-loaded aerogel was applied to the surface of the broth using sterile forceps, ensuring good contact between the aerogel and the liquid surface. Unloaded aerogels were applied to control wells. Biofilm plates were then incubated at 37 °C in a static incubator for 24 hours or 48 hours. After incubation aerogels and remaining planktonic cells were removed from each well and the wells were stained, destained and biofilm biomass quantified as outlined in section 4.3.5.2.

4.3.9.2 Application of furanone-loaded aerogels using a delayed treatment approach

The efficacy of aerogel application of furanones was tested using a more clinically relevant delayed treatment approach. Furanone-loaded aerogels were prepared as per section 3.3.5.1. The protocol was performed as described previously in section 4.3.9.1 with one amendment. Once biofilms had been grown for the required 24 or 48 hours, rather of adding a volume of furanone solution, a furanone-loaded aerogel was applied to each well using sterile forceps and the plates were then incubated for a further 24 hours or 48 hours. Biofilms were stained and quantified as detailed in section 4.3.5.2.

4.3.10 – Assessment of furanone resistance to furanones

As a number of genes with potential involvement in furanone resistance were identified from the literature (Maeda *et al.*, 2012; García-Contreras *et al.*, 2013; Heacock-Kang *et al.*, 2018), the whole genome data previously gained from MicrobesNG was interrogated to identify the presence or absence of these genes in the strain used in this work. Strains deficient in *nalC* and *mexR* have been shown to have a greater resistance to furanones through enhanced efflux due to limited repression of the MexAB-oprM efflux transporter which is ordinarily repressed by *nalC* / *mexR*. Further, both MdrR1 and MdrR2 have both been shown to be repressors of MexAB-

oprM and an additional efflux transporter, EmrAB. Absence of the genes encoding for these proteins would suggest the strain has an increased capacity for furanone efflux.

First, a previously published sequence for DSM50071 was interrogated for the presence or absence of the four genes. This was achieved using the National Centre for Biotechnology Information (NCBI) BlastN tool to search the genome for areas that had high sequence homology compared to the sequence of the genes of interest.

Secondly, the annotated genome of the strain used in this work (constructed by MicrobesNG) was searched for the presence of four separate genes; *nalC*, *mexR*, *MdrR1*, and *MdrR2*. If named genes were not found within the annotated genome, the complete FASTA sequence of the strain was interrogated for sequences showing high homology when compared with previously published base sequences of each gene. If no areas of high homology were found in the FASTA sequence it was concluded that the genes were not present within the genome.

4.4 Results

The antibiofilm efficacy of 4 furanone compounds; MTHF, sotolon, HDMF and L-ascorbic acid, was tested using a number of methods. The efficacy of each compound was tested against *P. aeruginosa* PAO1 (DSM50071) biofilms.

4.4.1 Basic characterisation of PAO1 DSM50071

Some basic tests were conducted to assess the behaviour of PAO1 DSM50071 under ideal growth conditions. The growth kinetics in liquid medium, biofilm formation kinetics and the viable cell count in the liquid phase of biofilm cultures were assessed.

A growth curve at 37 °C and 200 rpm shaking showed the expected growth kinetics with a lag in growth until 2 hours and logarithmic growth thereafter. A final culture optical density of approximately 3 (measured at 600 nm) was observed (Figure 4.3 a). Biofilm kinetics were assessed using the O'Toole and Kolter crystal violet method adapted for use in a 12-well tissue culture plate. Biofilm growth showed the expected gradual increase in biofilm biomass over the first 8 hours followed by a period of fluctuation in overall biofilm biomass (Figure 4.3 b). The numbers of CFU mL^{-1} in the culture liquid phase of the biofilm cultures was also assessed and the data showed a gradual increase in CFU mL^{-1} over the first 12 hours followed by a stationary phase until approximately 24 hours followed by a gradual decline in viable cell numbers thereafter (Figure 4.3 c).

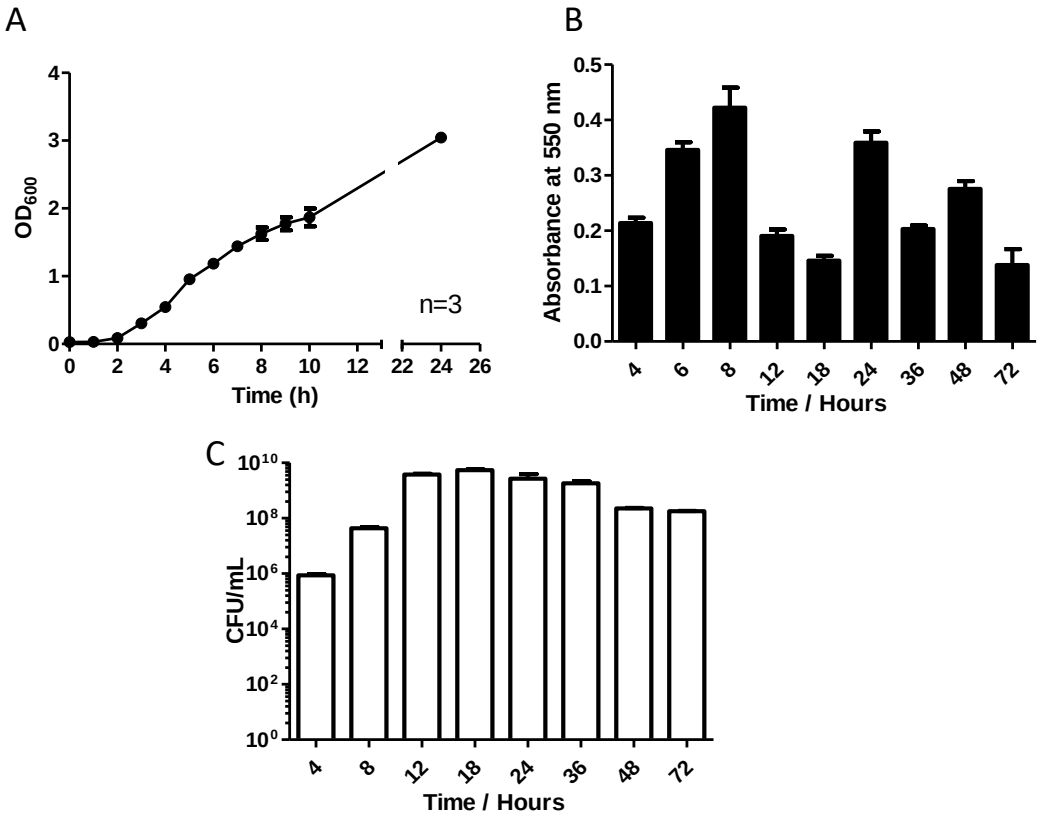

Figure 4.3 – Basic characterisation of PAO1 DSM50071 growth and biofilm formation.

(*a) A growth curve of the organism under ideal conditions showed a lag phase of 2 hours followed by exponential growth as expected. (b) Examination of biofilm formation kinetics of PAO1 DSM50071 showed variable biofilm biomass over time as expected. (c) Assessment of the number of viable bacteria in the liquid phase of the biofilm cultures showed a gradual increase in CFU/mL over 12 hours followed by a decline in CFU/mL after 24 hours.*

4.4.2 Assessment of the antimicrobial and antibiofilm activity of furanones

The minimum bacteriostatic concentration of each furanone was assessed using a TTC colorimetric assay and the minimum bactericidal concentration was confirmed using a streak plate method.

4.4.2.1 Determination of the minimum bactericidal concentration of furanone compounds

Each furanone was assessed for antimicrobial activity and the MBC was identified. Using a TTC assay HDMF was shown to have an MBC of 8 mg mL^{-1}, MTHF showed an MBC of 3.9 µg mL^{-1}, ascorbic acid had an MBC of 11.01 mg mL^{-1} and sotolon showed an MBC of 8.65 mg mL^{-1}. Each of these concentrations was further confirmed using a streak plate method (Figure 4.4).

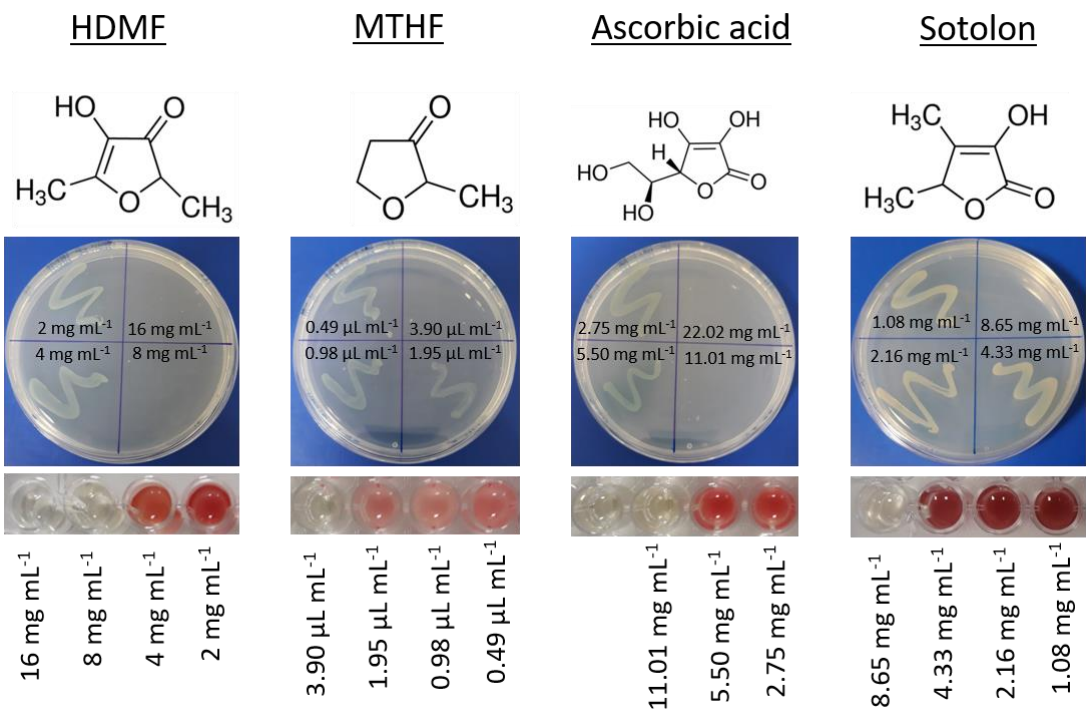

Figure 4.4 – Determination of the minimum bactericidal concentration (MBC) of each furanone using a streak plate method and a 2,3,5 triphenyl tetrazolium chloride (TTC) assay.

The streak plate method showed that P. aeruginosa PAO1 was effectively killed when treated with 8 mg mL^{-1} of HDMF, 3.90 µg mL^{-1} of MTHF, 11.01 mg mL^{-1} of ascorbic acid and 8.65 mg mL^{-1} of sotolon. These results were confirmed using a TTC assay. Lack of a colour change to red indicated a lack of metabolically active cells in the sample. All results shown are representative images of 3 independent replicates.

4.4.2.2 Antibiofilm effects of sub-inhibitory concentrations of furanones

An assessment of the antibiofilm effects of each furanone at a concentration of between half of the MBC and one thirty second of the MBC was conducted. It was found that after treatment for 24 hours there was no significant reduction in biofilm in cultures treated with any concentration ascorbic acid (Figure 4.5 a). This was also seen to be the case for cultures treated with MTHF with no reduction in biofilm at any furanone concentration (Figure 4.5 b). However, in cultures treated with HDMF a significant reduction in biofilm at one half MBC and one quarter MBC concentrations of 62.36% and 58.7% was observed (Figure 4.5 c). These furanone concentrations correspond to 4 mg mL^{-1} (one half MBC) and 2 mg mL^{-1} (one quarter MBC) of HDMF in tryptone soy broth. When treated with sotolon, significant reductions in biofilm of 62.73% and 54.67% were seen in cultures treated with one half MBC and one eighth MBC respectively (Figure 4.5 d). These concentrations correspond to 4.33 mg mL^{-1} (one half MBC) and 1.08 mg mL^{-1} (one eighth MBC).

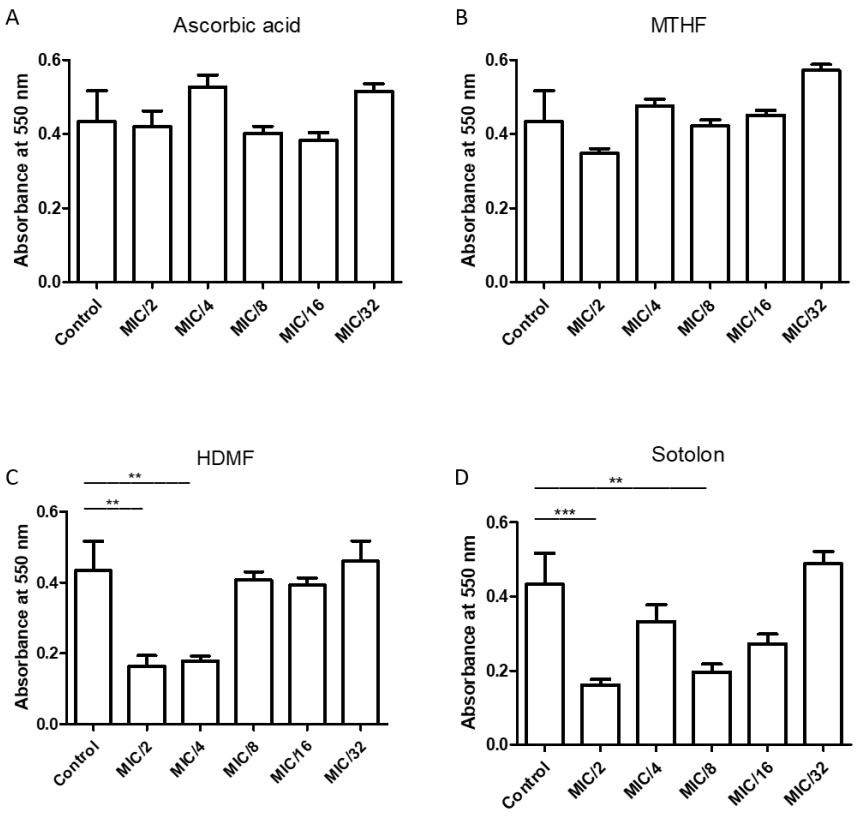

Figure 4.5 – The antibiofilm effects of a range of sub inhibitory furanone concentrations when applied at the point of inoculation.

(a) Ascorbic acid showed no antibiofilm effect at any sub inhibitory concentration. (b) MTHF showed no significant reduction in biofilm biomass at any concertation tested. (c) HDMF showed an antibiofilm effect (62.36% reduction) at one half and one quarter of the established MBC and an antibiofilm effect when treated with one quarter of the established MBC (58.7% reduction). (d) Sotolon showed an antibiofilm effect at one half and one eighth pf the established MBC (62.73% and 54.67% reductions respectively). Data represents the average of 3 biological replicates and 3 technical replicates ±S.D. Data was analysed using independent T tests.

4.4.2.3 Antibiofilm effects of sub-inhibitory concentrations of furanones over 72 h

The antibiofilm effects of sub-inhibitory concentrations of each furanone was assessed over 72 hours. When treated with a sub-inhibitory concentration (5.5 mg mL^{-1}) of ascorbic acid, no antibiofilm effects were seen at 24 hours or 48 hours. However, at 72 hours an increase in biofilm biomass was of 406% was observed (Figure 4.6 a). When treated with a sub-inhibitory concentration of MTHF (1.95 µL mL^{-1}), no antibiofilm effects were seen at 24 hours. A slight reduction in biofilm biomass of

26.45% was observed at 48 hours and a slight increase in biofilm biomass of 47.23% was observed at 72 hours (Figure 4.6 b). When treated with a sub-inhibitory dose of HDMF (4 mg mL^{-1}), consistent reduction in biofilm biomass were seen when compared with an untreated control. Reductions of 76.67%, 77.02% and 88.33% were seen at 24 hours, 48 hours and 72 hours respectively (Figure 4.6 c). When cultures were grown in the presence of a sub-inhibitory dose of sotolon (4.33 mg mL^{-1}) reductions in biofilm biomass of 87.20%, 86.58% and 66.13% were observed at 24 hours, 48 hours and 72 hours, respectively (Figure 4.6 d)

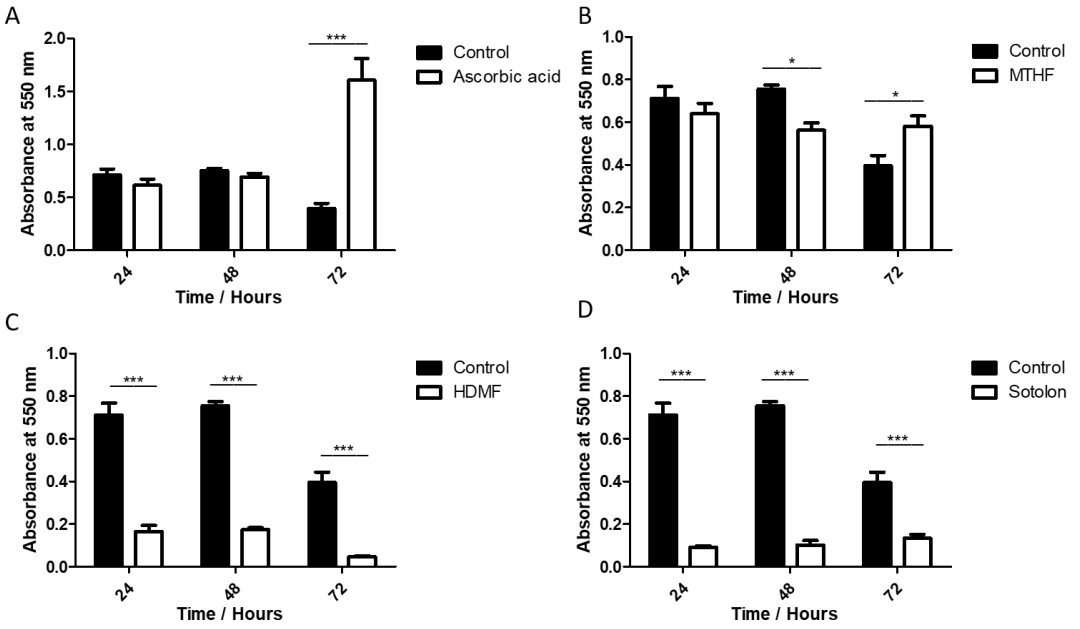

Figure 4.6 – Antibiofilm effects of each furanone at one half the established minimum bactericidal concentration when applied at the point of inoculation.

*(a) Ascorbic acid treatment did not result in any antibiofilm effect at 24 hours or 48h post infection but did show a strong promotion of biofilm formation at 72h post inoculation with an increase in biofilm biomass of 406%. MTHF (b) showed no significant antibiofilm activity 24h post inoculation but saw a significant reduction in biofilm biomass of 26.45% at 48 hours post inoculation and a significant increase of 47.23% at 72 hours post inoculation. HDMF (c) showed a 77.67% reduction in biofilm biomass 24 hours post inoculation, a 77.02% reduction at 48 hours post inoculation and an 88.33% reduction at 72 hours post inoculation. Sotolon (d) showed an 87.2% reduction in biofilm biomass 24 hours post inoculation, an 86.58% reduction 48 hours post inoculation and a 66.13% reduction at 72 hours post inoculation. Data represents the average of 3 biological replicates and 3 technical replicates ±S.D. Data was analysed using 2-way ANOVA. *** p<0.001, **p<0.01, * p<0.05*

4.4.3 Effects of furanones on cell viability in biofilms

The effect of furanone treatment on the viability of biofilm bound PAO1 cells was assessed using fluorescence microscopy and BacLight cell viability stain.

4.4.3.1 Cell viability in treated immature biofilms

PAO1 biofilms were grown in the presence or absence of a sub–inhibitory concentration of each furanone and visualised using BacLight cell viability stain with live cells being stained green by SYTO9 and dead cells being stained red by PI. At 24 hours untreated control biofilms presented as uniform in appearance with cell evenly spread across the growth substrate. Some non-viable cells are seen throughout the biofilm. At 48 hours the biofilms remain evenly populated, a slight increase in non-viable cells are noted in a small number of localised clumps (Figure 4.7).

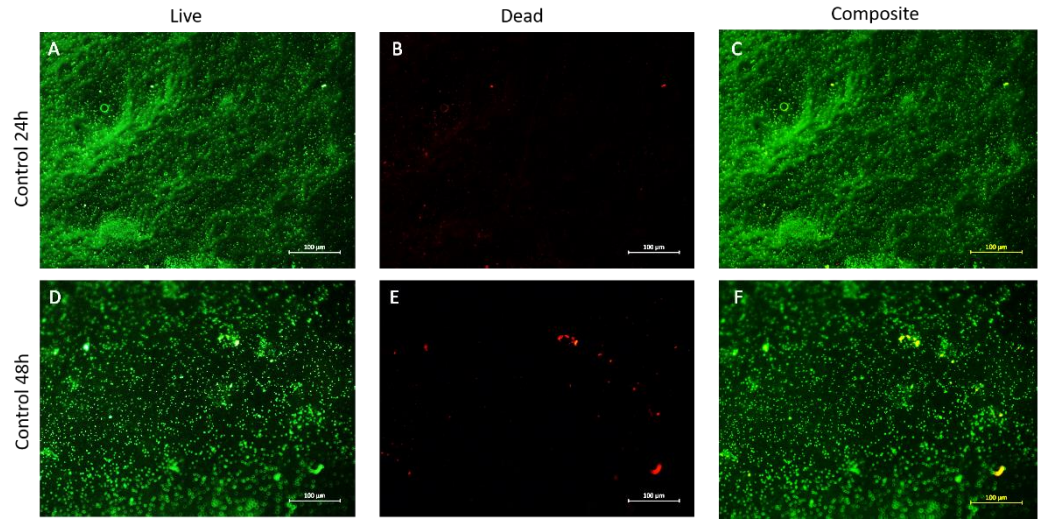

Figure 4.7- BacLight staining of an untreated control biofilm at 24 hours and 48 hours post inoculation.

Live cells are shown in green in images a and d. (a) At 24 hours the biofilm appears to be evenly populated with live cells evenly distributed across the substrate. (b) At 48 hours numbers of viable cells have increased and remain evenly distributed over the growth surface. Non-viable cells are shown in red in images b and e. (b) At 24 hours only small numbers of non-viable cells are present within the biofilm. (e) At 48 hours more non-viable cells are apparent. These cells appear localised to dense clumps of aggregated cells. Images c and f represent a composite of images a and b, and d and e respectively. All results shown are representative images of 3 independent replicates.

Biofilms grown in the presence of 4 mg mL^{-1} HDMF showed significant clumping and aggregation of cells with large areas of substrate with no cells apparent after 24 hours. No obvious increase in non-viable cells was seen. At 48 hours the clumping appeared to have dispersed although some small aggregates were apparent. Amounts of non-viable cells appeared to remain constant (Figure 4.8).

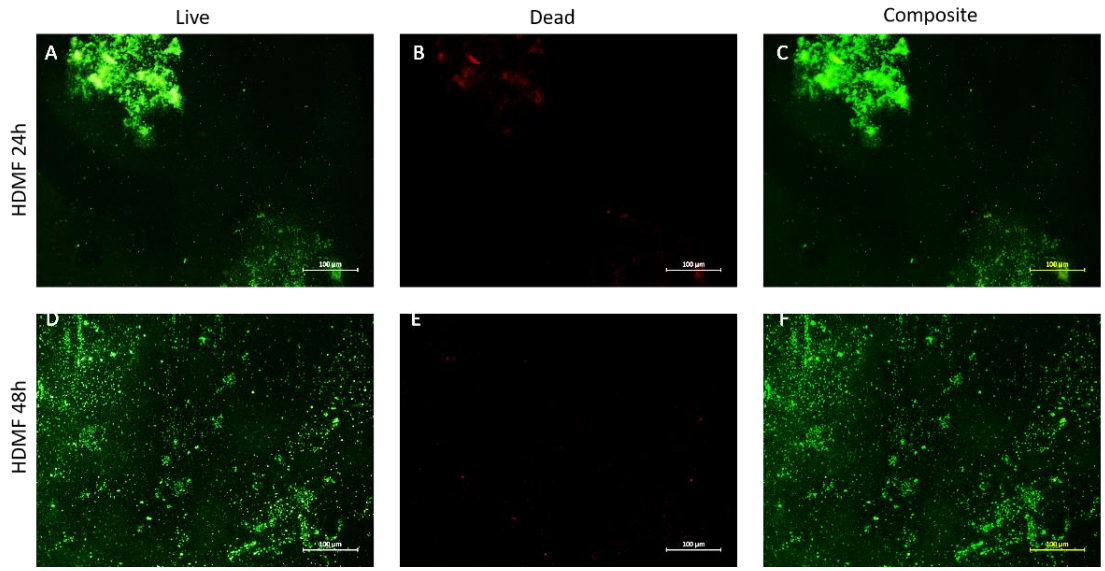

Figure 4.8- BacLight staining of an HDMF treated biofilm at 24 hours and 48 hours post inoculation.

Live cells are shown in green in images a and d. (a) significant clumping of cells was apparent in biofilms grown in the presence of HDMF. (d) this clumping then dispersed at 48 hours. Non-viable cells are shown in red in images b and e. (b) Small amounts of non-viable cells can be seen localised primarily in the larger cell aggregates. (e) After 48 hours the non-viable cells had been dispersed similarly to the live cells. Images c and f represent a composite of images a and b, and d and e respectively. All results shown are representative images of 3 independent replicates.

Biofilms grown in the presence of 4.33mg mL^{-1} of sotolon presented as poorly populated biofilms composed primarily of small aggregates on the growth substrate after 24 hours. Similar quantities of non-viable cells were observed when compared to both untreated controls and HDMF treated biofilms. At 48 hours aggregates had

dispersed but cells remained sparse on the substrate. No obvious increase in non-viable cells was observed over the 24 hours biofilms (Figure 4.9).

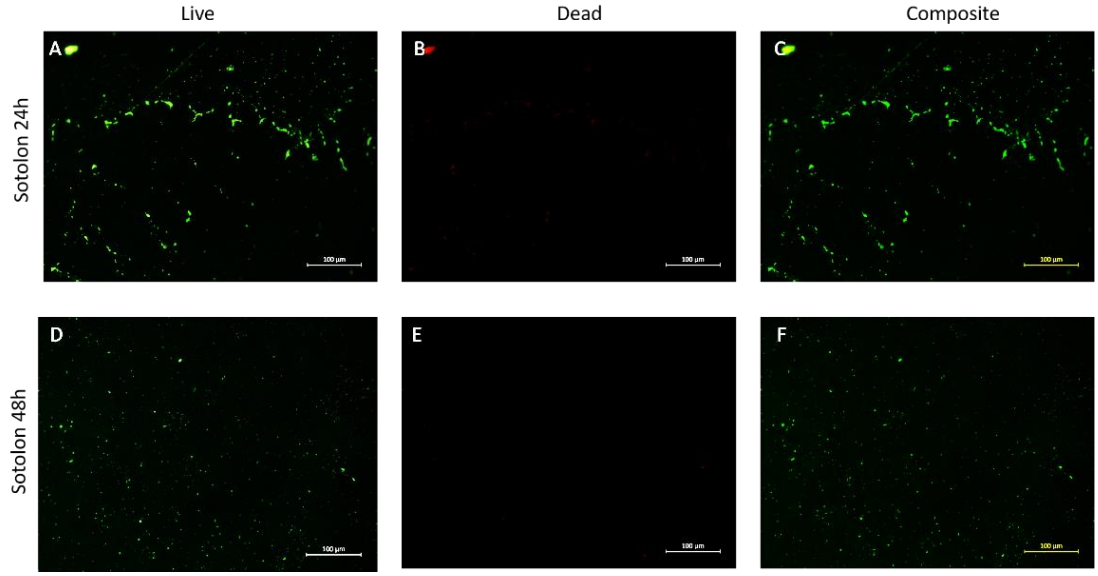

Figure 4.9- BacLight staining of a sotolon treated biofilm at 24 hours and 48 hours post inoculation.

Live cells are shown in green in images a and d. (a) Clumping of small amounts of cells was seen in the presence of sotolon. (d) this clumping then dispersed at 48 hours. Non-viable cells are shown in red in images b and e.(b) Small amounts of non-viable cells can be seen in the clumps of cells. (e) After 48 hours the non-viable cells had been dispersed similarly to the live cells. Images c and f represent a composite of images a and b, and d and e respectively. All results shown are representative images of 3 independent replicates.

When treated with 1.95µg mL^{-1} of MTHF, biofilms presented as well populated but heavily clumped films at 24 hours. At this point non-viable cells appeared to be located entirely within the clumps of cells which had formed. At 48 hours clumping was still apparent and it appeared that very few viable cells were present outside of the large aggregates which had formed. Non-viable cells again appeared primarily within the clumps of aggregated cells (Figure 4.10).

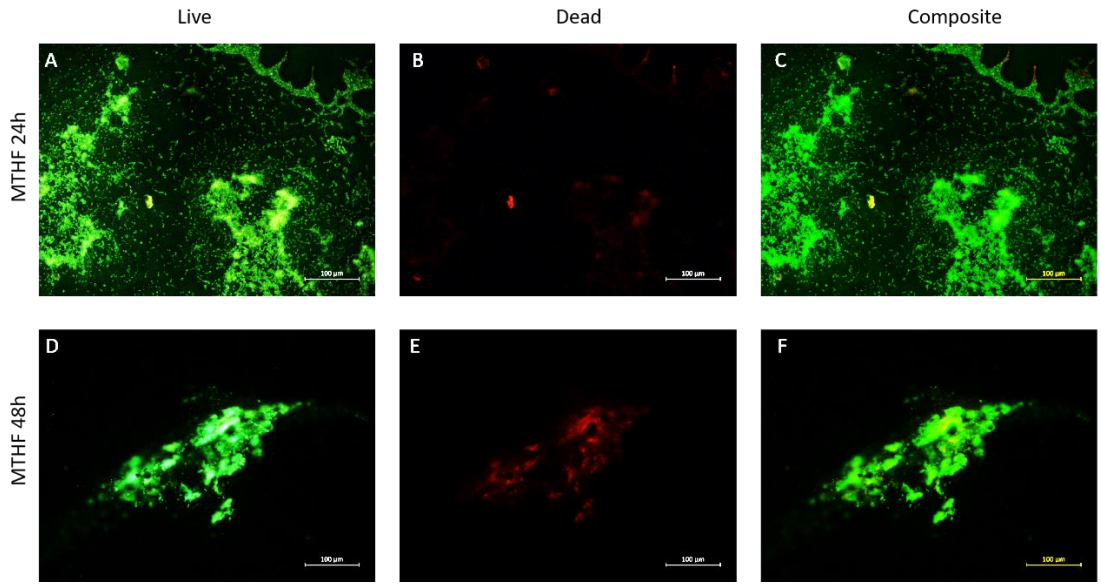

Figure 4.10 - BacLight staining of an MTHF treated biofilm at 24 hours and 48 hours post inoculation.

Live cells are shown in green in images a and d. Non-viable cells are shown in red in images b and e. (a-b) At 24h biofilms were well populated but showed aggregation of both viable and non-viable cells. (d-e) At 48h clumping remained apparent in biofilms and few viable cells were present on the growth substrate outside of the aggregates. Non-viable cells were located primarily within the clumps. Images c and f represent a composite of images a and b, and d and e respectively. All results shown are representative images of 3 independent replicates.

When treated with 5.50mg mL^{-1} of ascorbic acid, biofilms were well populated but appeared to show a degree of clumping of both viable and non-viable cells. At 48 hours biofilms remain well populated a clumping remains present for both viable and non-viable cells (Figure 4.11).

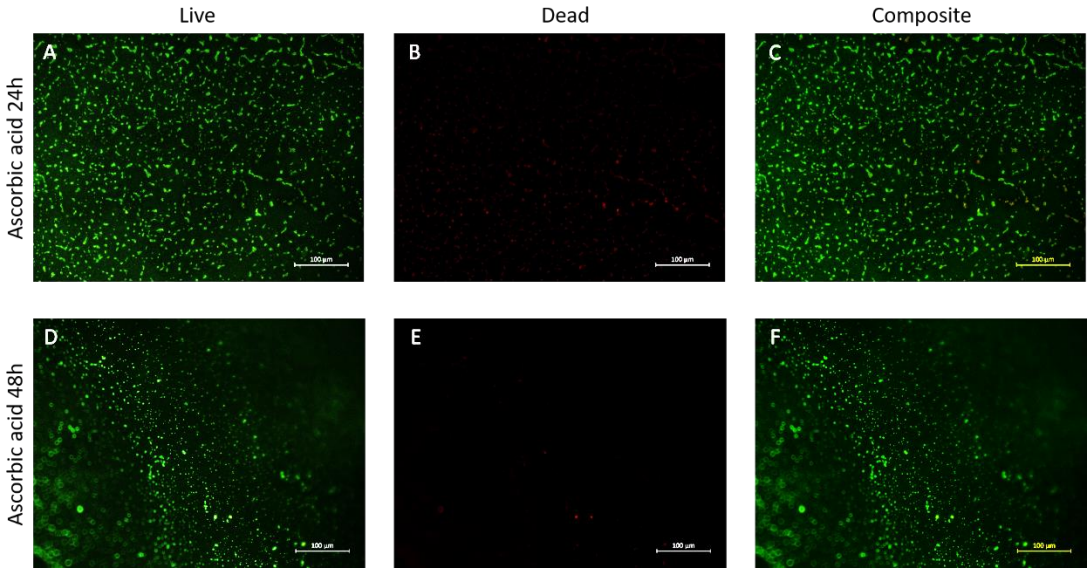

Figure 4.11- BacLight staining of an ascorbic acid control biofilm at 24 hours and 48 hours post inoculation.

Live cells are shown in green in images a and d. Non-viable cells are shown in red in images b and e. (a-b) At 24 hours biofilms were evenly populated with small aggregates of viable and non-viable cells evenly distributed across the growth substrate. (d-e) At 48 hours biofilms remained well populated and clumping was still apparent. Images c and f represent a composite of images a and b, and d and e respectively. All results shown are representative images of 3 independent replicates.

Viability staining of biofilms grown in the presence of sub-inhibitory concentrations of each furanone demonstrated that both HDMF and sotolon resulted in significantly less biofilm formation compared to untreated controls. Conversely, biofilm growth in the presence of sub inhibitory concentrations of MTHF appeared to be enhanced. Finally, treatment with sub inhibitory concentrations of ascorbic acid had no apparent effect on biofilm formation when compared with an untreated control.

4.4.4 Antibiofilm effects of sub-inhibitory concentrations of furanones on mature biofilms

The effects of furanone treatment on mature biofilms was also assessed as this represents a more accurate scenario likely to be encountered with a chronic wound.

When treated with 4 mg mL^{-1} HDMF, 24 hours old biofilms were shown to be reduced by 60.01% after 24 hours of treatment and 67.13% after 48 hours treatment (Figure 4.12 ai). When treated with a similar concentration of HDMF, 48 hours old biofilms were increased by 226% after 24 hours of treatment and showed no significant difference after 48 hours of treatment (Figure 4.12 a ii). When treated with 4.33mg mL^{-1} of sotolon, a 24 hours old biofilm showed a reduction in biofilm biomass of 77.66% and 56.12% at 24 hours post treatment and 48 hours post treatment respectively (Figure 4.12 bi). When treated with the same dose of sotolon, 48 hours old biofilms showed no significant changes in biofilm biomass (Figure 4.12 b ii). Delayed treatment with 1.95 µL mL^{-1} of MTHF a 46.36% reduction in biofilm biomass was seen in 24 hours old biofilms after 24 hours treatment. No significant reduction was seen after 48 hours of treatment (Figure 4.12 ci). No significant reductions in biofilm biomass was seen when a 48 hours old biofilm was treated with MTHF (Figure 4.12 cii). When both 24 hours and 48 hours old biofilms were treated with 5.50mg mL^{-1} of ascorbic acid, no significant reductions in biofilms were seen at any time point (Figure 4.12 di-ii).

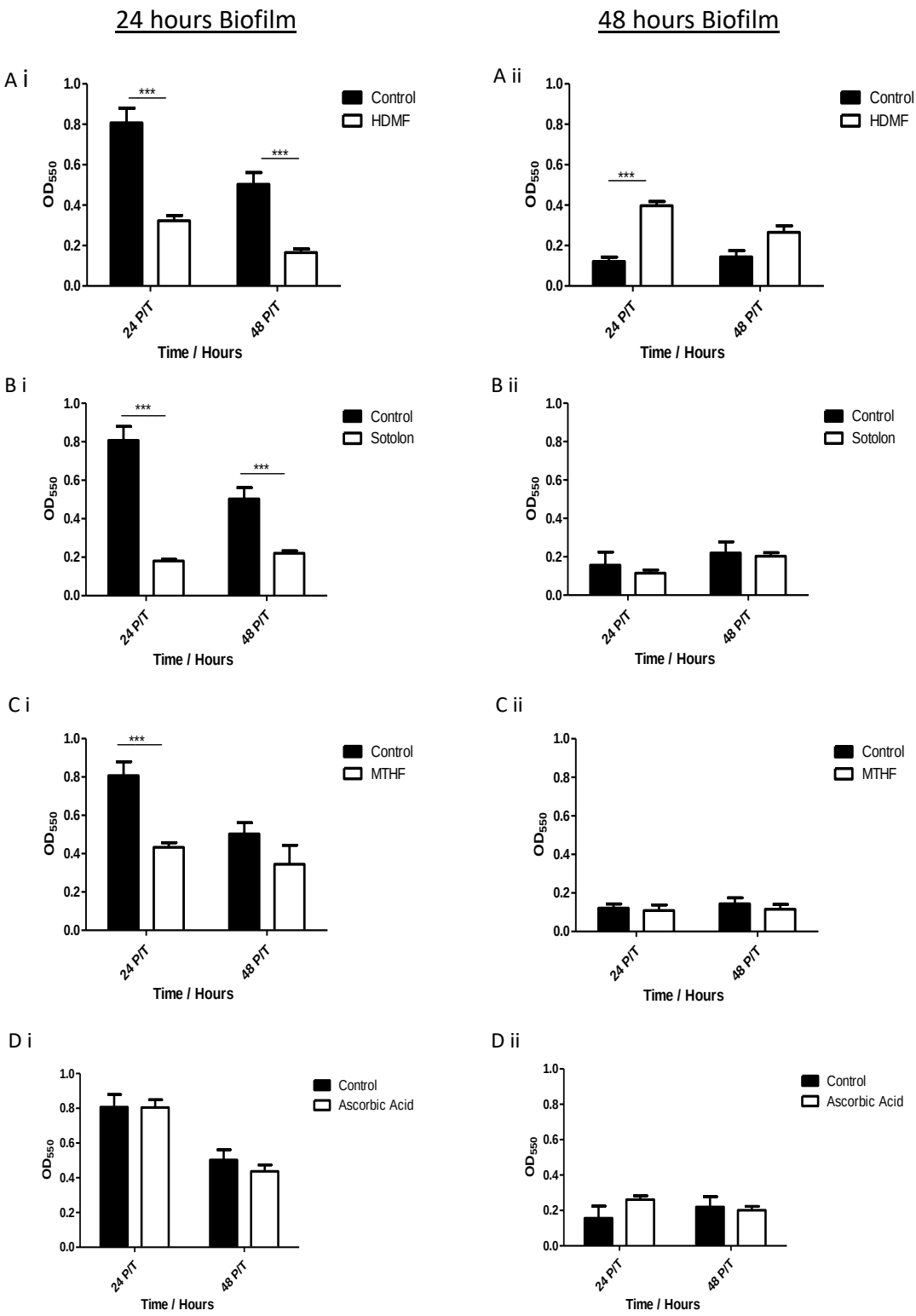
24 hours Biofilm
48 hours Biofilm
A i
A ii
B i
B ii
C i
C ii
D i
D ii
Control
HDMF
Sotolon
MTHF
Ascorbic Acid
OD550
Time / Hours
24 P/T
48 P/T
***

Figure 3.12 - Treatment of mature PAO1 biofilms with furanone compounds.

(a i) Treatment with 8mg mL-1 HDMF resulted in a 60.01% and 67.13% reduction in the biomass of a 24 hours old biofilm at 24 and 48 hours post treatment respectively. (a ii) This treatment cause a 226% increase in biofilm biomass and no significant change in biofilm biomass of a 48 hours old biofilm at 24 and 48 hours post treatment respectively (b i).Treatment with 4.33mg mL-1 of sotolon showed a 77.66% and a 56.12% reduction in biomass of a 24 hours old biofilm at 24 and 48 hours old biofilm respectively (b i). Treatment with 4.33mg mL^{-1} sotolon showed no significant decrease in biofilm biomass in a48 hours biofilm (b ii). When treated with 1.95µg mL-1 of MTHF, a 24 hours biofilm showed a 46.36% reduction in biofilm biomass 24 hours post treatment and no significant change in biofilm biomass 48 hours post treatment (c i). MTHF treatment of a 48 hours old biofilm showed no significant changes (c ii). Treatment with 5.50mg mL -1 ascorbic acid showed no significant changes in biofilm biomass in either a 24 hours old biofilm or a 48 hours old biofilm (d i-ii). Data represents the average of 3 biological replicates and 3 technical replicates ±S.D. Data was analysed using independent t-tests.

4.4.5 Aerogel-mediated delivery of furanones

The antibiofilm effects of furanone compounds when delivered using the novel aerogel system was assessed. Both HDMF and Sotolon-loaded aerogels were assessed using an unloaded aerogel as a control.

4.4.5.1 Treatment of immature biofilms with aerogel delivered furanones

The effects of application of aerogel delivered furanones to early stage PAO1 biofilms was assessed. When applied at the point of inoculation, an unloaded aerogel showed no significant decrease in biofilm biomass when compared to an untreated control at either 24 hours or 48 hours post treatment (Figure 4.13 a). When treated with an HDMF-loaded aerogel at the time of inoculation, a reduction of 81.08% and 70.00% in biofilm biomass was observed 24 hours and 48 hours post treatment respectively (Figure 4.13 b). When a sotolon aerogel was applied at the time of inoculation, a 100% and 94.72% reduction in biofilm biomass was observed at 24 and 48h, respectively, when compared to a blank aerogel control (Figure 4.13 c). This result was repeated

and verified independently, and a 98.37% and 100% reduction were observed at 24 and 48h post treatment respectively (data not shown).

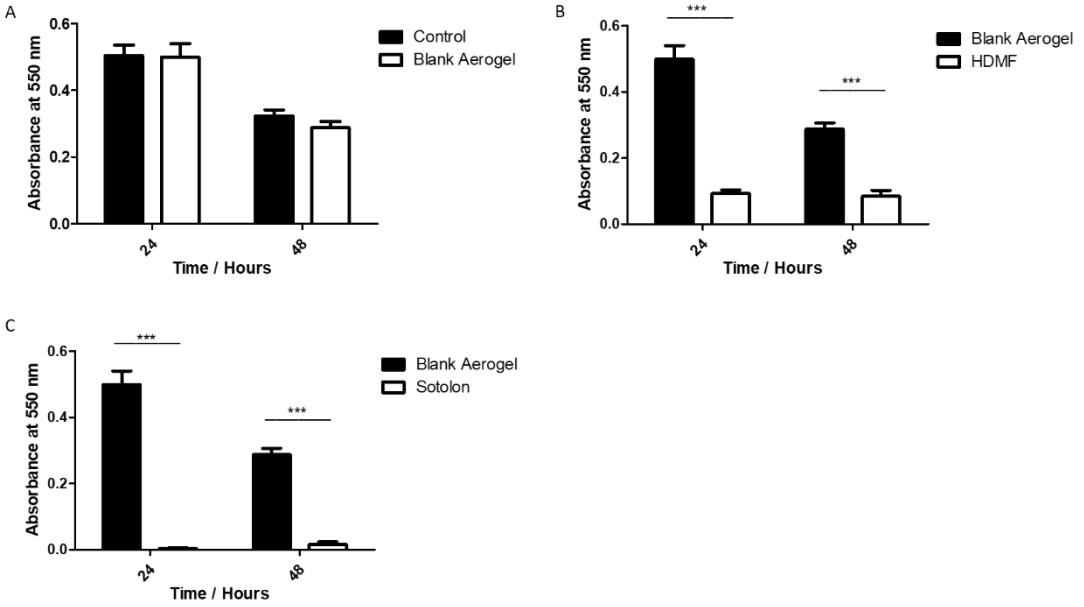

Figure 4.13 - The antibiofilm effects of aerogel delivered furanones when delivered at the time of inoculation.

(a) When treated with an unloaded aerogel cultures of PAO1 showed no significant decreases in biofilm biomass either 24 or 48 hours post treatment. (b) When treated with an HDMF-loaded aerogel biofilm biomass was reduced by 81.08% and 70.00% at 24 and 48 hours post treatment respectively. (c) When cultures of PAO1 were treated with a sotolon-loaded aerogel a 100% reduction in biofilm biomass was observed 24h post treatment as a 94.72% reduction was observed 48 hours post treatment. This finding was then confirmed using a new PAO1 culture and was validated as the repeated experiment showed a 98.37% and 100% reduction in biofilm biomass at 24 and 48h post treatment – data not shown. Data represents the average of 3 biological replicates and 3 technical replicates ±S.D. Data was analysed using independent t-tests

4.4.5.2 Treatment of mature PAO1 biofilms with aerogel delivered furanones

The antibiofilm effect of aerogel delivered furanones were assessed against mature biofilms. When a 24 hours old biofilm was treated with an unloaded control aerogel, an increase of 40.67% biomass was seen at 24 hours post treatment and no significant change was seen 48 hours post treatment (Figure 4.14 a). When a 48 hours old biofilm

was similarly treated, no significant effect was seen after 24 hours and a 35.24% reduction in biofilm biomass was seen 48 hours post treatment (Figure 4.14 b). When treated with an HDMF-loaded aerogel, a 24 hours old biofilm showed a 41.14% decrease in biofilm biomass 24 hours post treatment and a 41.87% reduction in biomass 48 hours post treatment when compared to an untreated control. These reductions increased to 58.41% and 54.80% respectively when compared to a blank aerogel treatment (Figure 4.14 a). When a 48 hours old biofilm was treated with an HDMF-loaded aerogel, a 43.64% reduction was seen 24 hours post treatment when compared to an untreated biofilm, but no significant difference was observed when compared to an unloaded aerogel treatment. A 71.01% reduction in biomass was seen 48 hours post HDMF aerogel treatment when compared to no treatment but only a 61.61% reduction when compared to an unloaded gel treatment (Figure 4.14 b). When a 24 hours old biofilm was treated with a sotolon-loaded aerogel, no significant changes in biofilm biomass were observed at either 24 hours or 48 hours post treatment when compared to the blank aerogel treatment but an increase in biofilm biomass of 25.75% was seen 24 hours post treatment of a 24 hours old biofilm when compared to the untreated control (Figure 4.14 a). Similarly, no significant reduction in biofilm biomass were observed when 48 hours old biofilms were treated with a sotolon aerogel after either 24 hours or 48 hours post treatment when compared to an unloaded aerogel (Figure 4.14 b). A decrease of 24.46% was observed 48 hours post treatment of a 48 hours old biofilm when sotolon treatment was compared to an untreated control.

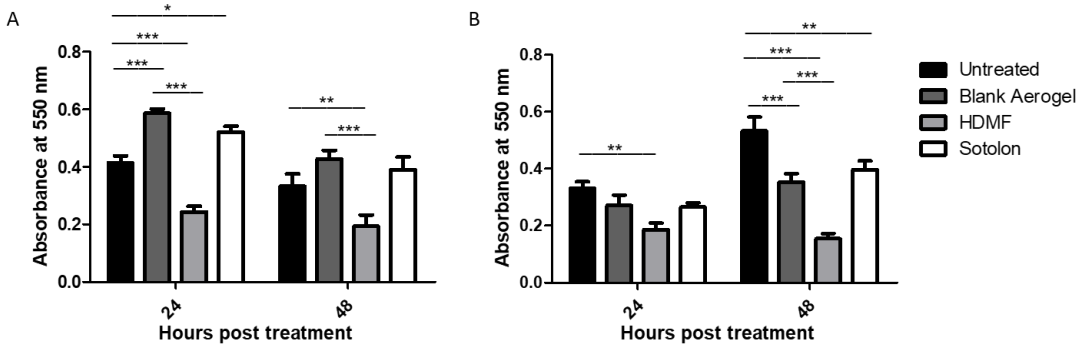

Figure 4.14 – Delayed treatment of mature biofilms with aerogel delivered furanones.

(a) When a 24 hours biofilm was treated with an unloaded aerogel a 40.67% increase was observed 24 hours post treatment. No significant change was noted following 48 hours of treatment when compared to untreated controls. HDMF treatment of a 24 hours old biofilm showed a 41.14% decrease in biofilm biomass 24 hours post treatment and a 41.87% reduction versus an unloaded aerogel treatment 48 hours post treatment. Sotolon treatment of a 24 hours old biofilm showed no significant changes in biofilm biomass over a blank aerogel treatment 24 hours and 48 hours post treatment. (b) When a 48 hours old biofilm was treated with a blank aerogel no effect was seen after 24 hours and a 35.24% reduction was observed after 48 hours treatment. HDMF treatment of a 48 hours old biofilm showed a 43.64% decrease in biofilm biomass 24h after treatment and no significant changes after 48 hours. Sotolon treatment of a 48h old biofilm showed no significant changes in biofilm biomass 24 or 48 hours post treatment when compare to a blank aerogel control. Data represents the average of 3 biological replicates and 3 technical replicates ±S.D. Data was analysed using independent t-tests

4.4.6 Assessment of DSM50071 genetic elements conferring resistance

A previously published genome for DMS50071 was interrogated using the NCBI Blastn tool for the presence or absence of 4 genes believed to be involved in furanone resistance; *nalC, mexR, MdrR1,* and *MdrR2.* These genes were found not to be present in the published genome for DSM50071. The whole genome sequence provided by MicrobesNG was interrogated to confirm the presence or absence these genes in the strain used in this work. It was found that the DSM50071 strain used in this work had no sequences within the genome that were homologous to *nalC, mexR, MdrR1* or

MdrR2, thus, confirming the hypothesis that the limited efficacy of furanones shown here are due to furanone resistance.

4.5 Discussion

P. aeruginosa is one of the most common pathogens isolated from chronic wounds (Serra *et al.*, 2015). When present in a wound, *P. aeruginosa* primarily grows in the form of a biofilm and it is the presence of these biofilms that often cause an acute wound to fail to heal, thus, becoming chronic (Wolcott, Rhoads and Dowd, 2008; Zhao *et al.*, 2013). Due to their prominent role in the development and maintenance of chronic wounds, novel treatments against *P. aeruginosa* biofilms are greatly needed. Therefore, the aim of this chapter was to conduct an assessment of furanones as potential QSIs and antibiofilm compounds against the common wound pathogen *P. aeruginosa* PAO1 (DSM50071).

Prior to applying furanone treatments an understanding of the baseline characteristics of the organism was required. Organism growth kinetics in liquid media were in keeping with expectations. Biofilm formation kinetics in a 12-well tissue culture plate showed continuous rise and fall of adhered biomass (as measured by retained crystal violet). This finding is in keeping with the work of Murray *et al.*(2017) who showed a similar pattern of increasing and decreasing biofilm biomass in *P. aeruginosa*. (Murray *et al.*, 2017). It is thought that these changes in biofilm biomass may be due to maturation and subsequent dispersal of the biofilm. The numbers of viable cells in the liquid phase of the biofilm cultures was also assessed. It was shown that a steady increase in planktonic cells occurred from 4 hours to 18 hours post-incubation after which stationary phase was reached and after 24 hours a decline in viable cell numbers in begins.

Following this initial characterisation of the strain, the MBC of each furanone was measured. For the purposes of this work a sub-inhibitory dose of each furanone were

used. The reason for doing so was twofold. First, if a sub-inhibitory concentration of furanone is used it is more likely that any reduction in biofilm is due to QSI effects rather than reductions in viable cell numbers. Second, when using a sub-inhibitory dose of furanone, a greatly reduced selection pressure is placed on the organism, therefore, minimising the chance of resistance developing. While the development of resistance to the compounds has little importance in *in vitro* testing, if the use of furanones was translated to use in humans, this would be a significant problem. Indeed, it has already been shown that some bacterial isolates have an inherent resistance to furanone compounds with some *P. aeruginosa* strains being able to efflux furanones more effectively (Maeda *et al.*, 2012; García-Contreras *et al.*, 2013). In this work it was shown that the MBC of HDMF, MTHF, ascorbic acid and sotolon were 8mg mL^{-1}, 3.90μL mL^{-1}, 11.01mg mL^{-1} and 8.65 mg mL^{-1}, respectively. To ensure concentrations used for each experiment were sub inhibitory half of the MBC was used. (4 mg mL^{-1}, 1.95 μL mL^{-1}, 5.50 mg mL^{-1} and 4.33 mg mL^{-1} for HDMF, MTHF, ascorbic acid and sotolon, respectively). The MBC values identified in this work are significantly higher than values previously reported for other organisms. For example, Sung *et al.* (2007) reported an MIC value 80 μg mL^{-1} for HDMF against wild type *P. aeruginosa* and a value of 120 μg mL^{-1} against vancomycin resistant enterococci (VRE)(Sung *et al.*, 2007). Similarly, Xu *et al*. reported MIC values for HDMF of between 19 and 39 μg mL^{-1} for a range of dental pathogens (Xu, Howard and Xie, 2016). In 2014 Choi *et al.* reported an MIC for HDMF when used against *P. aeruginosa* KCTC1637 of 624.8 μM or 80.06 μg mL^{-1}. This means that the MBC for HDMF presented here is more than thirty-three time greater than the highest previously reported MIC, and some fifty times higher than previously reported MIC values against *P. aeruginosa* specifically. One study reported the MIC of sodium

ascorbate (the sodium salt of ascorbic acid) to be 100 mg mL^{-1}. This is almost ten times greater than the MBC of ascorbic acid reported in this work. This may be due to an effect reported in 1992 by Oh and Marshall, who found that reducing the pH of a bacterial medium subsequently reduced the MIC of a surfactant known as monolaurin (Oh and Marshall, 1992). As ascorbic acid dissociates in an aqueous environment, such as bacterial growth media, it produces ascorbate mono ions and positively charged hydrogen ions. The production of excess hydrogen ions would lower the pH of the medium. If the effect reported by Oh and Marshall holds true for ascorbic acid this reduction in pH may potentially reduce the MBC of the compound below the reported MBC for sodium ascorbate. Unfortunately, due to the limited use of furanones in the literature reliable, reports of MBC values for MTHF and sotolon are not available and so comparisons to the findings reported here cannot be made. Despite this, the MBC values identified in this chapter were shown to be accurate using both a streak plate method and orthogonally validated using a colorimetric TTC assay. As such these data are robust.

The antibiofilm effects of each furanone at a range of concentrations were rapidly assessed by incubating *P. aeruginosa* PAO1 with a range of furanone concentrations from half MBC to one thirty second of the established MIC. Biofilm inhibition was assessed and reported as a reduction in total biofilm biomass after 24 hours. It was shown that neither ascorbic acid nor MTHF showed any effects on PAO1 biofilm biomass at any tested concentration. HDMF showed a significant reductions of equal magnitude in biofilm at one half and one quarter MBC (4mg mL^{-1} and 2mg mL^{-1}) while sotolon showed significant decreases (also similar in magnitude) in total biofilm biomass at half MBC and one eighth MBC (4.33mg mL^{-1} and 1.08mg mL^{-1}). It was,

therefore, decided that half MBC would be used as the treatment dose of each furanone for all subsequent experiments.

The antibiofilm effect of each furanone was assessed at a concentration of half MBC over 72 hours when administered at the point of inoculation. It was shown that ascorbic acid had no effect on quantities of biofilm biomass at 24 hours or 48 hours post inoculation. However, at 72 hours ascorbic acid treated biofilms were seen to have 406% more biomass when compared to untreated controls. This is in direct contrast to the two recent studies by El-Mowafy *et al.* (2014) and Pandit *et al.* (2017). It was demonstrated by El-Mowafy that sodium ascorbate effectively reduces the formation of biofilm by *P. aeruginosa* PAO1 by over 60% at one eighth of the established MBC (equal to 12.5 mg mL^{-1} in their study) and by approximately 50% at one twentieth of the established MIC (equivalent to 5 mg mL^{-1} in their study) (El-Mowafy, Shaaban and Abd El Galil, 2014). These findings suggest that the concentration of ascorbic acid used in this work (5.5 mg mL^{-1}) should have had a significant effect on biofilm formation. Similarly the work of Pandit *et al.* showed a biofilm inhibitory effect of sodium ascorbate at a concentration of 3.96 mg mL^{-1} and greater (Pandit *et al.*, 2017). This, again, indicates that the concentration used in this work should have shown an antibiofilm effect. As it has been previously shown that ascorbic acid is unstable in aqueous environment it is hypothesised that one or more degradation products of ascorbic acid caused the increase in biofilm. This may occur either by the degradation product acting as a QS agonist or simply by providing a chemical insult causing the bacteria to rapidly form a protective biofilm.

The use of MTHF showed no notable effect on biofilm biomass 24 hours post treatment, a 26.45% reduction at 48 hours and a 47.23% increase in biomass at 72

hours. As no previous reports exist of the use of MTHF for the inhibition of biofilm these findings cannot be compared to previous work. However, as with ascorbic acid the previously demonstrated instability of MTHF may have resulted in degradation product which cause an increase in biofilm formation in *P. aeruginosa*. While ascorbic acid and MTHF were largely unsuccessful in inhibiting biofilm formation in PAO1 both HDMF and sotolon showed high levels of biofilm inhibition when applied at the point of inoculation. HDMF treatment resulted in reductions in biofilm biomass of 77.67%, 77.02%, and 88.30% at 24 hours, 48 hours and 72 hours respectively. These reductions are in excess of those reported in other studies. For example, the work of Choi *et al*. in 2014 showed that when applied at a concentration of 0.1 μM (12.81 ng mL^{-1}) and 1.0 μM (128.13 ng mL^{-1}) HDMF reduced biofilm biomass 27.8% and 42.6% after 24 hours and 66.3% and 84.8% at 48 hours respectively. While the reductions reported in this work were greater than in the work of Choi *et al.,* the concentration of furanone used here was several orders of magnitude greater. This may be problematic as the requirement for a larger concentration of compound may result in greater pressure on the organism forcing the development of resistance. Furthermore, if furanones were taken forward to be tested *in vivo* the greater the required dose, the greater the possibility of adverse reactions and toxicity (Liebler and Guengerich, 2005). Under the same test conditions as HDMF, sotolon showed reductions in biofilm biomass of 87.20%, 86.50%, and 66.13% at 24 hours, 48 hours and 72 hours post-treatment. Again, these reductions are substantial.

It was decided that, despite the poor performance of MTHF and ascorbic acid, all furanones would be carried forward for testing in the treatment of mature biofilms.

The effect of furanone treatment on bacterial cell viability was assessed using BacLight cell viability staining. It was shown that when compared to untreated biofilms, those grown in the presence of HDMF showed a high degree of clumping with large aggregates being apparent at 24 hours and smaller but more numerous aggregates present after 48 hours. This change in morphology was also observed in biofilms grown in the presence of sotolon. MTHF biofilms appeared to be more densely populated after 24 hours and large, densely populated aggregates were apparent compared to untreated controls. Finally, ascorbic acid appeared as well populated biofilms similar to those seen in controls. Several studies have shown that interference with QS signalling can lead to the formation of biofilms with altered morphology (Huber *et al.*, 2001; Francolini *et al.*, 2004; Cady *et al.*, 2012). Francolini *et al.* showed that biofilms grown on polymer discs impregnated with the biofilm inhibitor usinic acid resulted in a *P. aeuginosa* biofilm that was less wide spread and which appeared to be clumped (Francolini *et al.*, 2004). Similarly, Cady *et al.* (2012) showed that treatment with various organosulfur compounds resulted in a poorly populated biofilm in which cells had aggregated into small clumps as shown by confocal microscopy. It is, therefore, likely that the altered biofilm morphology observed in the HDMF and sotolon treated biofilms was a result of quorum sensing inhibition leading to disordered biofilm formation. The changes observed in the MTHF biofilms may simply be a response of the cells to a non-lethal chemical insult. Indeed, in 2018 Wu *et al.* demonstrated that treatment of Enterococci with sub-inhibitory doses of antibiotics resulted in enhanced biofilm formation (Yu, Hallinen and Wood, 2018). If the same is true for the use of MTHF against *P. aeruginosa* this may explain the apparent increase in biofilm population density when the compound was present. Finally, the presence of these furanones did not appear to cause an

increase in non-viable cells. This was in keeping with previous reports of the use of furanones for the inhibition of biofilm which showed that these compounds could be used as QSIs at sub inhibitory concentration (Hentzer *et al.*, 2002; Choi *et al.*, 2014).

Mature biofilms (24 hours or 48 hours old) were then treated with each furanone. This approach was used as the majority of chronic wounds already have a biofilm present and assessing delayed treatment of a wound biofilm was more clinically relevant. When treated with ascorbic acid, it was shown that the compound had no effect on the levels of biofilm biomass of PAO1 at any time point tested. When measured 24 hours post MTHF treatment, a 24 hours old biofilm was reduced in biomass by 46.36%. However, in the following 24 hours this reduction became non-significant. Treatment of a 48 hours old biofilm with MTHF showed no obvious reduction in biofilm biomass. HDMF treatment of a 24 hours old biofilm resulted in reductions of 60.01% and 67.13% 24h and 48h post treatment. This represents a lower reduction than was seen when treatment was applied at the point of inoculation. This may be due to poor penetration of the compound into the pre-formed biofilm leading to poorer disruption of QS. It has been previously reported that, with antimicrobials such as vancomycin, as little as 20% of the administered dose is able to penetrate a bacterial biofilm (Dunne, Mason and Kaplan, 1993). If this also the case for furanones and *P. aeruginosa* biofilms, it may be that biofilm bound cells are receiving lower doses of furanone than anticipated. In contrast to the treatment of 24 hours old biofilms, HDMF treatment of 48 hours old biofilms caused an increase in biofilm biomass 24 hours after the application of the furanone and no significant increase 48 hours post treatment (though a trend was seen). This was highly unexpected as treatment with HDMF had caused significant reduction in biofilm biomass under all other conditions. It is hypothesised that 48 hours old biofilms differ vastly from 24 hours old biofilms both metabolically

and transcriptomically. This hypothesis is supported by the findings of Waite *et al.* (2005) who showed that developing and mature *P. aeruginosa* biofilms had distinct transcriptomic profiles. Mature biofilms showed upregulation of genes involved in carbon compound catabolism and general metabolism while developing biofilms favoured motility and small molecule transport (Waite *et al.*, 2005). This idea is supported by the subsequent work of Waite *et al.* (2006) who showed that in developing biofilms (8 hours post inoculation), gene expression was largely focused around cell motility and attachment, with over a quarter of upregulated genes being involved in these processes. However, gene expression in mature biofilms (48 hours post inoculation) was primarily focused on DNA repair and metabolism (Waite *et al.*, 2006; Schmidt *et al.*, 2011). The differences in transcription profiles between mature and immature biofilms would likely make them respond to treatments and chemical insults very differently, possibly accounting for the differences in response to furanone treatment. Finally, treatment of a 24 hours old biofilm with sotolon showed a decrease in biofilm biomass of 77.66% and 56.12% after 24 hours and 48 hours respectively. This reduction was not seen when treating a 48 hours old biofilm and no significant reduction in biomass was seen at any time point tested. This is likely also explained by the inherent differences between a newly formed, 24 hours old biofilm, and a more mature 48 hours old biofilm. However, it may also be the case that 24 hours after inoculation, when the early treatment was applied, the biofilm was still forming and the presence of the furanone prevented further QS and subsequent biofilm formation during the following 24 hours. This would not have been the case for the untreated biofilm which was able to continue growing in the subsequent 24 hours prior to quantification. In samples grown for 48 hours, prior to the application of the late treatment, biofilms will have been more fully formed, thus, quorum sensing controlled

biofilm formation was likely limited. This would have meant that the application of the furanones would have no significant effect. This is strongly supported by the findings of Waite *et al.* (2006) who showed, using gene clustering, that no significantly upregulated genes in a 48 hours old biofilm were related to cell division or chemotaxis. This is in contrast to a developing biofilm (represented in their work by an 8 hours old biofilm) in which approximately 7.5% of significantly upregulated genes were dedicated to cell division. This suggests that, by 48 hours, *P. aeruginosa* biofilms have slowed in the division of cells and may no longer be producing significant amounts of biomass.

Following the success of both HDMF and sotolon in the preceding experiments, it was decided that these compounds would be tested against biofilms using loaded aerogels as a delivery mechanism. Due to their limited effects, MTHF and ascorbic acid were omitted from further testing.

Furanone-loaded aerogels were applied to bacterial cultures at the point of inoculation to imitate a rapid treatment scenario in which a furanone aerogel dressing is applied to a wound as soon as it is sustained. Firstly, it was shown that the application of an unloaded aerogel had no effect on biofilm formation at any tested time point. HDMF-loaded aerogels were shown to reduce biofilm biomass by 81% and 70% at 24 hours and 48 hours post treatment respectively. When treated with sotolon, biofilm biomass was reduced by 100% and 94.72% over the same time period. The very high levels of reduction in biofilm biomass by sotolon were subsequently replicated using a new overnight culture and aerogels produced in a different batch. The substantial reductions in biofilm seen here indicate that both HDMF and sotolon retain their biological activity after being loaded into a PVA aerogel. Additionally, it clearly

demonstrates that controlled release of HDMF and sotolon is a potentially viable treatment to prevent the formation of *P. aeruginosa* biofilms in acute wounds. This would be advantageous in a real-world scenario as it has been shown that, in acute wounds, biofilms begin to form within 6 hours of the injury being sustained (Bowen and Richardson, 2016). As the presence of a biofilm is a major contributing factor to wounds progressing to a chronic state (Leaper, Assadian and Edmiston, 2015; Malone *et al.*, 2017; Schultz *et al.*, 2017), a reduction of this initial biofilm formation would likely lead to a reduction in number of chronic wounds.

The effect of aerogel delivered furanones on mature biofilms was then assessed. This experiment mimicked the use of furanone-loaded aerogels to treat established chronic wounds in which a biofilm was already present. A significant decrease in biofilm formation (41.14%) was seen 24 hours post treatment when HDMF was used to treat a 24 hours old biofilm. This reduction was maintained after 48 hours post treatment when compared to an untreated control. Conversely, when sotolon was used to treat a 24 hours old biofilm, it was found that a small increase in biofilm biomass was seen 24 hours post-treatment and no effect on biofilm biomass was observed 48 hours after treating a 24 hours old biofilm When used to treat a 48 hours old biofilm, a modest reduction in biofilm biomass was seen 48 hours after the application of the treatment. These results are largely contradictory to those seen when furanones were applied directly to the biofilm cultures. While the reason for the differences between the two methods of furanone application are unclear it may be that, when applied using the aerogel, the concentration of furanone in the culture is gradually increased (due to the controlled release of furanone from the gel). This would mean that the therapeutic dose of furanones was reached sometime after the application of the aerogel. This is in contrast to the direct application of the furanone which would have resulted in an

instantaneous therapeutic concentration of furanone. While the release studies reported in chapter 3 of this thesis showed that approximately 60-100% of the total loaded compound should have been released from the formulations, the aerogels used here are highly novel and as such several unidentified factors may have an effect on their drug release properties. For example, several factors such as pH of the solution into which a drug is being released can affect the drug release profile (Park *et al.*, 1998; Kenawy *et al.*, 2008). It is therefore possible that furanone release into the bacterial growth medium is not the same as was measured in chapter 3, causing the biofilms to be under dosed. However, this does not appear likely as results showing that aerogel delivered furanone performed better than directly added furanone when applied at the point of inoculation. This suggests that furanone release into the bacterial growth medium is not significantly altered when compared to the previously conducted release studies. Another explanation may be that, due to their protected nature, mature biofilms have a degree of resistance to the furanones, just as they have increased resistance to antibiotics. This hypothesis would explain why, when applied at the point of inoculation, furanones showed a potent biofilm inhibition effect both when applied directly, and when applied using an aerogel. Furthermore, this may explain why the direct application of furanones to mature biofilms showed a greater effect than the controlled release of furanones from an aerogel. Immediate application would have resulted in an instantaneous, high concentration treatment, while controlled release from an aerogel may have allowed the bacterial cells to respond by enhancing furanone efflux or perhaps producing enzymes such as lactonases which may cause degradation of the furan ring structure of the furanones. This possibility was considered further.

Resistance to furanones has been previously reported (Maeda *et al.*, 2012; García-Contreras *et al.*, 2013; García-Contreras, Peréz-Eretza, *et al.*, 2015). Maeda *et al.* (2012) showed that resistance to the furanone C-30 is possible in *P. aeruginosa* with resistant strains showing no significant reduction in several QS controlled phenotypes following furanone treatment. The authors of this paper showed that furanone resistant mutants of *P. aeruginosa*, which were produced using random transposon mutagenesis, were deficient in *mexR* or *nalC*. Both of these genes encode repressors of the MexAB-oprM multidrug efflux transporter (Maeda *et al.*, 2012; Pseudomonas.com, 2020a, 2020b). The authors show that when treated with furanone C-30, the mutants showed no significant reduction in pyocyanin production when compared with C-30-treated wild-type *P. aeruginosa* PA14. As well as this, the authors showed that C-30 treatment of furanone resistant organisms (particularly those deficient in *mexR*) enhanced swarming motility rather than simply having no effect as was expected. The authors also demonstrated that C-30 treatment of *mexR* deficient strains induced the expression of 23 QS-related genes, including genes encoding for efflux pumps and the LasR and RhlR transcriptional regulators. Finally, the authors demonstrated that the ability of wild-type PA14 to kill *Caenorhabditis elegans* nematodes was ameliorated with the use of C-30, with a reduction in lethality from 50% in untreated worms to 20% in treated worms being observed. However, in worm infections caused by *mexR* deficient strains, the mortality of 60% in untreated worms was only reduced to 50% mortality in C-30 treated worms. This study clearly demonstrates that bacterial resistance to furanones is possible and that this resistance arises when repressors of the MexAB-oprM operon are lost (Maeda *et al.*, 2012). An additional study in 2015 showed that *P. aeruginosa* PA14 strains which were deficient in *mexR* (and thus resistant to furanones) showed significant changes in response to a

stress following furanone treatment. The authors showed that when treated with C-30, wild type strains sensitivity to various stressors (heat, hydrogen peroxide, cadmium chloride, and sodium chloride) was increased by up to 8.2-fold. This indicated that furanone treatment could render *P. aeruginosa* more sensitive to common stresses. Conversely, *mexR* deficient strains treated with furanone C-30, experiencing the same stressors showed a maximum 1.5-fold change in sensitivity when exposed to C-30. These data indicate that strains resistant to furanones were not as effectively sensitised to various stresses by furanone treatment (García-Contreras, Nuñez-López, *et al.*, 2015).

In light of the studies described above, the previously published genome of PAO1 DSM50071 (accession number CP012001) was assessed for the presence of the *mexR* and *nalC* genes. It was found that the published DSM50071 genome did not contain sequences homologous to the *mexR* and *nalC* genes. Furthermore, it was shown by whole genome sequencing that the DSM50071 strain used in this study also lacked these two genes.

As well as lacking the mexR and nalC genes, both the previously published genome and the genome sequence produced during this work lacked sequences homologous to two more genes; *MdrR1* and *MdrR2*. This is important as these genes have also previously been reported to be repressors of MexAB-oprM and another efflux pump known as EmrAB (Heacock-Kang *et al.*, 2018).

Taken together, these data suggest that the hypothesis stating that the limited efficacy of the furanones as an antibiofilm treatment was the result of furanone resistance in the strain used in this work is correct. This hypothesis is further supported by the established MBC values for each furanone in this work. As previously discussed, the

MBC values reported here were many orders of magnitude greater than those reported in the literature. Due to the deficiency of DSM50071 in the two efflux repressors, and the subsequent greatly increased capacity for furanone efflux, this strain would require significantly increased concentrations of furanones to kill the cells.

The possibility of increased furanone efflux may also help to explain other findings in this work such as the improved antibiofilm effects of furanones when applied at the point of inoculation. It may be that, as bacterial cell numbers were lower at the point of inoculation, the high concentration of furanone was not able to be effluxed as rapidly or effectively meaning that the furanone was able to bind the AHL receptors and the expected anti QS effects of the furanones were seen. This idea is further supported by our observation that when 24 hours old biofilms were treated with furanones, smaller reduction in biofilm biomass were seen. Enhanced efflux of furanones by the bacterial cells may also explain the increase in biofilm formation seen in several experiments after furanone treatment. Garcia-Contreras *et al.* (2015) showed that *mexR* deficient strains, when grown in the presence of a furanone, exhibited a difference in response to stresses compared to non-deficient strains (García-Contreras, Nuñez-López, *et al.*, 2015). It may hold true that, as DSM50071 is deficient in *mexR* and other repressors, exposure to the furanones tested here may cause an abnormal response to stresses, such as depletion of nutrients in liquid culture, changes in medium pH, and changes in oxygen levels. It has been shown that nutrient density can significantly impact on the process of biofilm formation inducing processes as formation of mushroom type structures, or biofilm dispersal (Sauer *et al.*, 2004; Ghanbari *et al.*, 2016). It has also been shown that stresses such as pH and temperature also affect levels of biofilm formation (Ramli *et al.*, 2012). Considering this, it is not unreasonable to assume that the altered stress responses reported by

Garcia-Contreras *et al.* in 2015 may extend to other stressors and that the conditions found in bacterial cultures would, therefore, impact upon levels of biofilm.

Resistance to furanones has also been shown in clinical *P. aeruginosa* isolates. One study showed that some clinical isolates from cystic fibrosis patients were able to more effectively efflux furanone C-30 when compared to wild-type PA14. Further, one strain in particular, named INP-42, was able to efflux the furanone at levels approximately equivalent to the *mexR* deficient strain (García-Contreras, Peréz-Eretza, *et al.*, 2015). An earlier study showed that several clinical isolates from a hospital in Mexico showed increased production of several virulence factors, particularly elastase and alkaline protease, when treated with C-30 (García-Contreras *et al.*, 2013). While the authors of these studies did not explore the mechanism of furanone resistance in these clinical isolates, both suggest that it is likely to be a similar mechanism to the *mexR* and *nalC* mutants previously described.

As the strain used in this chapter for the assessment of furanones as antibiofilm was itself likely resistant to furanones the findings detailed here are not broadly applicable to all *P. aeruginosa* strains. However, the work reported here has shown that with early application of high dose HDMF and sotolon, even furanone resistant strains may be inhibited from effectively forming a biofilm. This is an important finding as it suggests that furanone-loaded aerogels may, in fact, be a suitable first-line wound treatment which would lessen or entirely inhibit the early stages of biofilm formation that often occur within the first hours after a wound is sustained. While this is a promising prospect, the methods used here are limited in their applicability to a real wound and therefore further testing on a suitable wound model is needed.

4.6 Conclusion

The use of furanones for the inhibition of biofilm formation in *P. aeruginosa* DSM50071 was investigated. It was shown that, when applied at the point of inoculation, sub-inhibitory doses of both HDMF and sotolon were effectively able to inhibit biofilm formation when compared to an untreated control. Under the same circumstances MTHF and ascorbic acid showed no appreciable reduction in biofilm formation and after 72 hours of treatment the presence of ascorbic acid significantly increased biofilm biomass. Using cell viability staining it was shown that, when grown in the presence of HDMF and sotolon, biofilm morphology changed from a well populated homogenous biofilm to a poorly populated biofilm that appeared to consist primarily of bacterial cell aggregates. MTHF treatment resulted in a biofilm that appeared to be more densely populated than the control with large densely populated aggregates formed after 48 hours. Biofilms grown in the presence of ascorbic acid appeared similar to the controls. When added directly to mature biofilm, HDMF and sotolon retained their antibiofilm properties while MTHF and ascorbic acid were less effective. When applied at the point of inoculation using a furanone-loaded aerogel, HDMF remained effective and sotolon was shown to be highly effective in inhibiting biofilm formation. It was demonstrated that when applied to mature biofilms using loaded aerogels both HDMF and sotolon were less effective in the inhibition of biofilm than when applied early. Finally, the possibility of DSM50071 having high levels of resistance to furanone compounds by means of increased furanone efflux was explored. The findings that furanone-loaded aerogels could be an effective early treatment for the prevention of biofilm formation in wounds is promising. However, the methods used in this chapter have limited applicability to a real-world scenario and so furanone-loaded aerogels should be tested on an appropriate wound model.

4.7 References

Abisado, R. G. *et al.* (2018) 'Bacterial Quorum Sensing and Microbial Community Interactions', *mBio*, 9(3), p. e02331. doi: 10.1128/mBio.02331-17.

Ahmed, S. A. K. S. *et al.* (2019) 'Natural quorum sensing inhibitors effectively downregulate gene expression of *Pseudomonas aeruginosa* virulence factors', *Applied Microbiology and Biotechnology*, 103(8), pp. 3521–3535. doi: 10.1007/s00253-019-09618-0.

An, J. *et al.* (2014) 'Bacterial quorum sensing and metabolic slowing in a cooperative population', *Proceedings of the National Academy of Sciences of the United States of America*, 11(14), pp. 14912–14917. doi: 10.1073/pnas.95.13.7687.

Andersson, R. A. *et al.* (2000) 'Quorum Sensing in the Plant Pathogen *Erwinia carotovora* subsp. carotovora: The Role of expR Ecc', *Molecular Plant-Microbe Interactions*, 13(4), pp. 384–393.

Arevalo-Ferro, C. *et al.* (2003) 'Identification of quorum-sensing regulated proteins in the opportunistic pathogen *Pseudomonas aeruginosa* by proteomics.', *Environmental microbiology*, 5(12), pp. 1350–69.

Arihara, K., Yokoyama, I. and Ohata, M. (2019) 'DMHF (2,5-dimethyl-4-hydroxy-3(2H)-furanone), a volatile food component with attractive sensory properties, brings physiological functions through inhalation', *Advances in Food and Nutrition Research*, 89, pp. 239–258. doi: 10.1016/bs.afnr.2019.05.001.

Bao, J. *et al.* (2017) 'New Furanone Derivatives and Alkaloids from the Co-Culture of Marine-Derived Fungi Aspergillus sclerotiorum and Penicillium citrinum',

Chemistry & Biodiversity, 14(3), p. e1600327. doi: 10.1002/cbdv.201600327.

Bjarnsholt, T. *et al.* (2005) 'Garlic blocks quorum sensing and promotes rapid clearing of pulmonary *Pseudomonas aeruginosa* infections', *Microbiology*, 151(12), pp. 3873–3880. doi: 10.1099/mic.0.27955-0.

Bowen, G. and Richardson, N. (2016) 'Biofilm management in chronic wounds and diabetic foot ulcers', *The diabetic foot journal*, 19(4), pp. 198–204. doi: 10.1097/prs.0000000000002681.

Brackman, G. *et al.* (2008) 'Cinnamaldehyde and cinnamaldehyde derivatives reduce virulence in Vibrio spp. by decreasing the DNA-binding activity of the quorum sensing response regulator LuxR', *BMC Microbiology*, 8(1), p. 149. doi: 10.1186/1471-2180-8-149.

Brackman, G. *et al.* (2011) 'Quorum Sensing Inhibitors Increase the Susceptibility of Bacterial Biofilms to Antibiotics In Vitro and In Vivo', *Antimicrobial Agents and Chemotherapy*, 55(6), pp. 2655–2661. doi: 10.1128/AAC.00045-11.

Brackman, G. *et al.* (2012) 'Synthesis and evaluation of the quorum sensing inhibitory effect of substituted triazolyldihydrofuranones', *Bioorganic and Medicinal Chemistry*, 20(15), pp. 4737–4743. doi: 10.1016/j.bmc.2012.06.009.

Cady, N. C. *et al.* (2012) 'Inhibition of biofilm formation, quorum sensing and infection in *Pseudomonas aeruginosa* by natural products-inspired organosulfur compounds', *PLoS ONE*, 7(6). doi: 10.1371/journal.pone.0038492.

Caine, D. and Ukachukwu, V. (1985) 'A New Synthesis of 3-n-Butyl-4-bromo-5(Z)-(bromomethylidene)-2-95H)-furanone, a Naturally Occurring Fimbriolide from

Delisia fimbriata (Bonnemaisoniaceae)', *Journal of Organic Chemisty*, 50, pp. 2195–2198.

CDC (2019) *Antibiotic Resistance Threats in the United States, 2019*. Atlanta. Available at: www.cdc.gov/DrugResistance/Biggest-Threats.html. (Accessed: 3 March 2020).

Choi, S. C. *et al.* (2014) 'Inhibitory effects of 4-hydroxy-2,5-dimethyl-3(2H)-furanone (HDMF) on acyl-homoserine lactone-mediated virulence factor production and biofilm formation in *Pseudomonas aeruginosa* PAO1', *Journal of Microbiology*, 52(9), pp. 734–742. doi: 10.1007/s12275-014-4060-x.

Cvitkovitch, D. G., Li, Y.-H. and Ellen, R. P. (2003) 'Quorum sensing and biofilm formation in Streptococcal infections.', *The Journal of clinical investigation*. American Society for Clinical Investigation, 112(11), pp. 1626–32. doi: 10.1172/JCI20430.

Davies, D. G. *et al.* (1998) 'The involvement of cell-to-cell signals in the development of a bacterial biofilm.', *Science*, 280(5361), pp. 295–8. doi: 10.1126/SCIENCE.280.5361.295.

Di Domenico, E. G. *et al.* (2019) 'Microbial biofilm correlates with an increased antibiotic tolerance and poor therapeutic outcome in infective endocarditis', *BMC Microbiology*, 19(1), p. 228. doi: 10.1186/s12866-019-1596-2.

Dong, Y. H. *et al.* (2001) 'Quenching quorum-sensing-dependent bacterial infection by an N-acyl homoserine lactonase', *Nature*, 411(6839), pp. 813–817. doi: 10.1038/35081101.

Dunne, W. M., Mason, E. O. and Kaplan, S. L. (1993) 'Diffusion of rifampin and vancomycin through a Staphylococcus epidermidis biofilm', *Antimicrobial Agents and Chemotherapy*, 37(12), pp. 2522–2526. doi: 10.1128/AAC.37.12.2522.

Eberhard, A. *et al.* (1981) 'Structural identification of autoinducer of Photobacterium fischeri luciferase', *Biochemistry*, 20(9), pp. 2444–2449. doi: 10.1021/bi00512a013.

El-Mowafy, S. A., Shaaban, M. I. and Abd El Galil, K. H. (2014) 'Sodium ascorbate as a quorum sensing inhibitor of *Pseudomonas aeruginosa*', *Journal of Applied Microbiology*, 117(5), pp. 1388–1399. doi: 10.1111/jam.12631.

Francolini, I. *et al.* (2004) 'Usinic acid, a natural antimicroial agent able to inhibit bacterial biofilm formation on polymer surfaces', *Antimicrobial Agents and Chemotherapy*, 48(11), pp. 4360–4365. doi: 10.1128/AAC.48.11.4360.

Gambello, M. J., Kaye, S. and Iglewski, B. H. (1993) 'LasR of *Pseudomonas aeruginosa* is a transcriptional activator of the alkaline protease gene (apr) and an enhancer of exotoxin A expression.', *Infection and immunity*, 61(4), pp. 1180–4.

García-Contreras, R. *et al.* (2013) 'Resistance to the quorum-quenching compounds brominated furanone C-30 and 5-fluorouracil in *Pseudomonas aeruginosa* clinical isolates', *Pathogens and Disease*, 68(1), pp. 8–11. doi: 10.1111/2049-632X.12039.

García-Contreras, R., Peréz-Eretza, B., *et al.* (2015) 'High variability in quorum quenching and growth inhibition by furanone C-30 in *Pseudomonas aeruginosa* clinical isolates from cystic fibrosis patients', *Pathogens and Disease*, 73(6), p. ftv040. doi: 10.1093/femspd/ftv040.

García-Contreras, R., Nuñez-López, L., *et al.* (2015) 'Quorum sensing enhancement

of the stress response promotes resistance to quorum quenching and prevents social cheating', *The ISME Journal*, 9(1), pp. 115–125. doi: 10.1038/ismej.2014.98.

Ghanbari, A. *et al.* (2016) 'Inoculation density and nutrient level determine the formation of mushroom-shaped structures in *Pseudomonas aeruginosa* biofilms', *Scientific Reports*, 6(1), pp. 1–12. doi: 10.1038/srep32097.

Givskov, M. *et al.* (1996) 'Eukaryotic interference with homoserine lactone-mediated prokaryotic signalling', *Journal of bacteriology*, 178(22).

Green, S. K. *et al.* (1974) 'Agricultural plants and soil as a reservoir for *Pseudomonas aeruginosa*.', *Applied microbiology*, 28(6), pp. 987–91.

Hammer, B. K. and Bassler, B. L. (2003) 'Quorum sensing controls biofilm formation in Vibrio cholerae.', *Molecular microbiology*, 50(1), pp. 101–4.

Heacock-Kang, Y. *et al.* (2018) 'Two regulators, PA3898 and PA2100, modulate the *Pseudomonas aeruginosa* multidrug resistance MexAB-OprM and EmrAB efflux pumps and biofilm formation', *Antimicrobial Agents and Chemotherapy*, 62(12). doi: 10.1128/AAC.01459-18.

Hentzer, M. *et al.* (2002) 'Inhibition of quorum sensing in *Pseudomonas aeruginosa* biofilm bacteria by a halogenated furanone compound', *Microbiology*, 148(1), pp. 87–102. doi: 10.1099/00221287-148-1-87.

Hentzer, M. *et al.* (2003) 'Attenuation of *Pseudomonas aeruginosa* virulence by quorum-sensing inhibitors', *Embo J.*, 22(15), p. 3803. doi: 10.1093/emboj/cdg366.

Hirsch, E. B. and Tam, V. H. (2010) 'Impact of multidrug-resistant *Pseudomonas aeruginosa* infection on patient outcomes.', *Expert review of pharmacoeconomics &*

outcomes research, 10(4), pp. 441–51. doi: 10.1586/erp.10.49.

Huber, B. *et al.* (2001) 'The cep quorum-sensing system of *Burkholderia cepacia* H111 controls biofilm formation and swarming motility', *Microbiology*, 147(9), pp. 2517–2528. doi: 10.1099/00221287-147-9-2517.

Ishida, T. *et al.* (2007) 'Inhibition of quorum sensing in *Pseudomonas aeruginosa* by N-acyl cyclopentylamides', *Applied and Environmental Microbiology*, 73(10), pp. 3183–3188. doi: 10.1128/AEM.02233-06.

Kenawy, E.-R. S. *et al.* (2008) 'Effect of pH on the drug release rate from a new polymer-drug conjugate system.', *Polymer International*, 57, pp. 85–91. doi: 10.1002/pi.

Kostakioti, M., Hadjifrangiskou, M. and Hultgren, S. J. (2013) 'Bacterial biofilms: development, dispersal, and therapeutic strategies in the dawn of the postantibiotic era.', *Cold Spring Harbor perspectives in medicine*, 3(4), pp. 1–23. doi: 10.1101/cshperspect.a010306.

Koutsoudis, M. *et al.* (2006) 'Quorum-sensing regulation governs bacterial adhesion, biofilm development, and host colonization in *Pantoea stewartii* subspecies stewartii', *Proceedings of the National Academy of Sciences of the United States of America*, 103(15), pp. 5983–5988. doi: 10.1073/pnas.95.13.7687.

Kusada, H. *et al.* (2017) 'A novel quorum-quenching N-acylhomoserine lactone acylase from acidovorax sp. strain MR-S7 mediates mntibiotic resistance.', *Applied and environmental microbiology*, 83(13), pp. e00080-17. doi: 10.1128/AEM.00080-17.

Lam, J. *et al.* (1980) 'Production of mucoid microcolonies by *Pseudomonas aeruginosa* within infected lungs in cystic fibrosis', *Infection and Immunity*, 28(2), pp. 546–556.

Leaper, D., Assadian, O. and Edmiston, C. E. (2015) 'Approach to chronic wound infections', *British Journal of Dermatology*, 173(2), pp. 351–358. doi: 10.1111/bjd.13677.

Lee, J. *et al.* (2013) 'A cell-cell communication signal integrates quorum sensing and stress response', *Nature Chemical Biology*, 9(5), pp. 339–343. doi: 10.1038/nchembio.1225.

Lee, J. and Zhang, L. (2014) 'The hierarchy quorum sensing network in *Pseudomonas aeruginosa*', *Protein and Cell*, 6(1), pp. 26–41. doi: 10.1007/s13238-014-0100-x.

Liebler, D. C. and Guengerich, F. P. (2005) 'Elucidating Mechanisms of Drug-Induced Toxicity', *Nature Reviews Drug Discovery*, 4(May), pp. 410–420. doi: 10.1038/nrd1720.

Limoli, D. H., Jones, C. J. and Wozniak, D. J. (2015) 'Bacterial Extracellular Polysaccharides in Biofilm Formation and Function', *Microbiology Spectrum*, 3(3). doi: 10.1128/microbiolspec.MB-0011-2014.

Lin, Y. H. *et al.* (2003) 'Acyl-homoserine lactone acylase from Ralstonia strain XJ12B represents a novel and potent class of quorum-quenching enzymes', *Molecular Microbiology*, 47(3), pp. 849–860. doi: 10.1046/j.1365-2958.2003.03351.x.

Maeda, T. *et al.* (2012) 'Quorum quenching quandary: resistance to antivirulence compounds', *The ISME Journal*, 6(3), pp. 493–501. doi: 10.1038/ismej.2011.122.

Malone, M. *et al.* (2017) 'The prevalence of biofilms in chronic wounds: a systematic review and meta-analysis of published data.', *Journal of wound care*, 26(1), pp. 20–25. doi: 10.12968/jowc.2017.26.1.20.

McKnight, S. L., Iglewski, B. H. and Pesci, E. C. (2000) 'The Pseudomonas quinolone signal regulates rhl quorum sensing in *Pseudomonas aeruginosa*.', *Journal of bacteriology*, 182(10), pp. 2702–8.

Morohoshi, T. *et al.* (2007) 'Inhibition of quorum sensing in Serratia marcescens AS-1 by synthetic analogs of N-acylhomoserine lactone', *Applied and Environmental Microbiology*, 73(20), pp. 6339–6344. doi: 10.1128/AEM.00593-07.

Mukherjee, S. *et al.* (2018) 'The PqsE and RhlR proteins are an autoinducer synthase–receptor pair that control virulence and biofilm development in *Pseudomonas aeruginosa*', *Proceedings of the National Academy of Sciences*, 115(40), pp. E9411–E9418. doi: 10.1073/pnas.1814023115.

Murray, J. *et al.* (2017) 'Evaluation of bactericidal and anti-biofilm properties of a novel surface-active organosilane biocide against healthcare associated pathogens and *Pseudomonas aeruginosa* biolfilm', *PLOS ONE*, 12(8), p. e0182624. doi: 10.1371/journal.pone.0182624.

Mushin, R. and Ziv, G. (1973) 'An epidemiological study of *Pseudomonas aeruginosa* in cattle and other animals by pyocine typing.', *The Journal of hygiene*, 71(1), pp. 113–22.

Nakano, K. *et al.* (2015) 'First complete genome sequence of *Pseudomonas aeruginosa* (Schroeter 1872) Migula 1900 (DSM 50071T), determined using PacBio single-molecule real-time technology', *Genome Announcements*, 3(4). doi:

10.1128/genomeA.00932-15.

Nealson, K. H., Platt, T. and Hastings, J. W. (1970) 'Cellular control of the synthesis and activity of the bacterial luminescent system.', *Journal of bacteriology*, 104(1), pp. 313–22.

Ng, W.-L. and Bassler, B. L. (2009) 'Bacterial Quorum-Sensing Network Architectures', *Annual review of genetics*, 43, p. 197. doi: 10.1146/ANNUREV-GENET-102108-134304.

NNIS (2004) 'National Nosocomial Infections Surveillance (NNIS) System Report, data summary from January 1992 through June 2004, issued October 2004', *American Journal of Infection Control*, 32(8), pp. 470–485. doi: 10.1016/J.AJIC.2004.10.001.

de Nys, R. *et al.* (1993) 'New halogenated furanones from the marine alga delisea pulchra (cf. fimbriata)', *Tetrahedron*, 49(48), pp. 11213–11220. doi: 10.1016/S0040-4020(01)81808-1.

O'Toole, G. A. (2011) 'Microtiter dish biofilm formation assay.', *Journal of visualized experiments : JoVE*, (47). doi: 10.3791/2437.

Oh, D. H. and Marshall, D. L. (1992) 'Effect of pH on the minimum inhibitory concentration of monolaurin against *Listeria monocytogenes*', *Journal of Food Protection*, 55(6), pp. 449–450. doi: 10.4315/0362-028x-55.6.449.

Pan, J. *et al.* (2012) 'Reverting Antibiotic Tolerance of *Pseudomonas aeruginosa* PAO1 Persister Cells by (Z)-4-bromo-5-(bromomethylene)-3-methylfuran-2(5H)-one', *PLoS ONE*, 7(9), p. e45778. doi: 10.1371/journal.pone.0045778.

Pandit, S. *et al.* (2017) 'Low Concentrations of Vitamin C Reduce the Synthesis of

Extracellular Polymers and Destabilize Bacterial Biofilms', *Frontiers in Microbiology*, 8(DEC), p. 2599. doi: 10.3389/fmicb.2017.02599.

Park, H. Y. *et al.* (1998) 'Effect of pH on drug release from polysaccharide tablets', *Drug Delivery: Journal of Delivery and Targeting of Therapeutic Agents*, 5(1), pp. 13–18. doi: 10.3109/10717549809052022.

Pearson, J. P., Pesci, E. C. and Iglewski, B. H. (1997) 'Roles of *Pseudomonas aeruginosa* las and rhl quorum-sensing systems in control of elastase and rhamnolipid biosynthesis genes.', *Journal of bacteriology*, 179(18), pp. 5756–67.

Pesci, E. C. *et al.* (1997) 'Regulation of las and rhl quorum sensing in *Pseudomonas aeruginosa*.', *Journal of bacteriology*, 179(10), pp. 3127–32.

Pessi, G. and Haas, D. (2000) 'Transcriptional control of the hydrogen cyanide biosynthetic genes hcnABC by the anaerobic regulator ANR and the quorum-sensing regulators LasR and RhlR in *Pseudomonas aeruginosa*.', *Journal of bacteriology*, 182(24), pp. 6940–9.

Phainuphong, P. *et al.* (2017) 'γ-Butenolide and furanone derivatives from the soil-derived fungus Aspergillus sclerotiorum PSU-RSPG178', *Phytochemistry*. Pergamon, 137, pp. 165–173. doi: 10.1016/J.PHYTOCHEM.2017.02.008.

Proctor, C. R., McCarron, P. A. and Ternan, N. G. (2020) 'Furanone quorum-sensing inhibitors with potential as novel therapeutics against *Pseudomonas aeruginosa*', *Journal of Medical Microbiology*, p. jmm001144. doi: 10.1099/jmm.0.001144.

Pseudomonas.com (2020a) *Overview: mexR, Pseudomonas aeruginosa PAO1*. Available at: http://www.pseudomonas.com/feature/show?id=103585 (Accessed: 5

May 2020).

Pseudomonas.com (2020b) *Overview: nalC, Pseudomonas aeruginosa PAO1*. Available at: http://www.pseudomonas.com/feature/show/?id=110260&view=overview (Accessed: 5 May 2020).

Ramli, N. S. K. *et al.* (2012) 'The effect of environmental conditions on biofilm formation of *Burkholderia pseudomallei* clinical csolates', *PLoS ONE*, 7(9), p. e44104. doi: 10.1371/journal.pone.0044104.

Rasamiravaka, T. *et al.* (2015) 'The Formation of Biofilms by *Pseudomonas aeruginosa* : A Review of the Natural and Synthetic Compounds Interfering with Control Mechanisms', *BioMed Research International*, 2015, pp. 1–17. doi: 10.1155/2015/759348.

Ren, D. *et al.* (2001) 'Inhibition of biofilm formation and swarming of *Escherichia coli* by (5Z) -4-bromo-5- (bromomethylene) -3- butyl-2 (5H) -furanone.', *Environmental microbiology*, 3, pp. 731–736. doi: 10.1039/c0np00043d.

Rodin, J. O. *et al.* (1965) 'Volatile Flavor and Aroma Components of Pineapple. l. Isolation and Tentative Identification of 2,5-Dimethyl-4-Hydroxy-3(2H)-Furanone', *Journal of Food Science*, 30(2), pp. 280–285. doi: 10.1111/j.1365-2621.1965.tb00302.x.

Sanz, M. *et al.* (2017) 'Role of microbial biofilms in the maintenance of oral health and in the development of dental caries and periodontal diseases. Consensus report of group 1 of the Joint EFP/ORCA workshop on the boundaries between caries and periodontal disease', *Journal of Clinical Periodontology*, 44, pp. S5–S11. doi:

10.1111/jcpe.12682.

Sauer, K. *et al.* (2004) 'Characterization of nutrient-induced dispersion in *Pseudomonas aeruginosa* PAO1 biofilm', *Journal of Bacteriology*, 186(21), pp. 7312–7326. doi: 10.1128/JB.186.21.7312-7326.2004.

Schmidt, J. *et al.* (2011) 'The *Pseudomonas aeruginosa* chemotaxis methyltransferase CheR1 impacts on bacterial surface sampling', *PLoS ONE*, 6(3). doi: 10.1371/journal.pone.0018184.

Schultz, G. *et al.* (2017) 'Consensus guidelines for the identification and treatment of biofilms in chronic nonhealing wounds', *Wound Repair and Regeneration*, 25(5). doi: 10.1111/wrr.12590.

Serra, R. *et al.* (2015) 'Chronic wound infections: the role of *Pseudomonas aeruginosa* and *Staphylococcus aureus*', *Expert Review of Anti-infective Therapy*, 13(5), pp. 605–613. doi: 10.1586/14787210.2015.1023291.

Singh, P. K. *et al.* (2000) 'Quorum-sensing signals indicate that cystic fibrosis lungs are infected with bacterial biofilms', *Nature*, 407(6805), pp. 762–764. doi: 10.1038/35037627.

Slaughter, J. C. (1999) 'The naturally occurring furanones: Formation and function from pheromone to food', *Biological Reviews*, 74(3), pp. 259–276. doi: 10.1111/j.1469-185X.1999.tb00187.x.

Sung, W. S. *et al.* (2007) '2,5-dimethyl-4-hydroxy-3(2H)-furanone (DMHF); antimicrobial compound with cell cycle arrest in nosocomial pathogens', *Life Sciences*, 80(6), pp. 586–591. doi: 10.1016/j.lfs.2006.10.008.

Tanabe, Y. and Ohno, N. (1988) ‘A Novel and Efficient Synthesis of 2(5H)-Furanone Derivatives’, *Journal of Organic Chemisty*, 53, pp. 1560–1563.

Toder, D. S., Gambello, M. J. and Iglewski, B. H. (1991) ‘*Pseudomonas aeruginosa* LasA: a second elastase under the transcriptional control of lasR.’, *Molecular microbiology*, 5(8), pp. 2003–10.

Trautner, B. W. and Darouiche, R. O. (2004) ‘Role of biofilm in catheter-associated urinary tract infection’, *American Journal of Infection Control*, pp. 177–183. doi: 10.1016/j.ajic.2003.08.005.

Wade, D. S. *et al.* (2005) ‘Regulation of Pseudomonas quinolone signal synthesis in *Pseudomonas aeruginosa*.’, *Journal of bacteriology*, 187(13), pp. 4372–80. doi: 10.1128/JB.187.13.4372-4380.2005.

Waite, R. D. *et al.* (2005) ‘Transcriptome analysis of *Pseudomonas aeruginosa* growth: Comparison of gene expression in planktonic cultures and developing and mature biofilms’, *Journal of Bacteriology*, 187(18), pp. 6571–6576. doi: 10.1128/JB.187.18.6571-6576.2005.

Waite, R. D. *et al.* (2006) ‘Clustering of *Pseudomonas aeruginosa* transcriptomes from planktonic cultures, developing and mature biofilms reveals distinct expression profiles’, *BMC Genomics*, 7(1), p. 162. doi: 10.1186/1471-2164-7-162.

Wang, Y. and Ho, C. T. (2008) ‘Formation of 2,5-dimethyl-4-hydroxy-3(2H)-furanone through methylglyoxal: A maillard reaction intermediate’, *Journal of Agricultural and Food Chemistry*, 56(16), pp. 7405–7409. doi: 10.1021/jf8012025.

Welsh, M. A. *et al.* (2015) ‘Small molecule disruption of quorum sensing cross-

regulation in *Pseudomonas aeruginosa* causes major and unexpected alterations to virulence phenotypes.', *Journal of the American Chemical Society*. NIH Public Access, 137(4), pp. 1510–9. doi: 10.1021/ja5110798.

Wolcott, R. D., Rhoads, D. D. and Dowd, S. E. (2008) 'Biofilms and chronic wound inflammation.', *Journal of wound care*, 17(8), pp. 333–41. doi: 10.12968/jowc.2008.17.8.30796.

Wu, H. *et al.* (2004) 'Synthetic furanones inhibit quorum-sensing and enhance bacterial clearance in *Pseudomonas aeruginosa* lung infection in mice', *Journal of Antimicrobial Chemotherapy*, 53(6), pp. 1054–1061. doi: 10.1093/jac/dkh223.

Xu, Y., Howard, L. and Xie, D. (2016) 'A dental cement containing 4-hydroxy-2,5-dimethyl-3(2H)-furanone for enhanced antibacterial activity', *Oral Health and Care*, 1(1). doi: 10.15761/ohc.1000104.

Yu, W., Hallinen, K. M. and Wood, K. B. (2018) 'Interplay between antibiotic efficacy and drug-induced lysis underlies enhanced biofilm formation at subinhibitory drug concentrations', *Antimicrobial Agents and Chemotherapy*, 62(1), pp. 1–13. doi: 10.1128/AAC.01603-17.

Zhao, G. *et al.* (2013) 'Biofilms and Inflammation in Chronic Wounds', *Advances in Wound Care*, 2(7), pp. 389–399. doi: 10.1089/wound.2012.0381.

Zhou, Y. *et al.* (2018) 'Furanone derivative and sesquiterpene from Antarctic marine-derived fungus Penicillium sp. S-1-18', *Journal of Asian Natural Products Research*. Taylor and Francis Ltd., 20(12), pp. 1108–1115. doi: 10.1080/10286020.2017.1385604.

Chapter 5

Development of a novel in vitro chronic wound biofilm model

5.1 Introduction

A chronic wound is any wound which fails to progress through the normal healing process. This failure can be caused by a wide range of both internal and external factors. For example, the autoimmune disease diabetes mellitus often causes patients to develop chronically non-healing wounds by causing chronic inflammation, local hypoxia, and circulatory dysfunction (Baltzis, Eleftheriadou and Veves, 2014). However, one of the most common causes of chronic wound formation is bacterial colonization, and subsequent formation of a biofilm in the wound environment (Malone *et al.*, 2017). The warm and moist environment of a wound is ideal for the growth of bacteria. *S. aureus* and *P. aeruginosa*, are the two bacterial species which most commonly colonise and form biofilms in wounds (Fazli *et al.*, 2009; Rhoads *et al.*, 2012).

When present in a wound, a bacterial biofilm causes a prolonged state of inflammation. This inflammatory state is maintained long-term and, thus, the host's immune system is unable to progress to the final stages of wound healing. This failure to progress through the normal wound healing process gives rise to a chronic wound (Wolcott, Rhoads and Dowd, 2008).

Due to the significant role that biofilms play in the formation and persistence of chronic wounds, new treatments should always consider addressing biofilm as a priority. However, it is difficult, both logistically and ethically, to study chronic wound biofilms in humans (Grada, Mervis and Falanga, 2018). Due to the complexity of studying biofilms in humans, animal models of wound healing are considered the gold standard for such investigations. However, the development and testing of novel

antibiofilm wound therapies using these models is challenging in itself for a number of reasons.

5.1.1 In vivo *wound models*

There are several common choices of animal when using a wound model. There are rodent models such as mouse and rat, rabbit models, and pig models as well as many others which are less commonly used.

The use of mice is both cost effective and an efficient use of space and facilities. When using mice there are several model options. These include the use of a dorsal wound in transgenic, leptin deficient Db/Db, mice which are designed to model the impaired wound healing seen in diabetes (Beer, Longaker and Werner, 1997). However, the loose skin and striated subcutaneous muscle layer found in mice means such models are not truly representative. Wound healing in dorsally wounded animals occurs primarily through tissue contraction rather than the growth of new tissue as is the case in humans (Grada, Mervis and Falanga, 2018). While rats may be used as an alternative to mice, the similar dorsal skin and muscle structure presents the same issues. Another limitation of using mice and rats for the study of wound healing is the wound healing time. Wounds in mice and rats have been shown to heal much more rapidly than human wounds and are, therefore, not truly representative. To circumvent this, a mouse tail vein model was developed. (Falanga *et al.*, 2004). This model used a scalpel to produce wounds on the dorsal aspect of the tail of the mouse. These wounds were shown to require up to twenty-five days to fully heal making them more representative of a chronic wound healing time frame. However, despite this, this model does not appear to have been widely adopted in the literature to study wound infection.

Unfortunately, the differences in the wound healing mechanism and time are not the only barrier to using an animal model in wound biofilm studies. Other issues include the method of wound infliction. When initiating a wound in an animal, processes such as surgical wounding, friction or sanding and punch biopsies are all commonly used (Ermolaeva *et al.*, 2011; Gurjala *et al.*, 2011; Asada *et al.*, 2012; Petreaca *et al.*, 2012; Roche *et al.*, 2012; Thompson *et al.*, 2014; Watters *et al.*, 2014). While these methods allow researchers to induce reproducible wounds, they often leave the wound poorly representative of the conditions present in a chronic wound. This makes the translation of the findings to chronic wounds in humans difficult (Brackman and Coenye, 2016; Trøstrup *et al.*, 2016). Furthermore, the maintenance of both the biofilm and the wound itself for a chronic timeframe in such models is often highly challenging, further limiting their relevance to real-world clinical scenarios.

5.1.2* In vitro *wound models

In order to address these issues and establish a biofilm with a high degree of similarity to a real-world scenario, many researchers opt to use an *in vitro* wound biofilm model. There are numerous *in vitro* wound models described in the literature, each with a range of different characteristics designed to mimic the chronic wound environment so that representative biofilms can be grown. However, as with the *in vivo* models, each *in vitro* model has both strengths and weaknesses.

5.1.2.1 The Lubbock chronic wound model

The most well-known and widely used *in vitro* chronic wound model is the Lubbock Chronic Wound Model. This wound model, first reported by Sun *et al*. in 2008, most commonly uses a plastic pipette tip ejected into a liquid growth medium to act as the wound bed. While a pipette tip does indeed provide a good substrate for the formation of a biofilm it is poorly representative of a biotic surface, such as a wound bed.

Furthermore, the growth medium used in the Lubbock model consists of Bolton Broth with 50% bovine plasma and 5% laked horse blood. As Bolton Broth is a chopped meat based medium it was chosen made to mimic the excess of cellular debris and extracellular media components that would be found in the chronic wound environment (Sun *et al.*, 2008). While the presence of these components does help to mimic the nutrient profile of a wound environment, it is not a perfect representation as any standard bacterial growth medium will be rich in vitamins and minerals which may not be present in a wound environment. Subsequent models, which will be discussed here, attempt to rectify this through the use of a wound-like growth medium.

5.1.2.2 The collagen matrix model

This model, developed by Werthén *et al*. in 2010, replaced the Bolton broth with a simulated wound fluid solution consisting of 50% physiological saline and 50% foetal calf serum. Alternatively, they also suggest a mix of 50% TSB and 50% simulated wound fluid (Werthén *et al.*, 2010). The use of saline and calf serum does appear to be more representative of a wound environment, but this simulated wound fluid is likely lacking components, such as blood and other salts, that are be present in a wound environment. The use of TSB presents the same problems as the use of Bolton broth in the Lubbock model in that there are likely several nutrients what would be present in a wound that are not present in this simulated wound fluid. In this model, the authors grew biofilms on matrices consisting of rat tail collagen and simulated wound fluid. Although this model is good representation of the wound environment, its main disadvantage is the high cost of the materials such as rat tail collagen. For many researchers aiming to characterise novel antibiofilm compounds or to test the efficacy of novel delivery drug mechanisms, the potential cost of high throughput testing, in which large volumes of wound fluid or wound bed is required, may be prohibitive.

5.1.1.3 Poloxamer hydrogel model

Another, similar, wound model which has been proposed includes the use of a poloxamer hydrogel matrix hydrated with Mueller-Hinton broth as a growth substrate. The authors state that the use of this gel cause the organisms to display a more clinically relevant biofilm phenotype which allows for an accurate representation of a wound infection (Percival, Bowler and Dolman, 2007). The authors show that both antibiotic sensitive and antibiotic resistant strains grown on the poloxamer gel (*P. aeruginosa, C. albicans, Klebsiella pneumoniae, E. faecalis, E.coli*, and *S. aureus*) displayed a higher resistance to silver containing dressings when compared to organisms grown directly on Mueller-Hinton agar. While this model shows that the nutrient source and growth substrate used during an experiment may affect the response of an organism to a wound treatment, the model has the same limitations the previous two models considered above. Furthermore, the use of Mueller-Hinton broth as the nutrient source is not representative of a chronic wound environment.

5.1.2.4 Cellulose agar model

A model developed by Hammond *et al.* (2011) used cellulose discs as a growth substrate for biofilm growth (Hammond *et al.*, 2011). As with the previous models this approach used a standard bacteriological growth medium as the nutrient source. In this case, standard lysogeny broth (LB) agar was used. This work showed that number of viable cells in biofilms grown in this model were effectively reduced through treatment with either a single antibiotic ointment (containing 0.1% gentamicin sulphate or 2% mupirocin) or an ointment containing an antibiotic combination. The use of the cellulose discs allowed for the simple collection and quantification of the treated and control biofilms. This also allowed for the visualisation of the biofilms using a fluorescent stain. These are useful attributes for a wound model to have.

Despite this, the use of a standard nutrient medium is, again, limiting to the relevance of the results.

5.1.2.5 Artificial wound bed model

Finally, a wound model consisting of an artificial wound bed was developed by Kucera *et al.* in 2014 for the testing of antimicrobial wound dressings. This model adapted the Lubbock model discussed above for use in the production of an artificial wound bed. The model involved the growth of a biofilm on a plastic pipette tip as per the Lubbock model. The artificial wound bed was prepared by pouring a thin layer of wound-like agar (Bolton broth with 1.0% w/v gelatin and 1.2% w/v agar) into the bottom of a petri dish. Once set a sterile magnetic stir bar was placed on the surface of the agar and a second layer of agar was poured on top of the first. Once this layer was set, the stir bar was removed aseptically leaving an artificial wound-like void in the agar. Pre-formed biofilms were then placed into the formed artificial wound bed (Kucera *et al.*, 2014). It is unclear whether the biofilm was somehow removed from the pipette tip or if the pipette tip itself was placed in the wound bed to inoculate. This model has the same limitation as all other models discussed here as it uses a non-representative nutrient source.

It is clear that while there are many *in vitro* models of chronic wound biofilms they have a common set of problems including the use of a growth substrate which is poorly representative of a wound bed or use of a growth medium which is poorly representative of a chronic wound nutrient profile. (Percival, Bowler and Dolman, 2007; Thorn and Greenman, 2009; Kostenko *et al.*, 2010; Lipp *et al.*, 2010; Hammond *et al.*, 2011; Ngo, Vickery and Deva, 2012). It is, therefore, the aim of this chapter to develop a novel, low cost, wound biofilm assay consisting of a simulated soft wound

bed with a nutrient profile that is representative of a mammalian wound environment for the assessment of novel antimicrobial and antibiofilm compounds and the *in vitro* testing of novel drug delivery mechanisms.

5.2 Aims and objectives

The aim of this chapter is to develop a novel, representative, *in vitro* chronic wound model. Firstly, a suitable growth substrate on which to grow biofilms will be identified. An appropriate method of quantifying the biofilms will then be chosen. Several methods will be assessed including crystal violet staining, fluorescent staining of the biofilm matrix, live/dead fluorescent staining of the biofilm bound cells, and direct enumeration of viable cells per biofilm. A suitable nutrient source will then be identified for the growth of representative chronic wound biofilms. Finally, the developed wound model will be used to assess the efficacy of commonly used clinical wound dressings and then used to assess the effect of furanone-loaded aerogel on biofilm formation in chronic wounds.

5.3 Materials and Methods

5.3.1 Materials and equipment

All chemicals and reagents used in the work detailed here were purchased from Sigma Aldrich (Poole, UK) and used without further modification or purification unless otherwise stated.

Porcine muscle was purchased from a local butcher to ensure no additional water or preservatives had been added prior to use in the wound model.

Clinically relevant wound dressings were purchased from Medisave.

5.3.2 Identification of a suitable growth substrate and wound-like nutrient source

To develop a novel wound model an appropriate growth surface was identified. In parallel, a range of wound-like nutrient sources were developed and tested.

5.3.2.1 Preparation of simulated body fluid and body fluid agar

To prepare simulated body fluid (SBF), which is chemically similar to human serum, the method detailed by Huang *et al.* (2013) was used. This protocol was adapted to produce a 5 times concentrated stock solution (Huang *et al.*, 2013). To prepare the concentrated body fluid a solution of 0.68 M sodium chloride, 27 mM potassium chloride, 1.25 mM sodium phosphate dibasic, 2.2 mM potassium phosphate dibasic trihydrate, 6.5 mM calcium chloride, 5 mM magnesium sulphate, 21 mM sodium bicarbonate, and 27.5 mM glucose was prepare in deionised water. The concentrations and masses of each component used are shown in Table 5.1. This solution was sterilised as required by passing through a 0.2 μm syringe filter. The use of autoclaving resulted in the caramelisation and browning of the sugars which may have added variability between batches of the simulated wound fluid.

Table 5.1 – Concentrations and masses of each component used to prepare simulated wound fluid for both the 5x concentrated stock solution and the 1x working solution.

Component	Molar Concentration (5x)	g L^{-1} (5x)	Molar Concentration (1x)	g L^{-1} (1x)
Sodium chloride	0.685 mM	40	0.137 mM	8.0063
Potassium chloride	27 mM	2.1	5.4 mM	0.402
Sodium phosphate dibasic	1.25 mM	0.175	0.25 mM	0.085
potassium phosphate dibasic	2.2 mM	0.295	0.44 mM	0.059
Calcium chloride	6.5 mM	0.57	1.3 mM	0.114
Magnesium sulphate	5 mM	0.6	1 mM	0.12
Sodium bicarbonate	21 mM	1.76	4.2 mM	0.352
Glucose	27.5 mM	4.95	5.5 mM	0.99

To prepare simulated body fluid agar with blood the protocol described above was followed with the following amendment. A solution of 6 g of technical agar in 375 mL of deionised water (1.6% w/v) was prepared and sterilised by autoclaving. Once cool, 100 mL of sterile simulated body fluid and 25 mL of laked horse blood (Oxoid, UK) were added (final conc. 5% v/v of laked blood). Plates were poured and sterility was confirmed by incubating an uninnoculated plate for 24 hours at 37°C. Absence of visible growth was used as an indication of sterility.

5.3.2.2 Growth of biofilms on artificial growth surfaces

Biofilms were grown on a range of semi-permeable membranes to assess their suitability as a biofilm growth substrate. Polycarbonate, nylon and nitrocellulose membranes were assessed. Nylon and nitrocellulose membranes were prepared by cutting 13 mm discs of membrane from large sheets of each membrane. To ensure discs were reproducible, a 13 mm paper punch tool was used. Polycarbonate membranes were purchased as pre-prepared 13 mm discs (Merck Millipore, UK). To sterilise, membranes were placed in 70% ethanol for 15 minutes then placed in a sterile

dish in a laminar flow hood to dry. The use of a laminar flow hood ensured that sterility was maintained. Samples were then stored in the sterile drying dish until required.

To grow biofilms on the membranes, standard nutrient agar, simulated body fluid agar, and simulated body fluid agar with blood were prepared as detailed previously. Membranes were then placed on the surface of the nutrient media using sterile forceps. Membranes were gently pressed down to ensure that total contact between the membrane and the medium was achieved.

The biofilm inoculum was prepared by making a 1:100 dilution of a stationary phase, overnight, culture of PAO1 DSM50071 in fresh TSB as detailed in chapter 4. To each membrane, a 5 μL volume of the 1:100 dilution was added. Plates were left partially uncovered in a laminar flow hood for 10 minutes for the inoculum to dry. Once the inoculum was dry the plates were covered and incubated at 37 °C for 18 hours. Once incubated, biofilms were imaged using a Canon EOS 500D digital camera.

5.3.2.3 Preparation of a novel semi synthetic wound bed medium

A semi synthetic wound medium was produced using porcine myocyte lysate (PML), simulated wound fluid, bovine serum albumin (BSA) and laked horse blood. To produce the myocyte lysate, 100 g of porcine muscle tissue was processed in a commercial food processor with 150 g of deionised water for 3 minutes or until a homogenous mixture was formed. The mixture was then centrifuged at 13,000 rpm for 5 minutes and the supernatant was decanted and collected. The solid material, consisting of skin and connective tissue, was discarded. The collected supernatant was then gravity filtered through filter paper to remove any remaining solid material. The filtered liquid was then split into 10 mL aliquots and stored at -30 °C until required.

To prepare the wound bed medium, first a 5% solution of technical agar in deionised water was prepared and sterilised by autoclaving. The PML solution was then thawed at room temperature. Once totally thawed BSA was added to a final concentration of 56 mg mL^{-1} and the mixture was placed on a rocker at room temperature until all BSA was dissolved. Once no visible BSA aggregates remained the PML/BSA solution was sterilised using a 0.2 μm syringe filter. A 100 μL volume of the filtered PML/BSA solution was streaked on nutrient agar and incubated at 37 °C for 18 hours to confirm sterility. This solution was then pre-warmed to 40 °C in a water bath. It should be noted that warming should not exceed 40 °C as this caused denaturation of the BSA and other proteins in the solution. However, warming was necessary to prevent gelling agents from setting rapidly on addition to the mixture. Once warm, the wound bed medium was prepared by adding 30 mL of warm PML/BSA solution, 10 mL of concentrated simulated body fluid stock solution, 7.5 mL of molten 5% agar solution and, 2.5 mL of laked horse blood to a falcon tube. The percentage concentrations of each component are shown in Table 5.2. The tube was inverted several times to ensure total mixing. While the medium was still liquid 1 mL volumes were pipetted into the wells of a 12 well tissue culture plate. These plates were stored at 4 °C for 18 hours to allow for the complete gelation of the medium. The final wound medium contained appropriate (i.e. x1) concentrations of all simulated body fluid components.

Table 5.2 – Components of simulated wound medium and their percentage concentrations.

Component	Percentage concentration
Porcine myocyte lysate/bovine serum albumin	60%
5x simulated body fluid	20%
5% technical agar	15%
laked horse blood	5%

5.2.3.4 Growth of biofilm on simulated wound bed medium

To grow biofilms using the simulated wound bed medium as a nutrient source, plates were prepared as described above and 13 mm discs of each membrane were added to the surface of the medium and inoculated as detailed in section 5.3.2.2. Plates were then incubated at 37 °C for 18 hours. Biofilms were imaged using a Canon EOS 500 digital camera.

5.3.3 Methods of biofilm quantification

Several methods of quantifying the biofilm grown on each membrane type were tested. These methods included fluorescent staining of the biofilm matrix proteins, crystal violet staining of the total biofilm biomass, live/dead staining of the biofilm bound cells and direct enumeration of viable cells in the biofilm.

5.3.3.1 Fluorescent staining of biofilm matrix proteins

To stain the biofilm matrix proteins, it was decided that the protein stain SYPRO ruby would be used and stained biofilms would be resuspended. The SYPRO ruby would then be quantified in the solution. As this stain has never been used to quantify resuspended biofilms the accuracy of quantifying SYPRO ruby in suspension was tested.

A calibration curve of SYPRO ruby was prepared by making an 80 μL mL^{-1} solution of SYPRO ruby in deionised water. This solution was tested for fluorescence using a Varian fluorimeter (California, USA) set with an excitation wavelength of 450 nm and an emission wavelength of 610 nm. Doubling dilutions of this 80μL mL^{-1} stock solution were prepared in deionised water and each dilution was tested as described. Measurements were made in triplicate. The calibration curve was plotted as concentration of SYPRO Ruby against fluorescence (in arbitrary units).

To assess the accuracy of quantifying SYPRO Ruby in aqueous solution, three test samples were prepared. These solutions corresponded to a high concentration of SYPRO Ruby (25 μL mL^{-1}), a moderate concentration (15 μL ml^{-1}) and a low concentration (5 μL mL^{-1}). These samples were then analysed using the fluorimeter as described previously. The fluorescence reading obtained was used to calculate the measured concentration of SYPRO ruby in the test samples. The percentage error was then calculated.

5.3.3.2 Staining of the total biofilm biomass

To stain the total biofilm biomass the crystal violet method of O'Toole and Koulter was adapted for use with membrane bound biofilm. Briefly, biofilms were grown on membranes using nutrient agar as a medium as detailed in section 5.3.2.2. After incubation, membranes were removed from the surface of the medium and any unbound cells were removed by gently submerging the membrane and biofilm in sterile deionised water taking care not to disrupt the biofilm. Membranes were then allowed to air dry for 10 minutes in a fresh 12 well plate. Once dry the membranes were covered with 2 mL of 0.1% crystal violet solution to ensure the membrane is completely covered. Crystal violet was added to the well by slowly pipetting down the inner was of the well so as not to disrupt the biofilm. Membranes were incubated in the crystal violet for 10 minutes at room temperature on a plate rocker. Once fully stained membranes were removed from the crystal violet and rinsed of any excess stain by gently submerging the membrane in deionised water 3 times. The membranes were then allowed to air dry in a fresh 12 well plate for 10 minutes. Once dry, 2 mL of 30% acetic acid in deionised water was added to each well to destain the biofilm. Membranes were destained for 10 minutes at room temperature on a plate rocker. Once membranes were destained, 100 μL of the resolubilised crystal violet in 30% acetic

acid was transferred to a 96 well plate and diluted in fresh destain solution as required. Absorbance of the resolubilised crystal violet was measured at 450 nm using a Fluostar Omega plate reader (BMG Labtech, Aylesbury, UK). Uninnoculated membranes were used as a control. A sample of 30% acetic acid in deionised water was used as a blank. Each membrane type was tested in triplicate using three biological replicates.

5.3.3.3 Live/dead staining of biofilm bound bacterial cells

To stain biofilm bound bacteria based on cellular viability BacLight Live/Dead fluorescent stain was used. Biofilms were grown as detailed in section 5.3.2.2. A working solution of BacLight reagent was prepared as per section 4.3.8.1. Once biofilms had formed, membranes were removed from the surface of the agar any remaining unbound cells were rinsed off by gently submerging the membrane in sterile deionised water 3 times. Membranes were placed in a fresh 12 well plate and allowed to dry for 10 minutes in a laminar flow hood to maintain sterility. A 100 μL volume of BacLight working reagent was pipetted on to the biofilm ensuring the whole biofilm was covered in the staining solution. BacLight reagent was added slowly to the surface of the biofilm so as not to disrupt it. The 12 well plates were then covered with aluminium foil, to protect them from light, and were incubated at room temperature for 30 minutes. After 30 minutes of staining membranes were rinsed of excess BacLight reagent by gently submerging in sterile deionised water 3 times. Membranes were placed on a microscope slide and allowed to air dry in a laminar flow hood in the dark for 10 minutes. Biofilms were then imaged as per section 4.3.8.3.

5.3.3.4 Direct enumeration of viable biofilm bound cells

Biofilms were grown on all membrane types using nutrient agar as a medium as detailed previously. After incubation membranes were removed from the medium and unbound cells were removed by gently submerging the membranes in sterile deionised

water 3 times. Membranes were then placed in 10 mL of sterile PBS (pH 7.4) and biofilms were resuspended by mechanical agitation with a sterile inoculation loop for 15 s followed by three separate 10 s sets of vortexing to resuspend any aggregates. Once biofilms were resuspended and no aggregates were visible a 100 µL sample of the resuspended biofilm was serially diluted to 10^{-15}. Each of the dilutions were then streaked on nutrient agar. Inoculated plates were allowed to dry in a laminar flow hood for 10 minutes and were then incubated at 37 °C for 16-18 hours. Visible colonies on the nutrient agar plates were counted and the cells per biofilm were calculated using the equation:

$$CFU_{BF} = CC \times DF \qquad \text{Equation 4}$$

Where CFU_{BF} is the colony forming units per biofilm, CC is the colonies counted on the nutrient agar plate and DF is the dilution factor. Each membrane type was tested in triplicate using three biological replicates.

5.3.4 Assessment of biofilm growth kinetics on novel wound model

The biofilm formation kinetics of PAO1 DSM50071 were assessed on both nutrient agar and on the developed simulated wound medium. To assess growth kinetics plates were prepared and inoculated using polycarbonate membranes and either nutrient agar or simulated wound medium as the nutrient source. Plates were prepared by pipetting 1 mL of molten nutrient agar or simulated wound bed medium into the wells of a 12 well plate and storing at 4 °C overnight to allow for complete gelation of the medium. Polycarbonate membranes were sterilised in 70% ethanol and allowed to dry. Once dry, membranes were placed on the surface of the medium and inoculated. Once inoculated, biofilms were grown for 10 hours at 37 °C. Biofilms were sacrificed every 2 hours and viable cells were enumerated as described previously. Data was plotted as

CFU per biofilm over time. Experiments were conducted in triplicate using biological replicates.

5.3.5 Assessment of the antimicrobial efficacy of clinically relevant wound dressings against PAO1 biofilm

To test the developed wound model in assessing the efficacy of wound therapies, the antimicrobial efficacy of four clinically relevant wound dressings was investigated. The wound dressings tested were Aquacel AG, Telfa AMD, Actilite and Inadine. The active ingredients of these dressings were silver, polyhexamethylene biguanide (PHMB), Manuka honey and iodine respectively. Treatment with non-medicated cotton gauze and application of no treatment were used as controls.

Plates were prepared and biofilms grown on polycarbonate membranes as per section 5.3.2.2 with one amendment. After inoculation samples were incubated at 37 °C for 6 hours. This resulted in a reproducible biofilm with approximately 1 x 10^6 viable cells. This cell density was selected as it has been shown that wound healing ceases once an infected wound reached 1 x 10^6 CFU g^{-1} of infected tissue. After 6 hours of incubation plates were removed from the incubator and a 1 cm^2 piece of a wound dressing was placed on the biofilm. The dressing was gently pressed down to ensure good contact between the dressing and the biofilm. The membranes with wound dressings applied were incubated for a further 24 hours at 37 °C. Following the 24 hours incubation with treatments the wound dressings were carefully removed, and the membranes were transferred to 10 mL of sterile PBS (pH 7.4). Biofilms were resuspended, diluted and enumerated. Each wound dressing was assessed in triplicate using biological replicates.

5.3.6 Assessment of a the antibiofilm potential of furanone aerogels

The efficacy of furanone-loaded aerogels against clinically relevant PAO1 biofilms was assessed using the simple wound model described above.

5.3.6.1 Treatment of clinically relevant biofilms with furanone-loaded aerogels using a simple chronic wound biofilm model

Wound bed medium was made, and plates were prepared as described previously in section 5.3.2.3. Polycarbonate membranes were inoculated, and clinically relevant biofilms were grown. Once biofilms were grown either a furanone-loaded aerogel or an unloaded aerogel was added to the surface of the membrane. Aerogels were gently pressed down to ensure good contact with the biofilm and medium. Biofilms were then incubated for a further 24 hours to simulate a standard wound dressing cycle. After further incubation aerogels were removed and biofilms were resuspended, and viable cell numbers obtained.

5.3.6.2 Confirmation of furanone release into wound medium

To confirm the release of furanone into the developed wound medium a 5% technical agar solution was prepared. To prepare the release medium 7.5 mL of sterile 5% agar solution was made up to 50 mL with deionised water and while still molten the agar was pipetted into 12 well plates in 1 mL volumes. This produced a semi solid medium with the same consistency, water content and agar content as the wound medium. Once the agar was set, furanone-loaded aerogels were placed on to the surface of the set agar and plates were incubated at 37 °C for 24 hours. After incubation, the aerogels were removed from the agar plates and the agar was liquefied by adding an additional 2 mL of deionised water and mixing thoroughly. The dissolved agar/furanone solution was then diluted, and the absorbance read over the full range of wavelengths (200 nm to 800 nm) using a Varian Cary 50 UV Spectrophotometer (Varian, California, USA).

The total concentration of released furanone was calculated. The full absorbance spectrum of the released furanone was also assessed to ensure no changes in absorbance spectrum had occurred. Experiments were conducted in triplicate and data were expressed as absorbance (in arbitrary units) at each tested wavelength.

5.3.7 Preparation of a modified semi-solid and liquid system.

Due to limitations in the simple wound model, previously developed, a modified system in which a semi-solid artificial wound bed is kept in contact with a liquid phase beneath it was required. This system would be comprised of a synthetic wound fluid reservoir beneath a semi-solid wound bed held on a stainless-steel mesh platform. This method would allow for greater furanone release into the system.

5.3.7.1 Preparation of stainless-steel wound bed platforms

To prepare the wound bed platforms stainless-steel mesh was cut to 50 mm x 50 mm square pieces. Two opposite edges of the mesh square were folded to a 90° angle to give a platform that was 50 mm x 30 mm x 10 mm (Figure 5.1).

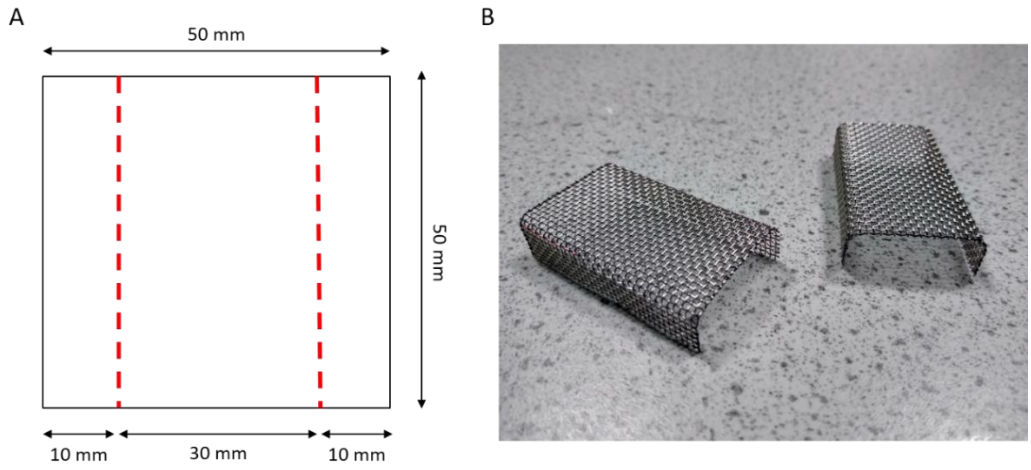

Figure 5.1 – (A) A plan view of the stainless-steel mesh and how it is measured and folded to prepare the wound bed platform. The mesh is folded along the red lines to an angle of 90° (B) The completed stainless-steel wound bed platform to be used in the modified wound model.

5.3.7.2 Preparation of a monolithic semi-solid wound bed

The same procedure as detailed in section 5.3.2.3 was used to prepare the wound bed mixture. The medium was poured into Teflon lined containers (KitchenCraft, Birmingham, UK) measuring 75 mm x 45 mm in 10 mL volumes. These were then stored at 4 °C overnight to allow for complete gelation of the medium. Once the medium was set, the wound beds were carefully removed from the Teflon containers and trimmed to an appropriate size. Once trimmed the wound beds were carefully transferred to the mesh platforms as shown in Figure 5.2 a-b.

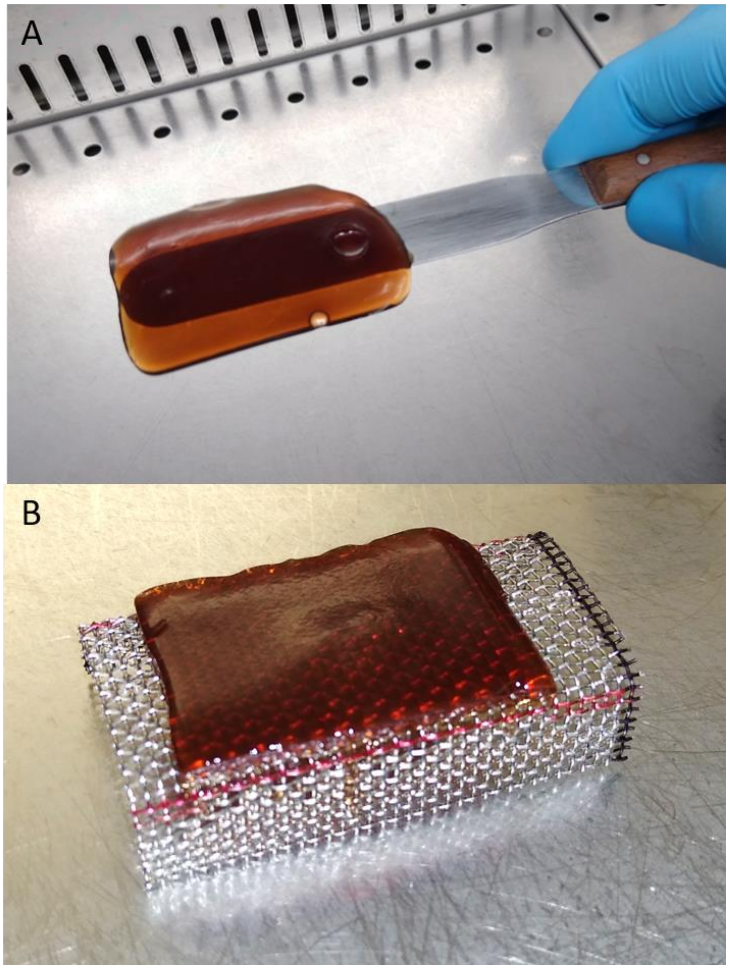

Figure 5.2 – (a) The cast monolithic wound bed was removed from the Teflon lined container using a sterile palette knife. (b) Wound beds were placed on the stainless-steel gel holder and trimmed using the palette knife. During trimming any irregular edges or imperfections (such as bubbles in the gel) can be removed from the wound bed.

5.3.7.3 Setting up the modified wound model system

Once the mesh platform and artificial wound beds were prepared the model was set up as follows. The mesh platforms were first sterilised by autoclaving. Wound beds were prepared and placed on sterile platforms as described above. These were placed in a plastic container (previously sterilised using 70% ethanol). Sterile simulated wound fluid was then added slowly to the container by allowing it to run down the inside of the container. This method of adding the fluid ensured that the delicate wound bed was not damaged or disturbed. A total volume of 20 mL of wound fluid was added to the container. This ensured that the surface of the liquid was in contact with the bottom of the wound bed. Once good contact between the liquid phase and the wound bed was achieved, a sterile polycarbonate membrane was placed on the surface of the wound bed. Membranes were inoculated as detailed in section 5.3.2.2. A cross section of a correctly set up wound model is shown in Figure 5.3 a and a top down image of an inoculated sample is shown in Figure 5.3 b.

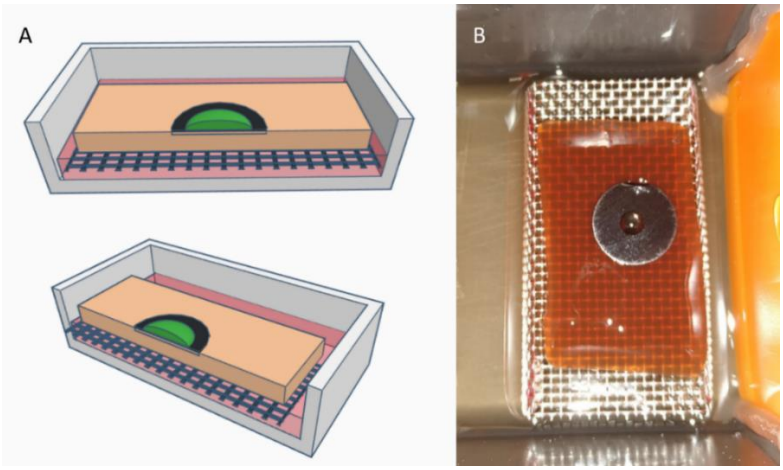

Figure 5.3 –A three-dimensional representation of a functioning modified wound model system and a correctly set up wound bed above a liquid phase

(a)The steel mesh (black) supports the semi solid wound bed (orange) over a reservoir of wound fluid (pink). If complete contact between the underside of the wound bed and the surface of the fluid reservoir is achieved, furanone release from the developed aerogel system will be unimpeded. (b) shows an image of a correctly set up wound bed above a liquid phase and a membrane that has been seeded with 5 µL of inoculum.

5.3.8 Assessment of furanone-loaded aerogels using the modified wound biofilm model

The efficacy of furanone-loaded aerogels for the treatment of wound biofilms was assessed using the developed modified wound bed/liquid model. Prior to treating biofilms with aerogels, the release of furanone into the modified model was investigated.

5.3.8.1 Assessing furanone release into the modified wound model

The release of furanones from the developed aerogel system into the modified wound model was assessed. The wound model was set up as described above with the omission of an inoculum. Furanone-loaded aerogels were placed onto the semi solid wound bed and were incubated at 37 °C temperature for 24 hours. After 24 hours the aerogel and membrane were removed and discarded. The semi solid wound bed was then placed into the fluid reservoir and the mixture was homogenised by vigorous pipetting. This was done so that any furanone that had been released from the aerogel but remained in the wound bed could be quantified along with the furanone in the liquid phase. The wound fluid/wound bed mixture was assessed using UV visible spectroscopy and concentrations of furanone release were calculated. The full absorbance spectrum of the released furanones were also assessed to measure any degradation that may have occurred.

5.3.8.2 Preparation of furanone-loaded aerogels

To prepare furanone-loaded aerogels for use in the developed wound model the previously detailed method was followed with one amendment. When adding furanone to the PVA sol, an excess was added so that the released portion (as determined in section 5.3.8.1) was equivalent to 4 mg for HDMF and 4.325 mg for sotolon. This was calculated using the following equation:

$$F_L = \frac{D_d}{F_r}$$ Equation 5

Where F_L is the amount of furanone to be loaded into the aerogel, D_d is the desired dose to be delivered to the biofilm and F_r is the percentage of total loaded furanone released into the wound medium (determined in 5.3.8.1). PVA sol phases with the adjusted furanone dose were then aliquoted and lyophilised as previously detailed.

5.3.8.3 Assessment of the antibiofilm potential of furanone-loaded aerogels

The efficacy of furanone-loaded aerogels was assessed using the protocol in 5.3.5 with one amendment. Once biofilms had been grown for 6 hours they were removed from the incubator and furanone-loaded aerogels were applied to the membranes ensuring good contact. Membranes treated with aerogels were then incubated for a further 24 hours. After 24 hours of incubation the biofilms were resuspended, diluted and enumerated.

5.3.9 Assessment of clinically relevant wound dressings using the modified wound biofilm model

The modified wound model system was prepared as described above. Membranes were inoculated, and biofilms grown to the clinically relevant density (approximately 10^6 CFU/biofilm). Five clinically relevant wound dressing materials (Sterile gauze, Aquacel Ag, Telfa AMD, Inadine, and Actilite) were trimmed to give 1 cm^2 pieces using sterile scissors in a laminar flow hood to ensure sterility. Sterile, non-woven, gauze was used as a non-medicated control. Once clinically relevant biofilms had been grown, they were removed from the incubator and the pieces of each wound dressing were applied to the surface of the biofilm. Wound dressings were pressed down gently to ensure good contact between the dressing and the biofilm. Biofilms were them returned to the incubator and incubated at 37 °C for a further 24 hours. Following 24

hours of incubation, wound dressings were removed from the biofilms and resuspended. Resuspended biofilms were then diluted and plated to enumerate viable cells as previously detailed.

5.4 Results

A novel *in vitro* chronic wound biofilm model was developed. Suitable growth surfaces and nutrient sources were assessed as well as methods of quantifying the biofilms formed. The model was then used to assess the efficacy of four common, clinically relevant, wound dressings against *P. aeruginosa* PAO1 biofilms. Finally, the model was used to assess the antibiofilm efficacy of the newly developed furanone-loaded aerogels.

5.4.1 Identification of a suitable growth substrate and nutrient source

Suitable growth surfaces and nutrient sources were identified during the development of the wound model as follows.

5.4.1.1 Identification of a suitable growth surface

Various semi permeable membranes were assessed as potential growth surfaces for biofilms. The membranes tested were polycarbonate, nylon and nitrocellulose. To ensure any variation in biofilms was due only to the membrane choice standard nutrient agar was used.

Biofilms formed easily on all membrane types on nutrient agar. Distinct morphological differences were seen between the three membrane types. Biofilms formed on polycarbonate presented as a dense central area of biofilm surrounded with a less dense ring of biomass surrounding it. Biofilms grown on nylon membranes were homogenous in terms of biomass density throughout the whole sample. A distinct beige/yellow colour was seen in samples grown on nylon. Biofilms grown on nitrocellulose were, again, homogenous in terms of biomass density. However, in these samples a clear green/blue colour was observed (Figure 5.4 a-c).

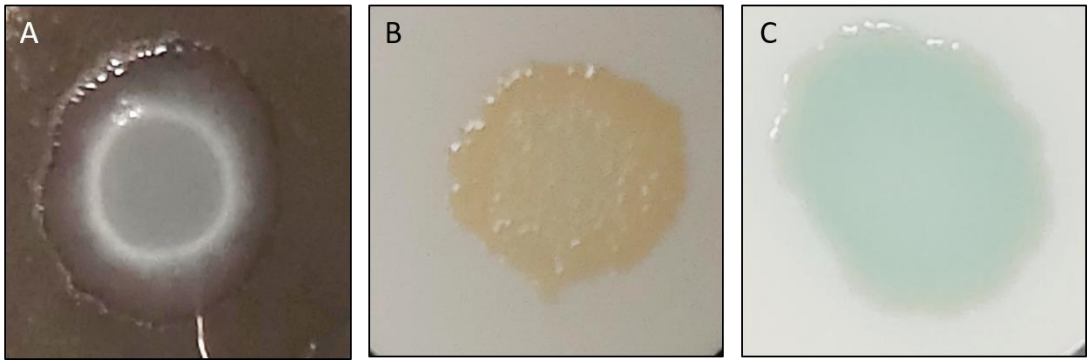

Figure 5.4 – Morphology of biofilms grown on (a) polycarbonate membranes, (b) nylon membrane, and (c) nitrocellulose membrane using nutrient agar as a medium.

Biofilms grown on polycarbonate had a distinct central mass surrounded by a less dense area of biomass. Biofilms grown on nylon appeared homogenous in terms of biomass distribution and had a distinct yellow colour. Biofilms grown on nitrocellulose membranes presented as a green/blue biofilm with a homogenous biomass density. Images shown are representative of 3 independent replicates. Each image shows a 10mm field of view.

5.4.1.2 Identification of an appropriate wound-like nutrient source

Biofilms were grown on all membrane types on SBF agar and SBF agar supplemented with laked horse blood. When grown with simulated body fluid agar as a nutrient source, biofilms on polycarbonate formed as very low-density biofilms which did not spread from the site of initial inoculation (Figure 5.5 a). When grown on nylon and nitrocellulose membranes with simulated body fluid agar, biofilms did not form at all (Figure 5.5 b - c). When simulated body fluid agar supplemented with laked horse blood was used, biofilms grown on polycarbonate membranes appeared denser than with SBF alone but still did not spread from the site of initial inoculation (Figure 5.5 d). Biofilms grown on nylon membranes showed the same distinct yellow colour but were much less dense than was seen on nutrient agar (Figure 5.5 e). Finally, biofilms grown on nitrocellulose in the presence of simulated body fluid agar with blood did not appear to form any visible biofilm (Figure 5.5 f).

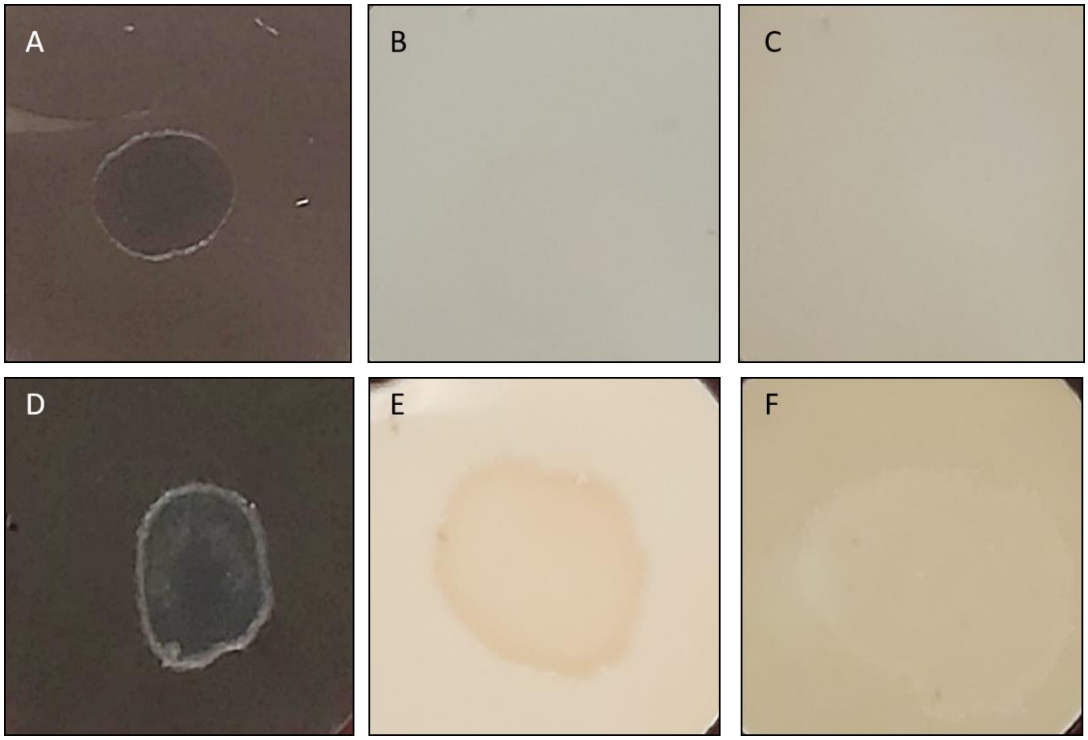

Figure 5.5 – Biofilms grown on simulated body fluid agar (a-c) and simulated body fluid agar supplemented with 5% laked hose blood (d-f) on three semi permeable membranes.

On non-supplemented SBF agar biofilms grown on polycarbonate membranes (a) were low density and showed no spread from the initial inoculation point. Biofilms did not form on nylon (b) and nitrocellulose (c) membranes on this medium. In the presence of supplemented body fluid agar biofilms on polycarbonate membranes (d) were denser than with non-supplemented agar but still showed no spreading. Biofilms grown on nylon membranes (e) were low density but retained the yellow colour noted previously. (f) Biofilms did not form on nitrocellulose membranes in the presence of body fluid agar with blood. Images shown are representative of 3 independent replicates. Each image shows a 10mm field of view.

Biofilms were then grown on a novel semi-synthetic wound bed agar (SWBA) with and without laked horse blood. On the SWBA, biofilms grown on polycarbonate, presented as well populated biofilms with distinct edges and an area of less dense biofilm at the edge (Figure 5.6 a). When grown on nylon membranes with SWBA, biofilms were low density with a yellow colour. Biomass density appeared homogenous throughout the biofilm (Figure 5.6 b). Biofilms grown on nitrocellulose membranes with SWBA appeared as dense biofilms with a cream/yellow colour and

homogenous biomass distribution (Figure 5.6 c). When grown in the presence of SWBA with 5% blood, biofilms on polycarbonate presented as very dense biofilms with no evidence of spreading but a noticeable three-dimensional architecture (Figure 5.6 d). Biofilms grown on nylon membranes were low density and difficult to identify visually from the underlying membrane (Figure 5.6 e). Biofilms grown on nitrocellulose appeared as white/cream biofilms with low biomass density (Figure 5.6 f).

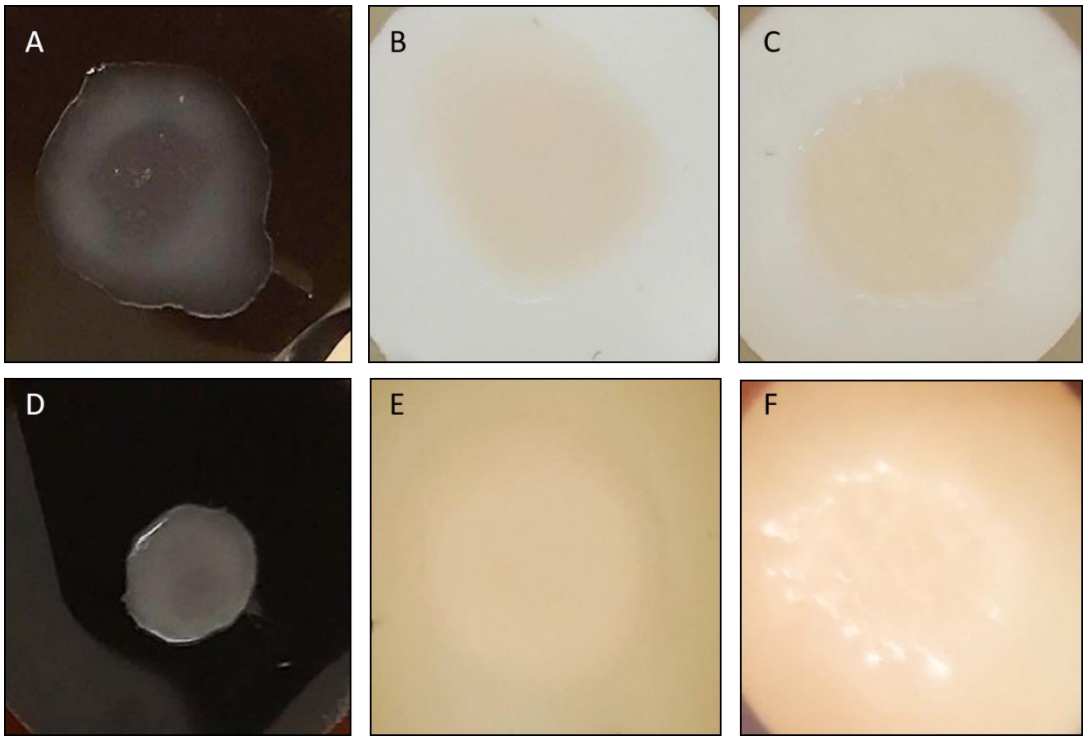

Figure 5.6 – Biofilms grown using simulated wound bed agar (a-c) and simulated wound bed agar supplement with 5% blood (d-f).

When grown using simulated wound bed agar only biofilms on polycarbonate membranes (a) formed moderately dense biofilms with some heterogeneity in the distribution of biomass throughout the biofilm. Biofilms grown on nylon membranes (b) had low amounts of biomass and a yellow colour. Biofilms grown on nitrocellulose were dense cream/yellow biofilms. When using SWBA with blood as a nutrient source, biofilms on polycarbonate membranes (d) appeared as very dense with an obvious three-dimensional architecture. Biofilms grown on nylon membranes (e) were difficult to identify but appeared as low-density, diffuse, biofilms. Nitrocellulose bound biofilms (f) were seen to be white/cream masses with low to moderate biofilm density. Images shown are representative of 3 independent replicates. Each image shows a 10mm field of view.

5.4.2 Selection of a biofilm quantification method

To assess the antibiofilm effects of wound dressings using the newly developed model, a method of quantifying both treated and untreated biofilms was required. Several methods were considered, including staining of biofilm proteins, staining of whole biofilm biomass, viability staining of biofilm bound cells and direct enumeration.

5.4.2.1 Biofilm matrix protein staining

In order to stain biofilm proteins, the fluorescent protein stain SYPRO Ruby was used. The accuracy of SYPRO Ruby quantification in aqueous solution was investigated. A calibration curve of the fluorescence intensity of SYPRO Ruby against the concentration in simple aqueous solution was constructed and the curve was found to be acceptable for the interpolation and estimation of the concentration of SYPRO Ruby in an unknown solution ($R^2 = 0.9835$). This calibration curve was then used to estimate the SYPRO Ruby concentration in three stock solutions of known concentration. It was found that estimating SYPRO Ruby concentration in aqueous solution was highly inaccurate despite the calibration curve being of acceptable quality for the purpose. When analysing the concentration of a 5 μL mL^{-1} solution, interpolation using this method gave an estimated concentration of 0.07 μL mL^{-1}. Similarly, a 15 μL mL^{-1} solution was estimated to contain 2.73 μL mL^{-1} and a 25 μL mL^{-1} solution estimated to contain 20.43 μL mL^{-1}. These estimates give average percentage errors of 98.67%, 81.79% and 18.28% respectively (Table 5.3). These data indicate that the use of SYPRO Ruby staining of biofilm proteins is an unsuitable method of biofilm quantification.

Table 5.3 - The estimated concentration of SYPRO Ruby in a low, moderate and high concentration solution of SYPRO Ruby in simple aqueous solution. Estimation using the previously developed calibration curve was shown to be inaccurate resulting in 98.67%, 81.79% and 18.28% reductions in estimated concentrations compared to actual concentration for the low, moderate and high concentration solution respectively.

Sample	Actual SYPRO Ruby Concentration (µL mL^{-1})	Estimated Concentrations (µL mL-1)			Average Estimated Concentration (µL mL-1)	Percentage Error
Low Concentration	5	0	0.2	0	0.07	98.67
Moderate Concentration	15	3.516	3	1.68	2.73	81.79
High Concentration	25	20.11	21.66	19.52	20.43	18.28

5.4.2.2 Staining of total biofilm biomass

To stain total biofilm biomass crystal violet was used. Prior to staining biofilms, each membrane type was used as a substrate to grow a biofilm with nutrient agar as a medium. It was found that quantitative crystal violet staining of each membrane type was possible. Nitrocellulose showed the lowest over all variability between replicates, while nylon showed the highest variability (Figure 5.7).

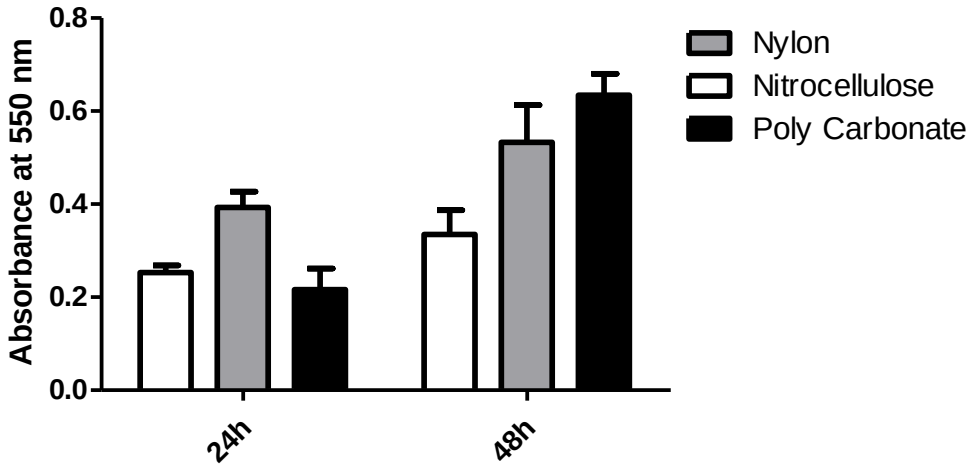

Figure 5.7 – Quantitative crystal violet staining of total biofilm biomass of membrane bound biofilms.

Biofilms grown on each membrane type were grown for either 24 or 48h on nutrient agar and biomass was quantified using crystal violet. Differences in biomass between the 24- and 48-h time points was apparent on each membrane type with nitrocellulose having the lowest overall inter replicate variability. Data shown represents the mean of three independent replicates ± S.D.

It was also noted that biofilms grown on nitrocellulose membranes were very well destained, appearing as white masses on a stained membrane following the destaining step. This data suggests that the nitrocellulose substrate strongly binds the crystal violet stain. Conversely, the biofilm grown on the nylon membrane appeared as a purple mass on a partially destained membrane. The degree of biofilm destaining was difficult to establish with biofilms grown on the black polycarbonate membranes (Figure 5.8).

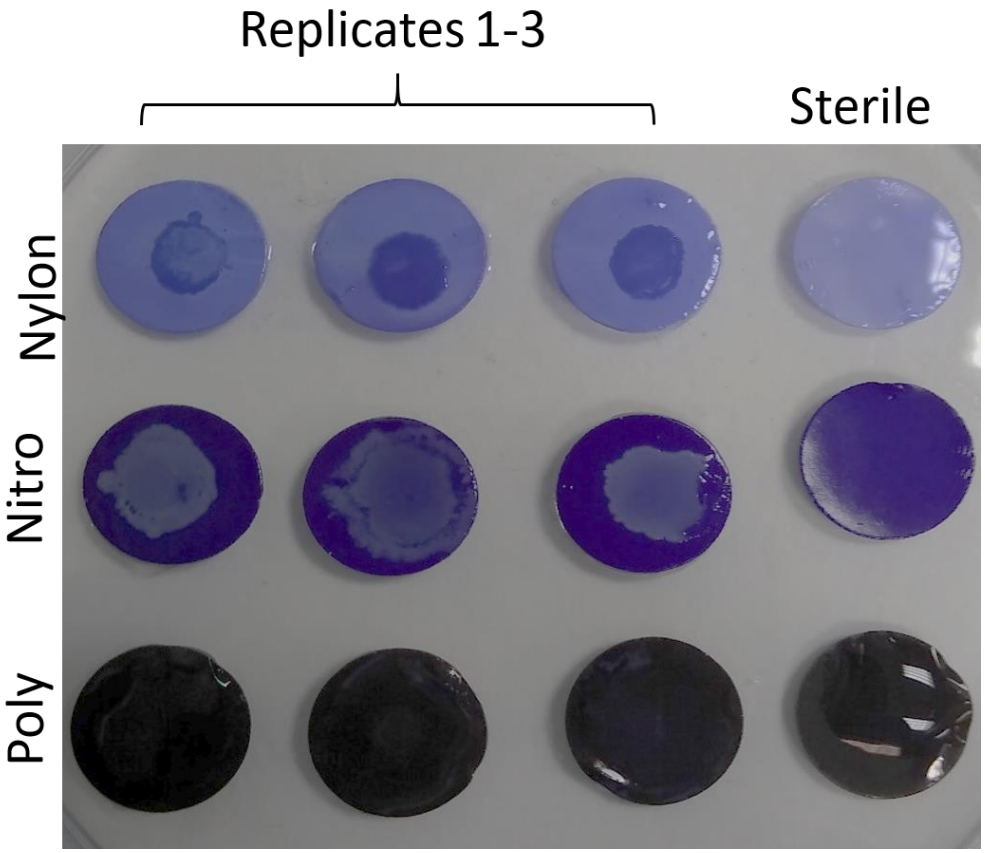

Figure 5.8 – Membrane bound biofilms following destaining with acetic acid.

Following destaining it was found that biofilms formed on nitrocellulose were well destained appearing as white areas on a heavily stained membrane. Nylon bound biofilms were found to be destained less readily than those on nitrocellulose while the nylon membrane was easily destained. Assessment of the extent of biofilm destaining on black polycarbonate membranes was not possible.

5.4.2.3 Viability staining of biofilm bound cells

To quantify cell viability in membrane bound biofilms the use of BacLight bacterial cell viability staining was investigated. It was found that BacLight was an unsuitable method of biofilm assessment. Both nylon and nitrocellulose membranes were white in colour and, as such, excessive reflection of the illuminating light occurred. This resulted in very bright images with little to no visible detail which persisted even when exposure time was significantly reduced. When BacLight stained biofilms, on black polycarbonate membranes, were imaged it was found that excessive non-specific staining of biofilm matrix occurred and, as such it, was not possible to enumerate stained cells within the biofilm. Washing away the surface biofilm matrix prior to staining was attempted but, when stained, the washed biofilm showed little to no cells present.

5.2.4.4 Direct enumeration of biofilm bound cells

Finally, direct enumeration of viable, biofilm bound, cells was assessed. It was discovered that biofilms grown on nitrocellulose membranes using nutrient agar as a medium contained $2.88 \times 10^8 \pm 5.70 \times 10^7$ viable cells after 24 hours of incubation at 37 °C. This increased to $4.54 \times 10^{11} \pm 4.80 \times 10^{10}$ viable cells after 48 hours. Similarly, biofilms grown on polycarbonate membranes were found to contain $2.89 \times 10^{11} \pm 2.55 \times 10^{10}$ viable cells after 24 hours and $6.99 \times 10^{13} \pm 1.55 \times 10^{13}$ after 48 hours. However, biofilms grown on nylon membranes did not follow this pattern. At 24 hours biofilms on nylon membranes consisted of $4.17 \times 10^{11} \pm 3.79 \times 10^{11}$ viable cell which subsequently decreased after 48 hours to $4.34 \times 10^8 \pm 1.72 \times 10^8$ viable cells (Figure 5.9). It was noted that biofilms grown on polycarbonate were generally larger and more reproducible than those grown on either nylon or nitrocellulose membranes. For

this reason, polycarbonate membranes were selected as the substrate for the developed wound model.

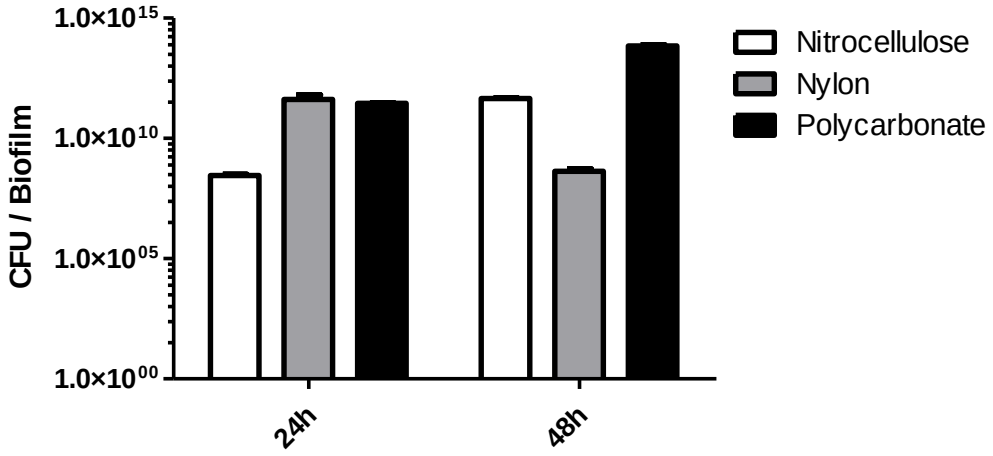

Figure 5.9 – Viable cells isolated from biofilms grown on nitrocellulose, nylon and polycarbonate membranes using nutrient agar as a medium.

Biofilms grown on nitrocellulose membranes had 2.88 x 10^8 ± 5.70 x 10^7 viable cells at 24 hours increasing to 4.54 x 10^{11} ± 4.80 x 10^{10} at 48 hours. Biofilms grown on nylon membranes had 4.17 x 10^{11} ± 3.79 x 10^{11} cells at 24 hours which decreased to 4.34 x 10^8 ± 1.72 x 10^8 at 48 hours. Biofilms grown on polycarbonate membranes 2.89 x 10^{11} ± 2.55 x 10^{10} viable cells at 24 hours and 6.99 x 10^{13} ± 1.55 x 10^{13} after 48 hours. Data shown represents the mean of three independent replicates ± S.D. on a log10 scale.

5.4.3 Characterisation and validation of the developed simple wound model

Following the selection of a growth surface, nutrient source and method for quantifying the produced biofilm, characterisation of the biofilm formation kinetics was performed. To validate the model, the efficacy of clinically used wound dressings was assessed using the developed method.

5.4.3.1 Biofilm formation on simulated wound bed medium

Biofilm formation kinetics on both simulated wound bed medium and nutrient agar were investigated and compared. When using nutrient agar as a nutrient source, biofilms grown on polycarbonate membranes reached a peak viable cell density of 1.9

x10^9 CFU per biofilm. However, over the same 10-hour experimental period, biofilms grown on polycarbonate membranes using the newly developed simulated wound bed medium as a nutrient source reached a total viable cell density of 5.37 x 10^7 cells per biofilm. One-way ANOVA analysis of each time point (comparing biofilms grown on nutrient agar to biofilms grown on wound bed medium) showed that there was, in fact, no significant difference between the samples at any time point. A clinically relevant biofilm viable cell density was achieved after 6 hours incubation with a viable cell count of 1.69 x 10^6 ± 1.32 x 10^5 cells per biofilm (Figure 5.10).

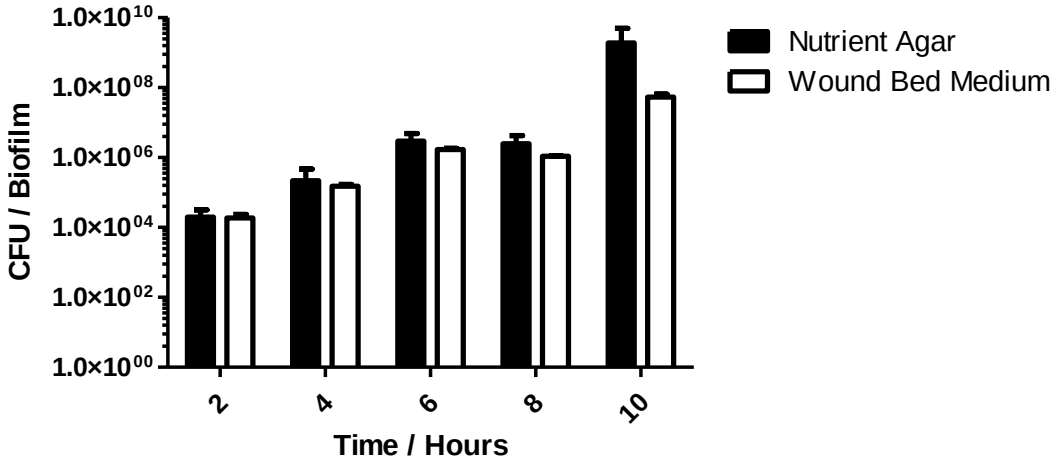

Figure 5.10 – Biofilm formation kinetics of *P. aeruginosa* PAO1 DSM50071 on polycarbonate membranes using nutrient agar and simulated wound bed media as nutrient sources.

In the presence of nutrient agar, POA1 biofilm total viable cell count steadily increased to a total viable cell density of 1.9x10^9 CFU per biofilm after 10 hours incubation. On wound bed medium a peak viable cell count of 5.37 x 10^7 per biofilm was reached after 10 hours and a clinically relevant bacterial load of 1.69 x 10^6 was reached in 6 hours. Data shown represents the mean of three independent replicates ± S.D. on a log10 scale. One-way ANOVA analysis showed no significant difference in biofilms at any time point.

5.4.3.2 Assessment of common antimicrobial wound dressings using a simple wound biofilm model

The effect of common, clinically relevant, antimicrobial wound dressings against *P. aeruginosa* PAO1 biofilms was investigated. Biofilms grown on the simulated wound bed medium were found to be generally resistant to all dressings tested with no significant reduction in viable cells following any of the four treatments. It was noted that while the application of wound dressings did not reduce viable cell numbers in the biofilms, it did prevent the rapid growth of the biofilm which was observed when no treatment was applied. This effect was apparent for both the medicated dressings and the non-medicated gauze control (Figure 5.11).

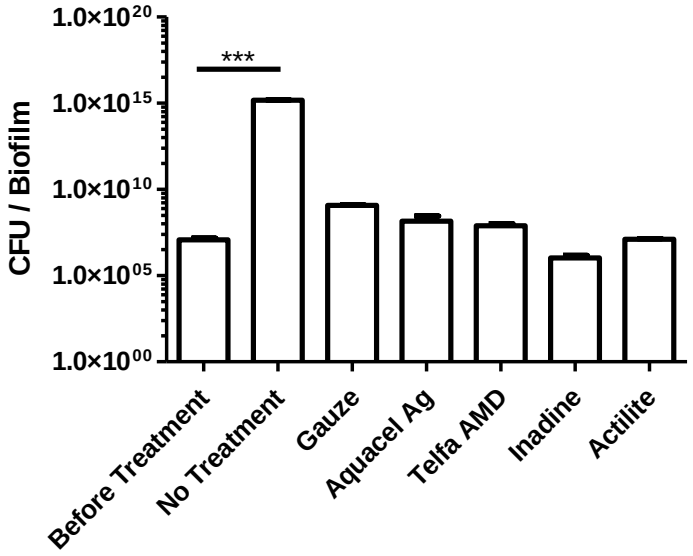

Figure 5.11 – The effects of treatment with common antimicrobial wound dressings on viable cell numbers in polycarbonate bound *P. aeruginosa* PAO1 biofilms grown on simulated wound bed medium.

When grown in the presence of the simulated wound bed medium PAO1 biofilms were found to be totally resistant to treatment with all dressings with no significant reductions in viable cell numbers after 24 hours. It was noted that the presence of any dressing (medicated and non-medicated) prevented further growth of the biofilm when compared to no treatment controls. Data shown represents the mean of three independent replicates ± S.D. on a log10 scale. Statistical analysis was by one-way ANOVA with a Dunnet's post-hoc test to compare all columns to the control (before treatment).

5.4.3.3 Assessment of a the antibiofilm potential of furanone aerogels using a simple wound biofilm model

The effect of furanone-loaded aerogels was assessed using the simple wound model. Clinically representative biofilms, containing approximately 10^6 CFU, were either left untreated or treated with an unloaded or furanone-loaded aerogel for a further 24 hours. Again, when no treatment was applied, the biofilm continued to proliferate and, after 24 hours, contained approximately 9.36 x 10^{14} CFU. When treated with a blank aerogel the biofilm was also able to proliferate, though not significantly. Biofilms treated with blank aerogels contained 9.42 x 10^8 CFU after 24 hours of treatment. HDMF aerogel treated biofilms showed no significant increase in CFU numbers and sotolon aerogel treated biofilm showed a non-significant increase in CFU (containing 1.55 x 10^8 CFU after 24 h) (Figure 5.12).

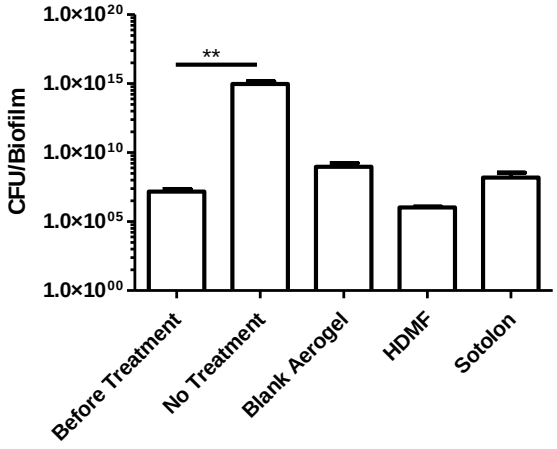

Figure 5.12 - The effects of treatment with blank and furanone-loaded aerogels on viable cell numbers in polycarbonate bound *P. aeruginosa* PAO1 biofilms grown using the simple wound biofilm model.

When grown on wound bed medium PAO1 biofilms were not susceptible to treatment with any aerogel treatment with no significant reductions in cell numbers after 24 hours. It was noted that the presence of any aerogel (blank and furanone-loaded) prevented any significant further growth of the biofilm when compared to no treatment controls. Data shown represents the mean of three independent replicates ± S.D. on a log10 scale. Statistical analysis was by one-way ANOVA with a Dunnet's post-hoc test to compare all columns to the control (before treatment).

These data indicate that the developed simple would model is not suitable for the assessment of furanone-loaded aerogels against *P. aeruginosa* PAO1 biofilms.

5.4.3.4 Furanone release and integrity in a simple wound bed model

The ability of the aerogels to release their furanone pay load into the wound bed medium was assessed. As the furanone compounds have been shown to be unstable under several conditions, degradation of released furanones was assessed as well as the total concentration of released furanone. It was shown that, following release into the wound bed medium, both HDMF and sotolon remained unchanged in their λ_{max}. The observed λ_{max} of HDMF was 285 nm while the λ_{max} of sotolon was 230 nm indicating that the furanones did not degrade upon release (Figure 5.13).

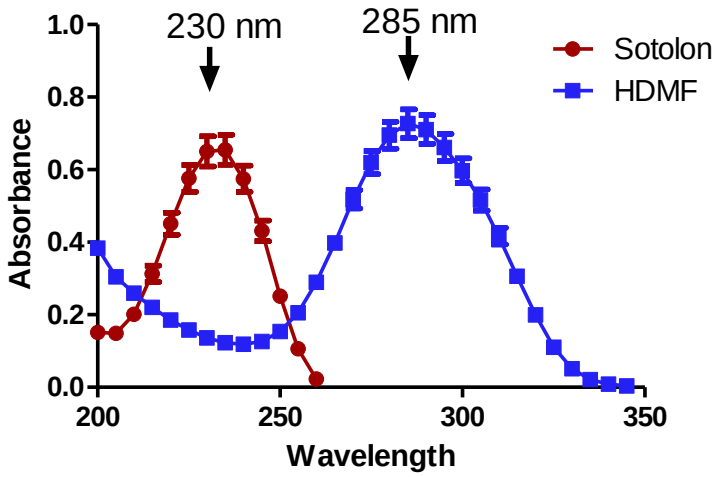

Figure 5.13 – Absorbance spectra of HDMF and Sotolon after being released from a PVA aerogel into the developed semi solid wound medium.

Spectra recorded for both Sotolon and HDMF remained unchanged in their λ_{max} showing maximum absorbances at 230 nm and 285 nm respectively. Data shown represents the mean of three independent replicates ± S.D.

When the total quantity of furanone released into the simple wound model was assessed it was found that aerogels loaded with 4 mg of HDMF were able to release only 8.61% of their total pay load (0.344 mg total release) into the simple wound

model. Conversely, aerogels loaded with 4.33 mg sotolon were able to release 72.34% of their total loaded volume (3.13 mg total release) (Figure 5.14).

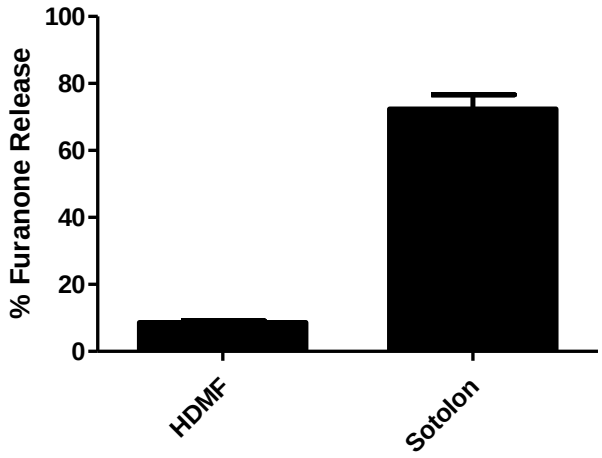

Figure 5.14– Quantification of furanone release from loaded aerogels into the newly developed wound model.

Aerogels loaded with an antibiofilm concentration of HDMF (4 mg) and Sotolon (4.33 mg) released 8.61% and 72.34% of their total payload into the wound model, respectively. Data shown represents the mean of three independent replicates ± S.D.

The limited release of HDMF into the simple wound model necessitated the optimisation of the wound model to allow for greater release of HDMF, thus, maximising the potential for successful inhibition of biofilm formation.

5.4.4 Assessment and validation of the developed modified wound model.

Following the failure of the simple model to assess the antibiofilm efficacy of aerogels a modified wound model system, consisting of a simulated wound bed and a wound fluid reservoir, was developed (section 5.3.7). This method was assessed for its ability to allow furanone release. It was then used to assess furanone-loaded aerogels and clinically used wound dressings.

5.4.4.1 Furanone release and integrity in a modified chronic wound bed model

The release of furanones into the new modified wound model was assessed. It was found that the furanone released into the new model was not degraded. Released HDMF showed a single clear peak at 285 nm when assessed using UV-Visible spectroscopy. Similarly, released sotolon was found to have a λ_{max} of 230 nm (Figure 5.15).

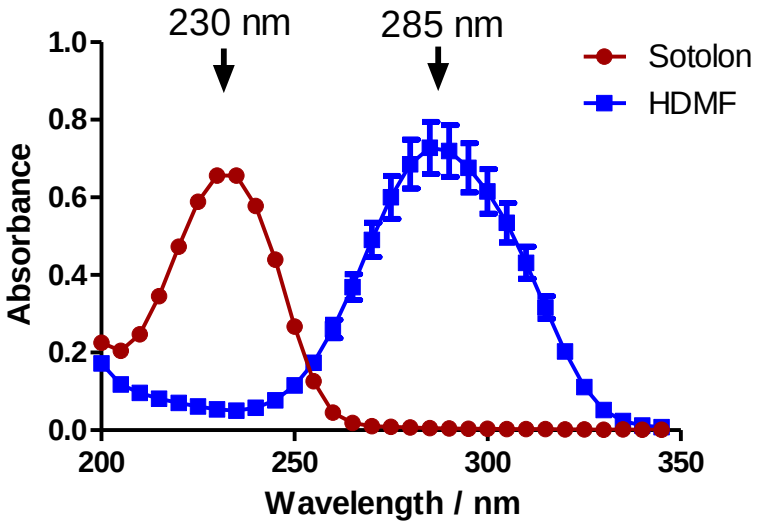

Figure 5.15 - Absorbance spectra of both HDMF and Sotolon after being released from a 10% PVA aerogel into the novel modified chronic wound model.

Both Sotolon and HDMF remained unchanged in their λ_{max} showing maximum absorbances at 230 nm and 285 nm respectively. Data shown represents the mean of three independent replicates ± S.D.

Further, the concentration of each furanone released into the modified wound model over 24 hours was examined. It was found that aerogel, loaded with 4 mg of HDMF, released 57.47% of the total loaded drug (2.3 mg total HDMF release). This was an improvement over the 8.61% release in the simple wound model. Aerogels loaded with 4.33 mg of sotolon released just 39.10% of the total loaded volume (1.69 mg total

sotolon release). This was considerably lower than the 72.34% release observed for the simple model.

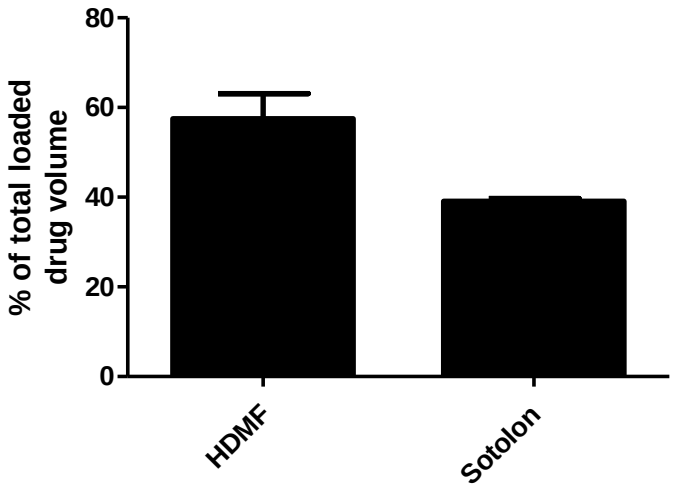

Figure 5.16 - Quantification of furanone release from loaded aerogels into a modified wound model.

Aerogels loaded with an antibiofilm concentration of HDMF (4 mg) and Sotolon (4.33 mg) released 57.47% and 39.10% of their total payload into the wound model respectively. Data shown represents the mean of three independent replicates ± S.D.

5.4.4.2 Treatment of biofilms with furanone-loaded aerogels on a modified wound model

Following confirmation that furanone was released into the modified wound model at acceptable concentrations, loaded aerogels were assessed for their ability to treat clinically relevant biofilms. It was discovered that, as was the case in the simple model, a clinically relevant biofilm, left untreated for a further 24 hours would continue to proliferate. Such biofilms contained an average of 3.3×10^{13} cells per biofilm. This represented a 7.52 log increase in viable cells. Treatment of clinically relevant biofilms with an unloaded aerogel contained 1.10×10^{9} cells per biofilm following treatment, representative of a 2.68 log increase in viable cells. Similarly, treatment with HDMF yielded biofilms containing 1.67×10^{8} cells per biofilm after 24 hours treatment (a

2.20 log increase). Finally, when treated with sotolon-loaded aerogels, biofilms contained only 233 viable cells on average. This represents a log reduction of 3.65 (Figure 5.17 a-b). It should be noted that statistical analysis was performed on log10 transformed CFU values. This action limited any skew in the data making statistical analysis by one-way ANOVA appropriate.

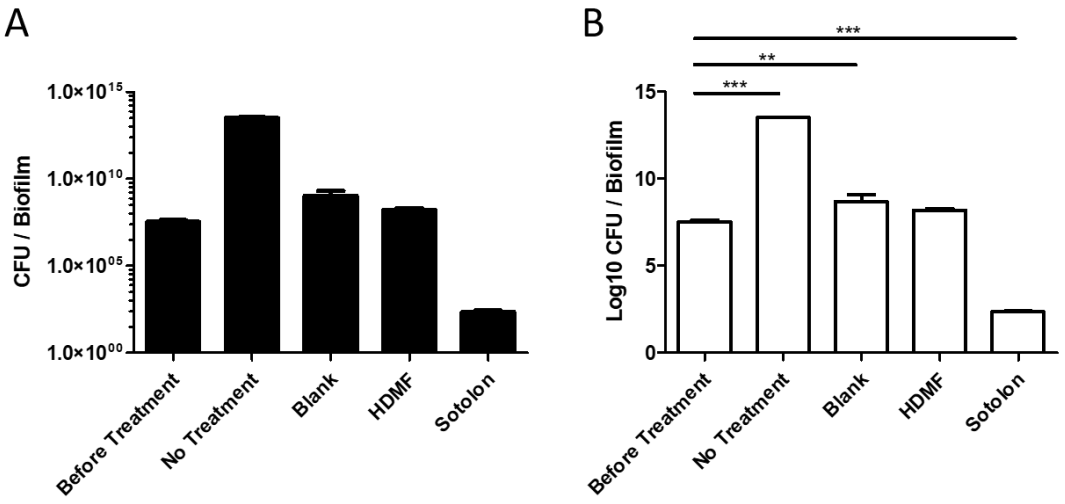

Figure 5.17 – Changes in bacterial cell numbers following treatment with unloaded and furanone-loaded aerogels expressed as (a) CFU/biofilm on a log scale and (b) Log10 CFU / biofilm.

*Controls in which no treatment was applied resulted in a 7.52 log increase in viable cells per biofilm (final CFU/ biofilm of 3.3 x 10^{13}) treatment with an unloaded aerogel resulted in a 2.68 log increase giving a final biofilm with 1.10 x 10^{9} CFU. Treatment with HDMF-loaded aerogel resulted in a 2.20 log increase in viable cells (final CFU/biofilm 1.67 x 10^{8}) this was not found to be significant. Treatment with sotolon-loaded aerogels showed a significant log decrease in viable cells of 3.65 and resulted in biofilms with an average of 233 CFU/biofilm. Data shown represents the mean of three independent replicates ± S.D. Analysis is by one-way ANOVA of the log10 values. *p=0.05, **p=0.01, *** p=0.001*

5.4.4.3 Assessment of clinically used wound dressings using the modified wound model.

Currently used, clinically relevant wound dressings were re-evaluated using the newly developed model. It was shown, that when clinically representative biofilms were treated with non-medicated gauze, the biofilm proliferated and gave a biofilm with

7.36 x 10^{11} cells after 24 hours of treatment. This corresponded to a 4.39 log increase in viable cells during treatment. When treated with Aquacel Ag, viable cell numbers were reduced to 136 per biofilm or a 3.87 log decrease in 24 hours. Similarly, treatment with Inadine resulted in a 2.54 log reduction in cells with biofilm containing just 3273 cells on average following treatment. When treated with Telfa AMD, biofilms continued to proliferate and contained 5.60 x10^{10} viable cells after 24 hours. This corresponds to a 3.88 log increase (Figure 5.18 a-b). Finally, treatment with Actilite for 24 hours showed no significant increase or decrease in viable cell numbers. As before, data was transformed to the Log10 values prior to data analysis

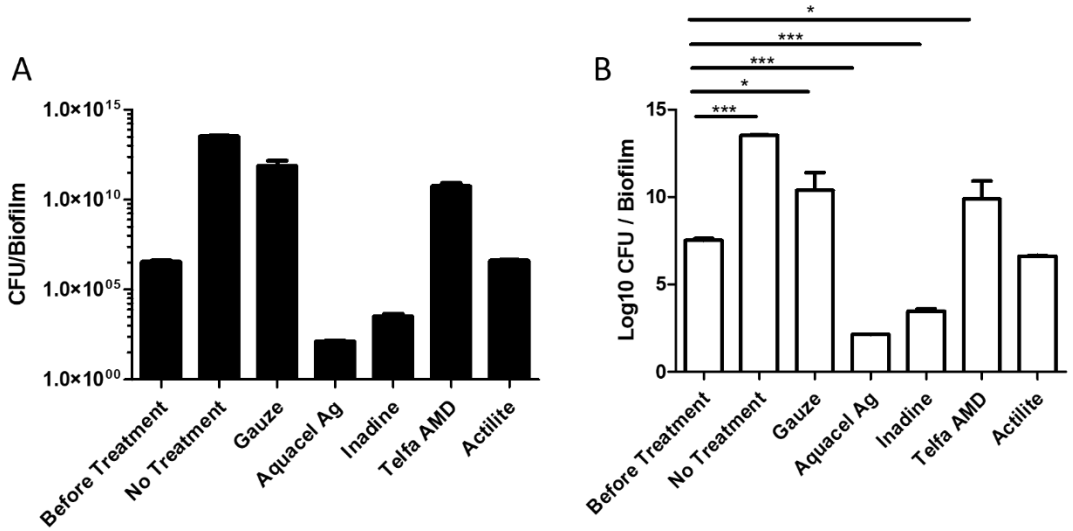

Figure 5.18 – Changes in viable cell numbers following treatment with clinically used wound dressings using a modified wound model.

*Treatment with gauze caused cells to proliferate with 7.36 x 10^{11} cells after 24 hours (4.39 log increase). Aquacel AG reduced bacterial numbers to approximately 136 per biofilm (3.87 log decrease). Inadine treatment reduced cell numbers to 3273 viable cells (2.54 log decrease). Telfa AMD had no bactericidal effect and biofilms proliferated during treatment with a final bacterial load of 5.60 x10^{10} cells per biofilm (3.88 log increase). Treatment with Actilite showed no significant change in viable cell numbers. Data shown represents the mean of three independent replicates ± S.D. Analysis is by one-way ANOVA of the log10 values. *p=0.05, **p=0.01, *** p=0.001*

5.5 Discussion

Chronic wounds are highly complex environments that rely heavily on the delicate balance of pro- and anti-inflammatory cytokines, immune cells and external conditions such as moisture and pressure (Guo and DiPietro, 2010). When infected, the wound environment only becomes more complex. This inherent complexity presents a number of difficulties for anyone hoping to research wounds, wound infections, and the development of novel wound therapeutics. The most significant issue with such research is the challenge of accurately representing an infected wound using an *in vitro* model. While there are many *in vitro* wound infection models reported in the literature (Sun *et al.*, 2008; Werthén *et al.*, 2010; Kucera *et al.*, 2014) these models often have one or more limitations. These can include the use of a nutrient profile that is not representative of a wound, a growth substrate that is not representative of a wound bed, or simply using materials with a high cost.

The work detailed in this chapter aimed to develop a novel, low cost wound biofilm model that is suitable for the assessment of not only furanone-loaded aerogels but other wound dressings as well.

The first stage of developing a novel wound model was to select a growth substrate. This work investigated the use of semi-permeable membranes (made from nylon, nitrocellulose and polycarbonate) as a growth substrate. Such membranes have been used in the colony biofilm model previously detailed in the literature (Merritt, Kadouri and O'Toole, 2005). The use of membranes as a substrate was investigated as precise quantification of the biofilm would be required at a later stage, and easy removal of the biofilm from the model was vital. This work showed that changes in growth substrate (while nutrient source remains the same) can have a significant effect on the

morphology of a *P. aeruginosa* PAO1 biofilms. When grown on polycarbonate membranes, biofilms appeared as an off-white mass with central area of high biomass and an outer ring of lower biomass. When grown on nylon, biofilm biomass was uniform across the sample and a more yellow biofilm was formed. When grown on nitrocellulose, biofilm biomass was relatively evenly distributed, but the biofilm presented as a blue/green colour. While these specific morphological changes have not previously been reported in the literature the idea that growth substrate can impact on biofilm properties has. For example, in 2019, Williams *et al,* showed that when biofilms grown using a CDC reactor were grown on polycarbonate, their susceptibility to antibiotics was significantly different to biofilms grown on collagen substrates. Further, this work showed that when grown on polycarbonate, biofilms formed by a wide range of organisms were often more susceptible to treatment with antibiotics. The authors showed that *P. aeruginosa* was more resistant to treatment with both tobramycin and ciprofloxacin when grown on collagen substrates. The authors suggest this may be due to a number of factors. They note that differences in substrate surface morphology may allow biofilms to penetrate deeper into the collagen substrate, allowing cells to better evade exposure to antibiotics (Williams *et al.*, 2019). However, as the surface morphologies of the membranes used in this thesis are likely very similar to each other this may not explain the differences observed in this work. Further, the presence of a blue/green colour in the biofilm grown on nitrocellulose indicates a greater production of pyocyanin. Changes in the production of this virulence factor may not be explained by changes in substrate morphology. However, pyocyanin has been shown to increase the binding of eDNA (which is vital for biofilm formation) to *P. aeruginosa* cells (Das *et al.*, 2013, 2016). If the surface of the nitrocellulose resulted in the formation of a poorly stable biofilm an increase in pyocyanin production, and

the subsequent increase in eDNA-cell linkages, may have increased biofilm integrity. However, this hypothesis would require further investigation to fully understand and this was not within the scope of this work.

Due to the differences in biofilm morphology on each membrane, it was decided that all three membrane types would be assessed as a growth substrate alongside a range of different nutrient sources. This work showed that biofilms did not grow well on any tested substrate when SBF agar was used as a nutrient source. This medium contained only salts that are present in human serum and 5.5 mM glucose. As such, both carbon and nitrogen were limited and, therefore, minimal biofilm growth was expected. However, when biofilms were grown in the presence of simulated body fluid agar supplemented with 5% v/v of laked horse blood obvious biofilms were formed on both the polycarbonate and nylon membranes. No biofilm formed on the nitrocellulose membrane. Finally, biofilms were grown on each membrane using simulated wound medium, consisting of a mix of simulated wound fluid, protein, and muscle cell lysate (with and without laked horse blood). This experiment showed that the densest biofilms were grown on polycarbonate membranes using simulated wound bed medium with laked blood. This was an important finding because it is well known that the nutrients available to various species of bacteria can have a significant impact on their ability to form biofilms, the metabolic profile of the cells, and the long term maintenance of the biofilms (Anderl *et al.*, 2003; Sauer *et al.*, 2004; Cherifi *et al.*, 2017; She *et al.*, 2019). The selection of simulated wound bed medium with laked blood ensured that the biofilms grown in the developed model closely resemble *in vivo* wound biofilms.

Once a suitable nutrient source and growth substrate had been selected, a method of

quantifying the biofilms was required. Four potential options were identified; staining of matrix proteins with fluorescent SYPRO Ruby, staining of total biofilm biomass with crystal violet, staining live and dead cells using BacLight, and direct enumeration of viable, biofilm bound, cells. These methods were selected as each has been previously reported for the quantification of biofilm (Merritt, Kadouri and O'Toole, 2005; O'Toole, 2011; Bauer *et al.*, 2013; Stiefel *et al.*, 2016).

It was found that the use of SYPRO ruby as a biofilm stain was not appropriate as the quantity of the stain in simple aqueous solution could not reliably be measured, resulting in large underestimations. For this reason, the use of SYPRO ruby was not examined further as a method of biofilm biomass quantification.

Crystal violet is a simple and effective method for measuring total biofilm biomass in microtitre plates (O'Toole, 2011). This work aimed to show that it is possible to use crystal violet staining to determine total biomass of membrane bound biofilms. It was found that when exposed to crystal violet stain, both the nitrocellulose and nylon membranes were heavily stained along with the biofilm. However, when the membranes and biofilms were washed and destained it was clear that the nitrocellulose membranes were not destained while the biofilm was effectively destained, appearing as a white mass on the purple membrane. Conversely, the nylon membranes appeared to be partially destained while the biofilm remained heavily stained (appearing as a light purple membrane with a dark purple biofilm). Due to their dark colour it was unclear if polycarbonate membranes were significantly stained by crystal violet. Following visual inspection of the membranes the biofilm, biomass was quantified by measuring the resolubilised crystal violet. Biofilm biomass was inconsistent between the three membrane types. However, it was expected that biofilms grown on different

membranes would be of different sizes following the observed differences in biofilm morphology on different membrane materials.

The use of BacLight staining was then tested as a method for quantifying biomass of membrane bound biofilms. It was demonstrated that when used on the white nylon and nitrocellulose membranes the light used to excite the fluorescent stains was heavily reflected and, thus, the biofilms could not be visualised. When visualising biofilms grown on black polycarbonate membranes it was found that there was a significant amount of background staining of the biofilm matrix in addition to the staining of the bacterial cells. This meant that the numbers of viable and non-viable cells could not be accurately determined. Due to these issues the use of BacLight was not selected for use in this wound model.

Finally, the use of direct enumeration of viable cells was assessed as a method of quantifying membrane bound biofilm. It was found that of all the quantification methods assessed, direct enumeration was the most accurate, giving the least amount of variability between replicates. This assessment showed a marked difference in the numbers of biofilm bound cells on each membrane type at the same time point. It was demonstrated that both nitrocellulose and polycarbonate membrane bound biofilms showed the expected increase in viable biofilm bound cells between the 24 hours and 48 hour time points. However, it was found that the biofilm grown on polycarbonate had a greater number of viable cells after 48 hours growth (6.99×10^{13} per biofilm) when compared to those biofilms grown on nitrocellulose membranes (4.54×10^{11}) at the same time point. These data suggest that the biofilm may not grow as well, or as rapidly, on a nitrocellulose membrane when compared to polycarbonate. Alternatively, the difference may be due to difficulties in removing all of the biofilm

from the nitrocellulose membrane. It was clear that the use of a polycarbonate membrane for use in the wound model was preferable. For this reason, it was decided that the wound model being developed would use the wound-like medium supplemented with laked horse blood as a nutrient source, polycarbonate membranes as the growth substrate, and direct enumeration as the method of biofilm quantification.

Once all elements of the wound model had been selected, the biofilm growth kinetics in the new wound model were investigated. For this, biofilms were grown on the developed simple wound model (wound medium and membrane only) and biofilms were sacrificed and quantified every two hours by direct enumeration. It was found that, for the first 10 hours, biofilm growth using the wound like medium supplemented with blood was not significantly different than biofilms grown using nutrient agar as a medium. This indicated that the developed wound-like medium had all the nutrients required for biofilm formation and that nutrient availability was not a limiting factor in biofilm growth during this time frame. After 12 hours of growth, the biofilms grown on the wound like medium had fewer viable cells per biofilm than those grown using nutrient agar. However, this difference was not found to be statistically significant. It was also noted that the biofilms grown using the wound like medium reached a CFU density of approximately 1 x 10^6 cells per biofilm after 6 hours. This is a significant cell density as it has been shown that once an infected wound surpasses 10^6 CFU per gram of tissue, wound healing stops and a wound becomes chronic (Bendy *et al.*, 1964). Following the assessment of biofilm growth kinetics, the finalised wound model protocol was developed. Biofilms would be grown on polycarbonate membranes using the wound-like nutrient medium. Biofilms would be grown for 6 hours (to achieve a clinically representative cell density of approximately 10^6 cells per

biofilm) prior to treatment. Treatments would be applied for 24 hours and the treated biofilm would be quantified using viable cell counting.

The developed model was then validated by assessing the efficacy of wound dressings that are in current use by tissue viability specialists and wound care clinics. The wound dressings included Aquacel AG, Telfa AMD, Inadine, and Actilite. These dressings contain a range of active ingredients (silver, PHMB, iodine, and manuka honey respectively). Non-woven gauze was used as a non-medicated control. When clinically representative biofilms, grown using the simple, wound medium only, model were left untreated, biofilms continued to proliferate as expected. However, when wound dressings were applied, the biofilms failed to grow beyond their pre-treatment state. Despite this stall in biofilm growth there was no significant reduction in viable cell numbers. The data generated here showed that the dressings which contained active ingredients were no more effective than non-medicated gauze. This finding was highly unexpected. Each of the active components of the tested dressings have been shown to be effective in killing biofilm bound bacteria using a range of methods such as fermenter grown biofilms, zone of inhibition assays, and crystal violet assays (Hill *et al.*, 2010; Park *et al.*, 2013; Lu *et al.*, 2019; Salisbury *et al.*, 2019). As well as this, each of these dressings have been proven to be clinically effective as an antimicrobial dressing prior to commercialisation. The lack of efficacy observed using the simple wound model suggested that one or more aspects of model do not allow for the wound dressings to exert their antimicrobial effect. Alternatively, this finding may suggest that the biofilms grown using this model are not clinically representative and so respond to treatment very differently than *in vivo* biofilms.

The simple wound model was then used to assess the efficacy of the furanone-loaded

aerogels as a treatment of wound biofilm. Again, the untreated biofilm continued to grow as expected. Treatment with the blank and furanone-loaded aerogels yielded similar results to the clinical wound dressings. No significant changes in biofilm bound viable cell numbers was observed when biofilms were treated with blank aerogels or aerogels loaded with either furanone. Again, this was unexpected. When the aerogels were removed following the 24 hours treatment period, they were fully rehydrated. This rehydration of the aerogel should have allowed the release of the furanone. It was hypothesised that the wound medium was limiting the release of the furanone. As there was only a 1 mL volume of wound medium for the furanone to release into it was hypothesised that the aerogel did release the furanone appropriately but that an equilibrium between the furanone concentration in the medium and the rehydrated gel was reached very rapidly. This equilibrium would have meant that no further drug release into the wound medium was possible (Frenning, 2011). An alternative hypothesis was that the furanones were released from the aerogel as expected but that they were rapidly degraded by an interaction with one or more components of the wound medium.

To test these two hypotheses, loaded aerogels were prepared and allowed to release into soft agar of identical polymer concentration and volume as was used in the wound model. The quantity and integrity of the furanone released into the agar was assessed. It was found that the furanone released into the agar remained intact as evidenced by no changes in the UV absorbance spectrum. Both the HDMF and sotolon retained their expected λ_{max}. However, when the concentration of furanone released into the agar measured it was found that HDMF released just 8.61% of the aerogel's total loaded drug and sotolon released 72.34% of the total loaded drug. The incomplete release of each furanone may explain the limited effect against biofilm. As each aerogel was

loaded with an anti-biofilm concentration of each furanone, incomplete release would have meant that the therapeutic dose was never reached in the wound model. As previously stated, it was hypothesised that this was due to the limited volume of wound medium for the furanone to release into. This prompted work to modify the wound model to have a larger reservoir so that furanone release could be improved.

Following the discovery that furanone release into the developed wound model was limited, the wound model was modified into a hybrid system that consisted of a wound bed made from the developed wound medium and a reservoir containing simulated body fluid. These modifications were made so that the wound model system provided a larger receiver phase for drug release. It has been noted previously that in diffusion-based drug release systems (which the developed aerogels are believed to be) drug release will gradually reduce until an equilibrium state is reached (Frenning, 2011). The addition of a greater receiver volume would allow significantly more drug to be released before equilibrium is reached. When furanone release into the modified wound model was assessed, the release of HDMF was significantly increased while the release of sotolon was reduced when compared to the total release observed in the simple model. While the improvement observed in the release of HDMF into the modified wound model is promising, the reason for the reduction in sotolon release is unclear. However, despite this the modified wound model was used to assess the efficacy of both furanone-loaded aerogels and clinically used wound dressings.

When assessed using the modified wound model, treatment of a clinically representative PAO1 wound biofilm with HDMF-loaded aerogels showed no significant reduction in biofilm bound cells after 24 hours of treatment. However, as no other work has assessed the use of HDMF against wound biofilm or using a wound

model, comparisons cannot be made. However, as noted in chapter 4, HDMF has been used to treat PAO1 biofilms using a standard microtitre plate assay (Choi *et al.*, 2014). Here the authors showed that treatment of PAO1 biofilms grown in microtitre dishes with 0.1 µM and 1.0 µM HDMF resulted in 27.8% and 42.6% reductions in total biomass respectively. However, due to differences in strain, growth substrate, and nutrient medium it can be expected that the biofilms grown in this work would respond very differently to treatment when compared to this work. Furthermore, as detailed in chapter 4 of this work the strain used is deficient in four genes, *mexR, nalC, mdrR1*, and *mdrR2*. As previously noted these genes all encode repressors of either the MexAB-oprM or ErmAB multidrug efflux transporters (Maeda *et al.*, 2012; Heacock-Kang *et al.*, 2018). It has been reported in the literature that that strains that lack the *mexR* and *nalC* genes in particular are more resistant to furanone treatment via enhanced furanone efflux. This increased resistance may explain the lack of antibiofilm effect observed when treating clinically representative biofilms with HDMF-loaded aerogels. However, when such biofilms were treated with sotolon-loaded aerogels, a significant reduction in biofilm bound cells was observed. Following treatment, a 3.65 log decrease in biofilm bound cells was observed. This significant reduction resulted in post-treatment biofilms containing approximately 233 viable cells. This indicates that sotolon-loaded aerogels are a potentially viable option for the reduction of biofilm bound viable bacterial cells in chronic wounds infected with *P. aeruginosa* PAO1. Further, if the hypothesis proposed in chapter 4 is correct and the strain used in this study has increased resistance to furanone treatment, a similar reduction in biofilm may be possible with significantly lower concentrations of sotolon for non-resistant strains.

Finally, the efficacy of clinically used wound dressings was reassessed using the

modified wound model. It was found that the efficacy of the wound dressings was significantly impacted by the model. When assessed using the simple model no dressing was found to be more effective than the non-medicated control in killing biofilm bound cells. However, when these dressings were assessed using the modified model both Aquacel Ag and Inadine showed excellent antimicrobial action against biofilm bound PAO1 cells. Aquacel Ag treatment resulted in a 3.87 log decrease in viable biofilm bound cells. Inadine treatment gave 2.54 log decrease in biofilm bound cells. The significant reduction in viable cell numbers observed after treatment with Inadine is in keeping with the literature. In their 2010 study Hill *et al.* showed that *P. aeruginosa* biofilms, grown using an *in vitro* chronic wound infection model based on continuous drip feed growth, could be totally eradicated after treatment with Inadine (Hill *et al.*, 2010). However, this same study showed that viable cell numbers in these biofilms were not significantly affected by treatment with Aquacel Ag. This is further supported by a 2015 study conducted by Priscilla *et al.* who also showed no significant antimicrobial effect of Aquacel Ag against mature *P. aeruginosa* biofilms grown on porcine skin explants (Phillips *et al.*, 2015). An explanation for the observed differences between these studies and the results reported in this thesis may be found in the biofilms themselves. Both the work of Hill *et al.* and Priscilla *et al.* reported control biofilms containing approximately 10^8 cells per biofilm. This is a significantly higher cell density than was used in this thesis. The use of larger, more robust biofilms by Hill *et al.* and Priscilla *et al.* may have limited the efficacy of Aquacel Ag and of silver as an antimicrobial. Further, these variations in the efficacy of silver may have been caused by differences in bacterial strains used. For example, several papers have identified mechanisms of silver resistance including genetic elements such as plasmids, bacterial cooperation, and the production of virulence factors such as

pyocyanin (Silver, 2003; Muller and Merrett, 2014; Muller, 2018). Therefore, if the strains used in the published works had a greater resistance to ionic silver the results would differ greatly from the work reported here.

The differences in antimicrobial data obtained using the simple wound model, the modified model, and other models reported in the published literature clearly highlight the need for accurate, clinically representative *in vitro* models of chronic wound infection. It is obvious that even small differences in nutrient availability, inoculum density, bacterial strain, and growth substrate can have a profound effect on the efficacy of the treatments being tested. With such a wide range of models available for researchers aiming to develop and assess novel antimicrobial wound therapies, it is vital that a model which is simple, robust, and which can yield clinically representative biofilms is chosen.

5.6 Conclusion

In order to grow biofilms that were representative of real-world wound biofilms a novel wound-like medium was developed. This wound bed medium was used to develop a simple chronic wound biofilm model. This model was shown to be effective in rapidly growing *P. aeruginosa* biofilms on a polycarbonate substrate. While biofilms grew on the model rapidly, they were found to not be susceptible to treatment with clinically used antimicrobial wound dressings and furanone-loaded aerogels alike. It was suggested that this may be due to the limited amount of the wound medium available for the active ingredients of the treatments to release into. This was subsequently shown to be the case for HDMF-loaded aerogels. The wound model was then redesigned to give a modified wound bed model. This modified model consisted of a wound bed prepared from the wound-like medium and a reservoir of simulated body fluid that would provide a greater receiver phase, thus allowing for greater release of the active antimicrobial ingredients to release from the dressing into the model. The modified model was then used to show that treatment of clinically representative chronic wound biofilms with HDMF-loaded aerogels had no significant effect on numbers of biofilm bound cells. However, treatment of such biofilms with sotolon-loaded aerogels resulted in significant reductions of biofilm bound cell numbers. This suggests that not only might sotolon make an effective treatment for the reduction of biofilm biomass in wounds chronically infected with *P. aeruginosa*, but also that minimally crosslinked PVA aerogels are an effective mechanism for delivering this compound directly to the biofilms.

5.7 References

Anderl, J. N. *et al.* (2003) 'Role of nutrient limitation and stationary-phase existence in Klebsiella pneumoniae biofilm resistance to ampicillin and ciprofloxacin', *Antimicrobial Agents and Chemotherapy*, 47(4), pp. 1251–1256. doi: 10.1128/AAC.47.4.1251-1256.2003.

Asada, M. *et al.* (2012) 'Novel models for bacterial colonization and infection of full-thickness wounds in rats', *Wound Repair and Regeneration*, 20(4), pp. 601–610. doi: 10.1111/j.1524-475X.2012.00800.x.

Baltzis, D., Eleftheriadou, I. and Veves, A. (2014) 'Pathogenesis and Treatment of Impaired Wound Healing in Diabetes Mellitus: New Insights', *Advances in Therapy*, pp. 817–836. doi: 10.1007/s12325-014-0140-x.

Bauer, J. *et al.* (2013) 'A combined pharmacodynamic quantitative and qualitative model reveals the potent activity of daptomycin and delafloxacin against Staphylococcus aureus biofilms.', *Antimicrobial agents and chemotherapy*, 57(6), pp. 2726–37. doi: 10.1128/AAC.00181-13.

Beer, H. D., Longaker, M. T. and Werner, S. (1997) 'Reduced expression of PDGF and PDGF receptors during impaired wound healing', *Journal of Investigative Dermatology*, 109(2), pp. 132–138. doi: 10.1111/1523-1747.ep12319188.

Bendy, R. H. *et al.* (1964) 'Relationship of Quantitative Wound Bbacterial Counts to Healing of Decubiti: Effect of Topical Gentamicin.', *Antimicrobial agents and chemotherapy*, 10, pp. 147–155.

Brackman, G. and Coenye, T. (2016) 'In Vitro and In Vivo Biofilm Wound Models

and Their Application.', *Advances in experimental medicine and biology*, 897, pp. 15–32. doi: 10.1007/5584_2015_5002.

Cherifi, T. *et al.* (2017) 'Impact of Nutrient Restriction on the Structure of Listeria monocytogenes Biofilm Grown in a Microfluidic System', *Frontiers in Microbiology*, 8(MAY), p. 864. doi: 10.3389/fmicb.2017.00864.

Choi, S. C. *et al.* (2014) 'Inhibitory effects of 4-hydroxy-2,5-dimethyl-3(2H)-furanone (HDMF) on acyl-homoserine lactone-mediated virulence factor production and biofilm formation in *Pseudomonas aeruginosa* PAO1', *Journal of Microbiology*, 52(9), pp. 734–742. doi: 10.1007/s12275-014-4060-x.

Das, T. *et al.* (2013) 'Pyocyanin Facilitates Extracellular DNA Binding to *Pseudomonas aeruginosa* Influencing Cell Surface Properties and Aggregation', *PLoS ONE*, 8(3). doi: 10.1371/journal.pone.0058299.

Das, T. *et al.* (2016) 'Role of Pyocyanin and Extracellular DNA in Facilitating *Pseudomonas aeruginosa* Biofilm Formation', in *Microbial Biofilms - Importance and Applications*. doi: 10.5772/63497.

Ermolaeva, S. A. *et al.* (2011) 'Bactericidal effects of non-thermal argon plasma in vitro, in biofilms and in the animal model of infected wounds', *Journal of Medical Microbiology*, 60(1), pp. 75–83. doi: 10.1099/jmm.0.020263-0.

Falanga, V. *et al.* (2004) 'Full-thickness wounding of the mouse tail as a model for delayed wound healing: Accelerated wound closure in Smad3 knock-out mice', *Wound Repair and Regeneration*, 12(3), pp. 320–326. doi: 10.1111/j.1067-1927.2004.012316.x.

Fazli, M. *et al.* (2009) 'Nonrandom distribution of *Pseudomonas aeruginosa* and *Staphylococcus aureus* in chronic wounds.', *Journal of clinical microbiology*, 47(12), pp. 4084–9. doi: 10.1128/JCM.01395-09.

Frenning, G. (2011) 'Modelling drug release from inert matrix systems: From moving-boundary to continuous-field descriptions', *International Journal of Pharmaceutics*, pp. 88–99. doi: 10.1016/j.ijpharm.2010.11.030.

Grada, A., Mervis, J. and Falanga, V. (2018) 'Research Techniques Made Simple: Animal Models of Wound Healing', *Journal of Investigative Dermatology*, pp. 2095-2105.e1. doi: 10.1016/j.jid.2018.08.005.

Guo, S. and DiPietro, L. A. (2010) 'Critical review in oral biology & medicine: Factors affecting wound healing', *Journal of Dental Research*, 89(3), pp. 219–229. doi: 10.1177/0022034509359125.

Gurjala, A. N. *et al.* (2011) 'Development of a novel, highly quantitative in vivo model for the study of biofilm-impaired cutaneous wound healing.', *Wound repair and regeneration*, 19(3), pp. 400–10. doi: 10.1111/j.1524-475X.2011.00690.x.

Hammond, A. A. *et al.* (2011) 'An in vitro biofilm model to examine the effect of antibiotic ointments on biofilms produced by burn wound bacterial isolates.', *Burns : journal of the International Society for Burn Injuries*, 37(2), pp. 312–21. doi: 10.1016/j.burns.2010.09.017.

Heacock-Kang, Y. *et al.* (2018) 'Two regulators, PA3898 and PA2100, modulate the *Pseudomonas aeruginosa* multidrug resistance MexAB-OprM and EmrAB efflux pumps and biofilm formation', *Antimicrobial Agents and Chemotherapy*, 62(12). doi: 10.1128/AAC.01459-18.

Hill, K. *et al.* (2010) 'An in vitro model of chronic wound biofilms to test wound dressings and assess antimicrobial susceptibilities', *Journal of Antimicrobial Chemotherapy*, 65(6), pp. 1195–1206. doi: 10.1093/jac/dkq105.

Huang, C. H. *et al.* (2013) 'Simulated body fluid electrochemical response of Zr-based metallic glasses with different degrees of crystallization', *Materials Science and Engineering: C*, 33(7), pp. 4183–4187. doi: 10.1016/J.MSEC.2013.06.007.

Kostenko, V. *et al.* (2010) 'Impact of silver-containing wound dressings on bacterial biofilm viability and susceptibility to antibiotics during prolonged treatment.', *Antimicrobial agents and chemotherapy*, 54(12), pp. 5120–31. doi: 10.1128/AAC.00825-10.

Kucera, J. *et al.* (2014) 'Multispecies biofilm in an artificial wound bed-A novel model for in vitro assessment of solid antimicrobial dressings', *Journal of Microbiological Methods*, 103, pp. 18–24. doi: 10.1016/j.mimet.2014.05.008.

Lipp, C. *et al.* (2010) 'Testing wound dressings using an in vitro wound model.', *Journal of wound care*, 19(6), pp. 220–6. doi: 10.12968/jowc.2010.19.6.48468.

Lu, J. *et al.* (2019) 'Honey can inhibit and eliminate biofilms produced by *Pseudomonas aeruginosa*', *Scientific Reports*, 9(1), pp. 1–13. doi: 10.1038/s41598-019-54576-2.

Maeda, T. *et al.* (2012) 'Quorum quenching quandary: resistance to antivirulence compounds', *The ISME Journal*, 6(3), pp. 493–501. doi: 10.1038/ismej.2011.122.

Malone, M. *et al.* (2017) 'The prevalence of biofilms in chronic wounds: a systematic review and meta-analysis of published data.', *Journal of wound care*, 26(1), pp. 20–

25. doi: 10.12968/jowc.2017.26.1.20.

Merritt, J. H., Kadouri, D. E. and O'Toole, G. A. (2005) 'Growing and Analyzing Static Biofilms', in *Current Protocols in Microbiology*, p. Unit. doi: 10.1002/9780471729259.mc01b01s00.

Muller, M. (2018) 'Bacterial silver resistance gained by cooperative interspecies redox behavior', *Antimicrobial Agents and Chemotherapy*, 62(8). doi: 10.1128/AAC.00672-18.

Muller, M. and Merrett, N. D. (2014) 'Pyocyanin production by *Pseudomonas aeruginosa* confers resistance to ionic silver', *Antimicrobial Agents and Chemotherapy*, 58(9), pp. 5492–5499. doi: 10.1128/AAC.03069-14.

Ngo, Q. D., Vickery, K. and Deva, A. K. (2012) 'The effect of topical negative pressure on wound biofilms using an in vitro wound model', *Wound Repair and Regeneration*, 20(1), pp. 83–90. doi: 10.1111/j.1524-475X.2011.00747.x.

O'Toole, G. A. (2011) 'Microtiter dish biofilm formation assay.', *Journal of visualized experiments : JoVE*, (47). doi: 10.3791/2437.

Park, H. J. *et al.* (2013) 'Biofilm-inactivating activity of silver nanoparticles: A comparison with silver ions', *Journal of Industrial and Engineering Chemistry*, 19(2), pp. 614–619. doi: 10.1016/j.jiec.2012.09.013.

Percival, S. L., Bowler, P. G. and Dolman, J. (2007) 'Antimicrobial activity of silver-containing dressings on wound microorganisms using an in vitro biofilm model', *International Wound Journal*, 4(2), pp. 186–191. doi: 10.1111/j.1742-481X.2007.00296.x.

Petreaca, M. L. *et al.* (2012) 'Deletion of a tumor necrosis superfamily gene in mice leads to impaired healing that mimics chronic wounds in humans', *Wound Repair and Regeneration*, 20(3), pp. 353–366. doi: 10.1111/j.1524-475X.2012.00785.x.

Phillips, P. L. *et al.* (2015) 'Antimicrobial dressing efficacy against mature *Pseudomonas aeruginosa* biofilm on porcine skin explants', *International Wound Journal*, 12(4), pp. 469–483. doi: 10.1111/iwj.12142.

Rhoads, D. D. *et al.* (2012) 'Comparison of culture and molecular identification of bacteria in chronic wounds', *International Journal of Molecular Sciences*, 13(3), pp. 2535–2550. doi: 10.3390/ijms13032535.

Roche, E. D. *et al.* (2012) 'A model for evaluating topical antimicrobial efficacy against methicillin-resistant Staphylococcus aureus biofilms in superficial murine wounds', *Antimicrobial Agents and Chemotherapy*, 56(8), pp. 4508–4510. doi: 10.1128/AAC.00467-12.

Salisbury, A. M. *et al.* (2019) 'Efficacy of poloxamer-based wound dressings on acinetobacter baumanni biofilms', *Advances in Wound Care*, 8(10), pp. 463–468. doi: 10.1089/wound.2018.0854.

Sauer, K. *et al.* (2004) 'Characterization of nutrient-induced dispersion in *Pseudomonas aeruginosa* PAO1 biofilm', *Journal of Bacteriology*, 186(21), pp. 7312–7326. doi: 10.1128/JB.186.21.7312-7326.2004.

She, P. *et al.* (2019) 'Effects of exogenous glucose on *Pseudomonas aeruginosa* biofilm formation and antibiotic resistance', *MicrobiologyOpen*, 8(12). doi: 10.1002/mbo3.933.

Silver, S. (2003) ‘Bacterial silver resistance: molecular biology and uses and misuses of silver compounds’, *FEMS Microbiology Reviews*, 27(2–3), pp. 341–353. doi: 10.1016/S0168-6445(03)00047-0.

Stiefel, P. *et al.* (2016) ‘Is biofilm removal properly assessed? Comparison of different quantification methods in a 96-well plate system’, *Applied Microbiology and Biotechnology*, 100(9), pp. 4135–4145. doi: 10.1007/s00253-016-7396-9.

Sun, Y. *et al.* (2008) ‘In vitro multispecies Lubbock chronic wound biofilm model’, *Wound Repair and Regeneration*, 16(6), pp. 805–813. doi: 10.1111/j.1524-475X.2008.00434.x.

Thompson, M. G. *et al.* (2014) ‘Validation of a novel murine wound model of Acinetobacter baumannii infection.’, *Antimicrobial agents and chemotherapy*, 58(3), pp. 1332–42. doi: 10.1128/AAC.01944-13.

Thorn, R. M. S. M. S. and Greenman, J. (2009) ‘A novel in vitro flat-bed perfusion biofilm model for determining the potential antimicrobial efficacy of topical wound treatments’, *Journal of Applied Microbiology*, 107(6), pp. 2070–2079. doi: 10.1111/j.1365-2672.2009.04398.x.

Trøstrup, H. *et al.* (2016) ‘Animal models of chronic wound care: the application of biofilms in clinical research’, *Chronic Wound Care Management and Research*, Volume 3, pp. 123–132. doi: 10.2147/CWCMR.S84361.

Watters, C. *et al.* (2014) ‘Insulin treatment modulates the host immune system to enhance *Pseudomonas aeruginosa* wound biofilms’, *Infection and Immunity*, 82(1), pp. 92–100. doi: 10.1128/IAI.00651-13.

Werthén, M. *et al.* (2010) ‘An in vitro model of bacterial infections in wounds and other soft tissues’, *Apmis*, 118(2), pp. 156–164. doi: 10.1111/j.1600-0463.2009.02580.x.

Williams, D. L. *et al.* (2019) ‘Growth substrate may influence biofilm susceptibility to antibiotics’, *PLOS ONE*. Edited by N. J. Hickok, 14(3), p. e0206774. doi: 10.1371/journal.pone.0206774.

Wolcott, R. D., Rhoads, D. D. and Dowd, S. E. (2008) ‘Biofilms and chronic wound inflammation.’, *Journal of wound care*, 17(8), pp. 333–41. doi: 10.12968/jowc.2008.17.8.30796.

Chapter 6

General Discussion

6.1 Introduction

The focus of this thesis was broad. The development of a novel delivery method for furanone compounds has spanned several key areas including pharmaceutics, microbiology and materials science. Due to the highly multidisciplinary nature of this work, each chapter includes a discussion of the main findings of that section in the context of the relevant, field specific, literature. This chapter will discuss the primary findings from each chapter in the context of the project as a whole and consider the potential of delivering furanones in a controlled manner to inhibit biofilm formation in chronic wounds by *P. aeruginosa*.

The main conclusions from this work have been:

1. Amorphous PVA-borate hydrogels are an unsuitable vehicle for delivery of furanones to chronic wounds.
2. Simple PVA aerogels can be loaded with, and release, furanone compounds.
3. Furanones can effectively inhibit early biofilm formation by *Pseudomonas aeruginosa* PAO1 and can reduce biofilm biomass in established biofilms.
4. The developed wound model is suitable for the growth of clinically representative *P. aeruginosa* wound biofilms.
5. Sotolon-loaded PVA aerogels show potential as anti-biofilm treatments for wounds containing a *P. aeruginosa* biofilm.

6.2 Hydrogels are unsuitable delivery vehicles for furanones

PVA-borate hydrogels were assessed as potential delivery mechanisms for furanones. While a suitable production method and formulation of hydrogel were identified it was found that, during the process of loading the hydrogel, the furanone compounds were significantly degraded. This degradation presented primarily as changes in the UV

absorbance though other changes, such as changes in the colour of the solution were also observed. Three of the tested compounds; HDMF, sotolon and ascorbic acid all showed changes in their maximum UV absorbance (see chapter two) and an overall decrease in total absorptivity. Both HDMF and ascorbic acid showed a change in colour when loaded into the formulated hydrogel. While the colour change for HDMF was rapid, the change observed in ascorbic acid samples was delayed and occurred slowly over several days. Finally, while one furanone compound, MTHF did not display any obvious change in λ_{max}, the total UV absorbance spectrum was altered and showed a compound that was absorbing across a broad range of wavelengths.

Due to the process of preparing the hydrogels the furanones were exposed to a number of conditions that could potentially cause compound degradation. These were extended exposure to high temperature (90 °C for up to 3 hours), exposure to a solution of the borate crosslinker, and exposure to the elevated pH caused by the presence of the borate. Each of these scenarios was examined independently of the others to identify the cause of the degradation. However, it was found to be a combination of all of these factors that caused the changes in the compounds. Interestingly, it was shown that the effects of each factor were not the same for each furanone. A simple summary each tested condition and their effect on the furanone compounds can be seen in Table 6.1

While this degradation of the furanone compounds was unexpected, it was in keeping with the available literature. As previously discussed in section 2.5 of chapter two, increased temperature and changes in pH have been shown to cause degradation in HDMF and ascorbic acid in aqueous solution (Shu, Mookherjee and Ho, 1985; Roscher, Schwab and Schreier, 1997; Yuan and Chen, 1998). This work showed that

the combination of factors needed to bring about changes in λ_{max} and total absorptivity of a furanone was unique to each compound. This meant that for each of the four furanones to remain stable they could not be exposed to high temperatures, borate or significantly altered pH.

Table 6.1 - A summary of the effect of each tested factor and its effect on each of the four furanone compounds. Cells highlighted in green showed no change in either total absorbance or λ_{max}. Yellow highlighted cells indicate a change in either total absorbance or λ_{max} and red highlighted cells show a change in both. The specific changes are detailed in each cell.

	Water 25°C	Water 90°C	1% Borate 25°C	1% Borate 90°C	Altered pH 25°C	Altered pH 90°C
MTHF				↑ Abs		
HDMF		↓ Abs	↑ λ_{max}	↑ λ_{max} ↓ Abs		↓ Abs
Ascorbic acid	↓ Abs	↓ Abs	↑ λ_{max} ↓ Abs	↑ λ_{max} ↓ Abs	↑ λ_{max} ↓ Abs	↑ λ_{max} ↓ Abs
Sotolon		↑ Abs	↑ λ_{max}	↑ λ_{max} ↓ Abs	↑ λ_{max} ↓ Abs	↑ λ_{max} ↓ Abs

One potential solution for this issue would be to different hydrogel types such as physically crosslinked gels prepared by freeze thaw. The use of such gels could minimise the conditions that degrade each compound (Hennink and van Nostrum, 2012; Zhang, Zhang and Wu, 2013). The findings of these experiments prompted the development of both a novel cold-loading method for loading furanones into a hydrogel while minimising interactions with free borate as well as the development and characterisation of a novel PVA aerogel.

6.3 Furanones can be loaded into simple PVA aerogels for direct delivery to chronic wounds

To circumvent the issues caused by exposure to heat and free borate ions, furanones were first loaded into a hydrogel by rehydrating a lyophilised and powdered hydrogel

with a furanone solution. It was hypothesised that, as this process was performed at room temperature, it would minimise the thermal degradation caused by the traditional hydrogel production method. Further, it was hypothesised that, because the hydrogel was crosslinked prior to drying, the presence of free borate in the system would be minimised, as much of it would be bound in crosslinks. It was found that a powdered form of the dried hydrogel was well rehydrated with deionised water, giving a high-quality hydrogel that was not rheologically different to its pre-dried state. However, despite these promising findings, when the dried hydrogels were rehydrated with a furanone solution, the hydrogel either became discoloured, as was the case with HDMF and ascorbic acid-loaded samples, or the hydrogels remained entirely liquid when rehydrated, as with ascorbic acid and sotolon-loaded samples. This meant that, while exposure to high temperature could be minimised, the presence of any amount of borate would cause HDMF, sotolon and ascorbic acid to be degraded. Indeed, chemical crosslinking agents are known to potentially cause negative effects in the production of hydrogels. While this is not widely supported by the primary literature, many studies claim the use of physical crosslinking to be more advantageous as it can ameliorate issues with chemical crosslinking agents such as potential toxicity, crosslinker leeching, and interactions with drug payloads (Berger *et al.*, 2004; Hu *et al.*, 2019).

These findings prompted the development of a drug delivery system that required no heating to produce and contained no borate crosslinker. To achieve this, a PVA aerogel was developed.

The developed aerogels showed an interesting microstructure that appeared to be dependent on the concentration of the polymer solution used to produce them. It was

shown that at higher polymer concentrations (and therefore higher aerogel density) the internal structure was highly ordered with the fibrous structure aligning spontaneously. This structure became less ordered at lower polymer concentrations (and lower aerogel density). As discussed in chapter three it was believed that this was due to directional freeze concentration of the polymer (Butler, 2002; Zhang *et al.*, 2005). Whether this structure affected drug loading or drug release remains unclear. While optical and electron microscopy showed an ordered structure, X-ray CT scanning showed that this structure was not homogenous throughout the entire material, with many areas having a higher overall density than others. Despite this PVA aerogels could be loaded with furanone easily.

As no heating or crosslinker were required for their production, it was hypothesised that each compound would be stable when loaded into the aerogels. This was found not to be the case for all furanones. When loaded with furanones, aerogels appeared to contain significantly higher concentrations of MTHF and ascorbic acid after lyophilisation when compared to the actual loaded dose. Conversely, concentrations of HDMF and sotolon were significantly decreased. This increase in concentration of MTHF was similar to that observed in the loaded hydrogels. The apparent increase in ascorbic acid was unexpected and was believed to be due to a form of degradation caused by exposure to an aqueous environment. The significant decrease in the concentrations of HDMF and sotolon was hypothesised to be due to the inherent volatility of the compounds. It was thought that the furanones were being lost while under vacuum during the lyophilisation process. Though there are no reports of this from the pharmaceutical sector, the loss of volatile compounds following lyophilisation is a known phenomenon in the food industry (Huang *et al.*, 2016; Nöfer *et al.*, 2018). However, when examining data from the food industry the effect of

drying method on furanones specifically is not clear as other factors such as enzymatic browning can produce furanones and furan derivatives, thus, making the true impact of lyophilisation on furanone loss unclear (de Torres *et al.*, 2010). Despite this, it is clear that drying can impact on volatile compounds and so the aerogel freeze-drying protocol was optimised to minimise furanone loss. This optimisation greatly improved the concentration of retained furanone post freeze-drying.

The final stage of aerogel characterisation was to demonstrate furanone release from a loaded gel. This was achieved in two formulations of aerogel for both HDMF and sotolon. MTHF and ascorbic acid showed total furanone release of more than 100% and so it was decided that these two compounds would be excluded from further formulation work.

The work conducted in chapter two demonstrated that not only were PVA-borate hydrogels unsuitable for furanone delivery, but that the issues observed were caused by a combination of exposure to the borate crosslinker and the elevated temperatures required for hydrogel formation. The experiments detailed in chapter three showed that the use of a minimally crosslinked PVA aerogel can ameliorate these problems. These aerogels are easily loaded with furanones and do not cause significant degradation of HDMF and sotolon. These aerogels were then carried forward for assessment as a system for delivering furanones to bacterial biofilms.

6.4 Furanones have potential as antibiofilm therapies against *P. aeruginosa*

With a furanone delivery mechanism having been formulated and characterised, furanones were assessed for their ability to inhibit biofilm formation in *P. aeruginosa*.

It was shown, through differential staining, biochemical assays, and genetic characterisation, that the chosen strain was indeed *P. aeruginosa* DSM50071. It was also shown that the strain grew appropriately in the chosen medium and that it formed biofilm.

The minimum inhibitory concentrations of each furanone were then assessed. It was found that the MIC for HDMF was significantly higher than previously reported in the literature (Choi *et al.*, 2014). The MIC for ascorbic acid could not be compared to a similar study, but the reported MIC of the similar compound, sodium ascorbate, was significantly higher than the established MIC in this work. These differences were initially attributed to the use of a different bacterial strain to the published literature (Choi *et al.*, 2014; El-Mowafy *et al.*, 2014). The MIC for sotolon and MTHF could not be compared to other studies as there have been no published works using these compounds.

It was then shown that both ascorbic acid and MTHF were not able to inhibit biofilm formation in *P. aeruginosa* at any fraction of the established MIC after 24 hours. While no data is available for MTHF, previous studies have shown the sodium salt of ascorbic acid is capable of reducing biofilm formation by *P. aeruginosa* at concentrations as low as one twentieth the MIC established in that study (El-Mowafy *et al.,* 2014). Conversely, both HDMF and sotolon were able to significantly reduce biofilm at a one half the established MIC during the same time frame. HDMF could also inhibit biofilm formation at one quarter MIC. Following longer furanone treatments, it was shown that both HDMF and sotolon significantly reduced biofilm formation and maintained the reduction for up to 72 hours post treatment. This was then confirmed by using BacLight staining. It was also shown that the furanone

treatment did not result in significantly higher numbers of non-viable cells in the formed biofilm.

Subsequently, both HDMF and sotolon were shown to be effective in reducing the mass of mature, 24 hours old biofilms while both ascorbic acid and MTHF had no effect. However, when applied to a mature, 48 hours old, biofilm it was found that HDMF caused a significant increase in biofilm biomass and sotolon showed no effect when applied to a similar biofilm. These data suggested that, while furanones could be very effective in reducing the biomass of wound biofilms, the time frame in which they remained effective may be narrow. As ascorbic acid and MTHF showed no effect they were excluded from further microbiological testing.

Finally, it was demonstrated that both HDMF and sotolon retained their antibiofilm effects when delivered to a biofilm using the developed aerogel system. It was shown that when applied at the point of inoculation, both HDMF and sotolon-loaded aerogels were highly effective in reducing biofilm biomass versus an unloaded control. Sotolon reduced biomass by up to 100%. When applied to mature, 24 hour and 48 hours old biofilms, aerogel delivered HDMF showed a significant decrease in biofilm biomass. Conversely, aerogel delivered sotolon showed a significant reduction in biofilm biomass 48 hours post application to a 48 hours old biofilm. These findings, again, reinforce the hypothesis that furanones, even when delivered using the developed aerogels, can be an effective treatment, but only if used at the right time.

The data presented in this chapter, while promising, had low applicability to real-world chronic wounds. Due to this limited applicability, it was decided that a more clinically relevant wound model would be developed in order to further assess the furanone-loaded aerogels.

6.5 The development of a clinically relevant wound model

While promising, the data collected using the microtitre dish assays were of limited relevance to an *in vivo* wound infection. For these reasons, it was decided that an appropriate wound infection model should be used. However, when reviewing the literature to select the most appropriate model it was apparent that the available models had several limitations including non-representative nutrient profiles or poorly representative growth substrates. Therefore, the final experimental chapter of this thesis focused on the development of a novel *in vitro* chronic wound biofilm assay.

The development of the wound model involved formulating a novel wound-like growth medium. This medium consisted of protein, salts, blood and muscle cell lysate. This growth medium, with a wound-like nutrient profile, was essential as it has been shown that nutrient availability can effect many aspects of biofilm formation and response to treatments (Anderl *et al.*, 2003; Sauer *et al.*, 2004; Cherifi *et al.*, 2017; She *et al.*, 2019). This medium proved to be excellent for biofilm growth and showed rates of growth similar to those observed with nutrient agar.

However, the use of the wound-like medium as a nutrient source for biofilms gown on polycarbonate membranes alone was not a sufficient wound model. When testing both the loaded aerogels and the clinically relevant wound dressings there was no significant reduction in biofilm or bacterial killing. It was subsequently shown that this lack of antibiofilm effect was due to limited release of the active components from the aerogels into the medium. This prompted a modification of the model to add a fluid reservoir, consisting of a volume of simulated body fluid. This modification increased the volume of material into which the furanones could release. This modification vastly improved the efficacy of the furanone-loaded aerogels. Results showed that

treatment with subinhibitory concentrations of sotolon resulted in a 3.65 log decrease in viable cell numbers in biofilms. In addition to this, using the modified wound model to assess clinically used wound dressings showed clear antimicrobial efficacy for both Aquacel Ag and Inadine, as expected.

This chapter aimed to develop a wound model capable of growing clinically representative *P. aeruginosa* wound biofilms for the assessment of novel wound dressings. A successful model was developed and used to show that PVA aerogels are a potentially excellent method to deliver antimicrobial compounds to infected chronic wounds. Furthermore, the data presented in this chapter clearly demonstrate that furanones, and sotolon in particular, have potential as novel anti-biofilm wound therapeutics.

6.6 Conclusion

The data presented in this thesis are promising. While the work of chapter two demonstrated that furanones are not suitable for use in every drug delivery mechanism, they can be delivered to bacterial biofilms using polymer aerogels. However, when used as antibiofilm agents the efficacy of furanones was variable. It is hypothesised that the efficacy of furanones largely depends on the time and, therefore, stage of biofilm formation at which they are applied. Unfortunately, it has not been possible to fully investigate this during the course of this project.

The development of a novel PVA aerogel for the delivery of active compounds to bacterial biofilms during this project has opened up many possibilities for further study. The aerogels used here have undergone minimal optimisation and characterisation due to time and funding constraints. As such, in order to realise the full potential of the developed aerogels, significantly more work is needed. To this

end, an extensive research proposal has been developed and included as the final chapter in this thesis. The work described in this proposal will aim to further develop the polymer aerogel drug delivery system and do so specifically in the context of delivering and optimising furanones and their use as an antibiofilm wound therapy.

6.7 References

Anderl, J. N. *et al.* (2003) 'Role of nutrient limitation and stationary-phase existence in *Klebsiella pneumoniae* biofilm resistance to ampicillin and ciprofloxacin', *Antimicrobial Agents and Chemotherapy*, 47(4), pp. 1251–1256. doi: 10.1128/AAC.47.4.1251-1256.2003.

Berger, J. *et al.* (2004) 'Structure and interactions in covalently and ionically crosslinked chitosan hydrogels for biomedical applications', *European Journal of Pharmaceutics and Biopharmaceutics*, 57(1), pp. 19–34. doi: 10.1016/S0939-6411(03)00161-9.

Butler, M. F. (2002) 'Freeze Concentration of Solutes at the Ice/Solution Interface Studied by Optical Interferometry', *Crystal Growth and Design*, 2(6), pp. 541–548. doi: 10.1021/cg025591e.

Cherifi, T. *et al.* (2017) 'Impact of Nutrient Restriction on the Structure of Listeria monocytogenes Biofilm Grown in a Microfluidic System', *Frontiers in Microbiology*, 8, p. 864. doi: 10.3389/fmicb.2017.00864.

Choi, S. C. *et al.* (2014) 'Inhibitory effects of 4-hydroxy-2,5-dimethyl-3(2H)-furanone (HDMF) on acyl-homoserine lactone-mediated virulence factor production and biofilm formation in *Pseudomonas aeruginosa* PAO1', *Journal of Microbiology*, 52(9), pp. 734–742. doi: 10.1007/s12275-014-4060-x.

El-Mowafy, S. A., Shaaban, M. I. and Abd El Galil, K. H. (2014) 'Sodium ascorbate as a quorum sensing inhibitor of *Pseudomonas aeruginosa*', *Journal of Applied Microbiology*, 117(5), pp. 1388–1399. doi: 10.1111/jam.12631.

Hennink, W. E. and van Nostrum, C. F. (2012) ‘Novel crosslinking methods to design hydrogels’, *Advanced Drug Delivery Reviews*, 64, pp. 223–236. doi: 10.1016/J.ADDR.2012.09.009.

Hu, W. *et al.* (2019) ‘Advances in crosslinking strategies of biomedical hydrogels’, *Biomaterials Science*, 7, p. 843. doi: 10.1039/c8bm01246f.

Huang, Q. *et al.* (2016) ‘Effect of Different Drying Method on Volatile Flavor Compounds of Lactarius deliciosus’, *J Food Process Technol*, 7(8). doi: 10.4172/2157-7110.1000615.

Nöfer, J. *et al.* (2018) ‘The Influence of Drying Method on Volatile Composition and Sensory Profile of Boletus edulis’. doi: 10.1155/2018/2158482.

Roscher, R., Schwab, W. and Schreier, P. (1997) ‘Stability of naturally occurring 2,5-dimethyl-4-hydroxy-3[2H]-furanone derivatives’, *European Food Research and Technology*, 204(6), pp. 438–441. doi: 10.1007/s002170050109.

Sauer, K. *et al.* (2004) ‘Characterization of nutrient-induced dispersion in *Pseudomonas aeruginosa* PAO1 biofilm’, *Journal of Bacteriology*, 186(21), pp. 7312–7326. doi: 10.1128/JB.186.21.7312-7326.2004.

She, P. *et al.* (2019) ‘Effects of exogenous glucose on *Pseudomonas aeruginosa* biofilm formation and antibiotic resistance’, *MicrobiologyOpen*, 8(12). doi: 10.1002/mbo3.933.

Shu, C.-K., Mookherjee, B. and Ho, C.-T. (1985) ‘Volatile Components of the Thermal Degradation of 2,5 - dimethyl-4-hydroxy-3(2H)-furanone’, *Journal of Agricultural and Food Chemistry*, 07735, pp. 446–448.

de Torres, C. *et al.* (2010) 'Effect of freeze-drying and oven-drying on volatiles and phenolics composition of grape skin', *Analytica Chimica Acta*. Elsevier, 660(1–2), pp. 177–182. doi: 10.1016/j.aca.2009.10.005.

Yuan, J. P. and Chen, F. (1998) 'Degradation of Ascorbic Acid in Aqueous Solution', *Journal of Agricultural and Food Chemistry*, 46(12), pp. 5078–5082. doi: 10.1021/jf9805404.

Zhang, H. *et al.* (2005) 'Aligned two- and three-dimensional structures by directional freezing of polymers and nanoparticles', *Nature Materials*, 4(10), pp. 787–793. doi: 10.1038/nmat1487.

Zhang, H., Zhang, F. and Wu, J. (2013) 'Physically crosslinked hydrogels from polysaccharides prepared by freeze–thaw technique', *Reactive and Functional Polymers*, 73(7), pp. 923–928. doi: 10.1016/J.REACTFUNCTPOLYM.2012.12.014.

Chapter 7

Proposal for future work:

"In-situ degrading polymer aerogels as drug delivery systems for use in both acute and chronic wounds"

7.1 Introduction

The work conducted during this project has provided promising data that suggests furanones have may potent antibiofilm effects when applied to early stage infections. This effect was apparent when applied both directly to the biofilm as a bolus dose, and when using an aerogel delivery system. Furthermore, it was shown that when added to a late-stage biofilm directly, furanones were able to effectively reduce biofilm biomass. It was suggested that the organism used in this work had a significantly higher resistance to furanones than expected when it was originally selected (through enhanced furanone efflux) and thus was able to remove the compound from the intracellular environment. This means that an effective intracellular dose was difficult to achieve. While interesting, the findings of this work are not broadly applicable to all *P. aeruginosa* strains and infections. This finding has provided an opportunity to further investigate the use of furanones and furanone-loaded aerogels as wound therapeutics.

Based on findings detailed in the preceding experimental chapters, this chapter will discuss ways in which this research may be further developed and translated to gain maximum benefit from the use of furanones and furanone-loaded aerogels. This discussion will be presented in the form of a detailed project proposal and will have several primary objectives. First, to optimise and characterise the aerogels developed as part of this work. This will ensure a robust delivery vehicle for the furanone compounds. Aerogels will be optimised as *in-situ* degrading dressings which do not require removal from a wound upon dressing change. Second, to investigate the anti-biofilm and anti-virulence effects of furanones against both susceptible and resistant organisms. This will take the form of furanone only treatments and furanones used in combinations with other therapeutics (such as currently used antimicrobials) under

both early and late infection conditions. Third, to characterise the effects of the most potent furanone treatments (both furanone only and combination treatments) on mammalian cells. Finally, robust *in vivo* assessment of the developed wound dressings will be conducted.

7.2 Project summary

Chronic wounds do not heal and, as such, present a significant socio-economic burden to health services and patients worldwide. Currently, there is no effective treatment (Martinengo *et al.*, 2019) and chronic wounds are set to cost the UK NHS £9 billion per annum by 2023 (Guest *et al.*, 2016). Those suffering from a chronic wound experience debilitating comorbidities such as persistent pain, reduced mobility, social isolation and negative effects on mental health (Renner and Erfurt-Berge, 2017).

Chronic wounds are caused by an acute wound becoming stuck in an inflammatory state. This can be due to a number of factors including presence of foreign bodies, poor circulation or continued physical trauma (Frykberg and Banks, 2015). However, bacterial infection is the most common reason for this failure to heal. When present in wounds, bacteria mainly grow in the form of a biofilm. Here, the bacteria are protected by a self-produced polymer matrix (Malone *et al.*, 2017), making them much more difficult, if not impossible to eradicate (Flemming *et al.*, 2016).

Topical antibiotics are not routinely used in the treatment of chronic wounds due to potential side effects such as irritation of the surrounding skin, sensitivity reactions, and potential systemic toxicity from prolonged use (Healy and Freedman, 2006). As an alternative, dressings which contain silver, iodine, and biguanide compounds are commonly used (e.g. AquacelAg, Inadine and Telfa AMD, respectively). However, these antiseptic dressings are expensive (some costing more than £20 per dressing). While they are the preferred course of treatment for such wounds, often the use of advanced dressings does not produce better clinical outcomes for patients in terms of wound healing (Dumville, Keogh, *et al.*, 2015; Dumville, Stubbs, *et al.*, 2015). Furthermore, these dressings require removal upon dressing change. This removal can

cause additional trauma to the wound site by damaging newly formed epithelial and granular tissues, as well as potentially removing of portions of the stratum corneum, thus, affecting the overall integrity of the skin (Matsumura *et al.*, 2013). Indeed, some 97% of wound care specialists have reported further damage such as wound enlargement, pain or bleeding upon removal dressings (Charlesworth *et al.*, 2014). In addition to the physical damages wound dressings can cause, the pain of removing an adhered dressing is a significant source of anxiety and worry for patients (Woo, 2010).

It is clear, therefore, that alternative wound treatments are needed. This project will develop wound dressings which undergo complete matrix dissolution in the wound environment (therefore, not requiring removal upon dressing change) in order to deliver antibiofilm drug compounds to both acute and chronic wounds. Development of a material with these properties will allow clinicians to apply a dressing which will effectively prevent biofilm formation in contaminated wounds and promote the removal of biofilms in established chronic wounds. Further, this dressing will not become adhered to the wound bed, thus, removing the potential for further trauma upon dressing change. This would represent a significant improvement over current therapies.

During this PhD, a minimally crosslinked PVA aerogel formulation has been developed for use as a wound drug delivery system. The developed aerogel has unique properties including high drug loading capacity and effective delivery of phytochemicals to bacterial biofilms. Further work is now required to optimise both physical and chemical characteristics of the aerogel in order to control parameters such as the polymer matrix dissolution rate, drug release kinetics, and physical properties

(such as material porosity) in order to realise the potential of this PVA aerogel as a wound therapeutic.

To achieve this, aerogels will be produced while modifying variables including polymer composition, polymer concentration, and cross-linking density. The produced aerogels will be extensively physically and structurally characterised to determine the effect of these changes on pore density, size, homogeneity, and structural homogeneity. Aerogels will then be loaded with a series of furanone compounds and drug release kinetics established via experimentation using an in-house method. Further, release mechanisms will be elucidated by using an appropriate mathematical model of drug release.

The developed aerogel material undergoes complete dissolution in the wound environment and therefore 100% release of the loaded drug is achievable, facilitating the application of highly targeted doses of active compounds to patients.

Following successful development of drug loaded aerogels, their antibiofilm efficacy against common wound pathogens will be demonstrated *in vitro* and their biocompatibility with human cells will be shown. The aerogels developed during this project will greatly improve clinical outcomes by simultaneously addressing issues surrounding antimicrobial compound delivery to wounds and potential trauma associated with dressing removal.

7.3 Background

A chronic wound is any wound which fails to progress through the normal process of wound healing. The development of a chronic wound can have a significant impact on patients, not only in terms of their physical health but their also mental well-being.

7.3.1 The process of wound healing

Normal wound healing involves several distinct but overlapping processes in which numerous cell types coordinate both spatially and temporally to successfully close a wound. The first stage of wound healing is the haemostasis phase. After a wound is sustained, blood vessels constrict and platelets aggregate and form a fibrinous clot (Zaidi and Green, 2019). Haemostasis is followed by an inflammatory stage in which immune cells such as neutrophils are recruited to the injury site and act as a primary defence against infection. Following this, other immune cells are recruited. Cells, such as monocytes, are activated to become macrophages which further protect against bacterial infection. Numerous other cells including dendritic cells and T-cells are also involved in this complex stage. After the inflammatory stage is the proliferative phase. During this phase the formation of new blood vessels at the wound site occurs in a process known as angiogenesis. Angiogenesis is accompanied by the production of new connective tissue by dermal fibroblasts. This mix of new blood vessels and connective tissue is known as granulation tissue. This is followed closely by reepithelialisation in which new epithelial cells begin to form, beginning at the wound edge, and regenerate the protective layer of skin, thus, restoring barrier function (Rodrigues *et al.*, 2019). When an acute wound is sustained in a healthy individual these stages progress seamlessly from one to the next and the wound is able to heal rapidly.

7.3.2 The development of a chronic wound

Under normal circumstances wounds will progress through the processes detailed above and the wound will heal appropriately. However, both intrinsic and extrinsic factors can interrupt the transition from one phase to the next. When this occurs, wound healing will fail, and a chronic wound is formed. Internal factors capable of interrupting the wound healing process include underlying health conditions such as diabetes and genetic disorders like sickle cell disease (Morton and Phillips, 2016; Dewi and Hinchliffe, 2019). External factors include those such as the presence of a foreign body in the wound, or persistent low-grade trauma to the wound bed (Frykberg and Banks, 2015; Han *et al.*, 2017; Waquad *et al.*, 2020). However, the most common cause of failure to heal in wounds is bacterial infection (Leaper, Assadian and Edmiston, 2015). When present in a wound, bacteria primarily grow in communities encased in a polymer matrix known as a biofilm. When growing in this form, bacteria have high levels of protection against host immune defences (Pier *et al.*, 2001). These biofilms elicit an inflammatory response from the hosts immune system but, due to the biofilms resilience against processes such as opsonisation and subsequent phagocytosis, they cannot be cleared (Mishra *et al.*, 2012). When a biofilm is not cleared, the inflammatory processes continue, and this results in a persistent inflammatory state within the wound. As the inflammatory stage of wound healing is unable to be resolved the process of wound healing cannot continue and a chronic wound results (Schultz *et al.*, 2017). These biofilms also provide the bacteria with greatly increased protection against treatment with antimicrobials, making them incredibly difficult, and often impossible, to eradicate (Mah and O'Toole, 2001; Mah, 2012). Due to the resilience of biofilms, chronically infected wounds may persist for months or years. During this time, they will require regular wound care (usually

provided daily) and regular consultation with clinicians, such as tissue viability specialists, general practitioners, infection specialists, and vascular teams. The prolonged and involved nature of chronic wound care makes their treatment very expensive.

7.3.3 The socio-economic impact of chronic wounds

The treatment of wounds and their associated complications currently costs the NHS £5.3 billion per year (Guest *et al.*, 2016). This is on par with the total cost of cancer care for the NHS in 2009/10 (Sullivan *et al.*, 2011). Furthermore, this figure is predicted to increase to £9 billion per annum by 2023 (Guest *et al.*, 2016). Chronic wounds are a persistent problem worldwide with some reports stating their prevalence at 2.21 per 1000 population (Martinengo *et al.*, 2019). If these estimates are indeed correct that would suggest that, in the UK, approximately 150,000 people currently suffer from a chronic wound. However, it is likely that these estimates are significantly lower than the actual prevalence as chronic leg ulcers alone have been shown to affect 731,000 people in the UK each year. With an associated cost to the NHS of £1.94 billion per annum (Guest, Vowden and Vowden, 2017), leg ulcers represent a significant economic burden for the NHS. Furthermore, chronic ulcers (a chronic wound that was caused by an internal factor rather than an external injury) as a whole have been estimated to affect between 0.6-3% of people over 60 and up to 5% in people over 80 (Rayner *et al.*, 2009). With over 390,000 people in the UK being over the age of 80 in 2019 (Office for National Statistics, 2020) this would suggest a potential 20,000 chronic ulcers in this age group alone. It is clear that chronic wounds are highly prevalent and, when the increasing age of the general population is considered, their incidence will likely continue to rise further adding to costs.

7.3.4 Current chronic wound therapies

Current guidance on the treatment of infected chronic wounds is contradictory and decisions on treatment are made on a case by case basis by clinicians. However, many clinicians are confused about when to use antimicrobial treatments or if their use is appropriate at all (Lipsky and Hoey, 2009). Many clinicians tend to avoid the use of topical antimicrobials as studies surrounding their efficacy remain inconclusive, and many cite other concerns such as difficulty in accurate dosing for topical preparations like creams and ointments (Lipsky and Hoey, 2009). Indeed, many health boards in England advise against the use of topical antimicrobials in wound treatment due to their broad spectrum of activity and concerns regarding the development of antimicrobial resistance (Cambridgeshire and Peterborough Foundation Trust, 2012; Brawn, 2015). The difficulty in accurate dosing of topical antimicrobials may, in fact, be a significant contributor to the development of resistance when using them. With inaccurate dosing, it is more likely that bacteria will be continuously exposed to sub-lethal doses of antimicrobial compounds. This is well known to be a driver for the development of resistance. Further, the very design of some antimicrobial dressings greatly increases dosing inaccuracies. Examples of this include antimicrobial wound dressings such as Aquacel Ag, Inadine and Telfa AMD which contain silver, iodine, and PHMB respectively. While these compounds are effective antimicrobials, the dressings mechanism of drug release means that compound release from these dressings to the wound site is not consistent or repeatable. Dressings such as these require a moist environment in which to work as they must be rehydrated in order to initiate release of their active components. Other dressings made of alginates and foams also require a moisture in order to release their antimicrobial payload. This means that day to day variations in wound exudate will cause variations in

administered doses from such dressings (Thomas and McCubbin, 2003). In addition to this, some clinical guidelines suggest cutting antimicrobial dressings to fit the wound size and shape (Cambridgeshire and Peterborough Foundation Trust, 2012). This will effectively reduce the levels of antimicrobial being applied to the wound and further encourage underdosing. These limitations make it impossible for clinicians to be certain that an effective dose of antimicrobial has been delivered to the wound. The same holds true of topical antibiotic creams and ointments. Anabact gel containing 0.75% metronidazole is occasionally applied to infected wounds. However, doses will vary considerably if applied in a thin layer or generously. Without applying exact weights, accurate dose measurement is impossible. Chronic underdosing in cases such as these has significant potential to encourage the development of antimicrobial resistance in infected wounds, which only makes eradication of the infection harder (Williamson, Carter and Howden, 2017; Carter *et al.*, 2018).

7.3.5 Preventing acute wound infection

Infection in acute wounds can come from a number of sources. Several types of wounds present a significantly increased risk of wound infection. These include bite wounds (both bites by animal and humans), those wounds with visible contamination (for example with soil or gravel), wounds with foreign bodies present (such as shards of glass) and burn wounds (Church *et al.*, 2006; Rothe, Tsokos and Handrick, 2015; WHO, 2020). Even simple injuries such as clean lacerations of the hand have been shown to have an infection rate of approximately 4.8% (Roodsari, 2015). It has also been shown that in wounds a biofilm can be identified as soon as 6 hours after initial infection (Percival, McCarty and Lipsky, 2015). It is this biofilm that can eventually cause the prolonged inflammatory response that leads to failure to heal. Disinfection of acute wounds should be a priority in order to prevent the development of infections

leading to biofilm development and chronic wound formation. Current treatment guidelines recommends the application of disinfectants such as iodine, or antimicrobials like silver sulfadiazine to high risk wounds such as animal bites and burns respectively (Rothe, Tsokos and Handrick, 2015; Cartotto, 2017). While effective, these treatments have the same limitations as those used in chronic wound. This means that, although antimicrobials are being used, it is likely that total disinfection will not be achieved and the possibility of remaining organisms forming a biofilm persists. The use of an antibiofilm agent in wound dressings may help to ameliorate this. Even if some bacterial cells remain in a wound following infection, the presence of a biofilm inhibitory compound would be of benefit. This would prevent any remaining cells from forming a biofilm and causing a chronic wound to form. Thus, a method of delivering biofilm inhibitory compounds to acute wounds would be of great value.

7.3.6 Addressing chronic wound biofilm

Over 90% of all chronic wounds contain microorganisms living within a biofilm (Attinger and Wolcott, 2012). Any effective treatment aimed at improving healing in chronic wounds must address bacterial biofilms as a priority. This means that quorum sensing inhibitors are excellent candidate molecules for use in chronic wound therapeutics. The use of furanones as effective quorum sensing inhibitors against a range of pathogens has been demonstrated (Ren, Sims and Wood, 2001; Hentzer *et al.*, 2002, 2003; Wu *et al.*, 2004; Lianhua *et al.*, 2013; Choi *et al.*, 2014). However, the application of non-optimal doses of compounds to wounds is not only problematic when delivering antimicrobials but would also likely be problematic when delivering antibiofilm compounds such as furanones. Indeed, it has been shown previously that resistance to furanone compounds is possible, and such resistance is also present in

many clinical isolates already (Maeda *et al.*, 2012; García-Contreras *et al.*, 2013). Underdosing must, therefore, be addressed in the development of an antibiofilm dressing. It is clear that a method of delivering precise doses of compounds, whether they are antimicrobials or antibiofilm agents, to infected wounds would be invaluable.

The work proposed here will further develop a novel polymer aerogel drug delivery system capable of delivering active compounds directly to chronic wounds through *in situ* matrix dissolution (Figure 7.1). Further, the developed aerogels will be loaded with a range of furanone compounds with proven antibiofilm activity and their efficacy against a range of common biofilm forming wound pathogen under chronic wound conditions will be shown. By undergoing total matrix dissolution, the aerogels described here will deliver 100% of their drug payload allowing for precise dosing to be achieved in wounds for the first time.

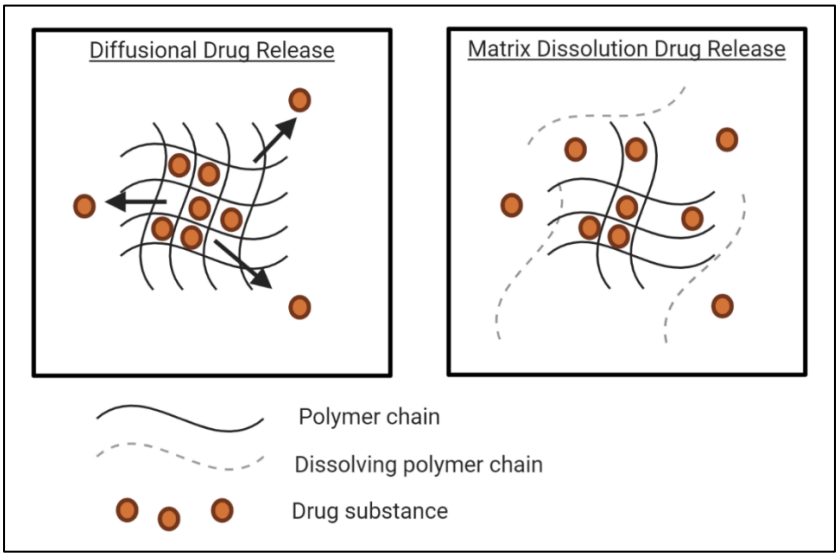

Figure 7.1 – A comparison of diffusional drug release achieved by formulations such as some polymeric hydrogels with the matrix dissolution mediated drug release of the aerogels proposed here.

Diffusional drug release occurs with a concentration gradient where drug substances move from a higher concentration (within the drug delivery system) to a lower concentration (in the wound bed). When mediated by matrix dissolution drug is steadily liberated as the aerogel matrix dissolves releasing the drug substance.

This project will address the significant problem of chronic wounds on two fronts. Firstly, by developing novel therapies for acute wounds which will prevent the early infections that cause a wound to become chronic. Secondly, by developing a wound dressing which will effectively reduce bacterial biofilm in chronic wounds which will allow the wounds to heal normally. The developed aerogel dressings will not require removal from the wound upon dressing change and so the trauma of dressing adherence, which commonly causes worsening of a wound, will be avoided. This represents a significant improvement over current clinically used chronic wound therapies.

7.4 Aims and objectives

To deliver *in situ* degrading aerogels for drug delivery to acute and chronic wounds this project has five primary aims. This project will determine:

1. the effects of polymer choice, concentration and crosslinking density on the matrix dissolution properties of polymer aerogels so that aerogels with precise drug release profiles can be made.
2. that antimicrobial aerogels deliver effective doses of furanones to ensure chronic wound bacterial biofilms can be eradicated
3. that furanone-loaded aerogels effectively prevent biofilm formation by low concentrations of bacteria in an acute wound environment so that initial wound infection can be prevented.
4. the biocompatibility of the developed antimicrobial aerogels so that aerogel treatments do not negatively impact mammalian cells and the wound healing process.

5. the *in vivo* efficacy of the developed aerogels in a mouse model of chronic wound infection and acute burn wound infection.

7.5 Proposed methods

This project will deliver novel antibiofilm therapies for both acute wounds and chronic wounds, preventing early infections that cause wounds to become chronic and, in the case of chronic wounds, eradicating the bacterial biofilms that prevent normal healing. In order to generate primary project outcomes, the following research activities will be undertaken.

7.5.1 Work Package 1 – Preparation of aerogel formulations (0-16 months)

Over 450 aerogel formulations with varying polymer types and concentrations will be prepared in order to identify those formulations with appropriate matrix dissolution properties. This work will generate aerogel formulations designed for drug release to chronic wounds and acute wounds. This work package will also increase understanding of the factors affecting aerogel matrix dissolution and drug release.

It is hypothesised that:

- Aerogels with lower polymer concentrations will dissolve more rapidly in aqueous environments.
- Aerogels with higher porosity will dissolve more rapidly in wound environments.
- Higher degrees of polymer crosslinking will attenuate matrix dissolution rates and prolong drug release times.
- Higher concentration of hydrophobic polymers in dual polymer aerogels will slow matrix dissolution.

To assess these hypotheses, over 450 aerogel formulations will be prepared using 17 polymers. A selection of 6 biocompatible synthetic polymers, or polymer precursors, will be used;

- poly vinyl alcohol (PVA)
- polyvinylpyrrolidone (PVP)
- polyacrylic acid (PAA)
- poly ethyene glycol (PEG)
- Gantrez,
- trimethyl orthosilicate (TMOS)

In addition to these, 11 natural biocompatible polymers will be used:

- xanthan gum
- pectin
- chitosan
- carrageenan
- guar gum
- hydroxypropyl methylcellulose (HPMC)
- albumin
- starch
- gelatin
- agar
- alginate

Each of these polymers has previously been used to make hydrogels for biomedical purposes. As such, production of an aerogel for wound therapeutics using these polymers is possible but has never been explored.

Single polymer aerogels will be produced from gels or sols containing 5% of each polymer by weight in an appropriate solvent. These single polymer aerogels will be prepared using three separate methods namely the lyophilisation method previously used in this work, the widely used critical point drying method (Baldino *et al.*, 2020) and the less frequently used ambient temperature and pressure drying. Following the

preparation of single polymer aerogels, aerogels containing a blend of 2 polymers will be prepared.

Aerogels containing each possible 2 polymer combination will be prepared. Gels and sols used to prepare the polymer blend aerogels will contain 5% total polymer by weight (i.e. 2.5% by weight of each polymer). Aerogels containing each polymer blend will be produced using the three methods named above. This work package will yield a potential 51 homopolymer aerogel formulations, and 408 dual polymer aerogels.

Each viable aerogel formulation will be loaded with a standardised concentration of a furanone. Formulations will be subjected to *in vitro* drug release testing using standard dissolution apparatus. Release data will be interrogated using the, first and zero order, Higuchi, and Hopfenberg mathematical models to identify the method of drug release from the aerogels. This will give detailed data on the viable aerogel formulations to release both hydrophilic and hydrophobic drugs as well as the method of release of each. Those formulations exhibiting drug release by matrix dissolution rather than, for example, simple diffusion will be carried forward for physical characterisation.

I will use SEM to obtain qualitative data on pore size and homogeneity and, in association with Professor Phillip Withers at the University of Manchester's X-ray Imaging Facility, I will use micro CT to assess internal structural homogeneity and pore type. Our partnership with Dr Volkan Degirmenci, an expert in the assessment of porous materials, at the University of Warwick will allow me to use nitrogen physisorption porosimetry to assess total pore volume, pore size, and pore size distribution in the developed aerogels. These research activities will lead to robust physical data that will facilitate our understanding of the relationships between aerogel structure, physical properties and drug release profiles. This information will underpin

the subsequent tuning of selected formulations (total polymer concentration, polymer ratio for dual polymer aerogels and presence or degree of crosslinking) to generate novel aerogels with precise drug release profiles and matrix dissolution times. This data will show that a high degree of control over drug dissolution is practically achievable and that tailored release kinetics can be designed *via* selective changes in formulation. Changes in drug release profiles will be correlated to changes in the measured physical properties of the aerogels (higher porosity, overall pore size etc.). These activities will generate vital knowledge regarding the relationship between aerogel formulation, physical properties, and drug release, therefore allowing greater control over, and rational design of, aerogel properties in future materials.

7.5.2 Work Package 2 – In vitro demonstration of aerogel-mediated delivery of furanones (16-24 months)

Firstly, it will be shown that aerogel-delivered furanones effectively inhibit the formation of bacterial biofilms, demonstrating the potential of drug-loaded aerogels for application to chronic wounds. Biofilm inhibition will be defined as at least a 3-log reduction in viable biofilm-bound bacterial cells, for which I will use the newly developed chronic wound biofilm model described in Chapter 5 of this work. I hypothesise that:

- aerogels will be effective in delivering therapeutic doses of furanones to bacterial biofilms.
- aerogels will be capable of delivering cocktails of several furanones to bacterial biofilms to achieve synergistic effects.
- treatment with furanone-loaded aerogels will cause a reduction levels of secreted virulence factors including degradative enzymes and siderophores in a wound-like environment.

To achieve these outcomes, loaded aerogels will be used to deliver furanones to biofilms under standard laboratory conditions. The efficacy of furanone-loaded aerogels to inhibit biofilm formation and reduce virulence factor production under chronic wound conditions will also be demonstrated.

Six representative wound organisms will be used; *Pseudomonas aeruginosa*, *Escherichia coli*, *Enterococcus faecalis*, *Staphylococcus aureus*, *Klebsiella pneumoniae*, and *Streptococcus pyogenes* (Bowler, Duerden and Armstrong, 2001). In addition to being commonly isolated from wound environments, each of the named species has been shown to use either homoserine lactones or a furanosyl borate diester known as autoinducer-2 in its intercellular signalling (Balestrino *et al.*, 2005; Li *et al.*, 2007; Siller *et al.*, 2008; Zhao *et al.*, 2010; Shao *et al.*, 2012). This means that each of these organisms may be susceptible to the antagonistic effects of furanone treatment.

The natural furanones HDMF and sotolon and the synthetic furanones C-30 and C-56 will be investigated. The MIC of these furanone compound against each organism, in the planktonic growth state, will be established using the standard EUCAST microdilution method and validated using a colorimetric TTC bacterial cell viability assay.

Following identification of the MIC of each furanones the minimum concentration of each furanone that effectively inhibits biofilm formation will be identified. Bacterial biofilms will be grown in nutrient rich medium (Deligianni *et al.*, 2010) in both the absence and presence of each furanone. A range of decreasing concentrations of each of the four furanones (beginning with the established MIC for planktonic cells) will be added directly to biofilm the growth medium. The rate of biofilm inhibition will be assessed using bacterial cell viability staining with BacLight live/dead stain (Murray

et al., 2017) and validated by direct enumeration of viable bacterial cells. Combination therapy consisting of two furanones will also be assessed for biofilm inhibitory effects using a standard checkerboard assay (Orhan *et al.*, 2005). This will identify synergistic effects that may allow for reductions in the concentrations of each furanone required to achieved effective biofilm inhibition. Similarly, combination treatments consisting of a furanone and classical antibiotics will also be tested to investigate the possibility of furanones potentiating biofilm killing by classical antimicrobials.

Confocal microscopy and SEM will be used to assess the effects of treatments on biofilm morphology (Reichhardt and Parsek, 2019). Changes including loss of 3D biofilm architecture and alterations to bacterial size, shape and distribution of both live and dead cells within the biofilm will be assessed. Treatments causing the greatest reduction in viable, biofilm bound, cells and the greatest impact on biofilm morphology will be taken forward for antimicrobial aerogel preparation.

Optimal aerogel formulations (as identified in work package 1) will be loaded with the most effective furanone treatments. This will be achieved by incorporating active compounds into the sol or gel phase prior to drying. I will also explore alternative drug loading strategies such as adsorption-based drug loading during supercritical drying (Lovskaya and Menshutina, 2020) to mitigate the effects of poor compound solubility on drug loading.

To assess the efficacy of furanone-loaded aerogels, the novel chronic wound biofilm model that was developed during this PhD, which is highly representative of the *in vivo* wound scenario, will be used. Biofilms will be grown at a physiological temperature on semipermeable polycarbonate membranes with a wound-like, semisolid, nutrient medium consisting of porcine muscle lysate, simulated body fluid,

blood and proteins. This medium was developed to represent the nutrient profile in a wound environment and has been used, during this PhD, to assess the efficacy of both clinically used antimicrobial wound dressings and novel aerogel dressings against bacterial biofilms. Biological activity of aerogels in this model will be assessed using cell viability staining and direct enumeration. In addition, the activity of relevant bacterial virulence factors including degradative enzymes such as protease, elastase and collagenase, that increase tissue damage and delay wound healing will be measured. These virulence factors will be measured using commercially available protease and collagenase assay kits, and a congo-red elastase assay (Oshri *et al.*, 2018). This will demonstrate that furanone-loaded aerogel treatment reduces virulence factor production, leading to important data on the likely amelioration of tissue damage resulting from aerogel treatment.

Secondly, it will be demonstrated that the developed aerogels deliver effective doses of furanones, preventing biofilm formation in acute traumatic wounds using *in vitro* models of burn wound infection and contaminated lacerations. I hypothesise that:

- rapidly degrading aerogels will effectively deliver a furanone payload to burn wounds and acute lacerations
- the application of furanones to early stage infections in acute wound environments will prevent biofilm formation

Furanone loaded aerogels will be prepared as described previously. Efficacy in treating and preventing infection in burn wounds will be tested using a well-established *ex vivo* burn wound model (Alves *et al.*, 2018) in which burns on porcine skin samples are infected with a selected organism. Aerogel treatments will be applied

to the infected skin and following treatment antimicrobial efficacy will be assessed using direct enumeration and cell viability staining.

To assess the efficacy of furanone-loaded aerogel dressings in acute lacerations with a foreign body, an adaptation of the model described by Kucera *et al.* (Kucera *et al.*, 2014) will be used in combination with the previously developed and more physiologically relevant wound bed medium. Firm polycarbonate coupons coated with 10^4 bacterial cells will be used to represent a contaminated foreign body. Once wounds have been inoculated, aerogels will be applied to the wound and antibiofilm efficacy will be assess as previously described.

7.5.3 Work Package 3 – Assessing the biocompatibility of developed aerogel wound treatments (24-36 months)

This work package will establish the biocompatibility of the developed furanone aerogels in the context of wound healing. I hypothesise that:

- Loaded aerogels will not induce significant cytotoxicity or genotoxicity in a range of mammalian cells vital in wound healing.
- Furanone aerogels will not induce significant release of inflammatory cytokines from relevant cells
- Furanone aerogels will not be detrimental to cell proliferative capacity during or after treatment.

To test these hypotheses, cell death, proliferation, migration, genotoxicity and cytokine release in human skin cell lines (keratinocytes and primary fibroblasts) will be measured. Skin immune cell types will also be used (macrophages, dendritic cells and bone marrow-derived mast cells). These experiments will provide complete data on the overall biocompatibility of the furanone aerogels in a wound environment. Cell

viability following aerogel treatment will be assessed using a simple colorimetric assay such as MTT cytotoxicity assay. In parallel, alkaline comet assays will demonstrate any genotoxicity as a result of aerogel treatment (Baldrick *et al.*, 2018). Clonogenic assays will assess post-treatment proliferation capacity of aerogel treated cells and wound scratch assays will assess the impact of aerogel exposure on cellular proliferation and migration and wound healing during treatment. The stimulation of cytokine release by aerogels will be demonstrated by measuring the release of several inflammation markers, including interleukin-1β, monocyte chemoattractant protein 1 (MCP1 / CCL2), Tumour Necrosis Factor alpha (TNF-α) and interleukin 6 using commercially available ELISAs.

An aerogel will be deemed suitable for further assessment if it shows a significant antibiofilm activity and is biocompatible as indicated by favourable response in all safety assays.

7.5.4 Work Package 4 – In vivo demonstration of aerogel-mediated delivery of furanones to acute and chronic wounds (37-48 months):

Once the *in vitro* efficacy and biocompatibility of furanone-loaded aerogels have been robustly demonstrated using clinically relevant model systems, *in vivo* effectiveness will then be demonstrated. Aerogels will be prepared aseptically to ensure sterile dressings are used throughout this *in vivo* work which will prove the clinical utility of then new dressings. To achieve this, two mouse models developed by collaborators at the Rumbaugh Lab in Texas Technical University will be used. These models have been used previously to study acute and chronic wound infections (Dalton *et al.*, 2011; Everett *et al.*, 2017). Firstly, a mouse model of chronic wound infection will be used to show the effective eradication of wound biofilms. Increases in wound closure rate, reductions in bacterial load will be measured. Reduction in bacterial load will be

through the use of the *In Vivo* Imaging System (IVIS) (Fleming and Rumbaugh, 2018) and direct enumeration of bacteria. Histological analyses will allow for measurements of underlying tissue damage, inflammation and bacterial infiltration of deeper tissues. Secondly, an *in vivo* model of acute burn wound infection will be used to show antimicrobial aerogel efficacy in reducing bacterial loads (Rumbaugh *et al.*, 1999). We will assess improvements in total acute wound closure and acute wound bacterial loads. Full details of the experimental design can be found in section 7.9.

7.6 Beneficiaries

The primary beneficiaries of this work will be patients, both in the UK and worldwide, suffering from a chronic wound. A highly effective antimicrobial wound dressing would significantly reduce bacterial burden in established wounds allowing for normal wound healing to resume. This will reduce wound healing time, improve clinical outcomes, and reduce the incidence of comorbidities such as sepsis and mental health effects. Additionally, individuals such as those who sustain burns or heavily contaminated wounds who are at greater risk of developing a chronic wound will also benefit. By preventing or eradicating early infection in these individuals the number of wounds becoming chronic will be significantly reduced. Further, the development of an *in situ* dissolving wound dressing will eliminate the need for dressing removal. As the removal of adhered dressings is a source of significant anxiety and worry for patients, this too will be eliminated.

Clinicians, such as the tissue viability teams in the South Eastern and Northern Health and social care trusts in Northern Ireland and the wider UK will also benefit from the development of these dressings. By completely dissolving in the wound environment these aerogels will allow clinicians to accurately monitor doses of antimicrobials being

administered to patients. This will be the first time that clinicians have been able to monitor doses of topically applied antimicrobials as closely as systemic antibiotics. This will allow clinicians to apply topical antimicrobials more sparingly and, thus, help to reduce the development of antimicrobial resistance in infected wounds. As such, consultant microbiologists such as Dr David Farren whose role in infection control seeks to reduce the development of antimicrobial resistance will see numerous benefits from this research. Furthermore, the successful use of extensive clinical input from project partners will effectively allow wound healing and tissue viability clinicians to have a direct effect on the development of new wound therapies. Having this clinical input will allow other clinicians to have greater confidence in the utility of the final product.

The research detailed here will also benefit academic researchers in a range of disciplines including materials science and tissue engineering such as Prof. Shiela Macneil and Dr Ilida Ortega, University of Sheffield and Prof. Phillip Withers and Prof. Sarah Cartmell and their teams at the University of Manchester. By developing *in situ* dissolving polymer aerogels, new information on the relationship between the microstructure of porous materials and their ability to release active compounds by undergoing matrix dissolution will be gained. This information can then be used by local, national, and international research groups investigating drug delivery and materials for biomedical applications. Researchers in pharmaceutics and pharmaceutical technologies such as Dr Gareth Williams, (Fabrication and Synthetic Technologies for Advanced Drug Delivery cluster, University College London), and Dr Eneko Larraneta of Queens University Belfast will benefit from this greater understanding of the relationship between material structure and drug release.

Finally, the UK Industrial sector will benefit from this project. Specifically, companies who focus on designing wound therapeutics and smart dressings such as the University of Bath spinout company SmartWound. Similarly, larger international pharmaceutical companies such as ConvaTec and Systagenix will also benefit from research into *in-situ* dissolving dressings. If successfully translated to the clinical setting the aerogel will need to be produced in large quantities by an industrial partner. As this product would be the first of its kind and the UK would be the sole producer of a product that can be used worldwide. This will provide revenue for the industrial manufacturer and also help to bolster the UK economy as well.

7.7 Relevance to Research Councils/Innovate UK

The project described here directly aligns with a number of Innovate UK (IUK) and research council themes and strategies and as such it is highly complementary to the current research profiles of the Medical Research Council (MRC) and UK Research and Innovation (UKRI), the Engineering and Physical Sciences Research Council (EPSRC), and of IUK

This work directly aligns with the MRC priority challenge of tackling antimicrobial resistance (AMR). AMR currently causes approximately 700,000 deaths annually and this is set to rise to 10 million if suitable measures are not taken. This work will develop a method for delivering non-antibiotic antimicrobials or tightly controlled doses of antibiotics directly to infected wounds. It, therefore, has the potential to help reduce the use of both topical and systemic antibiotics for the treatment of chronic wound infections which can contribute to the development of AMR (Carter *et al.*, 2018). The successful prevention of infections in acute wounds will reduce the incidence of more severe wound infections subsequently reducing the need for

systemic antibiotics. This will result in reduced selection pressures which encourage the development of resistance in bacterial populations. Additionally, the developed aerogel will allow delivery of 100% of the antimicrobial payload allowing for more accurate dosing of active compounds. For these reasons this project also falls under the UKRI general theme of "Tackling Antimicrobial Resistance".

This work also aligns with the EPSRC "Healthcare Technologies" theme. As this project proposes the development, characterisation and assessment of novel materials for use as an efficient and versatile drug delivery vehicle it will address the "Developing Future Therapies" grand challenge as stated by the EPSRC. It will also address the cross-cutting capability of "Advanced Materials". This material will be used for the delivery of both classical antimicrobials and novel non-antibiotic antimicrobial materials (such as metallic nanoparticles and graphene family materials) as well as complex drug cocktails. As such this work addresses several aspects of the challenge; administration of a novel therapeutic agents, targeting of a specific site, allowing co-delivery of multiple compounds and achieving controlled release of any agents delivered.

Finally, this work is in-line with the ethos of IUK as it will produce a novel and innovative product which, to the author's knowledge, would be the first of its kind. In addition to this, this project has significant potential to impact upon the UK economy through the possibility of spin-out company development to take advantage of any intellectual property. As well as the innovative nature of the proposed project the work detailed here aims to address the IUK "Ageing Society" grand challenge. This strategy aims to ensure that people have a minimum of 5 additional, good quality, years of life by 2035. As chronic wounds are primarily a condition associated with increased age

this project is designed to address this grand challenge. With chronic wounds come other health effects such as chronic pain, risk of sepsis and even mental health effects. Chronic wounds can clearly impact on the quality of life of patients who experience them. Therefore, any new intervention aimed at reducing the impact of chronic wounds on patients could make a significant difference in the quality of life of the elderly.

7.8 Project partners

This project will have both academic and clinical partners. Collaboration with the Welsh Wound Innovation Centre (WWIC) will provide vital clinical input from the beginning of the project. This clinical input will involve advice from practicing and research wound management clinicians on the design of the aerogel wound dressings. The development of novel materials for healthcare purposes has primarily been within the remit of engineering and materials science only. As such many novel materials are poorly optimised for clinical use. By involving wound management clinicians, steps can be taken to ensure that any developed materials meet the needs of both clinicians and patients. This needs driven design approach will greatly increase the likelihood of successful clinical translation.

To assist in the physical characterisation of the developed materials a collaboration has been sought with Professor Phillip Withers at the Royce Institute, part of the University of Manchester. Professor Withers will assist in the micro CT analysis of the developed aerogels. In addition to the collaboration with Professor Withers, a partnership with Dr Volkan Degirmenci of the University of Warwick has been established. Dr Degirmenci will provide access to, and assistance in using, the nitrogen physisorption facilities at Warwick's school of engineering.

Finally, to conduct robust *in vivo* investigations into the efficacy of the developed aerogels a collaboration has been established with Dr Kendra Rumbaugh at the Texas Technical University in Lubbock Texas. Dr Rumbaugh will provide assistance with conducting *in vivo* experiments using two mouse models which have been developed by her group. These models include a model of acute burn wound infection and a biofilm associated chronic wound infection model.

7.9 Ethical implications

Adult, Swiss Webster mice will be used in the project detailed in this application. Swiss Webster is a well-characterized outbred strain of white mice, which is susceptible to infection with both pathogens proposed for use in this work (*Pseudomonas aeruginosa* and *Staphylococcus aureus*) and have been used extensively by the Rumbaugh group at Texas Technical University. The use of mice in this work is appropriate as no sufficient *in vitro* model of wound healing is available.

7.9.1 Experimental design

Mice will be anesthetized by intraperitoneal injection of sodium pentobarbital. Once effective anaesthesia is reached, the backs of the animals will be shaved and a full-thickness, dorsal, 1.0 x 1.0 cm excisional skin wound will be administered. Wounds will be to the level of panniculus muscle and will be made with surgical scissors. Wounds will then be infected with approximately 10^4 - 10^5 colony-forming units of bacteria. Wounds will then be covered with a semipermeable polyurethane dressing (such as OPSITE). Warmed Ringer's lactate will then be administered to mice as fluid replacement and animals will be allowed to recover under heating pads. The use of an adhesive dressing prevents contractile wound healing and ensures that the administered wounds heal by deposition of granulation tissue. This means that the

wound healing is more representative of human processes. It has previously been shown that this infection is biofilm-associated and is therefore representative of human chronic wound infection.

A modified burned-mouse model of Stieritz and Holder (Stieritz and Holder, 1975) will be used as it closely resembles human acute wound sequelae. Briefly, adult, male and female Swiss Webster mice will be anesthetized, their backs will be shaved, and a non-lethal, third-degree thermal injury will be induced by scalding a 4.5 × 1.8 cm area of shaved skin with 90°C water. Fluid replacement therapy will be administered immediately following the burn, by the subcutaneous administration of 900 mL warm lactated rings. Wounds will then be infected with approximately 10^2 colony-forming units of bacteria.

7.9.2 Experimental endpoints

Endpoints for chronic wound experiments will be at 0, 7, 14, and 21 days post infection. Endpoint for acute wound experiments will be 72 h post infection. However, any animal found to be showing 3 or more of the NIH's morbidity endpoint clinical signs, or to be moribund, or unable to obtain food or water, will be judged to be at or near the endpoint and humanely euthanized.

7.9.3 Justification of sample size

Prior work and G-power software calculations performed in the Rumbaugh lab has shown that, typically, 9-12 mice will be needed per group to detect changes in bacterial load and wound closure at a P value of 0.05, at 95% confidence. However, as this is a first exploration of the efficacy of these dressings exact sample size estimates cannot be made. Experiments have been carefully designed so that data from as many parameters as possible will be obtained while using a minimal number of animals.

7.9.4 Addressing bias

Animals will be randomly assigned into treatment groups upon arrival to the animal facility. Treatments with either drug-loaded, or non-loaded aerogels will be blinded to the staff administering them and groups will be given letter identifiers. This identifier will be carried through the entire experiment and all tissues and samples obtained will be similarly labelled. All subsequent evaluation including histopathology, bacterial load determination, and wound closure rates, and statistical analysis will be performed on blinded samples.

7.9.5 Statistical analysis

Dr Rumbaugh will retain the blinded identifier key until statistical analysis of the data is performed by the applicant. Statistical analysis will be conducted utilizing GraphPad Prism, employing statistical ANOVA tests, with post-hoc Tukey tests. The data will be tested appropriately depending on normality and P values less than 0.05 will be considered significant.

7.10 Stakeholder engagement and dissemination plan

Stakeholder engagement will be considered a priority throughout this project. Engagement with potential clinical end users of the developed aerogel wound dressings will be through established collaborations with WWIC. By having clinicians involved in the design and development of the aerogel wound dressings from the early stages we aim to increase end user confidence that this dressing will meet both their needs and the needs of their patients.

As they are important stakeholders, patient involvement will also be used during this project. By engaging with patient groups, such as those run through organisations like The Wound Healing Foundation and The Scar-Free Foundation, we can gain a better

understanding of patients' needs and therefore tailor the design of the aerogels appropriately.

We will engage with academic stakeholders by disseminating our findings in high impact academic and clinically relevant journals as well as presenting at relevant conferences. We will also engage with academic stakeholder by hosting visits to the laboratories at Ulster University so that individuals may learn to use our chronic wound model for the assessment of antimicrobial wound therapies.

Initially, the objectives and then the findings of the project will be shared widely with potential stakeholders via web-based press releases (1-2 per year) from the communication office at Ulster University. A dedicated web page will be hosted on the University website and provide project information, updates and contact details to any interested parties for further engagement. Links to this information will be posted on the individual web page and social media profiles of each investigator. Tackling AMR–including chronic wound causing bacteria, and healthcare acquired infections–is a UKRI Cross Council initiative and to ensure relevant researchers benefit from our work, we will publish high impact papers in peer reviewed journals (e.g. Advanced Materials, Nature Microbiology) and deliver keynote presentations at leading conferences (e.g. Advanced Materials and Nanotechnology, Wounds UK and the Microbiology Society Annual Conference).

Once expected outcomes are achieved, we have identified follow on funding streams to translate our technology to the clinic. Firstly, we will seek UKRI research councils and charities funding, namely MRC (infection & immunity or antimicrobial resistance panel), MRC CiC (confidence in concept/P2D), Life Arc (MRC tech), Blond McIndoe Research Foundation and the Healing Foundation.

The generated knowledge will be useful not only for wound healing but also be important for other biomedical applications in which aerogel materials could be of use. Additionally, the findings of this work may be important to understand the in vivo efficacy profile of quorum sensing inhibitors (particularly in wound infections) as knowledge in this area is limited

7.11 Justification of Resources

7.11.1 Staff Directly Incurred Costs

Funds are requested for 100% time of a PDRA across the 4-year period in order to complete the detailed research activities.

7.11.2 Travel and Subsistence

Total funds requested: £11350. Funds are requested for attendance at 4 UK conferences of relevant disciplines (Advanced Materials and Nanotechnology, Wounds UK conference, Microbiology Society General conference, and Porous Materials conference). Attendance at these conferences is required for dissemination of key project findings, networking and development of collaborations. Costs for travel to these conferences includes flights/travel £150, accommodation £150, subsistence £50, and registration fee £300. Cost of £650 per conference. **TOTAL COST FOR UK CONFERENCES = £2600**.

Funds are also requested for travel to 2 international conferences (European Wound Management Association). Attendance at these international meetings is also required for dissemination of key project findings, networking and development of collaborations. Costs include flights/travel £500, accommodation £750, subsistence £300, and registration fee £500. Cost of £2050 per conference. **TOTAL COST FOR UK CONFERENCES = £4100**.

Travel to project collaborators and partners. Travel will include 8 trips to UK based partners (x2 trips to University of Warwick for porosimetry experiments, x2 trips to University of Manchester for micro CT experiments, x 4 trips to Welsh Wound Innovation Centre). This travel is necessary for work essential to the completion of the project Travel costs to UK partners and collaborators includes flights/travel £150, accommodation £200, subsistence £50. This represents a cost of £400 per trip. **TOTAL COST FOR TRAVEL TO UK PARTNERS = £3200.**

Funds for travel to non-UK collaborators have also been requested (x1 trip to Texas Technical University). This travel is required for the completion of *in vivo* work essential to the completion of the project. Costs for travel include flights £1000, Accommodation £300 and Subsistence £150. **TOTAL COST OF TRAVEL TO NON-UK PARTNERS = £1450**

7.11.3 Other Directly Incurred Costs

Total funds requested: £206758. Funds requested for WP1 are detailed here. Chemicals and reagents including polymers £7250 and crosslinkers £1291 are required for the preparation of aerogel formulations. Funds for characterisation of aerogel formulations include 50h scanning electron microscopy £6,000, 20 days for micro CT (in collaborations with Prof. Phillip Withers at the University of Manchester/Royce Institute) using Zeiss Versa system £10155 and 25 h of staff time £1068. **TOTAL COST FOR WP1 = £25764**

Funds for WP2 include the purchase of microorganisms £600, furanones £3830, microbiological culture media (inc. tryptone soy broth, nutrient broth, Mueller Hinton broth and technical agar) £1500, bacteriological stains (crystal violet and BacLight cell viability stain) £1060, wound model components £1050, wound dressing materials

£1400, protease and collagenase kits and elastin-congo red substrate £1760, other laboratory consumables (inc plasticware and polycarbonate coupons for acute laceration model) £ 2320. Funds for imaging of microbiological samples are also requested (SEM 25h, Confocal 25h, Bright field 15h) £6200. Costs for bulk production of critical point dried aerogels for acute and chronic wound via Suprex are also requested. The production of these samples will cost £10000. **TOTAL COSTS FOR WP2: £29720**

Requested funds for biocompatibility testing in WP3 are; purchase of human cell lines for in vitro testing £3500, consumables for cytotoxicity, clonogenic and wound scratch assays £1660, ELISA kits, 96 well plates and lids for inflammatory marker panel £3270. Funds for RT-qPCR testing includes reagents (RNEasy, Light Cycler plates and seals, Sybr Stain, Bioanalyser kit and consumables) £5950. Funds for xCelligence plates and electrodes will be £1500. Other required materials include cell culture medium and medium supplements £920 and general laboratory consumables £1450. **TOTAL COST FOR WP3 = £18250**

Funds for WP4 – Note: all costs from collaborator Kendra Rumbaugh at Texas Technical University (all costs converted from USD). Funds for Animals and animal housing £4859, lab and pathology processing fees £1620, microscopy core facility (use of the IVIS system) £1620, consumables (chemicals, media, and plasticware) £4049. Staff costs - Kendra Rumbaugh time £7748, Research Technician time £22921, facilities and administrative costs £22693. **TOTAL COST FOR WP4 = £65510**

Funds are requested for collaboration with Welsh Wound Innovation Centre. Requested funds will cover x1 full-day focus group for clinical input on dressing design (Staff costs for 2 professor and 4 senior research nurses £12281.25, room hire

£160, facilities costs £112) £12553.25. Costs also included for x3 half day follow up meetings for clinical input on dressing design. **TOTAL COST: £40,544**

Finally, funds are requested for the purchase of equipment for the completion of this project. The equipment to be purchased includes;

1. WR CDL1000L UV Crosslinker for PVP and PAA aerogel synthesis £1500
2. QuorumTech E3100 critical point dryer for aerogel supercritical drying £6000
3. critical point dryer accessories (inc. sample pots, servicing kit and spare components, seals, washers etc) £3200
4. Cleaver Scientific SWB-20L-3 stirring water bath for gel preparation £1700
5. full set of Gilson pipettes (5 pipettes total) for RNA work £1190
6. Sciquip Mutichanel pipettes (2 pipettes total) and Sciquip serological pipette gun for cell biology work £450,
7. SiQuip DryBlock Heat block for use in ex vivo burn wound model £230
8. Thermo x4Pro 240V50/60Hz benchtop centrifuge for use in biocompatibility testing £9900
9. Kern inverted compound microscope for cell biology and biocompatibility work £2800.

TOTAL COST FOR EQUIPMENT FOR THIS PROJECT = £26970

7.12 References

Alves, D. R. *et al.* (2018) 'Development of a High-Throughput ex-Vivo Burn Wound Model Using Porcine Skin, and Its Application to Evaluate New Approaches to Control Wound Infection', *Frontiers in Cellular and Infection Microbiology*, 8, pp. 1–15. doi: 10.3389/fcimb.2018.00196.

Attinger, C. and Wolcott, R. (2012) 'Clinically Addressing Biofilm in Chronic Wounds.', *Advances in wound care*, 1(3), pp. 127–132. doi: 10.1089/wound.2011.0333.

Baldino, L. *et al.* (2020) 'Production of biodegradable superabsorbent aerogels using a supercritical CO2 assisted drying', *Journal of Supercritical Fluids*, 156, p. 104681. doi: 10.1016/j.supflu.2019.104681.

Baldrick, F. R. *et al.* (2018) 'Impact of a (poly)phenol-rich extract from the brown algae Ascophyllum nodosum on DNA damage and antioxidant activity in an overweight or obese population: A randomized controlled trial', *American Journal of Clinical Nutrition*, 108(4), pp. 688–700. doi: 10.1093/ajcn/nqy147.

Balestrino, D. *et al.* (2005) 'Characterization of type 2 quorum sensing in *Klebsiella pneumoniae* and relationship with biofilm formation', *Journal of Bacteriology*, 187(8), pp. 2870–2880. doi: 10.1128/JB.187.8.2870-2880.2005.

Bowler, P. G., Duerden, B. I. and Armstrong, D. G. (2001) 'Wound microbiology and associated approaches to wound management', *Clinical Microbiology Reviews*, pp. 244–269. doi: 10.1128/CMR.14.2.244-269.2001.

Brawn, K. (2015) 'Guidelines for the assessment & management of wounds',

Northamptonshire Healthboard Guidance. Available at: https://www.nhft.nhs.uk/download.cfm?doc=docm93jijm4n1793.pdf&ver=17402.

Cambridgeshire and Peterborough Foundation Trust (2012) 'Wound Care Guidelines and Dressings Formulary', (June), pp. 1–63. Available at: http://www.cambsphn.nhs.uk/Libraries/Woundcare/Wound_Care_Guidelines_and_Dressings_Formulary_June_2012.sflb.ashx.

Carter, G. P. *et al.* (2018) 'Topical antibiotic use coselects for the carriage of mobile genetic elements conferring resistance to unrelated antimicrobials in *Staphylococcus aureus'*, *Antimicrobial Agents and Chemotherapy*, 62(2). doi: 10.1128/AAC.02000-17.

Cartotto, R. (2017) 'Topical antimicrobial agents for pediatric burns', *Burns & Trauma*, 5(1), pp. 1–8. doi: 10.1186/s41038-017-0096-6.

Charlesworth, B. *et al.* (2014) 'Dressing-related trauma: Clinical sequelae and resource utilization in a UK setting', *ClinicoEconomics and Outcomes Research*, 6(1), pp. 227–239. doi: 10.2147/CEOR.S59005.

Choi, S. C. *et al.* (2014) 'Inhibitory effects of 4-hydroxy-2,5-dimethyl-3(2H)-furanone (HDMF) on acyl-homoserine lactone-mediated virulence factor production and biofilm formation in *Pseudomonas aeruginosa* PAO1', *Journal of Microbiology*, 52(9), pp. 734–742. doi: 10.1007/s12275-014-4060-x.

Church, D. *et al.* (2006) 'Burn wound infections', *Clinical Microbiology Reviews*, pp. 403–434. doi: 10.1128/CMR.19.2.403-434.2006.

Dalton, T. *et al.* (2011) 'An in vivo polymicrobial biofilm wound infection model to

study interspecies interactions', *PLoS ONE*, 6(11). doi: 10.1371/journal.pone.0027317.

Deligianni, E. *et al.* (2010) '*Pseudomonas aeruginosa* cystic fibrosis isolates of similar RAPD genotype exhibit diversity in biofilm forming ability in vitro', *BMC Microbiology*, 10, p. 38. doi: 10.1186/1471-2180-10-38.

Dewi, F. and Hinchliffe, R. J. (2019) 'Foot complications in patients with diabetes', *Surgery*, pp. 106–111. doi: 10.1016/j.mpsur.2018.12.003.

Dumville, J. C., Keogh, S. J., *et al.* (2015) 'Alginate dressings for treating pressure ulcers', *Cochrane Database of Systematic Reviews*, 2015(5). doi: 10.1002/14651858.CD011277.pub2.

Dumville, J. C., Stubbs, N., *et al.* (2015) 'Hydrogel dressings for treating pressure ulcers', *Cochrane Database of Systematic Reviews*, 2015(2). doi: 10.1002/14651858.CD011226.pub2.

Everett, J. *et al.* (2017) 'Arginine is a critical substrate for the pathogenesis of *Pseudomonas aeruginosa* in burn wound infections', *mBio*, 8(2). doi: 10.1128/mBio.02160-16.

Fleming, D. and Rumbaugh, K. (2018) 'The Consequences of Biofilm Dispersal on the Host', *Scientific Reports*, 8(1), pp. 1–7. doi: 10.1038/s41598-018-29121-2.

Flemming, H.-C. *et al.* (2016) 'Biofilms: an emergent form of bacterial life', *Nature Reviews Microbiology*, 14(9), pp. 563–575. doi: 10.1038/nrmicro.2016.94.

Frykberg, R. G. and Banks, J. (2015) 'Challenges in the Treatment of Chronic Wounds', *Advances in Wound Care*, 4(9), pp. 560–582. doi:

10.1089/wound.2015.0635.

García-Contreras, R. *et al.* (2013) 'Resistance to the quorum-quenching compounds brominated furanone C-30 and 5-fluorouracil in *Pseudomonas aeruginosa* clinical isolates', *Pathogens and Disease*, 68(1), pp. 8–11. doi: 10.1111/2049-632X.12039.

Guest, J. F. *et al.* (2016) 'Health economic burden that different wound types impose on the UK's National Health Service', *National Health Service. Int Wound J*. doi: 10.1111/iwj.12603.

Guest, J. F., Vowden, K. and Vowden, P. (2017) 'The health economic burden that acute and chronic wounds impose on an average clinical commissioning group/health board in the UK', *Journal of Wound Care*, 26(6), pp. 292–303. doi: 10.12968/jowc.2017.26.6.353a.

Han, G. *et al.* (2017) *Chronic Wound Healing: A Review of Current Management and Treatments, Advances in Therapy*. doi: 10.1007/s12325-017-0478-y.

Healy, B. and Freedman, A. (2006) 'ABC of Wound Healing: Infections', *BMJ*, 332(7545), pp. 838–841. doi: 10.1136/bmj.332.7545.838.

Hentzer, M. *et al.* (2002) 'Inhibition of quorum sensing in *Pseudomonas aeruginosa* biofilm bacteria by a halogenated furanone compound', *Microbiology*, 148(1), pp. 87–102. doi: 10.1099/00221287-148-1-87.

Hentzer, M. *et al.* (2003) 'Attenuation of *Pseudomonas aeruginosa* virulence by quorum-sensing inhibitors', *Embo J.*, 22(15), p. 3803. doi: 10.1093/emboj/cdg366.

Kucera, J. *et al.* (2014) 'Multispecies biofilm in an artificial wound bed-A novel model for in vitro assessment of solid antimicrobial dressings', *Journal of Microbiological*

Methods, 103, pp. 18–24. doi: 10.1016/j.mimet.2014.05.008.

Leaper, D., Assadian, O. and Edmiston, C. E. (2015) 'Approach to chronic wound infections', *British Journal of Dermatology*, 173(2), pp. 351–358. doi: 10.1111/bjd.13677.

Li, J. *et al.* (2007) 'Quorum sensing in *Escherichia coli* is signaled by AI-2/LsrR: Effects on small RNA and biofilm architecture', *Journal of Bacteriology*. A, 189(16), pp. 6011–6020. doi: 10.1128/JB.00014-07.

Lianhua, Y. *et al.* (2013) 'Effect of Brominated Furanones on the Formation of Biofilm by Escherichia coli on Polyvinyl Chloride Materials', *Cell Biochemistry and Biophysics*, 67(3), pp. 893–897. doi: 10.1007/s12013-013-9578-8.

Lipsky, B. A. and Hoey, C. (2009) 'Topical Antimicrobial Therapy for Treating Chronic Wounds', *Clinical Infectious Diseases*, 49(10), pp. 1541–1549. doi: 10.1086/644732.

Lovskaya, D. and Menshutina, N. (2020) 'Alginate-based aerogel particles as drug delivery systems: Investigation of the supercritical adsorption and in vitro evaluations', *Materials*, 13(2). doi: 10.3390/ma13020329.

Maeda, T. *et al.* (2012) 'Quorum quenching quandary: resistance to antivirulence compounds', *The ISME Journal*, 6(3), pp. 493–501. doi: 10.1038/ismej.2011.122.

Mah, T. F. (2012) 'Biofilm-specific antibiotic resistance', *Future Microbiology*, pp. 1061–1072. doi: 10.2217/fmb.12.76.

Mah, T. F. C. and O'Toole, G. A. (2001) 'Mechanisms of biofilm resistance to antimicrobial agents', *Trends in Microbiology*, 9(1), pp. 34–39. doi: 10.1016/S0966-

842X(00)01913-2.

Malone, M. *et al.* (2017) 'The prevalence of biofilms in chronic wounds: a systematic review and meta-analysis of published data.', *Journal of wound care*, 26(1), pp. 20–25. doi: 10.12968/jowc.2017.26.1.20.

Martinengo, L. *et al.* (2019) 'Prevalence of chronic wounds in the general population: systematic review and meta-analysis of observational studies', *Annals of Epidemiology*, pp. 8–15. doi: 10.1016/j.annepidem.2018.10.005.

Matsumura, H. *et al.* (2013) 'A model for quantitative evaluation of skin damage at adhesive wound dressing removal', *International Wound Journal*, 10(3), pp. 291–294. doi: 10.1111/j.1742-481X.2012.00975.x.

Mishra, M. *et al.* (2012) '*Pseudomonas aeruginosa* Psl polysaccharide reduces neutrophil phagocytosis and the oxidative response by limiting complement-mediated opsonization', *Cellular Microbiology*, 14(1), pp. 95–106. doi: 10.1111/j.1462-5822.2011.01704.x.

Morton, L. M. and Phillips, T. J. (2016) 'Wound healing and treating wounds Differential diagnosis and evaluation of chronic wounds', *Journal of the American Academy of Dermatology*, pp. 589–605. doi: 10.1016/j.jaad.2015.08.068.

Murray, J. *et al.* (2017) 'Evaluation of bactericidal and anti-biofilm properties of a novel surface-active organosilane biocide against healthcare associated pathogens and *Pseudomonas aeruginosa* biolfilm', *PLOS ONE*, 12(8), p. e0182624. doi: 10.1371/journal.pone.0182624.

Office for National Statistics (2020) *Overview of the UK population*. Available at:

https://www.ons.gov.uk/peoplepopulationandcommunity/populationandmigration/populationestimates/articles/overviewoftheukpopulation/august2019#the-uks-population-is-ageing (Accessed: 22 May 2020).

Orhan, G. *et al.* (2005) 'Synergy tests by E test and checkerboard methods of antimicrobial combinations against Brucella melitensis', *Journal of Clinical Microbiology*, 43(1), pp. 140–143. doi: 10.1128/JCM.43.1.140-143.2005.

Oshri, R. D. *et al.* (2018) 'Selection for increased quorum-sensing cooperation in *Pseudomonas aeruginosa* through the shut-down of a drug resistance pump', *ISME Journal*, 12(10), pp. 2458–2469. doi: 10.1038/s41396-018-0205-y.

Percival, S. L., McCarty, S. M. and Lipsky, B. (2015) 'Biofilms and Wounds: An Overview of the Evidence.', *Advances in wound care*, 4(7), pp. 373–381. doi: 10.1089/wound.2014.0557.

Pier, G. B. *et al.* (2001) 'Role of alginate O acetylation in resistance of mucoid *Pseudomonas aeruginosa* to opsonic phagocytosis', *Infection and Immunity*, 69(3), pp. 1895–1901. doi: 10.1128/IAI.69.3.1895-1901.2001.

Rayner, R. *et al.* (2009) 'Leg ulcers: atypical presentations and associated comorbidities', *Wound Practice and Research*, 17(4), pp. 168–185.

Reichhardt, C. and Parsek, M. R. (2019) 'Confocal Laser Scanning Microscopy for Analysis of *Pseudomonas aeruginosa* Biofilm Architecture and Matrix Localization', *Frontiers in Microbiology*, 10(APR), p. 677. doi: 10.3389/fmicb.2019.00677.

Ren, D., Sims, J. J. and Wood, T. K. (2001) 'Inhibition of biofilm formation and swarming of Escherichia coli by (5Z)-4-bromo-5-(bromomethylene)-3-butyl-2(5H)-

furanone', *Environmental Microbiology*, 3(11), pp. 731–736. doi: 10.1046/j.1462-2920.2001.00249.x.

Renner, R. and Erfurt-Berge, C. (2017) 'Depression and quality of life in patients with chronic wounds: ways to measure their influence and their effect on daily life', *Chronic Wound Care Management and Research*, Volume 4, pp. 143–151. doi: 10.2147/cwcmr.s124917.

Rodrigues, M. *et al.* (2019) 'Wound healing: A cellular perspective', *Physiological Reviews*, 99(1), pp. 665–706. doi: 10.1152/physrev.00067.2017.

Roodsari, G. S. (2015) 'The risk of wound infection after simple hand laceration', *World Journal of Emergency Medicine*, 6(1), p. 44. doi: 10.5847/wjem.j.1920-8642.2015.01.008.

Rothe, K., Tsokos, M. and Handrick, W. (2015) 'Animal and Human Bite Wounds', *Deutsches Arzteblatt international*, pp. 433–443. doi: 10.3238/arztebl.2015.0433.

Rumbaugh, K. P. *et al.* (1999) 'Contribution of quorum sensing to the virulence of *Pseudomonas aeruginosa* in burn wound infections.', *Infection and immunity*, 67(11), pp. 5854–62. Available at: http://www.ncbi.nlm.nih.gov/pubmed/10531240 (Accessed: 25 October 2017).

Schultz, G. *et al.* (2017) 'Consensus guidelines for the identification and treatment of biofilms in chronic nonhealing wounds', *Wound Repair and Regeneration*, 25(5). doi: 10.1111/wrr.12590.

Shao, C. *et al.* (2012) 'LuxS-dependent AI-2 regulates versatile functions in Enterococcus faecalis V583', *Journal of Proteome Research*, 11(9), pp. 4465–4475.

doi: 10.1021/pr3002244.

Siller, M. *et al.* (2008) 'Functional analysis of the group A streptococcal luxS/AI-2 system in metabolism, adaptation to stress and interaction with host cells', *BMC Microbiology*, 8(1), p. 188. doi: 10.1186/1471-2180-8-188.

Stieritz, D. D. and Holder, I. A. (1975) 'Experimental Studies of the Pathogenesis of Infections Due to *Pseudomonas aeruginosa*: Description of a Burned Mouse Model', *Journal of Infectious Diseases*, 131(6), pp. 688–691. doi: 10.1093/infdis/131.6.688.

Sullivan, R. *et al.* (2011) 'Delivering affordable cancer care in high-income countries', *The Lancet Oncology*, 12(10), pp. 933–980. doi: 10.1016/S1470-2045(11)70141-3.

Thomas, S. and McCubbin, P. (2003) 'An in vitro analysis of the antimicrobial properties of 10 silver-containing dressings.', *Journal of wound care*, 12(8), pp. 305–308. doi: 10.12968/jowc.2003.12.8.26526.

Waquad, A. *et al.* (2020) 'Retained iatrogenic foreign body causing persistent non-healing wound: a case report', *International Surgery Journal*, 7(3), p. 883. doi: 10.18203/2349-2902.isj20200837.

WHO (2020) *Prevention and management of wound infection*. Available at: https://www.who.int/hac/techguidance/tools/guidelines_prevention_and_management_wound_infection.pdf (Accessed: 26 July 2019).

Williamson, D. A., Carter, G. P. and Howden, B. P. (2017) 'Current and emerging topical antibacterials and antiseptics: Agents, action, and resistance patterns', *Clinical Microbiology Reviews*, pp. 827–860. doi: 10.1128/CMR.00112-16.

Woo, K. Y. (2010) 'Wound-related pain: anxiety, stress and wound healing', *Wounds*

UK, 6(4), pp. 92–98.

Wu, H. *et al.* (2004) 'Synthetic furanones inhibit quorum-sensing and enhance bacterial clearance in *Pseudomonas aeruginosa* lung infection in mice', *Journal of Antimicrobial Chemotherapy*, 53(6), pp. 1054–1061. doi: 10.1093/jac/dkh223.

Zaidi, A. and Green, L. (2019) 'Physiology of haemostasis', *Anaesthesia and Intensive Care Medicine*, pp. 152–158. doi: 10.1016/j.mpaic.2019.01.005.

Zhao, L. *et al.* (2010) '*Staphylococcus aureus* AI-2 quorum sensing associates with the KdpDE two-component system to regulate capsular polysaccharide synthesis and virulence', *Infection and Immunity*, 78(8), pp. 3506–3515. doi: 10.1128/IAI.00131-10.

Appendix 1

Publications arising from this work

Proctor, C. R., McCarron, P. A. and Ternan, N. G. (2020) 'Furanone quorum-sensing inhibitors with potential as novel therapeutics against Pseudomonas aeruginosa', *Journal of Medical Microbiology*, p. jmm001144. doi: 10.1099/jmm.0.001144.

Abstract: Micro- organisms use quorum sensing (QS), a cell density- dependent process, to communicate. This QS mode of interchange leads to the production of a variety of virulence factors, co- ordination of complex bacterial behaviours, such as swarming motility, degradation of host tissue and biofilm formation. QS is implicated in numerous human infections and consequently researchers have sought ways of effectively inhibiting the process in pathogenic bacteria. Two decades ago, furanones were the first class of chemical compounds identified as Pseudomonas aeruginosa QS inhibitors (QSIs). P. aeruginosa is a ubiquitous organism, capable of causing a wide range of infections in humans, including eye and ear infections, wound infections and potentially fatal bacteraemia and thus novel treatments against this organism are greatly needed. This review provides a brief background on QS and the use of furanones as QSIs. Based on the effectiveness of action, both in vivo and in vitro, we will explore the use of furanones as potential antimicrobial therapeutics and conclude with open questions.